Deciphering the role of STIM1 in nervous system development

Adrian Colin Thompson
BMedRes (Hons)

Submitted in fulfillment of the requirement for the
Degree of Doctor of Philosophy, Medicine.

School of Medicine,
University of Tasmania,
March 2017

Declaration of Originality

This thesis contains no material which has been accepted for a degree or diploma by the University or any other institution, except by way of background information and duly acknowledged in the thesis, and to the best of my knowledge and belief no material previously published or written by another person except where due acknowledgement is made in the text of the thesis, nor does the thesis contain any material that infringes copyright.

Adrian Thompson
March 2017

Authority of Access

This thesis may be made available for loan and limited copying and communication in accordance with the Copyright Act 1968.

Adrian Thompson
March 2017

Statement of ethical conduct

The research related to this thesis abides by international and Australian codes on human and animal experimentation, the guidelines by the Australian Government's Office of the Gene Technology Regulator and the Safety, Ethics and Institutional Biosafety Committees of the University.

Adrian Thompson
March 2017

Acknowledgments

Firstly, I would like to express my appreciation and gratitude to my primary supervisor, Associate Professor Lisa Foa. Thank you for continued support and guidance over the past four years. It feels like such a long time ago since that first chat about doing experiments with fish, and I'm glad that we made it happen! Thank you for believing in me, for continually pushing me to be a better scientist, and for sharing your passion for science. It was always so great to see your excitement for new data! I owe you such a huge debt, not only for your support over the past four years, but also for encouraging me to apply for Woods Hole. As you know, words cannot describe the experience, but I can't see anything but science in my future, and I have you to thank for that.

To my co-supervisor, Dr Rob Gasperini, thank you for all your advice and support. I am especially grateful for all your help in the lab, for teaching me imaging, for helping me look after the fish, and for answering all my questions. Thank you for helping me shape and articulate my ideas, for your encouragement, and for always pushing me to be better. Your guidance has been truly invaluable.

To Dr Kaylene all Young, thank you for your help and support. Thank you for always being willing to help and provide advice whenever I needed it. I am especially grateful for all your help in my first year, I would have been lost without your support.

A huge thank you to Macarena Pavez. I have been lucky that I have had you to share this PhD with. Thank you for being a great friend, for your support, for our many STIM chats, for listening to my rants, and for always being so cheerful! You have helped me stay somewhat sane, and I am so grateful for all your support.

Thank you to the amazing people that have been a part of the Foa, Small, Young and Lin labs, you have been such valued supports during my PhD. To Dr Lila Landowski, Dr Camilla Mitchell and Dr Edgar Dawkins: when I first joined the lab you three taught me

so much about what it means to be a scientist, and I am lucky to have such great friends! Thank you to Professor David Small, Dr John Lin and Dr Sharron Sann for your valuable advice, constructive feedback, ideas, and technical help throughout my PhD.

Thank you to Dr Ethan Scott for welcoming me into your lab during my visit, your advice and support in establishing this project, as well as being so gracious with your time whenever we crossed paths. Thank you also to Jason Cockington and the staff of the zebrafish facility at UQ for training me in the care of zebrafish. Your advice was so helpful in getting this project started.

To my fellow students, thanks you all for your friendship and support. I am so thankful that I have had such an amazing group of people to share this experience with. No matter what was going on, it was always good to know that there were people that understood. It has been so great to share this experience with you all.

Finally, I would like to thank my parents for being amazing. I have been so lucky to have your support during my university life. I could not have achieved this without all your encouragement and support.

Table of Contents

List of abbreviations:

$[Ca^{2+}]_i$	concentration of intracellular calcium
$\Delta F/F_0$	change in fluorescence from baseline fluorescence
+TIP	microtubule plus end binding protein
AChR	acetylcholine receptors
AP	alkaline phosphatase
APC	adenomatous polyposis coli
BCIP	5-bromo-4-chloro-3-indolyl-phosphate
BDNF	brain-derived neurotrophic factor
bFGF	basic fibroblast growth factor
BMP	bone morphogenic protein
Ca^{2+}	calcium
cAMP	cyclic adenosine monophosphate
CaN	calcineurin
CaMKII	calcium/calmodulin-dependent kinase II
cGMP	cyclic guanosine monophosphate
CaP	caudal primary motor neuron
CC1/2/3	coil-coiled 1/2/3
Cdk5	cyclin-dependent kinase 5
CNG	cyclic nucleotide gated channel
CNTF	ciliary neurotrophic factor
CP	cortical plate
Ctx	cortex
CICR	calcium-induced calcium release
CRAC	calcium release activated calcium
CTID	C-terminal inhibitory domain
DCC	deleted in colorectal cancer
DIG	digoxin
DEPC	diethyl pyrocarbonate
DH	dorsal horn
DP	dorsal pallium
DRG	dorsal root ganglion
dSTIM	*drosophila* STIM

E13/15/16	embryonic day 13/15/16
EB1	end binding 1
EF-SAM	EF-hand/sterile alpha motif
ER	endoplasmic reticulum
ERK1/2	extracellular regulated kinases 1 and 2
F-actin	filamentous actin
FGF	fibroblast growth factor
FITC	fluorescein isothiocyanate
FLIP	focal laser-induced photolysis
GFP	green fluorescent protein
GM	grey matter
Hz	hertz
hpf	hours post fertilisation
hr	hour
I_{CRAC}	calcium release activated calcium current
IICR	IP_3-induced calcium release
IP_3	inositol-3-phopshate
IP_3R	inositol-3-phopshate receptor
IR	immunoreactivity
LGE	lateral ganglionic eminence
MABT	maleic acid buffer containing Tween-20
MAG	myelin associated glycoprotein
MAPK	mitogen-activated protein kinase
MiP	middle primary motor neuron
mGluR	metabotropic glutamate receptor
mRNA	messenger ribonucleic acid
morpholino	antisense morpholino oligonucleotide
MP	medial pallium
NA	numerical aperture
NBT	nitroblue tetrazolium
NFAT	nuclear factor of activated T cells
NGF	nerve growth factor
P5	post-natal day 5
PBS	phosphate buffered saline

PDGFRα	platelet derived growth factor receptor alpha
PFA	paraformaldehyde
PIP_2	4,5-bisphosphate
PI3K	phosphatidylinositol-4,5-bisphosphate 3-kinase
PK	proteinase K
PKA	protein kinase A
PKG	protein kinase G
PLC	phospholipase C
PM	plasma membrane
RNAi	RNA interference
RoP	rostral primary motor neuron
RS	retrosplenial neocortex
RyR	ryanodine receptor
SAM	sterile-alpha motif
sema3a	semaphorin-3a
sema3A1/2	zebrafish semaphorin-3A1/2
Shh	sonic hedgehog
SOAR	STIM1 Orai1-activating region
SOCE	store-operated calcium entry
STIM1	stromal interaction molecule 1
STIM2	stromal interaction molecule 2
TAC	tip attachment complex
Tg	thapsigargin
TrkB	tropomyosin receptor kinase B
TRPA	transient receptor potential
TRPC	transient receptor potential canonical
TRPM	transient receptor potential melastatin
TRPML	transient receptor potential mucolipin
TRPN	transient receptor potential nompC
TRPP	transient receptor potential polycystic
TRPV	transient receptor potential vanilloid
UAS	upstream activation sequence
VAMP2	vesicle-associated membrane protein 2
VeLD	ventral-longitudinally descending interneuron

VH	ventral horn
VZ	ventricular zone
VDCC	voltage-dependent calcium channel
WM	white matter
xSTIM1	*Xenopus* STIM1
zOrai1a	zebrafish Orai1a
zOrai1b	zebrafish Orai1b
zSTIM1a	zebrafish STIM1a
zSTIM1b	zebrafish STIM1b
zSTIM2a	zebrafish STIM2a
zSTIM2b	zebrafish STIM2b

Abstract

The wiring of the nervous system during development requires each neuron to find and connect with a correct synaptic target in a process known as axon pathfinding. Defects in axon pathfinding cause significant neurodevelopmental disorders, and contribute to the inability of neural circuits to reconnect following injury or disease. Axon pathfinding is regulated by precise intracellular calcium signals produced by the influx of extracellular calcium and the release of calcium from internal stores, such as the endoplasmic reticulum (ER). Although the importance of discrete patterns of calcium signaling for determining axon pathfinding are well documented, the mechanisms that control such precise calcium signaling events are yet to be fully elucidated.

Stromal interacting molecule 1 (STIM1) is an ER-resident calcium sensing protein that activates a specific mode of calcium influx termed store-operated calcium entry (SOCE). STIM1 is activated by the depletion of calcium from the ER, with activated STIM1 triggering calcium influx via SOCE. The calcium that enters the cell via SOCE refills the depleted ER calcium store, and sustains elevated intracellular calcium to potentiate calcium-dependent intracellular signaling pathways. STIM1 has been shown to be necessary for correct growth cone motility *in vitro*, and correct axon pathfinding *in vivo*. However, the cellular expression of STIM1 during nervous system development, and the function of STIM1 in axon pathfinding *in vivo* remain poorly understood. To this end, the central hypothesis examined by this thesis is that there are discrete patterns of STIM1 protein expression during embryonic development, and STIM1-mediated calcium signaling is necessary for correct nervous system development.

The developmental expression of STIM1 was investigated in the mouse and zebrafish (*Danio rerio*) nervous systems. The pattern of STIM1 expression was highly conserved between mice and zebrafish nervous systems, suggesting that STIM1 has a conserved role in development. By examining the cellular expression of STIM1 in the embryonic mouse nervous system, it was confirmed that STIM1 is expressed by neurons during development, consistent with a function for STIM1 in the regulation of calcium signaling during nervous system development.

The function of STIM1 during nervous system development was assessed by investigating the requirement of zebrafish STIM1a (zSTIM1a) expression for axon pathfinding *in vivo*. A reduced expression of zSTIM1a impacted the survival, growth and correct development of zebrafish embryos, consistent with STIM1 having important functions in development. zSTIM1a was shown to regulate calcium influx via SOCE in zebrafish spinal motor neurons, confirming that STIM1 regulates calcium signaling in zebrafish neurons. When axon pathfinding by spinal motor neurons was examined in zSTIM1a morphant embryos, the axons of caudal primary (CaP) motor neurons were observed to stall at intermediate targets, exhibit defects in extension from intermediate targets, express fewer filopodia, and were less likely to be branched. Defects in axon pathfinding correlated with perturb calcium signaling in navigating CaP axons when zSTIM1a expression was reduced, with bursting calcium spikes decreased in axons navigating via intermediate targets. Together, these data provide evidence that STIM1-mediated calcium signaling is required for correct axon pathfinding *in vivo*. These findings have significant implications for our understanding of the molecular mechanisms that contribute to the regulation of discrete patterns of calcium signaling during axon pathfinding *in vivo* and, hence, nervous system development.

Chapter 1:
Introduction and literature review

Chapter 1: Introduction and literature review

1.1 Axon pathfinding is necessary for nervous system development

The nervous system is comprised of a highly complex, yet precise network of synaptic connections. The incredible fidelity with which these synaptic connections are formed is vital for nervous system development and function, with aberrant synapses causing developmental diseases including epilepsy, schizophrenia, autism spectrum disorders, as well as numerous mental retardation syndromes (Lewis and Levitt, 2002; Anitha et al., 2008; Li et al., 2009; Sbacchi et al., 2010; Cvetkovska et al., 2013). During development, each neuron extends an axon through the complex environment of the embryonic nervous system to find and synapse with an appropriate target (Stoeckli and Zou, 2009). The process by which axons navigate is termed axon pathfinding (Keshishian and Bentley, 1983; Bastiani et al., 1984; Kuwada, 1986).

Multiple cellular and molecular mechanisms exist to ensure the precision of axon outgrowth. The first axons to begin axon pathfinding are referred to as pioneer axons (Connor et al., 1990). Pioneer axons provide a crucial scaffold along which axons from later-born neurons (or follower axons) subsequently navigate (Keshishian and Bentley, 1983; Kuwada, 1986), in a process known as fasciculation (Van Vactor, 1998). Accordingly, ablation of pioneering axons, or defective axon pathfinding by pioneer axons, results in follower axons stalling, failing to extend, or extending along inappropriate trajectories (Raper et al., 1984; Pike et al., 1992; Hidalgo and Brand, 1997). Axon pathfinding is also controlled via intermediate targets (also referred to as choice points), which are sources of instructive guidance signals that trigger axons to pause and turn, such that each axon reaches an appropriate synaptic target (Lance-Jones and Landmesser, 1981; Bentley and Keshishian, 1982; Tosney and Landmesser, 1985). These guidance cues, which include soluble, cell-surface bound or extracellular matrix proteins, signal to the axon via the activation of cell-surface receptors [reviewed in (Tessier-Lavigne and Goodman, 1996; Dickson, 2002)]. Hence, axon pathfinding is dependent on axons sensing and translating environmental guidance cues into motility responses that guide the axon towards its target. This ability of axons to sense and respond to environmental guidance cues is conferred by the axonal growth cone.

1.2 The growth cone

The growth cone is a highly motile guidance structure located at the distal tip of growing axons (Cajal, 1890). Growth cones interpret environmental guidance signals to coordinate motile responses that guide each axon to its correct synaptic target (Tessier-Lavigne and Goodman, 1996; Dickson, 2002; Henley and Poo, 2004; Spitzer, 2004; Zheng and Poo, 2007). The morphology of the growth cone correlates with distinct motility behaviours (Tosney and Landmesser, 1985; Lankford and Letourneau, 1990; Halloran and Kalil, 1994; Tessier-Lavigne and Goodman, 1996; Mason and Erskine, 2000; Goodhill et al., 2015). Growth cones of pioneering axons are large and complex, a morphology that is consistent with pioneer axons pausing and spreading as they 'sample' their environment for guidance cues (Bovolenta and Mason, 1987; Kaethner and Stuermer, 1992; Halloran and Kalil, 1994; Mason and Erskine, 2000). In contrast, growth cones of follower axons are simpler, narrower, and more elongated. As follower axons predominantly navigate by fasciculating with axon scaffolds laid down by pioneering axons (Van Vactor, 1998), this morphology is consistent with growth cones of follower axons having less guidance cues to interpret. Hence, the capacity of growth cones to adopt a morphology in response to environmental guidance signals is key to the ability of growth cones to regulate axon pathfinding. Like all motile structures, the growth cone relies on the cytoskeleton to regulate motility.

1.2.1 Structure of the growth cone

The growth cone is comprised of two structurally distinct regions, referred to as the central and peripheral zones (Fig. 1.1). The central zone is located at the distal end of the axon shaft and is a microtubule-rich zone containing numerous membranous vesicles, as well as organelles such as the endoplasmic reticulum (ER) and mitochondria (Bridgman et al., 1986; Forscher et al., 1987). The central zone contains stabilised microtubules projecting from the axon shaft and dynamic microtubules that constantly probe into the peripheral zone, where they mediate directed growth cone stabilisation and axon outgrowth (Dent et al., 2011). By comparison, the peripheral zone is rich in actin and largely devoid of microtubules and organelles (Henley and Poo, 2004). However, the remodeling of microtubules and trafficking of vesicles and organelles into the peripheral

zone is crucial for growth cone motility (Forscher et al., 1987; Dent and Gertler, 2003; Tojima et al., 2007; Zhang and Forscher, 2009; Wada et al., 2016). A morphological hallmark of the peripheral zone is the presence of filopodia and lamellipodia (Fig. 1.1), which bestow the growth cone with its characteristic 'hand-like' appearance (Mueller, 1999). Filopodia are antennae-like projections comprised of actin bundles and dynamic microtubules that have extended from the central zone (Welnhofer et al., 1999; Buck and Zheng, 2002; Dent et al., 2011). In contrast, lamellipodia are sheet-like membranous structures that bridge the spaces between extending filopodia, containing an actin meshwork with few microtubules (Forscher and Smith, 1988; Krause and Gautreau, 2014). Filopodia and lamellipodia are dynamic structures that are constantly projecting and retracting to sample the environment for guidance signals, which is dictated by changes in the actin and microtubule cytoskeletons.

1.2.2 Growth cone motility

Growth cone motility is informed by filopodial and lamellipodial dynamics, which in turn are regulated by the remodeling of actin filaments and microtubules that comprise the growth cone cytoskeleton (Sabry et al., 1991; Williamson et al., 1996; Welnhofer et al., 1999; Schaefer et al., 2008; Ketschek et al., 2016). Growth cone protrusion is biased towards stabilised areas of the growth cone (Tosney and Landmesser, 1985; Buck and Zheng, 2002). This occurs in three stages: projection and stabilisation of filopodia and lamellipodia; infiltration of microtubules and organelles from the central zone into the stabilised periphery; and consolidation of directed motility by advancement of the central zone and axon shaft in the direction of the stabilised side of the growth cone [for reviews see (Gomez and Spitzer, 2000; Henley et al., 2004; Chilton, 2006; Zheng and Poo, 2007; Dent et al., 2011)]. Hence, attractive guidance cues promote the stabilisation of actin and microtubules, while repulsive guidance cues induce destabilisation of actin and microtubules.

Remodeling of the actin cytoskeleton is crucial for the dynamic motility of filopodia and lamellipodia (O'Connor and Bentley, 1993; Suter and Forscher, 2001; Dent et al., 2011). Filopodia and lamellipodia are primarily comprised of filamentous actin (F-actin), which conforms to two configurations within the growth cone: F-actin bundles and randomly

linked F-actin networks (Lewis and Bridgman, 1992; Lin and Forscher, 1995; Welnhofer et al., 1999; Schaefer et al., 2002; Zhou et al., 2002). F-actin bundles are principally found within filopodia, with the barbed or plus-end of the F-actin bundle directed towards the projecting tip of the filopodium (Gordon-Weeks, 1987; Forscher and Smith, 1988; Welnhofer et al., 1999; Zhou et al., 2002). In contrast, random F-actin networks are the predominant form of F-actin in lamellipodia, which facilitates the spreading and extension of membrane between filopodia (Forscher and Smith, 1988; Sobue, 1993; Krause and Gautreau, 2014). Actin filament assembly, which occurs by the addition of globular actin monomers (G-actin) to the barbed end of the actin filament, provides protrusion forces to the growth cone (Strasser et al., 2004; Hyland et al., 2014), leading to projection of the filopodia and lamellipodia (Mallavarapu and Mitchison, 1999). F-actin assembly is balanced by constant retrograde flow of actin (Lin and Forscher, 1995; Medeiros et al., 2006; Burnette et al., 2008), which provides traction forces to promote growth cone extension (Schaefer et al., 2008; Craig et al., 2012). Hence, the rate of actin polymerisation must exceed the rate of retrograde actin flow for the growth cone to extend (Lin and Forscher, 1995; Suter and Forscher, 2001). Accordingly, F-actin accumulation is observed at the leading edge of growth cones during directed motility, and denotes the direction of axon outgrowth (Marsick et al., 2010). Once actin remodeling has informed the direction of axon outgrowth, projection and stabilisation of microtubules is required to potentiate axon outgrowth.

Although the peripheral zone is relatively devoid of microtubules when compared with the central domain, extension and stabilisation of dynamic microtubules into the peripheral zone (in particular into filopodia) plays a vital role in facilitating growth cone motility (Forscher and Smith, 1988; Tanaka and Kirschner, 1995; Buck and Zheng, 2002; Dent and Gertler, 2003; Dent et al., 2011; Kahn and Baas, 2016). Although actin remodeling is considered to be the first action of growth cone motility (Sobue, 1993), it has been demonstrated that stabilisation of microtubules within the peripheral domain is sufficient to cause directed growth cone motility (Buck and Zheng, 2002), implying that microtubule stabilisation is an instructive signal for growth cone motility. In addition to providing structural support to filopodia, microtubule extension into the peripheral zone also enables ER, mitochondria and vesicles to be transported towards the leading edge of the growth cone, which in turn facilitates advancing growth cone motility (Forscher et al., 1987; Dailey and Bridgman, 1989; Tojima et al., 2007; Zhang and Forscher, 2009).

Hence, a model of axon outgrowth has been proposed in which asymmetric stabilisation of F-actin and microtubules within the peripheral zone leads to a biasing of growth cone motility in the direction of the stabilised filopodia and lamellipodia [for reviews see (Dickson, 2002; Chilton, 2006; Dent et al., 2011)]. While much has been discovered regarding the regulation of growth cone motility by actin and microtubule dynamics, the intracellular signaling pathways by which environmental guidance cues are transduced into cytoskeletal remodeling remain to be fully elucidated.

1.3 Axon pathfinding is regulated by intracellular signaling molecules

Growth cones navigate by sensing and responding to guidance cues to steer axons towards their final targets. To date, numerous guidance cue protein families have been discovered including netrins, semaphorins, ephrins, slits; while the neurotrophins [including brain-derived neurotrophic factors (BDNF), nerve growth factor (NGF), and fibroblast growth factors (FGF)], and morphogens [including bone morphogenic protein (BMP), sonic hedgehog (Shh) and Wnts] have also been shown to act as guidance cues (Gallo et al., 1997; Song and Poo, 1999; Wen et al., 2007; Killeen and Sybingco, 2008). Guidance cues are divided into soluble or contact-mediated attractants or repellants (Bastiani et al., 1984; Raper et al., 1984; Fambrough and Goodman, 1996), and further categorised based on their calcium-dependent or calcium-independent mechanism of action [reviewed in (Tessier-Lavigne and Goodman, 1996; Song and Poo, 1999; Dickson, 2002)]. Guidance cues act via intracellular signaling pathways that converge on the microtubule and actin cytoskeleton to inform motile responses, with cyclic nucleotides and calcium known to be key regulators of the intracellular signaling (Dickson, 2002; Henley et al., 2004; Zheng and Poo, 2007; Dent et al., 2011; Sutherland and Goodhill, 2013). Although much has been discovered regarding the importance of calcium and cyclic nucleotides as signaling molecules that control growth cone motility, the mechanisms that regulate these intracellular signaling pathways are not fully understood.

To ensure the precision of axon pathfinding, guidance cues not only elicit motile responses in appropriate axons at specific locations, but also act at distinct developmental times, otherwise axon pathfinding is perturbed (Vitriol and Zheng, 2012; Goodhill, 2016). Accordingly, complex regulatory mechanisms exist to control the response of an axon to each guidance cue. The repertoire of guidance cue receptors expressed by a growth cone

Figure 1.1: Illustration of an axonal growth cone.

The growth cone is comprised of two structurally distinct regions: the central zone located at the distal end of the axon shaft, and the peripheral zone with its numerous projecting filopodia interspersed with membranous lamellipodia (the boundary between the central and peripheral zones is demarcated by a dashed line). Filopodia contain F-actin bundles and projecting microtubules, while lamellipodia are formed by a meshwork of F-actin.

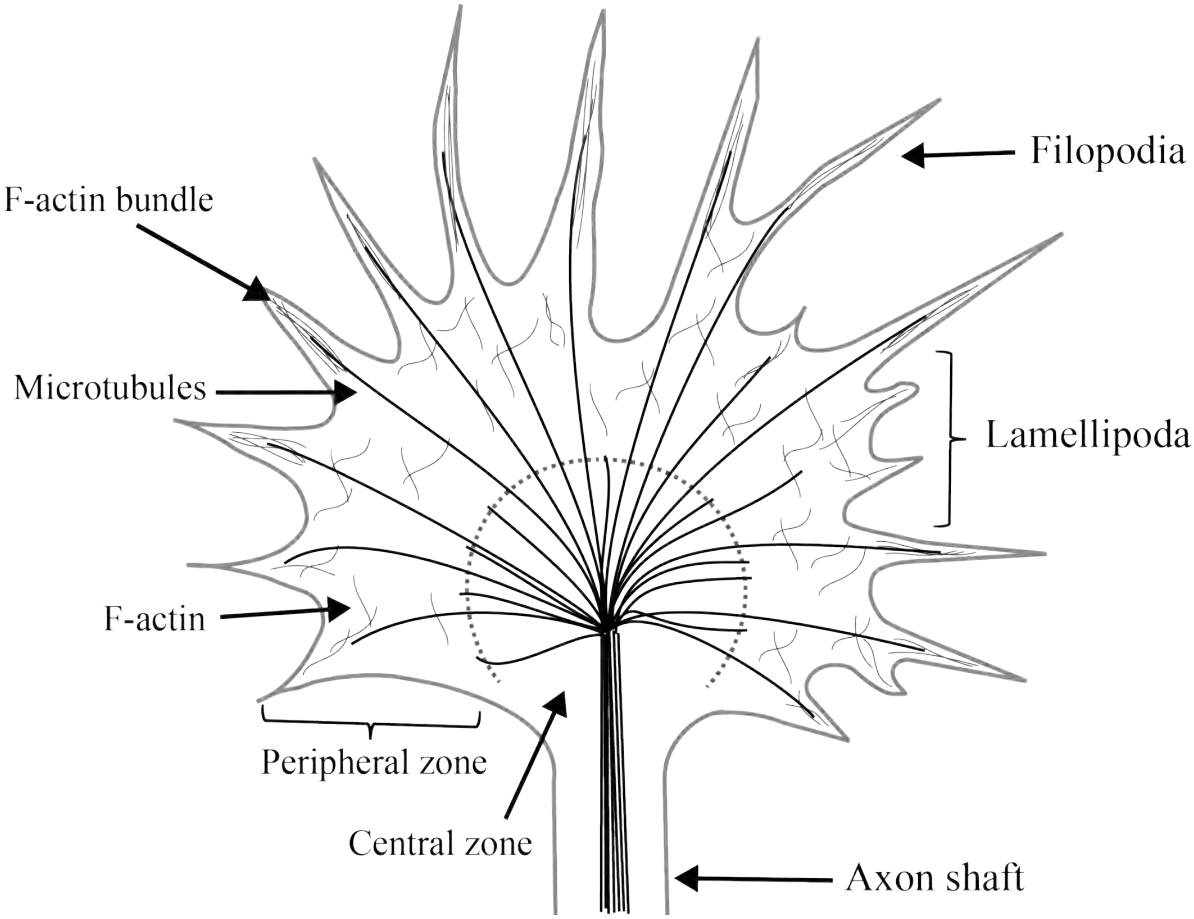
Filopodia
F-actin bundle
Microtubules
Lamellipoda
F-actin
Peripheral zone
Central zone
Axon shaft

is key for determining whether a guidance cue influences axon pathfinding (Stein and Tessier-Lavigne, 2001; Hanson and Landmesser, 2004; Sato-Maeda et al., 2006). For example, motor neurons exiting the mouse spinal cord encounter a proximal choice point that triggers axons from the medial motor column to turn and extend dorsally, but has no effect on the outgrowth of axons from the hypaxial and lateral motor columns that continue to extend ventrally (Bonanomi and Pfaff, 2010).

Selective expression of the ephrin-A receptors EphA3 and EphA4 by axons of the medial motor column, is thought to underlie the high selectivity of this EphrinA expressing choice point (Shirasaki et al., 2006; Gallarda et al., 2008), illustrating how gudaince cue receptor expression can control axon pathfinding descisions. However, regulating axon pathfinding by manipulating receptor expression can be more complex than simply expressing or not expressing a guidance cue receptor, with individual guidance cues capable of eliciting both attraction or repulsion depending on the stage of axon outgrowth (Brose et al., 1999; Stein and Tessier-Lavigne, 2001; Lieberam et al., 2005; Sato-Maeda et al., 2006; Hernandez-Fleming et al., 2017). This phenomenon is vital for axon guidance decisions that occur at intermediate targets where axons grow towards, and then away from, a certain point in space and time. The classic example is midline crossing by commissural interneuron axons at the floor plate, where growth cones of commissural axons are initially attracted to the midline by netrin-1, while remaining insensitive to repulsive cues such as slit and semaphorin3a (sema3a) (Kennedy et al., 1994; Serafini et al., 1994; 1996; Brose et al., 1999; Niclou et al., 2000; Stein and Tessier-Lavigne, 2001). However, once the growth cone reaches the midline, slit binding to its receptor roundabout (Robo) silences netrin-1 mediated attraction, with slit/sema3a triggering repulsion of the commissural axon away from the midline, preventing recrossing (Stein and Tessier-Lavigne, 2001). Intermediate targets can also express guidance cues at certain developmental stages and therefore the timing of when a growth cone reaches the intermediate target, as well as the timing of guidance cues expression by the intermediate target, can regulate the behaviour of navigating axons (Lauderdale et al., 1997; Sato-Maeda et al., 2006; Bonanomi and Pfaff, 2010; Tedeschi et al., 2016). Finally, as guidance cues ultimately act on the cytoskeleton to regulate growth cone motility, the intracellular signaling pathways activated downstream of guidance cue receptor activation are key determinants of axon pathfinding (Kaplan et al., 2013; Sutherland and Goodhill, 2013; Averaimo and Nicol, 2014). Two key signaling molecules known to be

responsible for transducing guidance signals into changes in the cytoskeleton are calcium and the cyclic nucleotides.

1.3.1 Cyclic nucleotides as regulators of axon pathfinding

Cyclic nucleotides are signaling molecules that play a crucial role in the regulation of axon guidance (Lohof et al., 1992; Ming et al., 1997; Song et al., 1997; Song and Poo, 1999; Nishiyama et al., 2003; Averaimo and Nicol, 2014). Cyclic nucleotides are generated by enzymatic degradation of adenosine triphosphate (ATP) and guanosine triphosphate (GTP) to cyclic adenosine monophosphate (cAMP) and cyclic guanosine monophosphate (cGMP) respectively (Defer et al., 2000; Padayatti et al., 2004). Cyclic nucleotides regulate growth cone attraction and repulsion in a manner that depends on the ratio of cAMP to cGMP (Lohof et al., 1992; Ming et al., 1997; Song et al., 1997; Tojima et al., 2009; Shelly et al., 2010). In principle, a higher level of cAMP compared to cGMP promotes growth cone attraction via the activation of protein kinase A (PKA), whilst a higher level of cGMP compared to cAMP induces growth cone repulsion via activation of protein kinase G (PKG) (Song et al., 1997; Song and Poo, 1999; Nishiyama et al., 2003; Shelly et al., 2010; Nicol et al., 2011; Averaimo and Nicol, 2014). By activating PKA and PKG, cyclic nucleotides regulate intracellular calcium signaling to impact growth cone motility [for reviews see (Tojima et al., 2011; Sutherland and Goodhill, 2013; Averaimo and Nicol, 2014)], and therefore will be discuused in terms of their interactions with the calcium signaling pathway.

1.3.2 Calcium as a regulator of axon guidance

Calcium is a key second messenger molecule in all cells, and a major function of calcium signaling is to communicate receptor activation to intracellular effector proteins that, in turn, elicit cellular responses (Berridge, 1998; Berridge et al., 2003). Calcium has long been implicated in the regulation of axon pathfinding (Gundersen and Barrett, 1980). It is believed that calcium signaling has dual functions in the regulation of axon pathfinding, with global calcium signals regulating the rate of axon extension, and localised calcium signals regulating ‘steering’ of the growth cone and therefore the direction of axon

outgrowth (Spitzer, 2006; Zheng and Poo, 2007; Averaimo and Nicol, 2014). Hence, mechanisms that regulate the spatial and temporal localisation of calcium signaling are believed to be vital for controlling axon pathfinding. To understand how calcium signals are regulated in space and time, it is important to understand the types of calcium signals observed in neurons.

1.3.3 Precise patterns of calcium signaling are expressed in neurons

Calcium signaling is crucial for correct nervous system development, with precise patterns of calcium signaling shown to regulate proliferation and differentiation, cell type specification, cell motility, axon pathfinding, as well as neurotransmitter specification and synaptogenesis (Gu et al., 1994; Komuro and Rakic, 1996; Owens and Kriegstein, 1998; Gomez and Spitzer, 1999; Blankenship and Feller, 2009; Kirkby et al., 2013). Patterns of calcium signaling observed include waves, spikes, puffs and sparks, which differ in their spatial and temporal properties, as well as the cellular processes that they mediate (Zheng and Poo, 2007; Rosenberg and Spitzer, 2011; Ross, 2012; Miyazaki and Ross, 2013).

Calcium waves are sustained, regenerative rises in intracellular calcium that propagate within a cell, or group of cells (Gu et al., 1994; Charles et al., 1996; Garaschuk et al., 2000; Lautermilch and Spitzer, 2000; Weissman et al., 2004; Ross, 2012). Calcium waves conform to a classical model of signaling (Bootman and Berridge, 1995), whereby an exogenous signal triggers calcium release from the ER to elevate intracellular calcium, which is subsequently amplified by further release of calcium from the ER (Clapham, 1995; Berridge, 1998; Weissman et al., 2004; Ross, 2012). As such, calcium waves begin as localised events, but propagate through the cell by sequential release of calcium from the ER, and are therefore confined by the diffusion limit of calcium within the cytosol and the spatial localisation of ER calcium release channels (Berridge, 2006; Rizzuto and Pozzan, 2006; Pani and Singh, 2009; Yang et al., 2010).

Calcium waves regulate cell proliferation and differentiation, as well as gene expression (Spitzer et al., 1994; Gu and Spitzer, 1995; Owens and Kriegstein, 1998; Jessell, 2000; Weissman et al., 2004; Bonanomi and Pfaff, 2010), suggesting that calcium waves are

responsible for long-term changes in neuronal function. Consistent with this hypothesis, gap junctions permit calcium waves to propagate between cells (Charles et al., 1996; Weissman et al., 2004; Jang et al., 2017). In this way, waves can synchronize activity between adjacent cells to orchestrate cell division, cell fate determination, as well as cell motility during nervous system development (Charles et al., 1996; Garaschuk et al., 2000; Jessell, 2000; Montoro and Yuste, 2004; Weissman et al., 2004; Bonanomi and Pfaff, 2010).

Similar to waves, calcium spikes are global calcium transients that are propagated within the cell by the sequential release of calcium form the ER (Meyer and Stryer, 1991; Gu et al., 1994; Rosenberg and Spitzer, 2011). However, spikes differ from waves in terms of the kinetics of the calcium transient (Spitzer and Gu, 1997; Rosenberg and Spitzer, 2011). While waves are slow and persist in the order of a minute, spikes are more rapid, lasting only a few seconds (Gu et al., 1994; Rosenberg and Spitzer, 2011). Spikes regulate axon pathfinding, neurotransmitter specification, and are therefore crucial for the wiring of neuronal circuits (Gomez et al., 1995; Feller, 1999; Gomez and Spitzer, 1999; Borodinsky et al., 2004; Kirkby et al., 2013; Plazas et al., 2013; Borodinsky et al., 2014).

Unlike spikes and waves, puffs and sparks are highly localised calcium transients that occur within subcellular compartments or microdomains (Bootman et al., 2001; Tovey et al., 2001; Ouyang et al., 2005; Berridge, 2006; Miyazaki and Ross, 2013). Sparks and puffs result from the activation of individual, or small numbers of ER calcium release channels (Brown and Griffith, 1983; Satin and Adams, 1987; Bootman and Berridge, 1995; Berridge, 1998; Tovey et al., 2001). Given that sparks and puffs occur in discrete sub-cellular compartments, they are thought to regulate spatially localised events such as synaptic remodeling (Mattson et al., 2000; Miyazaki and Ross, 2013; Chen et al., 2015), steering in cell motility (Laude and Simpson, 2009; Wei et al., 2009), as well as filopodial motility and growth cone turning (Lau et al., 1999; Gomez et al., 2001; Robles et al., 2003; Akiyama et al., 2009; Shim et al., 2013). Hence, by shaping calcium signals in space and time, neurons can activate distinct cellular processes, all of which are required for nervous system development.

Although the past two decades has seen an explosion in our understanding of the importance of precise patterns of calcium signaling for nervous system development

(Rosenberg and Spitzer, 2011; Toth et al., 2016), the molecular mechanisms responsible for the spatiotemporal control of calcium signaling in neurons remains to be fully elucidated. Given the exquisite correlation between distinct spatial and temporal patterns of calcium signaling and the motile behaviours expressed by navigating growth cones (Gomez and Spitzer, 1999; Zheng, 2000; Wen et al., 2004b), calcium signaling during axon pathfinding represents a good model to investigate the molecular mechanisms that regulate nervous system development.

1.3.4 Global calcium signals regulate axon extension

The calcium "set point" theory is a prevailing hypothesis for describing the regulation of axon extension by calcium. The set point theory suggests that axon outgrowth occurs over a narrow range of intracellular calcium concentration, with fluctuations above or below this set-point causing axons to accelerate, slow, pause or collapse (Kater and Mills, 1991; Fields et al., 1993; Gomez and Spitzer, 2000; Zheng, 2000; Henley et al., 2004; Wen et al., 2004b; Zheng and Poo, 2007; Sutherland et al., 2014). Growth cones generate spontaneous calcium transients *in vitro* and *in vivo*, and these transients modulate the rate of axon extension in a frequency-dependent manner (Gomez et al., 1995; Gomez and Spitzer, 1999; Tang and Kalil, 2005; Hutchins and Kalil, 2008). The frequency of spontaneous calcium transients is inversely related to the rate of axon outgrowth, with high frequency calcium transients causing axons to slow down and pause at intermediate targets (Gomez and Spitzer, 1999; Plazas et al., 2013), while growth cones expressing low frequency calcium transients exhibit accelerated axon extension (Gomez and Spitzer, 1999; Tang et al., 2003; Plazas et al., 2013). By maintaining a set-point for calcium, calcium-dependent effector proteins are able to discriminate between subtle differences in the change in concentration of intracellular calcium that occur with calcium oscillations (Tomida et al., 2003). Calcium/calmodulin-dependent protein kinase II (CaMKII) is activated by large amplitude increases in calcium, and as such is thought to act as a spike frequency detector (Malinow et al., 1989; Deisseroth et al., 1995; De Koninck and Schulman, 1998; Hudmon and Schulman, 2002). CaMKII has been shown to be activated by sustained increases in intracellular calcium that occur with higher frequency calcium transients resulting in axon branching, filopodial formation, and promotes filopodial dynamics (Borodinsky et al., 2003; Fink et al., 2003; Tang et al., 2003). Accordingly,

CaMKII is activated in growth cones that exhibit an increased frequency of calcium transients, with CaMKII activity correlating with larger, more complex growth cones (Tang et al., 2003), slowing axon extension and increasing the time spent sampling the local environment and slowing axon outgrowth (Ren and Suter, 2016). In contrast, lower frequency calcium transients activate the phosphatase calcineurin (CaN), which is activated by lower amplitude calcium signals and opposes the actions of CaMKII, leading to a less complex growth cone and increased axon extension (Lautermilch and Spitzer, 2000). Therefore, precise patterns of calcium signaling have distinct effects on axon outgrowth. Accordingly, increasing or decreasing the frequency of calcium transients in a navigating axons results in errors in axon pathfinding *in vivo* (Shim et al., 2005; Plazas et al., 2013), which illustrates the importance of precise patterns of calcium signaling for axon pathfinding. While global changes in intracellular calcium are crucial for mediating rates of axon outgrowth, the direction of growth cone motility is dependent on spatially localised calcium transients (Zheng, 2000; Wen et al., 2004b; Nicol et al., 2011).

1.3.5 Localised calcium signals regulate growth cone motility

Growth cone motility is biased in the direction of the stabilised filopodia and therefore signals that cause asymmetric stabilisation or destabilisation of the actin and microtubule cytoskeletons within the growth cone will induce a growth cone turning response (Dickson, 2002; Chilton, 2006; Dent et al., 2011). Calcium has been shown to mediate growth cone motility both towards (attraction) and away from (repulsion) a source of guidance cue, with the concentration of intracellular calcium highest on the side of the growth cone nearest to the source of guidance cue, irrespective of whether the guidance cue causes attraction or repulsion (Zheng, 2000; Henley et al., 2004; Tojima et al., 2011; Sutherland et al., 2014). Therefore, regulatory mechanisms must exist to differentiate between attractive and repulsive calcium signals, with the spatiotemporal localisation of calcium signaling proposed to be a key factor in determining growth cone motility in response to calcium signaling (Tojima et al., 2011).

The significance of spatially and temporally localised calcium signals for growth cone turning was elegantly demonstrated by the use of focal laser-induced photolysis (FLIP) to increase intracellular calcium concentration in a spatially restricted manner in *Xenopus*

growth cones (Zheng, 2000). In this study, a spatially localised calcium signal on one side of the growth cone was shown to be sufficient to induce attractive growth cone turning in the direction of the elevated intracellular calcium (Zheng, 2000). However, when the same experiment was conducted in zero extracellular calcium (which decreases intracellular calcium), the turning response to the same focal increase in intracellular calcium was switched to repulsion (Zheng, 2000), suggesting that both the spatial localisation and the magnitude of the calcium signal together determine whether calcium induces attraction or repulsion. Consistent with this hypothesis, the attractive guidance cue netrin-1 induced a large, asymmetric calcium signaling on the turning side of the growth cone (Hong et al., 2000). However, when calcium influx or calcium release from internal stores is inhibited prior to the application of netrin-1, the turning response was switched from attraction to repulsion (Hong et al., 2000). Moreover, the repulsive guidance cue myelin associated glycoproteins (MAG) induces a small calcium signal that induces turning away from the source of MAG (Henley et al., 2004). Together, these results provided crucial evidence that localised calcium signals are sufficient to cause both attraction and repulsion, and that the spatiotemporal dynamics of the calcium signal determine the polarity of the growth cone turning response. Hence, a model of growth cone turning has been proposed whereby spatially restricted, larger amplitude calcium signals promote growth cone turning towards the calcium signal, and spatially restricted, small amplitude calcium signals promote growth cone turning away from the calcium signal (Henley and Poo, 2004; Gomez and Zheng, 2006; Zheng and Poo, 2007). However, it remained to be determined how these precise spatiotemporal patterns of calcium signaling are transduced into distinct motile responses.

The microtubules of the growth cone cytoskeleton are key downstream targets of guidance cue mediated calcium signaling, with microtubule stabilisation and extension biasing growth cone motility in the direction of stabilised microtubules (Dent et al., 2011). Microtubules are constantly growing and shrinking as tubulin molecules are added or removed from the plus-end in a process termed ‘dynamic instability’ (Kirschner and Mitchson, 1986). The extension and stabilisation of microtubules is promoted by the activation of CaMKII (Goto et al., 1985; Yamamoto et al., 1985), and activation of CaMKII is required for attraction in response to guidance cues such as acetylcholine (Zheng et al., 1994; Wen et al., 2004b). In contrast, CaN opposes CaMKII activity and is associated with microtubule destabilisation (Goto et al., 1985; Yamamoto et al., 1985),

and growth cone repulsion (Chang et al., 1995; Wen et al., 2004b). Together, these studies suggest that CaN or CaMKII are activated upstream of microtubule stabilsaiton/destabilsation to control the direction of growth cone turning.

Evidence for a CaN-CaMKII switch in the growth cone was provided by an investigation of calcium-mediated growth cone turning in *Xenopus* spinal neurons (Wen et al., 2004b). In this study, FLIP was used to induce a localised calcium signal that is sufficient to induce growth cone attraction as previously reported (Zheng, 2000). When CaMKII was inhibited, FLIP-mediated attractive growth cone turning was abolished (Wen et al., 2004b), suggesting that CaMKII is required for growth cone attraction mediated in response to a localised larger amplitude calcium signals. However, when FLIP was used to cause growth cone repulsion in calcium-depleted conditions (Zheng, 2000), inhibition of CaN caused growth cone repulsion to be switched to attraction (Wen et al., 2004b). To determine if this switch to attraction is caused by CaMKII being activated when CaN is inhibited, CaMKII and CaN were inhibited concurrently. When CaMKII and CaN were both inhibited, growth cone turning in response to a localised calcium signal was abolished (Wen et al., 2004b). A mathematical model describing the relationship between CaMKII and CaN during growth cone turning was recently published by Forbes and colleagues (Forbes et al., 2012). This model describes how the higher affinity that CaN has for calcium-calmodulin binding compared to CaMKII leads to a preferential activation of CaN at lower calcium concentrations, whereas CaMKII is predominantly activated at higher calcium concentrations (Forbes et al., 2012). These studies illustrate the importance of precise spatial and temporal localisation of calcium signaling for the regulation of growth cone motility, and describe a mechanism by which distinct patterns of calcium signaling differentially signal to the growth cone cytoskeleton. However, regulation of growth cone motility by the CaN-CaMKII switch in response to distinct calcium signals does not fully explain how precise patterns of calcium signaling control growth cone motility.

In addition to the asymmetric stabilisation of the cytoskeleton, growth cone turning also relies on shifts in the balance between endocytosis and exocytosis. The repulsive guidance cues sema3A and myelin associated glycoprotein (MAG) trigger a localised low amplitude calcium signals (Henley et al., 2004; Togashi et al., 2008), as well as inducing clatherin-mediated endocytosis via β1-integrin internalisation (Carlstrom et al., 2010;

Hines et al., 2010). These data suggest that focal small amplitude calcium signals and localised endocytosis act together to trigger growth cone repulsion. In contrast, larger amplitude calcium signals promote microtubule-based trafficking of vesicle-associated membrane protein 2 (VAMP2) positive vesicles to the turning side of the growth cone, leading to VAMP2-dependent exocytosis (Tojima et al., 2007; Akiyama and Kamiguchi, 2013; Ros et al., 2015; Wada et al., 2016). Given that VAMP2-mediated exocytosis is reported to regulate insertion of guidance cue receptors into the plasma membrane (Singh et al., 2004; Tojima et al., 2007; Araki et al., 2010), these findings suggest that asymmetric trafficking and insertion of vesicles increases the sensitivity of the turning side of the growth cone to guidance cues, facilitating growth cone turning. In addition, CaMKII activates cyclin-dependent kinase 5 (Cdk5), which in turn inhibits clatherin-mediated endocytosis, inhibiting repulsion (Tojima et al., 2014). Hence, localised large amplitude calcium signals both promote attraction and inhibit repulsion. These studies illustrate how distinct spatial and temporal patterns of calcium signaling determine the polarity of growth cone motility by modulating microtubule stabilisation and membrane dynamics. Taken together, these studies inform a model of growth cone motility whereby distinct spatial and temporal patterns of calcium signaling regulate attraction versus repulsion (Fig. 1.2). While these studies highlight the importance of spatial and temporal patterns of calcium signaling for the regulation of growth cone motility, the mechanisms responsible for regulating the spatial and temporal localisation of calcium during growth cone motility remain to be fully elucidated.

One mechanism by which growth cones may control the spatial regulation of calcium signaling is to regulate ER remodeling within the growth cone. Rac is a small calcium-dependent G-protein, and activation of Rac triggers microtubule extension into the periphery of the growth cone (Jin et al., 2005; Zhang and Forscher, 2009; Dent et al., 2011). Rac-dependent microtubule extension is required for remodeling of the ER towards the leading edge of the growth cone (Zhang and Forscher, 2009). Given that the ER is a large intracellular pool of calcium that is released to generate calcium signals in response to guidance cues (Li et al., 2005; Akiyama et al., 2009; Gasperini et al., 2009; Sutherland et al., 2014), these findings suggested that ER remodeling to the leading edge of the growth cone is a regulatory mechanism for the localisation of sustained elevations in calcium within the growth cone.

1.4 Mechanisms of calcium influx and release in the growth cone

Given that precise patterns of calcium signaling determine the direction of growth cone motility, it is important to understand how distinct spatiotemporal patterns of calcium are produced. Calcium signals are shaped by the influx of extracellular calcium and the release of calcium from internal stores, with each calcium signal being the product of the calcium influx and release mechanism that contribute to the calcium signal. Hence, it has been hypothesised that guidance cues produce distinct calcium signals according to the source of calcium used to generate the calcium signal (Tojima et al., 2011). Calcium influx and release mechanisms of importance for growth cone motility include calcium influx via transient receptor potential (TRP) channels and voltage-dependent calcium channels (VDCC), release of stored calcium from the ER, as well as calcium influx via store-operated calcium entry (SOCE).

1.4.1 Mechanisms of calcium influx: TRP channels

TRP channels are a family of non-selective cation channels that trigger sustained calcium influx into the cell (Kennedy et al., 1994; Serafini et al., 1994; 1996; Brose et al., 1999; Niclou et al., 2000; Stein and Tessier-Lavigne, 2001; Ramsey et al., 2006). Mammalian TRP channels includes 6 sub-families, which are further divided into channel subtype [for reviews see (Ramsey et al., 2006; Nilius and Owsianik, 2011)]. Although many TRP family members are expressed in growth cones (Goswami et al., 2007; Goswami, 2010; Shibasaki et al., 2010; Kerstein et al., 2015), the best evidence for the requirement of TRP channels for growth cone motility exists for TRPC (canonical) channels (Greka et al., 2003; Li et al., 2005; Wang and Poo, 2005; Shim et al., 2013).

Calcium entry via TRPC channels is crucial for growth cone motility, with calcium influx via TRPC channels mediating growth cone attraction in response to BDNF, netrin-1 and glutamate (Li et al., 1999; Kim et al., 2003; Li et al., 2005; Wang and Poo, 2005), as well as repulsion in response to myelin-associated glycoprotein (MAG) (Shim et al., 2005).

Figure 1.2: The spatial and temporal properties of calcium signaling determines the polarity of growth cone motility.

In response to a repulsive guidance cue, a smaller amplitude calcium signal on the side of the growth cone facing towards the source of guidance cue activates calcineurin (CaN) in preference to calcium/calmodulin-dependent kinase II (CaMKII), which promotes destabilisation of the microtubule cytoskeleton and, hence, growth cone repulsion. Repulsive guidance cues also promote clatherin-mediated endocytosis. In contrast, attractive guidance cues elicit a larger amplitude calcium on the side of the growth cone facing towards the source of guidance cue. This larger amplitude calcium signal activates CaMKII in preference to calcineurin CaN, which promotes extension and stabilisation of microtubules to the turning side of the growth cone. In addition, larger amplitude calcium signal promotes the trafficking of VAMP2-coated vesicles to the turning side of the growth cone, with VAMP2-mediated exocytosis increases the sensitivity of the turning side of the growth cone to attractive guidance cues via the insertion of additional guidance cue receptors into the plasma membrane.

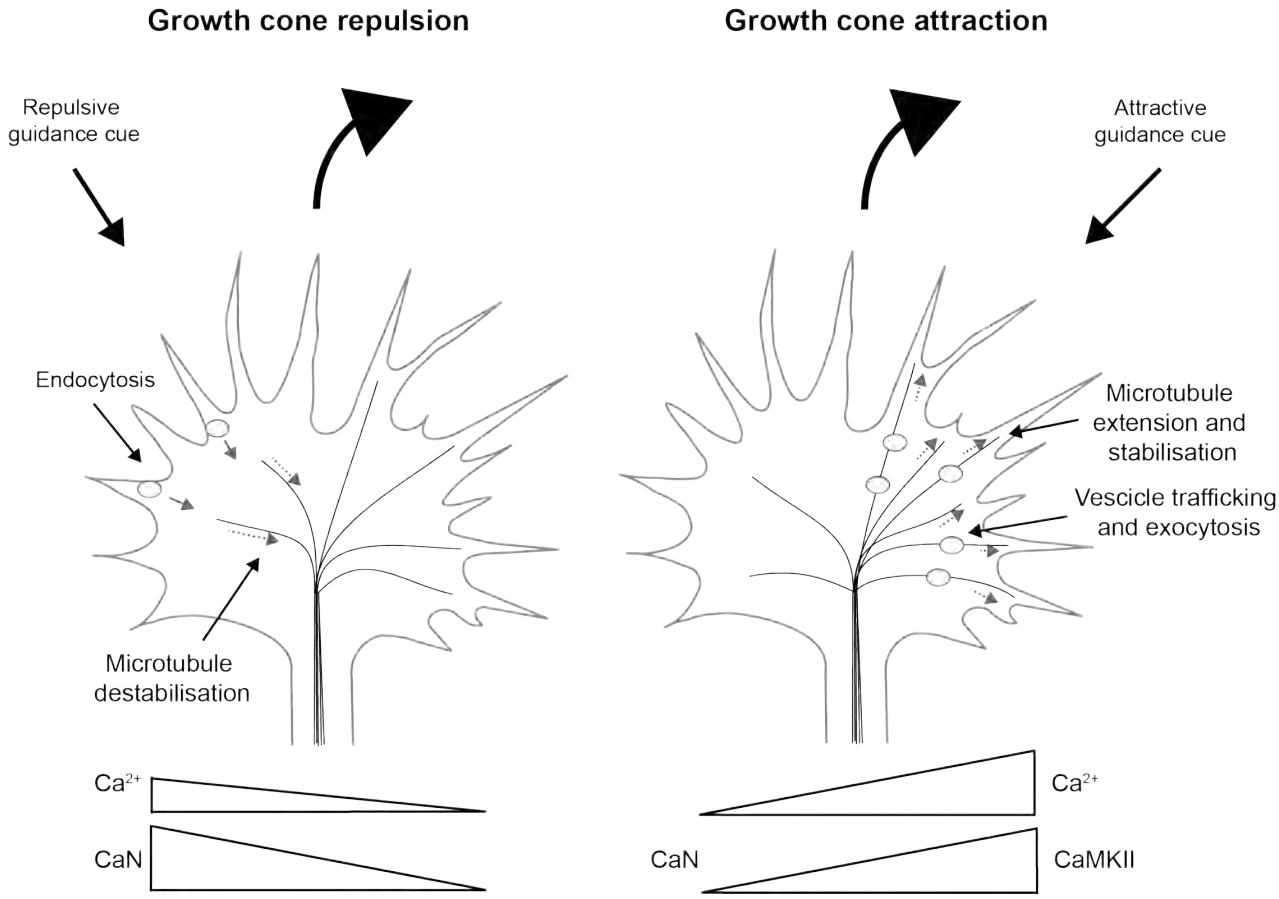
Growth cone repulsion
Growth cone attraction
Repulsive guidance cue
Attractive guidance cue
Endocytosis
Microtubule destabilisation
Microtubule extension and stabilisation
Vescicle trafficking and exocytosis
Ca2+
CaN
Ca2+
CaN
CaMKII

Therefore, calcium influx via TRPC channels can regulate both attraction and repulsion. When TRPC channels are inhibited, growth cone turning towards BDNF and netrin-1 is abolished (Li et al., 2005; Shim et al., 2005; Wang and Poo, 2005), suggesting that calcium influx via TRPC channels is important for the generation of large amplitude calcium signals associated with growth cone attraction. Receptor stimulation by BDNF and netrin-1 triggers asymmetric phosphoinositide-3-kinase (PI3K)-dependent production of PIP_3 within the growth cone (Li et al., 2005; Henle et al., 2011). This localised production of PIP_3 causes activation of the Akt (protein kinase B), which in turn phosphorylates and activates TRPC channels to cause localised calcium influx (Li et al., 2005; Henle et al., 2011). These findings suggest that calcium influx in response to BDNF and netrin-1 is mediated by TRPC channel opening, which is regulated by a PI3K-PIP_3-Akt pathway (Fig.1.3).

Inhibition of TRPC channels also abolishes growth cone repulsion away from MAG (Shim et al., 2005). Although evidence suggests that MAG interacts with β1-integrin to stimulate asymmetric endocytosis and growth cone repulsion (Goh et al., 2008; Hines et al., 2010; Tojima et al., 2010), MAG is also reported to cause a low amplitude rise in intracellular calcium on the side of the growth cone facing the source of guidance cue (Henley et al., 2004). Although this small rise in intracellular calcium has been attributed to calcium release from the ER (Henley et al., 2004), extracellular calcium is required for MAG induced repulsion (Song et al., 1998), and inhibition of TRPC channels abolishes MAG-dependent growth cone repulsion (Shim et al., 2005). Therefore, these studies suggest that calcium entry via TRPC channels is important for MAG induced repulsion, however the mechanisms that underlie this process remain to be fully elucidated. It should also be noted that not all guidance cues activate TRPC channels. A reduction of TRPC channel expression has no effect on growth cone repulsion to sema-3a (Shim et al., 2005), consistent with previous findings that sema-3a induces a small influx of calcium via cyclic nucleotide gated (CNG) channels, but not via TRPC channels (Togashi et al., 2008). These studies confirm the importance of calcium influx via TRPC channels for correct growth cone motility, however they also illustrate the complexity of calcium signaling. Given that calcium influx via TRPC channels is implicated in growth cone repulsion (Shim et al., 2005), it is predicted that calcium influx via TRPC channels alone is insufficient to generate the large amplitude calcium signals required for growth cone

attraction. Consistent with this prediction, calcium entry via TRPC channels is believed to activate further calcium influx via L-type VDCC.

1.4.2 Mechanisms of calcium influx: voltage-dependent calcium channels

VDCC have been reported to regulate axon outgrowth, however their role in steering growth cones in response to guidance cues remains controversial. Numerous VDCC subtypes are expressed in growth cones, including N-, L-, P- and T-type VDCC (Fox et al., 1987; Bean, 1989); with L-type VDCC the most extensively studied subtype in growth cone guidance (Gomez et al., 1995; 2001; Tang et al., 2003). Studies conducted in *Xenopus* spinal neurons have demonstrated that calcium influx via L-type VDCC is required for growth cone attraction in response to netrin-1 (Hong et al., 2000; Nishiyama et al., 2003). In *Xenopus* growth cones, netrin-1 stimulates an increase in the amplitude of VDCC-dependent calcium currents, which is blocked by the inhibition of L-type VDCC (Nishiyama et al., 2003). These findings confirmed results from a previous study which showed that L-type VDCC are required for netrin-1 induced elevations in intracellular calcium in *Xenopus* growth cones (Hong et al., 2000). Interestingly, inhibition of L-type VDCC was shown to convert netrin-1 induced attraction into repulsion (Hong et al., 2000). Given that L-type VDCC are reported to be activated downstream of TRPC channel activation in *Xenopus* spinal neurons (Wang and Poo, 2005), these findings inform a model of calcium signaling whereby guidance cues firstly activate calcium entry via TRPC, with increased intracellular calcium triggering a further influx of calcium via L-type VDCC that induces attractive growth cone turning downstream of CaMKII activation (Fig. 1.3). Hence, when L-type VDCC channels are inhibited, TRPC channels still trigger an influx of calcium, but there is no amplification of this calcium signal. As such, the small calcium signal induced by netrin-1 results in growth cone repulsion, presumably via the activation of CaN (Wen et al., 2004b). Taken together with function of TRPC channels, these findings are consistent with the hypothesis that the source of calcium is crucial for determining growth cone motility in response to calcium signaling.

Interestingly, studies carried out in rodent neurons have reported that inhibition of L-type VDCC has no effect on BDNF mediated growth cone turning in mammalian cerebellar

or dorsal root ganglion (DRG) neurons (Li et al., 2005; Gasperini et al., 2009). Similarly, unpublished observations from this laboratory suggest that inhibition of L-type VDCC has no effect on the attractive turning response to netrin-1 by growth cones of DRG sensory neurons (*unpublished observations*). These studies suggest that netrin-1 mediated calcium influxes via L-type VDCC may be specific to *Xenopus* spinal neurons, may function in a cell-type specific manner, or may be dependent on the maturation state of the cell (Ohbayashi et al., 1998). Nevertheless, many axon guidance studies have been conducted in *Xenopus* spinal neurons, therefore it is important to note the significance of calcium entry via L-type VDCC for growth cone turning in this model. These studies illustrate how the cell-type, the repertoire of guidance cue receptors expressed, as well as the ligands that each growth cone encounters, can add to the complexity of calcium signals observed in navigating growth cones. However, further complexity is introduced when calcium release from internal stores is considered.

1.4.3 Mechanisms of calcium release from the endoplasmic reticulum

The ER is a continuous membranous structure that spans the entire neuron, including the soma, axon, dendrites, as well as extending into the periphery of the growth cone (Yamada et al., 1971; Dailey and Bridgman, 1989; 1991; Terasaki et al., 1994; Berridge, 1998; de Juan-Sanz et al., 2017). ER calcium represents a large pool of intracellular calcium that can be released in response to guidance cue signaling (Henley and Poo, 2004; Tojima et al., 2011), and release of calcium from the ER plays a crucial role in the generation of localised calcium signals that mediate steering of the growth cone (Takei et al., 1998; Hong et al., 2000; Henley et al., 2004; Ooashi et al., 2005; Akiyama et al., 2009). ER calcium release occurs via two mechanisms: inositol triphosphate (IP_3)-induced calcium release (IICR), and/or calcium induced-calcium release (CICR).

1.4.3.1 IP_3-induced calcium release (IICR)

IICR refers to release of calcium from the ER that occurs in an IP_3-dependent manner via the activation of IP_3 receptors (IP_3R) on the ER membrane (Burgess et al., 1984; Berridge, 2002). IP_3 is an intracellular signaling molecule generated by phospholipase C (PLC)-

dependent hydrolysis of phosphatidylinositol-4-5-bisphophate (PIP_2), which diffuses within the cytoplasm to bind IP_3R located on the ER membrane, triggering calcium release from the ER (Berridge and Irvine, 1989). Calcium release by IICR is vital for axon pathfinding, with netrin-1, NGF, and BDNF found to initiate attractive growth cone turning via activation of the PLC-IP_3-IP_3R pathway (Ming et al., 1999; Li et al., 2005; Akiyama et al., 2009). Likewise, a gradient of guidance cues across the growth cone results in asymmetric generation of IP_3 on the side of the growth cone facing the source of guidance cue (Akiyama et al., 2009), correlating with sustained asymmetric rises in calcium observed in response to gradients of guidance cue (Wang and Poo, 2005; Gasperini et al., 2009). This attractive turning response is abolished by inhibition of PLC or by depletion of calcium from the ER (Li et al., 2005; Akiyama et al., 2009), implying that release of calcium from ER via IICR is sufficient to induce growth cone attraction. These data suggest that calcium release form the ER via the PLC-IP_3-IP_3R pathway regulates calcium entry via TRPC channels during the growth cone turning response (Fig. 1.3). Together, these findings demonstrate the importance of IICR for correct growth cone motility in response to guidance cue signaling, and illustrate the importance of calcium release from the ER as a source of calcium for correct growth cone motility.

1.4.3.2 Calcium-induced calcium release (CICR)

Calcium release from the ER via calcium-induced calcium release (CICR) is activated by increased intracellular calcium, with free calcium ions binding to ryanodine receptors (RyR) located in the ER membrane, causing potentiation of RyR-mediated calcium release (Berridge, 2002). Activation of CICR is required for growth cone attraction (Hong et al., 2000; Ooashi et al., 2005; Tojima et al., 2007), with inhibition of CICR switching netrin-1 mediated attraction to repulsion (Hong et al., 2000). Although CICR is required for netrin-1 mediated attraction, inhibition of CICR has no effect on BDNF mediated growth cone turning, or calcium signaling in response to BDNF (Li et al., 2005). Unlike IICR, activation of CICR alone with a low concentration of ryanodine causes growth cone repulsion (Hong et al., 2000), suggesting that CICR must be paired with an influx of extracellular calcium or IICR to generate large amplitude calcium signals that mediate attraction. This finding is consistent with the hypothesis that the source of calcium is important for determining growth cone motility in response to guidance cue

signaling (Ooashi et al., 2005; Tojima et al., 2007), and suggests that the mode of calcium release from the ER is an important factor in determining growth cone turning responses.

1.4.4 Calcium influx mechanisms: store-operated calcium entry

Growth cone motility is known to require sustained, localised calcium signals formed by calcium influx and release of calcium from the ER (Li et al., 2005; Ooashi et al., 2005; Gasperini et al., 2009; Tojima et al., 2011). However, intracellular calcium is rapidly buffered within the cytoplasm (Faas et al., 2011), and the ER is a finite source of calcium, that is rapidly depleted upon release via IICR and/or CICR (Ooashi et al., 2005; Gasperini et al., 2009). Therefore, an additional mechanism of calcium influx must exist to sustain elevated intracellular calcium and replenish the ER calcium store during growth cone motility. It has been suggested that this mechanism of calcium influx is store-operated calcium entry (SOCE) (Li et al., 2005; Gasperini et al., 2009; Mitchell et al., 2012; Shim et al., 2013). SOCE refers to a specific mode of calcium influx that is triggered in response to a depletion of calcium from the ER, which refills the ER calcium store and sustains elevated intracellular calcium (Putney, 1986). Briefly, SOCE occurs when the ER-resident, calcium sensing protein stromal interacting molecule 1 (STIM1) is activated by depletion of ER calcium, which triggers STIM1 to bind and activate Orai proteins in the plasma membrane, leading to the formation of calcium-release activated calcium (CRAC) channels and SOCE [*discussed in detail below* (Luik et al., 2008; Park et al., 2009)]. Recent studies have suggested that STIM1 is necessary for attractive growth cone turning in response to BDNF (Mitchell et al., 2012), and netrin-1 (Shim et al., 2013), as well as midline crossing by commissural neurons of the *Xenopus* spinal cord (Shim et al., 2013), which supports a hypothesis whereby SOCE is activated in growth cones to mediate growth cone motility during axon pathfinding.

Figure 1.3: The source of calcium is a key determinate of growth cone motility responses.

In growth cone repulsion, guidance cue receptor activation leads to a relatively small influx of extracellar calcium, or a small release of ER calcium, generating a small amplitude calcium signal that activates calcineurin in preference to CaMKII. Activation of calcineurin promotes growth cone repulsion, as well as inhibiting CaMKII to inhibit growth cone attraction.

In growth cone attraction, guidance cue receptor activation leads to activation of calcium influx via TRPC channels via the PI3K-PIP_3-Akt pathway, and potentially further calcium influx via the activation of L-type VDCC. Receptor activation also leads to IP_3 production, which diffuses in the cytosol to bind and activate IP_3R located on the ER membrane, triggering calcium release via IICR. The resulting increase in intracellular calcium produces a further release of ER calcium via CICR, leading to a large amplitude rise in intracellular calcium. As ER calcium is depleted, STIM1 activates SOCE by triggering CRAC channel formation, with the resulting influx of calcium via SOCE refilling the depleted ER calcium store, and potentiating elevated intracellular calcium. The resulting sustained, large amplitude rise in intracellular calcium activates CaMKII in preference to calcineurin and promotes growth cone attraction.

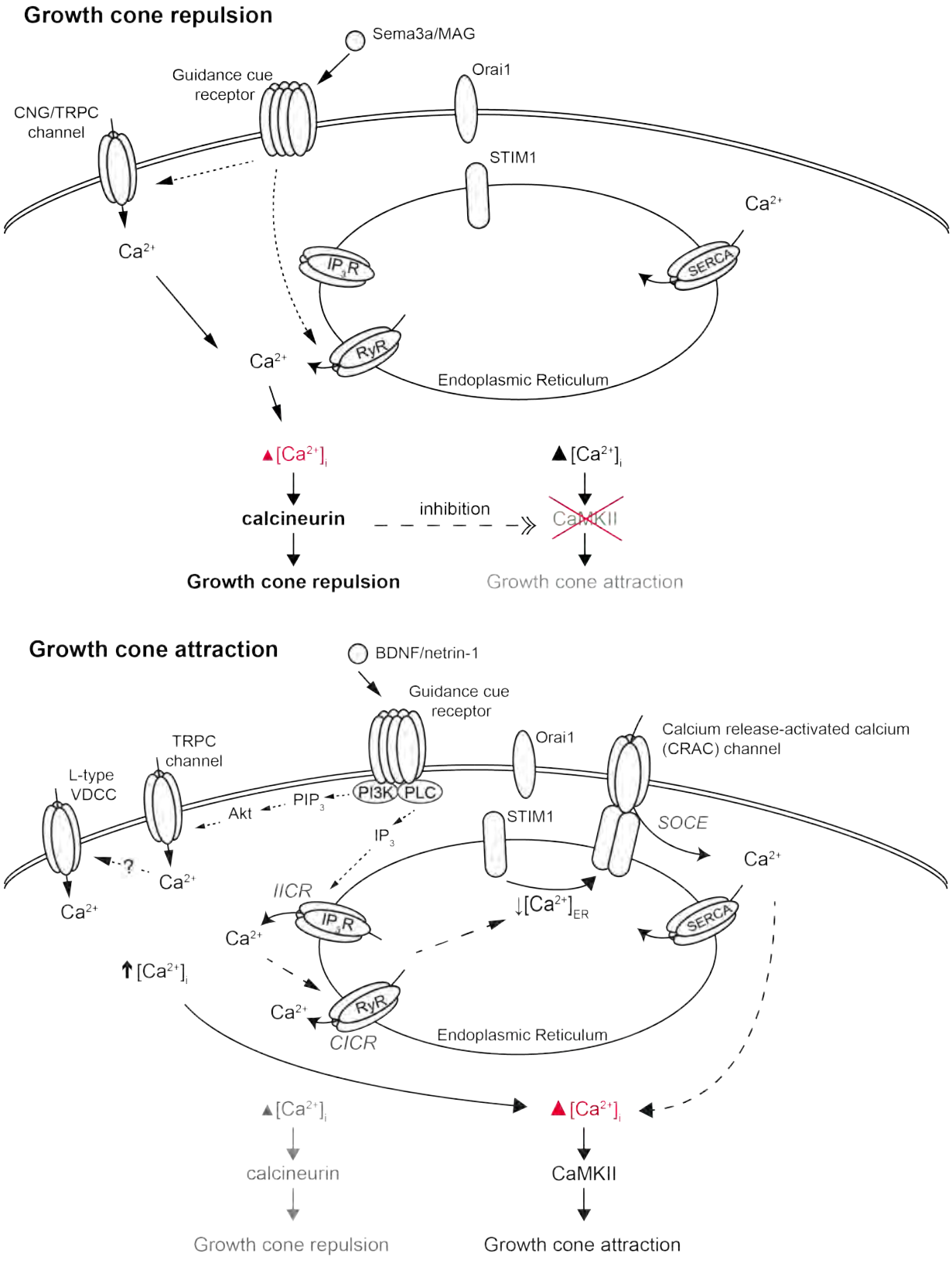
Growth cone repulsion
Sema3a/MAG
Guidance cue receptor
Orai1
CNG/TRPC channel
STIM1
Ca2+
Ca2+
IP3R
SERCA
RyR
Ca2+
Endoplasmic Reticulum
▲[Ca2+]i
▲[Ca2+]i
calcineurin
inhibition
CaMKII
Growth cone repulsion
Growth cone attraction
Growth cone attraction
BDNF/netrin-1
Guidance cue receptor
Orai1
Calcium release-activated calcium (CRAC) channel
TRPC channel
L-type VDCC
PIP3
PI3K
PLC
Akt
IP3
STIM1
SOCE
Ca2+
?
Ca2+
Ca2+
IICR
↓[Ca2+]ER
Ca2+
IP3R
SERCA
↑[Ca2+]i
Ca2+
RyR
CICR
Endoplasmic Reticulum
▲[Ca2+]i
▲[Ca2+]i
calcineurin
CaMKII
Growth cone repulsion
Growth cone attraction

1.5 Store-operated calcium entry (SOCE)

The concept of SOCE was first proposed by James Putney in the mid 1980s as a mechanism to explain the compensatory influx of extracellular calcium that is observed in response to the depletion of calcium from the ER (Putney, 1986). Although SOCE was initially predicted to be a mechanism of calcium entry for non-excitable cells (Hoth and Penner, 1992), SOCE was subsequently shown to be present in excitable cells (Putney, 2003), including neurons (Baba et al., 2003; Bouron et al., 2005; Kachoei et al., 2006). However, the mechanism of SOCE and its molecular components remained to be elucidated.

1.5.1.1 Store-operated channels: CRAC channels

CRAC channels were first described in mast cells as a calcium influx channels that mediates a sustained inward calcium current (termed I_{CRAC}) in response to ER calcium depletion, which occurrs independent of a change in membrane voltage (Hoth and Penner, 1992; 1993). As such, the CRAC channel was proposed to be the calcium permeable channel responsible for calcium influx during SOCE. However, despite electrophysiological evidence for the existence of CRAC channels (Hoth and Penner, 1992; 1993), the identity of the CRAC channel remained to be elucidated.

Orai1 (also termed CRAC modulator 1 (CRACM1)) was first identified as a candidate CRAC channel protein by a genetic screen of patients with severe combined immune deficiency (SCID) (Feske et al., 2006), a disease in which immune cells exhibit defective calcium influx via SOCE (Feske et al., 2005). At a similar time, Orai1 was identified by RNA interference (RNAi) screens aiming to identify regulators of SOCE in *Drosophila* S2 cells (Feske et al., 2006; Vig et al., 2006). However, the key pieces of data that revealed that Orai1 was the molecular constituent of the CRAC channel was that expression of Orai1 together with the ER-localised calcium sensing protein STIM1 activates SOCE with calcium influx that resembles I_{CRAC} (Peinelt et al., 2006; Soboloff et al., 2006b), and mutation of the pore-forming residue of Orai1 abrogated calcium influx via SOCE (Vig et al., 2006). Hence, it was concluded that Orai1 is a molecular constituent of the CRAC channel.

However, the Orai family of proteins includes three Orai homologs in mammals: Orai1, Orai2 and Orai3 (Feske et al., 2006), and all three Orai homologues are capable of forming CRAC channels (Prakriya et al., 2006; Schindl et al., 2008; 2009). Orai proteins are plasma membrane localised proteins that contain four transmembrane domains with both N- and C-termini located within the cytoplasm (Feske et al., 2006; Vig et al., 2006), and structural analysis has revealed that CRAC channels are formed by Orai hexamers (Hou et al., 2012; Cai et al., 2016), with Orai1-3 able to heteromultimerise to form CRAC channels containing multiple Orai family members (Inayama et al., 2015). Furthermore, each Orai protein confers the CRAC channel with distinct calcium conduction and inactivation kinetics (DeHaven et al., 2007; Lis et al., 2007), suggesting that calcium influx via SOCE can be shaped by the expression of different Orai proteins (Moccia et al., 2015).

1.5.2 Store-operated channels: TRPC channels

It was long argued that TRPC channels were CRAC channels (Putney et al., 2001), as evidence suggest that TRPC channels were activated in response to ER calcium depletion (Zitt et al., 1996; Kiselyov et al., 1998). However, these results were not reproducible in other laboratories (McKay et al., 2000). Furthermore, calcium influx via TRPC channels does not produce the highly specific I_{CRAC} (Feske et al., 2005), which is the hallmark of CRAC channel mediated SOCE (Hoth and Penner, 1992; 1993), suggesting that TRPC channels are not CRAC channels. However, given that STIM1 is able to activate a store-dependent calcium influx via TRPC channels (Huang et al., 2006; Yuan et al., 2007; Wang et al., 2008; Antigny et al., 2011; Li et al., 2012; Somasundaram et al., 2014; Ong and Ambudkar, 2015), it is now recognized that TRPC and CRAC channels can both function as store-operated channels activated in response to calcium depletion from the ER [for reviews see (Wang et al., 2008; Hogan and Rao, 2015; Majewski and Kuznicki, 2015)]. Consequently, herein SOCE refers to STIM-mediated calcium influxes elicited by CRAC and/or TRPC channels.

1.6 Stromal interacting molecule (STIM) proteins

For SOCE to occur, depletion of ER calcium must be communicated to store-operated channels located on the plasma membrane (Putney et al., 2001). Early studies in mast cells demonstrated that there is a delay between ER calcium depletion and the activation of SOCE (Hoth and Penner, 1992; 1993), implying that a signaling process activates CRAC channels in response to ER calcium depletion. Of the various signaling mechanisms proposed (Putney et al., 2001), experimental evidence supported a mechanism of direct coupling between ER and plasma membrane localised regulatory elements (Venkatachalam et al., 2002). A key piece of evidence for this direct coupling hypothesis was provided by the demonstration that calcium release from the ER and calcium influx via SOCE is highly colocalised (Jaconi et al., 1997), suggesting that proximity of the ER with the plasma membrane is required for SOCE to occur.

Stromal interacting molecule (STIM) proteins are a family of two type I transmembrane proteins first identified as candidate tumour suppressor genes (Parker et al., 1996; Sabbioni et al., 1997; Manji et al., 2000; Williams et al., 2001). The first STIM protein identified was human STIM1, which was discovered as a rhabdomyosarcoma-releated gene within chromosome region 11p15.5 (Parker et al., 1996), which was implicated in the development of several cancers including rhabdomyosarcoma, Wilms tumour and adrenal carcinoma (Parker et al., 1996; Sabbioni et al., 1997; Manji et al., 2000; Williams et al., 2001). A second STIM protein, termed STIM2, was also identified, which exhibited significant homology with STIM1 (Williams et al., 2001), suggesting a conserved function. Orthologs for STIM1 and STIM2 have been identified in all vertebrates, including zebrafish (*Danio rerio*), *Xenopus*, and rodents, whilst invertebrates such as *C. elegans* and *Drosophila* express a single STIM ortholog (Williams et al., 2001; Cai, 2007a). The high degree with which STIM proteins have been conserved during evolution (Williams et al., 2001; Cai, 2007a), coupled with the demonstration that STIM proteins exhibited near ubiquitous expression in most tissues (Williams et al., 2001), suggested that STIM proteins have highly important biological functions. As STIM1 had a putative role as a tumour suppressor gene (Parker et al., 1996; Williams et al., 2001; 2002), and possessed a sterile-α-motif (SAM) domain, α-helical coiled-coil domains, and numerous phosphorylated residues (Parker et al., 1996; Williams et al., 2001; 2002), it

was theorised that STIM1 would form higher order structures that function as part of a signaling pathway (Williams et al., 2002).

1.6.1 Regulation of SOCE by STIM proteins

The first evidence that STIM1 regulated SOCE was provided by RNAi screens aiming to identify the molecular mediators of SOCE (Liou et al., 2005; Roos et al., 2005). Using RNAi in *Drosophila* S2 cells, Roos and colleagues showed that of 170 candidate genes screened, only knockdown of *Drosophila* STIM (dSTIM) inhibited I_{CRAC}, with calcium influx reduced by 90% in cells lacking dSTIM (Roos et al., 2005). When similar experiments were conducted by reducing STIM1 expression in mammalian HEK293 cells, SOCE was reduced by 60% (Roos et al., 2005), suggesting that STIM1 is a conserved regulator of SOCE in both vertebrates and invertebrates. A similar RNAi screen of 2,304 proteins in HeLa cells identified both STIM1 and STIM2 as proteins required for SOCE (Liou et al., 2005). Together, these findings revealed that STIM proteins were molecular components of SOCE, however how the function of STIM protein during SOCE remained to be determined.

It was suggested that STIM proteins could function in several ways to regulate SOCE. Firstly, the simplest explanation of the above results would be that STIM proteins constitute the CRAC channel, whether as a constitutive plasma membrane protein, or by translation of ER-localised STIM1 into the plasma membrane upon activation (Roos et al., 2005; Zhang et al., 2005). Secondly, as STIM1 was observed on both the ER and the plasma membranes, it was proposed that homophilic interactions between STIM1 proteins initiates SOCE by activation of independent CRAC channels (Zhang et al., 2005). Lastly, it was hypothesised that activated STIM1 located within the ER membrane could directly interact with CRAC channels on the plasma membrane to trigger SOCE, without interactions with plasma membrane localised STIM1 (Liou et al., 2005; Roos et al., 2005). The final hypothesis was proven correct with the observation that STIM1 is an ER-localised protein that translocates towards the plasma membrane in response to depletion of calcium from the ER, but is not inserted into the plasma membrane (Liou et al., 2005). Subsequent studies would identify Orai proteins as the molecule constituents of CRAC channels (Feske et al., 2006; Peinelt et al., 2006; Vig et al., 2006), which are

directly bound and regulated by STIM1 (Muik et al., 2008; Derler et al., 2009; Yuan et al., 2009; Zhou et al., 2014), thus proving that STIM1 is an ER-localised calcium sensing protein responsible for the activation of SOCE.

In addition to STIM proteins, SOCE is also regulated by STIM interacting proteins including the ER-resident SOCE-associated regulatory factor (SARAF), which binds to STIM1 coupled with Orai to attenuate SOCE, preventing excessive store-refilling (Palty et al., 2012; Jha et al., 2013; Palty and Isacoff, 2015; Albarran et al., 2016). While acknowledging the important role that these regulatory proteins play in the fine tuning of calcium influx via SOCE, this thesis focuses on the regulation of SOCE mediated by STIM proteins.

1.6.2 Stromal interacting molecule 1 (STIM1)

STIM1 is a 77-kDa ER-resident calcium sensing protein that that is required to initiate SOCE in response to depletion of calcium from the ER. STIM1 is a type I transmembrane protein with an N-terminal region within the ER lumen, and a cytosolic C-terminal region (Williams et al., 2001; Roos et al., 2005; Zhang et al., 2005; Dziadek and Johnstone, 2007; Liou et al., 2007). The luminal N-terminal region of STIM1 is comprised of an ER-localisation sequence or signal motif, an EF-hand that binds calcium, a 'hidden' EF-hand that does not participate in calcium binding, and a SAM domain involved in STIM1 conformational changes and oligomerisation (Huang et al., 2006; Stathopulos et al., 2006; Zheng et al., 2008; Yuan et al., 2009; Covington et al., 2010; Zheng et al., 2011). While the calcium-binding EF-hand imparts STIM1 with the ability to sense ER calcium concentrations (Liou et al., 2005; Zhang et al., 2005; Mercer, 2006; Stathopulos et al., 2006), the remaining N-terminal protein domains are responsible for communicating changes in calcium binding to STIM1 C-terminal protein domains, which in turn regulate effector functions of STIM1, including CRAC channel activation (Stathopulos et al., 2006; Luik et al., 2008; Muik et al., 2011). Here, the structure of STIM1 will be reviewed to provide insight into the function of STIM1 during SOCE (Fig. 1.4).

The luminal region of STIM1 is involved in calcium binding, and regulates the activation state of STIM1. The STIM1 EF-hand is a low affinity calcium-binding motif that confers

STIM1 with its calcium sensory function (Liou et al., 2005). The low affinity of the STIM1 EF-hand for calcium, coupled with the 1:1 binding between calcium ions and the EF-hand (Stathopulos et al., 2006), means that STIM1 is able to sense changes in the concentration of calcium within the ER lumen. ER calcium is high under resting conditions and consequently STIM1 remains bound to calcium (Liou et al., 2005; Stathopulos et al., 2006). This inactive form of STIM1 is present as a dimer and is distributed throughout the ER (Zhou et al., 2014) (Fig. 1.4). When calcium concentration in the ER is decreased the low affinity of calcium for the EF-hand results in dissociation of calcium from the EF-hand (Liou et al., 2005; Stathopulos et al., 2006). As a result, conformational changes in the SAM domain occur that promote STIM1 oligomerisation, which activates STIM1 and causes SOCE via CRAC channels (Stathopulos et al., 2006; Luik et al., 2008; Shim et al., 2014). Accordingly, a constitutively active STIM1 (an EF-hand mutant STIM1 that is unable to bind calcium) is present in puncta and continuously activates calcium influx via SOCE (Zhang et al., 2005). These studies provide a mechanism for ER calcium-dependent SOCE by regulating the activation state of STIM1, however they do not explain how STIM1 interacts with CRAC channels to facilitate SOCE.

STIM1 contains three α-helical coiled-coil domains (CCD), termed CC1-3 (Fig. 1.4), which are responsible for controlling CRAC channel activation by STIM1 (Kawasaki et al., 2009; Muik et al., 2009; 2011). When STIM1 is inactive, an acidic region within CC1 (which shares high homology with the STIM1 binding site on CRAC channels) binds CC2/CC3 to inhibit STIM1-mediated CRAC channel activation (Korzeniowski et al., 2010). Conformational changes within STIM1 that result from calcium dissociation from the EF-hand promote STIM1 dimers to assemble into a higher order oligomer (Zhou et al., 2014). As a consequence of oligomer formation, STIM1 undergoes translocation (remaining within the ER) to areas of close apposition between the ER and plasma membrane (Liou et al., 2005; Soboloff et al., 2006b; Liou et al., 2007), which are known as ER-PM junctions (Wu et al., 2012; 2014; Hogan, 2015). Oligomerisation is critical for activation of CRAC channels, as demonstrated by the poor activation of SOCE when the full cytoplasmic region of STIM1 is expressed alone (Korzeniowski et al., 2010). It is believed that oligomer formation releases CC2/CC3 regions from CC1 (Korzeniowski et al., 2010; Kim and Muallem, 2011), which enables a STIM1 orai-activating region (SOAR) domain within the CC2/CC3 region to bind and activate CRAC channels (Derler

et al., 2009; Yuan et al., 2009; Kim and Muallem, 2011; Fahrner et al., 2014). This SOAR domain has previously been shown to be sufficient and necessary for STIM1-mediated activation of CRAC channels (Yeromin et al., 2006; Muik et al., 2008; Park et al., 2009; Kim and Muallem, 2011). Therefore, the structure of STIM1 informs a model of STIM1-mediated SOCE whereby calcium depletion from the ER causes dissociation of calcium from the EF-hand, stimulating conformational changes that trigger STIM1 oligomerisation, and subsequently the translocation of STIM1 to ER-PM junctions. Once localised at ER-PM junctions, STIM1 interacts with Orai to trigger calcium influx via SOCE (Fig. 1.4). However, this model does not take into account the important functions of the unstructured region located at the C-terminus of STIM1.

A key role of the C-terminus of STIM1 is to regulate the translocation of STIM1 to ER-PM junctions (Grigoriev et al., 2008; Sampieri et al., 2009; Asanov et al., 2013). The unstructured C-terminus of STIM1 contains a serine/proline-rich region that is proposed to be phosphorylated to regulate STIM1 interactions with the microtubule cytoskeleton to facilitate translocation of STIM1 (and the ER) within cells (Grigoriev et al., 2008; Pozo-Guisado et al., 2010; Asanov et al., 2013; Pozo-Guisado et al., 2013; Casas-Rua et al., 2015). This active translocation and localisation of STIM1 at ER-PM junctions is thought to occur via STIM1 interactions with the microtubule plus end tracking protein end binding (EB), and the actin binding protein adenomatous polyposis coli (APC) (Grigoriev et al., 2008; Asanov et al., 2013). The function of STIM1 as a regulator of ER remodeling has not been shown in neuronal cells. However, EB proteins and APC are expressed in the neuronal growth cone (Stepanova et al., 2003; Koester et al., 2007), suggesting that the ability of STIM1 to regulate trafficking of the ER within the growth cone may be a further mechanism by which calcium signals are regulated in space and time.

1.6.3 Stromal interacting molecule 2 (STIM2)

STIM1 and STIM2 homologues are conserved within vertebrates (Cai, 2007a), implying that both STIM proteins have an evolutionarily important role. Despite the high degree of homology between STIM1 and STIM2 (Williams et al., 2001), STIM proteins are believed to exhibit distinct functions, including in the regulation of SOCE (Soboloff et

al., 2006a; Brandman et al., 2007; Parvez et al., 2008). Early studies proposed that STIM2 inhibits SOCE, possibly by direct coupling to STIM1 to inhibit STIM-mediated SOCE (Soboloff et al., 2006a). However, other studies have shown that STIM2 is able to initiate SOCE (Liou et al., 2005; Soboloff et al., 2006b), suggesting that the inhibitory influence of STIM2 may have been an artifact of STIM2 overexpression. More recent studies have suggested that STIM2 activates SOCE to regulate basal calcium homeostasis (Brandman et al., 2007; Thiel et al., 2013). An RNAi screen of 2,304 proteins in HeLa cells aimed at identifying regulators of basal calcium concentration, identified STIM2 as the strongest positive regulator of basal calcium (Brandman et al., 2007). Accordingly, STIM2 is activated by smaller depletions of ER calcium compared to STIM1, while reduced expression of STIM2 causes a decrease in basal cytosolic and ER calcium concentrations (Brandman et al., 2007). One interpretation of these findings is that STIM2 primarily regulates basal calcium homeostasis, while STIM1 is responsible for regulating SOCE induced by receptor-activated depletion of ER calcium. Another interpretation is that STIM2 regulates cellular responses to sub-maximal receptor activation. Further studies are required to dissect the different roles of STIM1 and STIM2 in calcium signaling.

Figure 1.4: STIM1 is an ER-localised calcium sensing protein that regulates calcium influx via store-operated calcium entry.

(a) A schematic of STIM1 illustrating the major protein domains that confer STIM1 with the ability to activate SOCE in response to ER calcium depletion. In the inactive state, the EF-hand is bound to calcium and the auto-inhibitory function of the coiled-coil domain prevents STIM1 binding to Orai via the CRAC channel activation domain (CAD). However, upon the depleted of calcium from the ER, calcium dissociates from the EF-hand, activating STIM1. Activated STIM1 alters conformation leading to the release of the CAD domain, forms higher order structures via oligomerisation with other activated STIM1 proteins, and translocates to ER-PM junctions. The translocation of STIM1 to ER-PM junctions is regulated via the S/P rich region and the K-rich region, via interactions with EB and APC proteins. One located at ER-PM junctions, STIM1 binds and activate Orai proteins via the CAD domain, triggering calcium influx via CRAC channels.

(b) A diagram illustrating STIM1-medaited SOCE. In calcium replete conditions (top), STIM1 is observed throughout the ER bound to calcium. When the ER is depleted of calcium (b), activated STIM1 translocates together with the ER to form ER-PM junctions, triggering CRAC channel formation and calcium influx via SOCE.

Stromal interaction molecule 1 (STIM1)

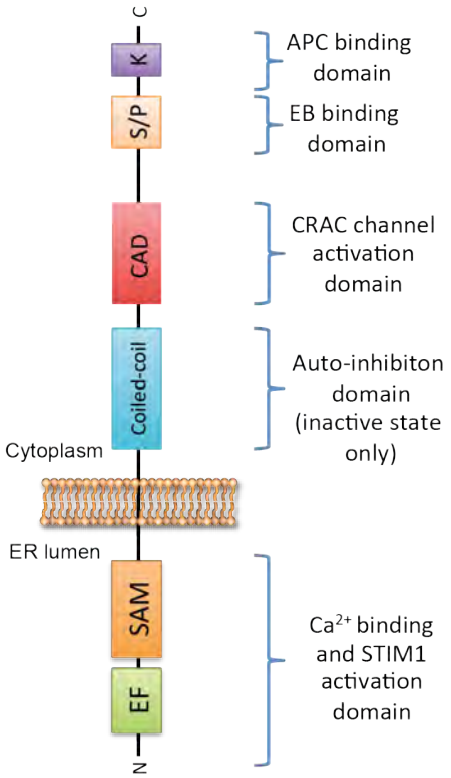

Calcium replete conditions

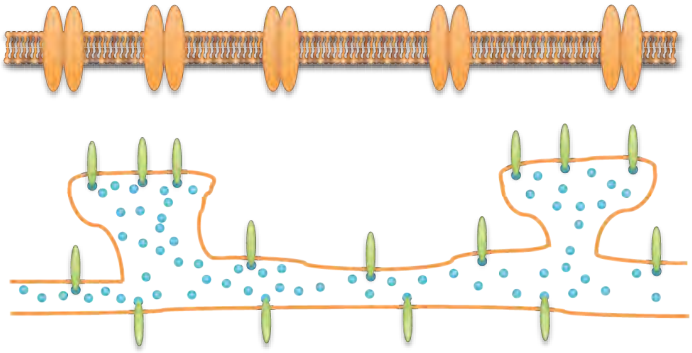

Calcium-deplete conditions

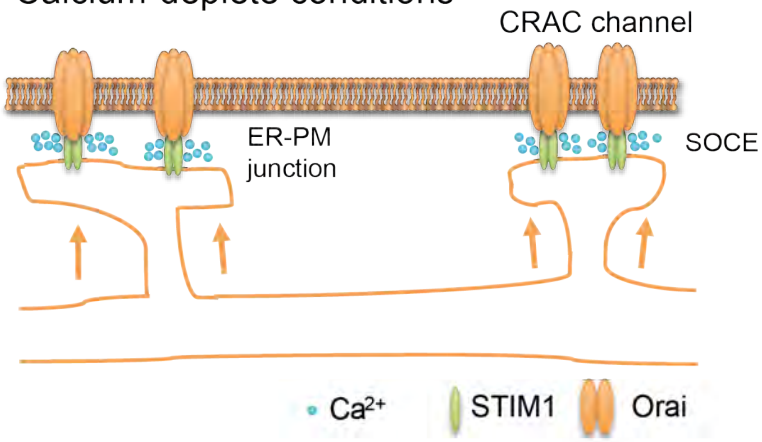

1.7 STIM1-mediated SOCE regulates calcium signaling in neurons

In neurons, STIM1 regulates SOCE to maintain basal intracellular calcium levels and sustain calcium signaling for the activation of calcium signaling pathways, which in turn modulate neuronal functions [recently reviewed by (Majewski and Kuznicki, 2015)]. STIM1 is widely expressed in the adult nervous system (Klejman et al., 2009; Skibinska-Kijek et al., 2009; Gemes et al., 2011), with an enrichment of STIM1 expression observed in layer V neurons of the cortex (Klejman et al., 2009; Skibinska-Kijek et al., 2009), the granule neurons of the dentate gyrus (Klejman et al., 2009), pyramidal cells of CA1-CA3 (Klejman et al., 2009), and by Purkinje cells of the cerebellum (Dziadek and Johnstone, 2007; Klejman et al., 2009; Skibinska-Kijek et al., 2009; Hartmann et al., 2014). These data suggest that STIM1 and SOCE have an important role in regulating the function of these neuronal subtypes in the mature nervous system. In contrast, the pattern of STIM1 expression in the developing nervous system is not as well understood. STIM1 is known to be expressed by mouse DRG neurons and peripheral axon tracts at embryonic day 16 (E16) (Dziadek and Johnstone, 2007), and by dorsal horn neurons from the neonatal spinal cord (Xia et al., 2014). Furthermore, *in vitro* studies have shown that STIM1 is expressed by hippocampal, cortical, and DRG neurons isolated from the embryonic nervous system (Gasperini et al., 2009; Klejman et al., 2009; Mitchell et al., 2012), suggesting that STIM1 is appropriately expressed to regulate SOCE in neurons during development. Evidence suggests that Orai1-3 are also expressed in the developing and adult nervous systems (Gross et al., 2007; Gwack et al., 2007; Takahashi et al., 2007; Berna-Erro et al., 2009; Hartmann et al., 2014), however the pattern of Orai expression in development remains to be determined.

As expected from the ubiquitous nature of STIM1 expression in the brain, defective SOCE has been associated with a wide range of diseases of the nervous system. Diseases in which SOCE has so far been implicated include Alzheimer's and Huntington's diseases (Yoo et al., 2000; Bojarski et al., 2008; Wojda et al., 2008; Sun et al., 2014a; Zhang et al., 2015), epilepsy (Steinbeck et al., 2011), hypoxia-induced neuronal cell death (Berna-Erro et al., 2009; Zhang et al., 2014), axonal injury (Gemes et al., 2011), as well as deleterious calcium signaling events induced by traumatic brain injury (Hou et al., 2014; Rao et al., 2015).

At the cellular level, STIM1-dependent SOCE is present in the dendrites of hippocampal neurons (Ng et al., 2011), with inhibition of SOCE reducing the ability of hippocampal synapses to undergo long term potentiation (Baba et al., 2003). In mice that have had STIM1 expression ablated from forebrain neurons, there is a delay in both memory acquisition and the reversal of learning (Garcia-Alvarez et al., 2015). In contrast, when SOCE is activated in the CA1 region of the hippocampus using an optically controlled STIM1 (OptoSTIM1), mice exhibit an increase in contextual memory formation (Kyung et al., 2015), suggesting that STIM1-mediated SOCE is an important regulator of synaptic plasticity. Furthermore, when the *STIM1* gene is knocked out of cerebellar Purkinje neurons, metabotropic glutamate receptor type 1 (mGluR1)-dependent synaptic calcium transients were attenuated, and this was associated with defects in motor coordination (Hartmann et al., 2014). Consistent with STIM1-mediateing SOCE at the synapse, both ER calcium release and the refilling of ER calcium stores following mGluR1-mediated synaptic calcium transients were attenuated (Hartmann et al., 2014). STIM1 is also important in the pre-synaptic axon, with STIM1 regulating neurotransmitter release by controlling ER calcium levels (de Juan-Sanz et al., 2017). Together, these findings suggest that spatially localised calcium signals at the synapse are regulated by the refilling of the ER calcium store via STIM1-mediated SOCE, providing evidence that STIM1 is important for the regulation of localised calcium signaling in neurons.

1.8 STIM1 in growth cone motility and axon pathfinding

Axon guidance requires discrete spatial and temporal patterns of calcium signaling to steer axons towards their final targets. Although the past few decades have seen a surge in our understanding of the processes that govern axon guidance, the mechanisms responsible for regulating the spatial and temporal localisation of calcium signaling within the pathfinding axon remains to be elucidated. Given that release of calcium from the ER is vital for the generation of sustained calcium signals in response to environmental guidance cues (Hong et al., 2000; Henley et al., 2004; Ooashi et al., 2005; Gasperini et al., 2009), it is predicted that release of calcium from the ER is a key source of calcium for correct growth cone motility (Tojima et al., 2011). However, the ER is a finite source of calcium, and further calcium influx is required to sustain increased intracellular calcium and refill the depleted ER calcium store. Interestingly, recent

evidence has implicated STIM1 in the regulation of growth cone motility *in vitro* (Mitchell et al., 2012; Shim et al., 2013), with STIM1 shown to be required for sustained elevations in intracellular calcium in response to guidance cue signaling (Mitchell et al., 2012). However, the function of STIM1 for axon pathfinding is not well understood. Here, I will outline what is known regarding the function of STIM1 in growth cone motility.

STIM1 expression has been shown in growth cones of cultured mammalian DRG sensory neurons (Gasperini et al., 2009; Mitchell et al., 2012), as well as growth cones of *Xenopus* spinal neurons (Shim et al., 2013), indicating that STIM1 is a conserved component of the calcium signaling machinery in growth cones. Depletion of growth cone ER calcium stores stimulates co-localisation of STIM1 and Orai1 on the turning side of the growth cone, and is associated with a sustained rise in intracellular calcium (Mitchell et al., 2012). This sustained rise in intracellular calcium was abolished when STIM1 expression was reduced (Mitchell et al., 2012), providing evidence that STIM1-mediated SOCE functions in the growth cones to refill depleted ER calcium stores. Significantly, when STIM1 expression was reduced, the growth cone turning response to BDNF was switched from attraction to repulsion (Mitchell et al., 2012). This finding is consistent with STIM1 being required for localised, larger amplitude calcium signals that trigger growth cone attraction. In similar experiments conducted on *Xenopus* spinal neurons, STIM1 was shown to be required for netrin-1 mediated growth cone attraction, with attraction switched to repulsion when STIM1 function was perturbed (Shim et al., 2013). In this experimental paradigm, reduced STIM1 function decreased the number of filopodia exhibiting calcium transients and reduced the frequency of calcium transients in freely growing growth cones *in vitro* (Shim et al., 2013), suggesting that STIM1-mediated SOCE regulates both localised and global calcium transients.

Interestingly, STIM1 expression is also necessary for sema3a induced growth cone repulsion (Mitchell et al., 2012). Sema3a is classically described as a calcium-insensitive repulsive guidance cue (Song and Poo, 1999). As such, STIM1 knockdown was not expected to alter sema3a induced repulsion. Although small influxes of calcium occur in response to sema3a via CNG channels (Togashi et al., 2008), CNG-mediated calcium influxes are minimal (Togashi et al., 2008; Mitchell et al., 2012). Accordingly, STIM1 knockdown had little effect on sema3a induced calcium influx, and sema3a-mediated

repulsion still occurred when calcium was depleted from the extracellular media (Mitchell et al., 2012). As such it is unlikely that STIM1 perturbs sema3a turning in a calcium-dependent manner. STIM1 has previously been described to interact with cAMP signaling via the store-operated cAMP pathway (Lefkimmiatis et al., 2009), suggesting that cAMP may be regulated by STIM1 in growth cones. Given that cyclic nucleotides play an important role in regulating growth cone motility (Song et al., 1997; Tojima et al., 2009; Nicol et al., 2011), defects in cyclic nucleotide signaling may underlie the attenuation of sema3a-mediated repulsion when STIM1 expression is reduced. Therefore, although STIM1 is best understood as the ER-localised regulator of SOCE, these findings suggest that STIM1 may also interact with other intracellular signaling pathways to regulate growth cone motility and, hence, axon pathfinding.

1.9 Hypothesis and aims

Over the past few decades, evidence has accumulated to support an important role for spatial and temporal localisation of calcium signaling during growth cone motility (Hong et al., 2000; Zheng, 2000; Henley et al., 2004; Akiyama et al., 2009; Gasperini et al., 2009). More recently, the hypothesis has emerged that the source of calcium is vital for determining the outcome of guidance cue signaling, with release of calcium from the ER being a crucial mechanism for the regulation of growth cone motility (Ooashi et al., 2005; Tojima et al., 2007), implying that the refilling of the ER calcium store is crucial for correct axon pathfinding. Previous studies have shown that expression of STIM1 is required for correct growth cone motility *in vitro* (Mitchell et al., 2012; Shim et al., 2013). Furthermore, when STIM1 function was perturbed in developing *Xenopus* embryos, errors were observed in midline crossing by spinal commissural axons (Shim et al., 2013). Although these data provide evidence that STIM1 has a role in axon pathfinding *in vivo*, the function of STIM1 during axon pathfinding remains unclear. Furthermore, the developmental expression of STIM1 remains poorly defined, and as such it is unknown whether STIM1 is correctly expressed in development to regulate axon pathfinding. As such, the central hypothesis to be addressed by this thesis is that STIM proteins exhibit discrete cellular patterns of expression during embryonic development, and STIM1-mediated calcium signaling is necessary for correct axon guidance during nervous system development.

For STIM1 to function as a regulator of calcium signaling in axon pathfinding, STIM1 should be expressed in the developing nervous system. Despite the expression of STIM proteins in the adult nervous system being well described (Skibinska-Kijek et al., 2009), little is known regarding the expression of STIM proteins in development. Therefore, the pattern of expression of STIM proteins in the developing rodent nervous system was compared with expression in the zebrafish (*Danio rerio*) nervous system to ascertain the conservation of STIM1 expression in nervous system development. Using zebrafish as an experimental model, the importance of STIM1 expression for embryonic development was determined, with a focus on the requirement of STIM1 expression for axon pathfinding by motor neurons in the live, intact nervous system. Finally, given that STIM1 functions to regulate SOCE, the requirement of STIM1 for the regulation of calcium signaling during motor neuron axon pathfinding *in vivo* was investigated.

Chapter 2:
STIM1 is expressed in the developing vertebrate nervous system

Chapter 2: STIM1 is expressed in the developing vertebrate nervous system

2.1. Introduction

The role of STIM1 in the nervous system, including the contribution of SOCE to neuronal calcium signaling, has been controversial [for recent reviews see (Hooper et al., 2014; Majewski and Kuznicki, 2015; Lu and Fivaz, 2016)]. The function of STIM1 as a regulator of SOCE was initially discovered and characterised in non-excitable cells such as immune cells and platelets (Hoth and Penner, 1993; Liou et al., 2005; Feske et al., 2006; Grosse et al., 2007), where SOCE is the primary mode of calcium influx (Putney, 2007). In contrast, neurons express an extensive array of calcium channels (Brini et al., 2014), with calcium influx into neurons having long been ascribed to voltage-dependent and receptor-operated channels (Berridge, 1998). Consequently, the importance of a low conductance calcium influx channel such as the CRAC channel for the regulation of neuronal function has been questioned (Putney, 2003; Lu and Fivaz, 2016). However, there is growing evidence that neurons harness STIM1-medaited SOCE to regulate cellular processes.

STIM1 is expressed in many neuronal subtypes, where it regulates calcium entry via SOCE (Kraft, 2015; Majewski and Kuznicki, 2015). STIM1-mediated SOCE has been shown to regulate neural precursor cell proliferation and differentiation (Li et al., 2012; Somasundaram et al., 2014; Hao et al., 2016), gene expression (Lalonde et al., 2014; Somasundaram et al., 2014; Kar and Parekh, 2015; Kar et al., 2016), cell migration (Tsai et al., 2014; Casas-Rua et al., 2015), axon pathfinding (Mitchell et al., 2012; Shim et al., 2013), as well as synaptic transmission (Bouron, 2000; Ng et al., 2011; Hartmann et al., 2014). Evidence also suggests that calcium influx via SOCE is required to maintain basal calcium levels in neurons, with SOCE opposing a continual ER calcium leak (Samtleben et al., 2015). Therefore, it is hypothesised that STIM1-mediated SOCE is an important regulator of calcium in the developing nervous system.

There is little experimental evidence that STIM1 is expressed by neurons in development *in vivo*. Indeed, most of what is known regarding STIM1 expression in the nervous system has been determined by studying the adult rodent nervous system (Dziadek and Johnstone, 2007; Klejman et al., 2009; Skibinska-Kijek et al., 2009; Hartmann et al.,

2014; Hou et al., 2014; Zhang et al., 2014; Rao et al., 2015), or by studying neurons and glia *in vitro* (Dziadek and Johnstone, 2007; Gasperini et al., 2009; Klejman et al., 2009; Gruszczynska-Biegala et al., 2011; Mitchell et al., 2012; Moreno et al., 2012; Michaelis et al., 2014; Sun et al., 2014b). However, STIM1 mRNA and protein have been detected in embryonic human and mouse brain lysates (Williams et al., 2001; Dziadek and Johnstone, 2007), as well as lysates of the neonatal mouse spinal cord (Xia et al., 2014). Moreover, STIM1 mRNA is present in the embryonic mouse brain at E16 (Stiber et al., 2008), and STIM1 protein is expressed in mouse DRG neurons and in peripheral axon tracts at E16 (Dziadek and Johnstone, 2007). Although these studies indicate that STIM1 is expressed in the embryonic nervous system, the ontogeny of STIM1 during development remains largely unknown. Similarly, the pattern of expression for Orai protein in the developing nervous system remains unknown. All three Orai isoforms have been isolated together with STIM1 from the neonatal mouse spinal cord (Xia et al., 2014), while Orai1 and Orai2 form discrete puncta with STIM1 in growth cones of embryonic DRG neurons *in vitro* (Mitchell et al., 2012). Therefore, it would be predicted that STIM and Orai proteins co-express during nervous system development.

STIM2, which is derived from a second mammalian STIM gene, is reported to be expressed in the adult and embryonic rodent nervous systems (Berna-Erro et al., 2009; Gruszczynska-Biegala et al., 2011; Steinbeck et al., 2011; Gruszczynska-Biegala and Kuznicki, 2013; Rao et al., 2015). The two STIM proteins have different roles in the regulation of calcium [for recent reviews see (Hooper et al., 2014; Kraft, 2015; Majewski and Kuznicki, 2015)]. STIM1 triggers SOCE in response to larger decreases in ER calcium (Stathopulos et al., 2006; Thiel et al., 2013), mediates larger calcium influx via SOCE (Soboloff et al., 2006a; 2006b; Zhou et al., 2009), and is associated with calcium signaling events that control cellular processes such gene expression, axon guidance and synaptic transmission (Ng et al., 2011; Mitchell et al., 2012; Shim et al., 2013; Hartmann et al., 2014; Hou et al., 2014; Kar and Parekh, 2015; Kyung et al., 2015). Conversely, STIM2 is activated in response to small decreases in ER calcium levels and mediates a less robust calcium influx via SOCE (Soboloff et al., 2006a; 2006b; Zhou et al., 2009), and is associated with the regulation of basal calcium homeostasis (Brandman et al., 2007; Thiel et al., 2013). Despite evidence that STIM1 and STIM2 function differently to regulate SOCE (Stathopulos et al., 2006; Brandman et al., 2007; Thiel et al., 2013), and the known importance of precise patterns of calcium signaling for regulating neural

development (Owens and Kriegstein, 1998; Borodinsky et al., 2004; Weissman et al., 2004; Komuro and Kumada, 2005), the cellular expression of STIM proteins in the developing nervous system has not been determined.

Zebrafish (*Danio rerio*) have emerged as a powerful tool to study nervous system development. Zebrafish embryos exhibit rapid, highly stereotypic development, and their tissues are transparent during early development (Kimmel et al., 1995), meaning that neurodevelopmental processes such as axon pathfinding can be studied in the live, intact nervous system (Del Bene et al., 2010; Seredick et al., 2012; Ahrens et al., 2013; Heap et al., 2013; Plazas et al., 2013; Portugues et al., 2013; Sainath and Granato, 2013; Koyama et al., 2016). Advances in genetic tools means that it is possible to investigate defined populations of cells within the developing embryo (Scott et al., 2007; Don et al., 2017). Combined with the recent evolution of genetically encoded calcium indicators, such as the GCaMP family of calcium indicators (Akerboom et al., 2012), this means that calcium dynamics can be studied in specific neuronal populations (Ahrens et al., 2012; 2013; Koyama et al., 2016). Furthermore, zebrafish motor neurons exhibit highly reproducible and well defined axon pathfinding behaviours at discrete developmental stages (Eisen et al., 1986; Myers et al., 1986; Beattie et al., 2000; Plazas et al., 2013). Accordingly, the zebrafish was chosen as a model to study the role of STIM1 in nervous system development.

There is no data to describe STIM1 expression or function in the zebrafish nervous system. A previous phylogenetic analysis of STIM1 has suggested that two STIM1 orthologs are present in the zebrafish, which were termed zebrafish STIM1a (zSTIM1a) and zSTIM1b (Cai, 2007a). Studies have shown that zSTIM1 is localised with zOrai1 to cleavage furrows during the first two cell divisions post fertilisation (Chan et al., 2016), mediating sustained, spatially restricted calcium signals that are important for furrow deepening and daughter cell apposition (Chan et al., 2015; 2016). Furthermore, zebrafish Orai1b (zOrai1b) has been shown to be important for skeletal and cardiac muscle function in zebrafish, with reduced zOrai1b expression resulting in cardiac failure and skeletal myopathy by 2 days post fertilisation (Volkers et al., 2012). Together, these findings suggest that SOCE is important for zebrafish development, supporting the utility of zebrafish as a model to study the role of STIM1 in the developing nervous system.

These studies aim to characterise and compare the expression of STIM1 proteins in the developing mouse and zebrafish nervous systems. The expression of STIM1, STIM2, and the three STIM binding partners, Orai1, Orai2 and Orai3, was investigated in developing mouse nervous system. Furthermore, given the conjecture surrounding the neuronal functions of STIM1 and STIM2, the ontogeny of STIM1 and STIM2 was compared during mouse nervous system development. As data suggested that STIM1 is the major STIM protein in neurons during development, the pattern of zSTIM1 expression was described in development and compared with the pattern STIM1 expression in mice to infer whether the function of STIM1 in the developing nervous systems is conserved across vertebrate species.

2.2. Materials and methods

2.2.1. Ethical declaration

Procedures relating to the care and use of animals were approved by the Animal Ethics Committee of the University of Tasmania (Ethics approval numbers: A0013470, A0013741 and A0016061). All procedures were consistent with the Australian code for the care and use of animals for scientific purposes, 8th edition (National Health and Medical Research Council (Australia), 2013).

2.2.2. Animals

Mouse embryos (C57BL/6 strain) were obtained at embryonic day 13 (E13), E15, or post-natal day 5 (P5). To obtain mouse embryos, adult pregnant C57BL/6 mice were euthanised by carbon dioxide asphyxiation, with embryos resected from the mother by caesarean section, removed from their yolk sac, and euthanised by chilling on ice followed by decapitation. C57BL/6 mice at P5 were euthanised by decapitation. Neural tissues were rapidly dissected and processed for experiments as outlined below.

Zebrafish were maintained in a laboratory colony on a 14-hour (hr) light/10-hr dark cycle. Embryos were obtained from natural spawning events, maintained at 28°C in 0.5X E2 medium and staged for experiments by external morphology according to established guidelines (Kimmel et al., 1995).

2.2.3. *In situ* hybridisation: riboprobes

Anti-sense riboprobes were synthesised by *in vitro* transcription using T3 or T7 RNA polymerase (New England Biolabs, MA, USA), and digoxin (DIG)-labeled or fluorescein isothiocyanate (FITC)-labeled deoxynucleotides (dNTPs; Roche, Basal, Switzerland). Riboprobe synthesis reactions were performed per Table 2.1, with riboprobes spanning the entire nucleotide sequence.

Table 1.1: Riboprobe synthesis reactions.

The synthesis of specific riboprobes was performed as outlined. The mRNA targeted by the riboprobe, the species of the mRNA target, the plasmid from which each DNA template was generated, the accession number corresponding to target DNA template, the source of the plasmid DNA, the restriction enzyme used to linearise the plasmid DNA (cutting at the 5' end), the RNA polymerase employed for the synthesis of the riboprobe, and whether riboprobe was generated using fluorescein isothiocyanate (FITC)-labeled or digoxin (DIG)-labeled deoxynucleotides (dNTPs) is defined.

Gene target	Species	Plasmid	Source	Linearisation enzyme	RNA pol. enzyme	dNTP label
STIM1	Mouse	pCMV-SPORT6-STIM1	SourceBiosciences, Nottingham, UK	SalI	T7	DIG
STIM2	Mouse	pCR4-TOPO-STIM2	SourceBiosciences, Nottingham, UK	NotI	T3	DIG
Orai1	Mouse	pCMV-SPORT6-Orai1	SourceBiosciences, Nottingham, UK	NotI	T3	FITC
Orai2	Mouse	pCR-BluntII-TOPO-Orai2	SourceBiosciences, Nottingham, UK	BamHI	T7	FITC
Orai3	Mouse	pDNR-LIB-Orai3	SourceBiosciences, Nottingham, UK	EcoRI	T3	FITC
PDGFRα	Mouse	pBluescript- PDGFRα	(Rivers et al., 2008)	HindIII	T7	FITC
zSTIM1a	Zebrafish	pExpress-1-zSTIM1a	SourceBiosciences, Nottingham, UK	EcoRI	T7	DIG

2.2.4. *In situ* hybridisation: cryosections

To investigate STIM and Orai expression in the embryonic nervous system, cryosections of mouse or zebrafish tissue were probed for STIM or Orai mRNA by *in situ* hybridisation. Tissues harvested from mice at E13, E15 and P5, as well as zebrafish embryos at 12, 24, 48, 72 and 96 hours (hr) post fertilisation, were fixed in 4% (w/v) paraformaldehyde (PFA; Sigma-Aldrich, MI, USA) in diethyl pyrocarbonate (DEPC)-treated phosphate buffered saline (PBS) overnight at 4°C. Mouse tissues were cryoprotected in DEPC-treated 20% sucrose solution overnight at 4°C. Zebrafish tissue was cryoprotected by sequential overnight incubations at 4°C in DEPC-treated 15, 20, and 30% sucrose solutions. Tissues were mounted in Tissue-Tek O.C.T. compound (Sakura Finetek, CA, USA), rapidly frozen, and stored at -80°C. Sections were cut on a CM 1850 cryostat (Leica Microsystems, Germany) at 15-20 μm, mounted onto glass slides (Dako FLEX IHC microscope slides; Agilent Technologies, CA, USA), air dried for 4 hr, and, if required, stored at -20°C

To perform *in situ* hybridisation on cryosections, each riboprobe was first denatured at 70°C for 5 min in pre-heated *hybridisation solution* [50% formamide (Sigma-Aldrich), 0.1 mg/mLyeast tRNA (Roche), 10% (w/v) dextran sulphate, 1X Denhardt's solution and 1X hydridisation salts solution (0.2 M NaCl, 5 mM EDTA, 10 mM Tris-HCl pH 7.5, 5 mM NaH_2PO_4, 5 mM Na_2HPO_4); 1:1,000 dilution]. Once denatured, riboprobes were immediately added to tissue sections and incubated in a sealed humidified hybridisation chamber overnight at 65°C. Following hybridisation, tissue sections were washed in 65°C wash buffer (50% formamide, 1X hydridisation salts solution, 0.1% Tween-20), and maleic acid buffer containing Tween-20 (MABT; 100 mM malaeic acid, 150 mM NaCl, 0.1% Tween-20). Sections were blocked at room temperature for 1 hr with *in situ* blocking solution [2% blocking reagent (Sigma-Aldrich) 10% heat inactivated sheep serum (Invitrogen) in DEPC-treated PBS], before riboprobes were labeled by overnight incubation at 4°C with alkaline phosphatase (AP)-conjugated anti-DIG Fab fragments or anti-FITC Fab fragments (Roche; 1:1,1000 in PBS pH 7.4). Anti-DIG and anti-FITC Fab fragments were subsequently detected using AP-catalysed fluorescent or chromogenic substrates as outlined below.

To detect riboprobes using a chromogenic reaction, sections were first incubated for 15 minutes at room temperature in *pre-developing buffer* (100 mM NaCl, 50 mM $MgCl_2$, 100 mM Tris pH 9.8). 5-bromo-4-chloro-3-indolyl-phosphate (BCIP; Roche) and nitroblue tetrazolium (NBT; Roche) containing developing buffer (BCIP/NBT at 1:1,000 in *pre-developing buffer*) was then applied to tissue sections and incubated at 37°C for 2-4 hr until colour had developed sufficiently. Sections were subsequently dehydrated in ascending concentrations of ethanol, xylene washed, and mounted in DPX mounting media (Sigma-Aldrich). Images were acquired using a DM2500 M microscope (Leica Microsystems) equipped with a HC Plan Fluotar 10x objective (Leica Microsystems), or a Zeiss Lab.A1 microscope equipped with a N-Achroplan 5x objective (Carl Zeiss, Germany).

To detect riboprobes by fluorescence microscopy, fast red solution [Fast Red tablet (Roche) dissolved in 0.1M Tris pH 8.0/0.4M NaCl] was applied to tissue and incubated at 37°C for 2-3 hr. To visualise nuclei, sections were incubated with 4',6-diamidino-2-phenylindole (DAPI; Sigma-Aldrich) for 10 min at 1:20,000 in PBS, before slides were mounted in fluorescence mounting medium (Agilent Technologies). Images were acquired using an BX50 microscope (Olympus, Tokyo, Japan) equipped with a UPlanSApo 60x-1.35-water immersion objective and a PlanApo 40x air objective (Nikon, Tokyo, Japan), a CoolSNAP HQ^2 CCD camera (Photometrics, AZ, USA), and NIS Elements 6 software (Nikon). Images were prepared for manuscript using ImageJ (National Institute Health (NIH), MD, USA) and Adobe Illustrator CS6 (Adobe Systems, CA, USA).

2.2.5. *In situ* hybridisation: zebrafish whole mounts

To prepare zebrafish embryos for whole mount *in situ* hybridisation, fixed embryos were first permeabilised by dehydration in ascending concentrations of methanol (50-100%), and then stored overnight at -20°C in 100% methanol. To aid the entry of riboprobes, embryos were permeabilised by digestion in Proteinase K (PK, 10 μg/mL in DEPC-treated PBS; ThermoFisher Scientific, CA, USA) for a maximum of 15 min (depending on developmental stage). To stop PK activity, embryos were rinsed twice in glycine (26.6 μM) and post-fixed for 20 min in DEPC-treated 4% PFA. For hybridisation of

riboprobes, embryos were first pre-incubated with hybridisation buffer for 10 min at 65°C. Riboprobes were denatured at 70°C for 5 min in hybridisation solution before being added to embryos and incubated at 65°C for 48 hr. To visualise riboprobes, embryos were incubated with anti-DIG-AP Fab fragments or anti-FITC-AP Fab fragments (1:500 in MABT) for 48 hr at 4°C, which were then detected by incubation with a chromogenic substrate (NBT/BCIP) for 4-8 hr at 37°C. For imaging, embryos were cleared by incubating overnight at 4°C with glycerol, before being mounted in glycerol. Images was acquired with a SZX16 zoom stereo-microscope (Olympus) equipped with a DFC295 CMOS camera (Leica Microsystems). Images were prepared using ImageJ (NIH) and Adobe Illustrator CS6 (Adobe).

2.2.6. Immunohistochemistry

Tissues from E13, E15 and P5 mice were fixed and sectioned for immunohistochemistry as described above for *in situ* hybridisation (Section 2.2.3). Cryosections were blocked and permeabilised for 1 hr at room temperature with 5% normal goat serum and 0.4% Triton X-100 in PBS pH 7.4. Primary antibodies for STIM1 (rabbit polyclonal, Sigma-Aldrich; 1:500), STIM2 (rabbit polyclonal, Alamone labs, Israel; 1:500), Nestin (mouse monoclonal, BD Biosciences, NJ, USA; 1:1,000) and NeuN (mouse monoclonal, Biosenses Laboratories, Norway; 1:750) were detected using Alexa Fluor-488/594 conjugated secondary antibodies (ThermoFischer; 1:1,000). Images were acquired with a BX50 microscope (Olympus) equipped with a UPlanSApo 60x-1.35 NA water immersion lens (Nikon), a PlanApo-40X lens (Nikon), a PlanApo-20X, or a PlanApo-4X lens with a CoolSNAP HQ^2 CCD camera (Photometrics), and NIS elements software (Nikon). ImageJ (NIH) and Adobe Illustrator CS6 (Adobe) was used to prepare images.

2.2.7. Analysis of STIM1 protein homology in zebrafish

Zebrafish STIM1 orthologs were identified from a library of translated nucleotides (tblastn tool; National Center for Biotechnology Information (NCBI)) using the human STIM1 sequence as a reference sequence. To confirm the specificity of this bioinformatic approach to identify zebrafish STIM1 orthologs, the same approach was used to identify

STIM1 orthologs in species where STIM1 function has previously been studied. Accordingly, STIM1 orthologs were also identified for mouse (*Mus musculus*), rat (*Rattus norvegicus*), *Xenopus* (*Xenopus tropicalis*) and *Drosophila* (*Drosophila melanogaster*). Furthermore, as two STIM1 orthologs were predicted to exist in zebrafish, the human STIM2 protein sequence was used to identify zebrafish zSTIM2 orthologs to exclude the possibility that a second zSTIM1 ortholog is zSTIM2.

To calculate the degree of protein sequence homology between human and zebrafish STIM1 proteins, the protein sequence alignment tools Megablast and Blastp (NCBI) were used to compare protein sequences with the human STIM1 protein sequence. To confirm the specificity of this approach, protein sequences for mouse, rat, *Xenopus* and *Drosophila* STIM proteins served as controls (for a list of STIM protein sequences used in the bioinformatic analyses see Table 2.2). Protein sequence homology was assessed by comparing protein sequence coverage and conservation. Domain coverage was calculated as the percentage of the total query protein sequence that aligned to the human STIM1 protein sequence. Whereas domain conservation was calculated as the percentage of identical amino acids to human STIM protein sequence within the across the aligned protein sequence. Together, these parameters provide information regarding the amount of the query protein that can be aligned to human STIM1, as well as the degree of homology in the region of the query protein that aligns with human STIM1.

Species	Protein	Protein accession number
Homo sapiens	STIM1	NP_003147.2
Homo sapiens	STIM2	NP_001162589.1
Mus musculus	STIM1	NP_033313.2
Rattus norvegicus	STIM1	NP_001101966.2
Xenopus tropicalis	xSTIM1	NP_001090506.1
Danio rerio	zSTIM1a	NP_001038264.1
Danio rerio	zSTIM1b	NP_001189470.1
Danio rerio	zSTIM2a	XP_002660454.3
Danio rerio	zSTIM2b	XP_692356.4
Drosophila melanogaster	dSTIM	NP_996470.2

Table 2.2: STIM protein sequences used for protein sequence analyses.

The species, protein name, and protein accession number are provided for each of the STIM proteins used in the bioinformatic analyses.

2.3. Results

2.3.1. STIM and Orai are expressed in the embryonic mouse nervous system

The expression of the molecular constituents of SOCE, STIM1-2 and Orai1-3, is poorly characterised in the developing nervous system. However, STIM1 transcripts are reported to be present throughout the mouse brain at E16 (Stiber et al., 2008), and presented in DRG sensory neurons express STIM1 at E16 (Dziadek and Johnstone, 2007), suggesting that the constituents of SOCE are expressed in the developing nervous system by E16. To examine the distribution of STIM and Orai mRNA in the embryonic mouse nervous system, coronal sections were taken through the developing telencephalon and spinal cord at E15 to perform *in situ* hybridisation.

STIM1 and STIM2 transcripts were enriched in the dorsal and medial pallium, as well as in the lateral ganglionic eminence (Fig. 2.2a-b), suggesting that STIM proteins are widely expressed in the developing brain. STIM1 transcripts were detected at similar levels in the ventricular zone and cortical plate of the developing cortex, while STIM2 transcripts were enriched in the ventricular zone compared with the cortical plate (Fig. 2.1a-b), suggesting that STIM1 and STIM2 are differentially expressed in development. STIM1 and STIM2 transcripts were also present in the mouse spinal cord and associated DRG at E15 (Fig. 2. 1g-h), which is consistent with the detection of both STIM proteins in neonatal mouse spinal cord lysates (Xia et al., 2014). STIM expression in the DRG is also consistent with mouse DRG neurons expressing STIM1 at E16 (Dziadek and Johnstone, 2007), and STIM1 being required for axon guidance by DRG sensory neurons (Mitchell et al., 2012). Together, these findings indicate that STIM1 and STIM2 mRNA are widely expressed in the developing mouse nervous system, which is consistent with *in vitro* observations that SOCE regulates cellular process involved in neuronal development (Li et al., 2012; Mitchell et al., 2012; Shim et al., 2013; Hao et al., 2014; Somasundaram et al., 2014).

In situ hybridisation analysis of coronal sections through the developing telencephalon and spinal cord at E15 also revealed that Orai1-3 transcripts were expressed in an overlapping pattern with STIM1 and STIM2 transcripts in the mouse brain and spinal cord at E15 (Fig. 2.1). Orai1 transcripts were widely distributed, but detected at low

levels in the brain, detected in the dorsal and medial pallium, as well as the lateral ganglionic eminence (Fig. 2.1c). This observation is consistent with previous findings that Orai1 is diffusely expressed in the adult brain (Klejman et al., 2009). In contrast, Orai2 transcripts were also observed in the dorsal/medial pallium and lateral ganglionic eminence, however Orai2 transcripts were enriched in the intermediate zone and cortical plate (Fig. 2.1d). Orai3 transcripts were also observed in the dorsal/medial pallium and lateral ganglionic eminence, and detected at higher levels than Orai1 (Fig. 2.1e). Similar to STIM1-2 transcripts, Orai1-3 transcripts were widely distributed in the spinal cord and associated DRG at E15 (Fig. 2.1i-k), which is consistent with STIM and Orai proteins being expressed together in the neonatal mouse spinal cord (Xia et al., 2014). Although expression of the molecular constituents of SOCE overlapped in some regions of the developing nervous system, STIM and Orai transcripts were also detected in discrete patterns. As Orai1-3 confer CRAC channels with distinct calcium influx properties (DeHaven et al., 2007; Lis et al., 2007), and STIM1 and STIM2 activate SOCE in response to different levels of calcium depletion from the ER (Stathopulos et al., 2006; Brandman et al., 2007; Thiel et al., 2013), these results suggest that cells express different molecular constituents of SOCE as a mechanism to regulate calcium signaling in development.

Figure 2.1: STIM1 and STIM2 transcripts are expressed with Orai1-3 transcripts in the embryonic mouse brain and spinal cord.

In situ hybridisation on coronal sections of the mouse brain and spinal cord at E15. **(a-e)** Coronal sections through the telencephalon at E15 illustrate STIM and Orai transcript expression in the developing brain. (a) STIM1 transcripts were distributed throughout the ventricular zone and cortical plate of the dorsal and medial pallium. STIM1 transcripts were also observed in the lateral ganglionic eminence. (b) The pattern of STIM2 transcript expression resembles STIM1 transcript expression in the developing brain at E15. However, more intense STIM2 transcript expression is observed in the ventricular zone of the dorsal and medial pallium, as well as the lateral ganglionic eminence. (c) Orai1 transcript expression parallels STIM1 and STIM2 transcript expression, and is diffusely observed in the ventricular zone of the dorsal and medial pallium, as well as the lateral ganglionic eminence. (d) Orai2 transcripts were most evident in the cortical plate of the dorsal and medial pallium, and exhibit intense expression in the intermediate/subplate zones between the ventricular zone and the cortical plate. (e) Orai3 transcript expression is diffuse within the developing brain. (f) *in situ* hybridisation for PDGFRα transcipts (specific for oligodendrocyte progenitor cells) was used as a positive control for the method (a-e). **(g-k)** Coronal sections through the rostral spinal cord at E15 demonstrates that STIM and Orai transcripts are similarly expressed in the developing spinal cord. (g) STIM1 transcripts were detected throughout the dorsal and ventral horns of the spinal cord at E15. STIM1 transcripts were also detected in the associated dorsal root ganglion. (h-k) STIM2 and Orai1-3 transcript expression parallels STIM1 transcript expression in the spinal cord at E15. (l) PDGFRα riboprobe is a positive control to show the specificity of the hybridisation reaction. *Scale bars illustrate 20 μm for (a-f) and 40 μm for (g-l). Anatomical landmarks in (a) and (g) are correct for all images of the brain and spinal cord respectively. Abbreviations: CP = cortical plate; DH = dorsal horn; DRG = dorsal rot ganglion; DP = dorsal pallium; IZ = intermediate zone; LGE = lateral ganglionic eminence; MP = medial pallium; VH = ventral horn; VZ = ventricular zone.*

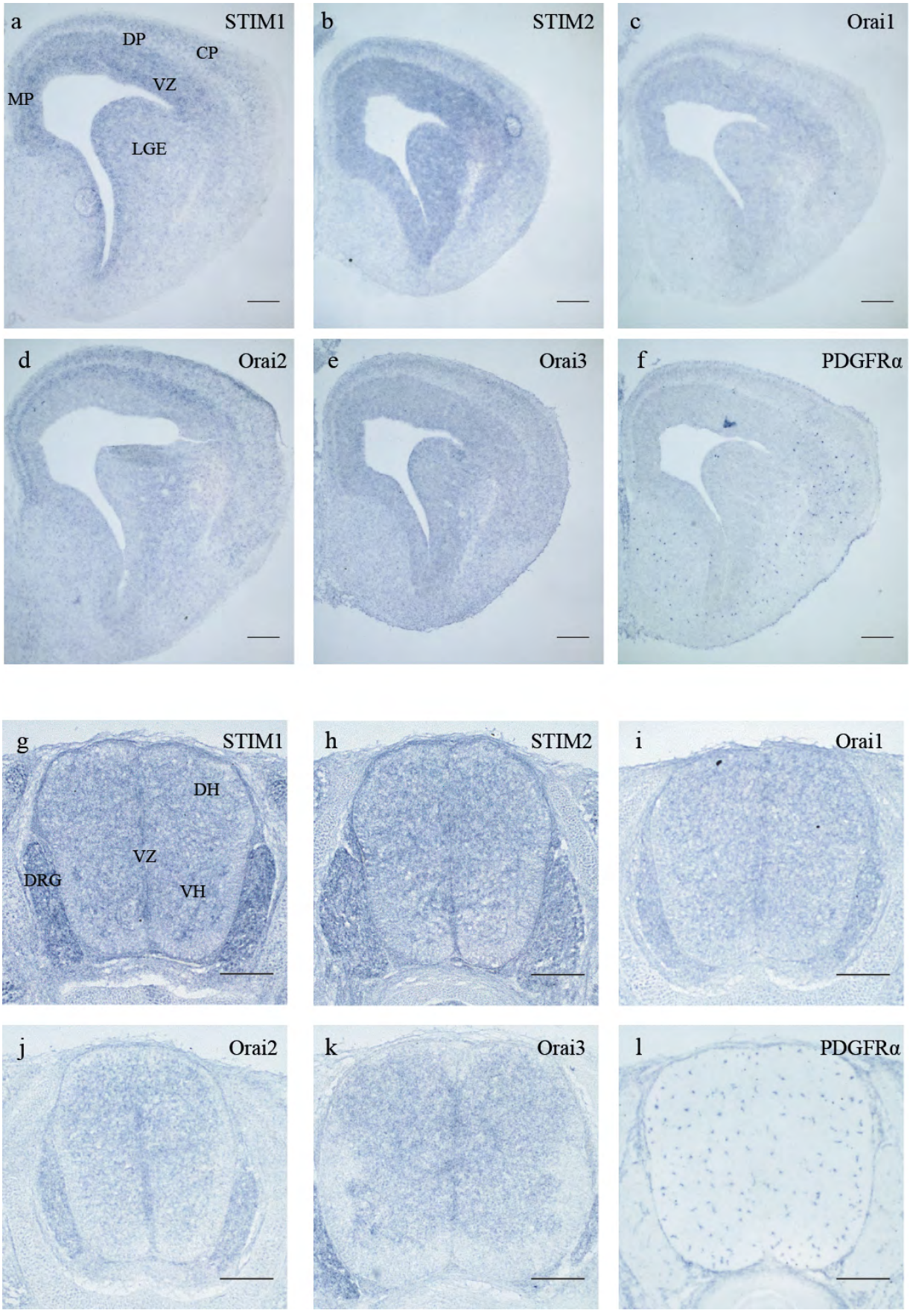
a
STIM1
DP
CP
VZ
MP
LGE
b
STIM2
c
Orai1
d
Orai2
e
Orai3
f
PDGFRα
g
STIM1
DH
VZ
DRG
VH
h
STIM2
i
Orai1
j
Orai2
k
Orai3
l
PDGFRα

To further investigate the regional expression of STIM1 and STIM2 in development, the expression pattern of STIM1 and STIM2 transcripts was examined at higher power using fluorescence *in situ* hybridisation. STIM1 and STIM2 transcripts exhibited distinct patterns of expression in the mouse cortex and spinal cord at E15 (Fig. 2.2 and Fig 2.3). Low power images confirmed that STIM1 and STIM2 transcripts were present throughout the brain at E15 (Fig. 2.2a-b, e-f). Higher power images showed that STIM1 transcripts are present at similar levels in the ventricular zone and cortical plate at E15 (Fig. 2.2c-d). While STIM2 transcripts were also present in the ventricular zone and cortical plate of the developing cortex, dissimilar to STIM1, STIM2 transcripts appeared abundant in the ventricular zone, but reduced in the cortical plate (Fig. 2.2g-h), suggesting that STIM2 expression may be downregulated with neuronal maturation. STIM1 transcripts were also detected throughout the grey matter of the spinal cord at E15 (Fig. 2.3a-b), with an enrichment of STIM1 transcripts in the ventricular zone and within the ventral horn (Fig. 2.3c-d). STIM1 transcripts were also enriched in the DRG (Fig. 2.3c-d), supporting previous studies that showed STIM1 expression in rodent DRG neurons (Dziadek and Johnstone, 2007; Gasperini et al., 2009; Mitchell et al., 2012). Furthermore, STIM2 transcripts detected in the spinal cord were more diffuse than STIM1 transcripts (Fig. 2.3e-h), providing further evidence that STIM1 and STIM2 have different patterns of expression in the developing nervous system. As STIM1 and STIM2 mRNA were previously reported to be expressed in most embryonic tissues (Williams et al., 2001; Dziadek and Johnstone, 2007; Oh-Hora et al., 2008; Stiber et al., 2008), a zero riboprobe control served as a negative control for the hybridisation reactions *in lieu* of tissue negative for STIM1 or STIM2. An absence of signal in the zero riboprobe control demonstrated specificity of the hybridisation reactions for STIM1 and STIM2 riboprobes (Fig. 2.2i-j and Fig. 2.3i-j). Taken together, these data confirm that STIM1 and STIM2 transcripts are present in the embryonic mouse nervous system and, for the first time, illustrate the distinct patterns of STIM1 and STIM2 mRNA localisation, which suggests that STIM proteins have different roles in development.

Figure 2.2: STIM1 and STIM2 transcripts exhibit distinct patterns of expression in the mouse cortex at E15.

In situ hybridisation for STIM1 and STIM2 on coronal sections taken from the caudal telencephalon at E15. **(a-b)** STIM1 transcripts are widely expressed in the mouse brain at E15. **(c-d)** Higher resolution images of the cortex, indicated by the box in (a-b), illustrate that STIM1 transcripts are present at similar levels in the ventricular zone and cortical plate of the cortex at E15. **(e-f)** STIM2 transcripts are also present in the mouse brain at E15. **(g-h)** Higher resolution images of the cortex, which is indicated by the box in (a-b), illustrate that STIM2 transcript expression is prominent in the ventricular zone, comparable with STIM1 transcript expression, but lower in the cortical plate compared with STIM1 transcripts. **(i-j)** Absence of fluorescence in the zero riboprobe control demonstrates the specificity of the hybridisation reaction for STIM1 and STIM2 riboprobes.

Scale bar denotes 200 µm for images (a), (b), (e), (f), (i) and (j), but 10 µm for (c), (d), (g) and (h). Abbreviations: CP = cortical plate; Ctx = cortex; GE = ganglionic eminence; IZ = intermediate zone; VZ = ventricular zone.

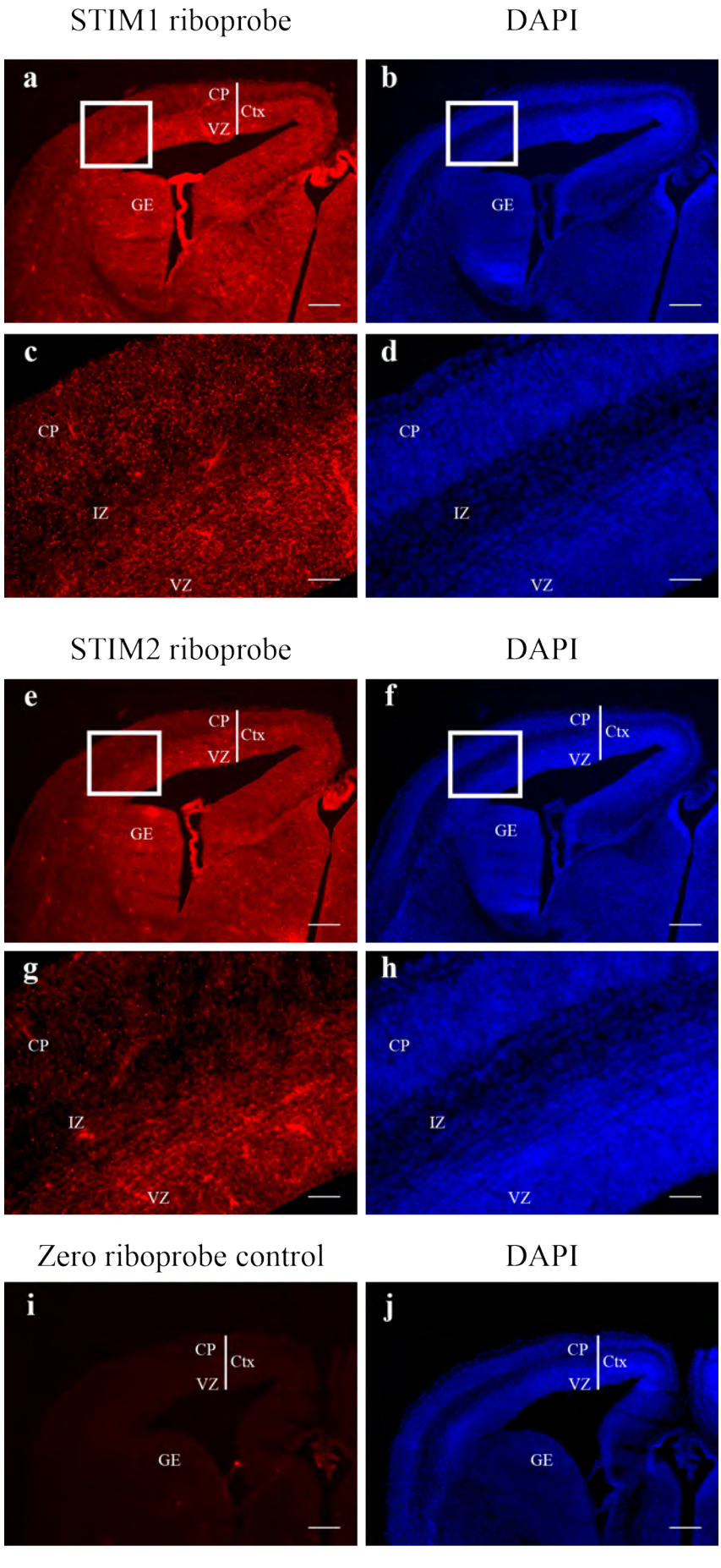
STIM1 riboprobe
DAPI
a
b
CP
Ctx
VZ
GE
c
d
CP
IZ
VZ
STIM2 riboprobe
DAPI
e
f
g
h
Zero riboprobe control
DAPI
i
j

Figure 2.3: STIM1 and STIM2 transcripts exhibit distinct patterns of expression in the spinal cord at E15.

In situ hybridisation on coronal tissue sections of the rostral mouse spinal cord at E15. **(a-d)** STIM1 transcripts are present in the mouse spinal cord at E15 throughout the grey matter (dashed line denotes the boundary between the grey and white matter), including in the ventricular zone and ventral horn. STIM1 transcripts are also present in the accompanying dorsal root ganglion. **(e-h)** STIM2 transcripts are widely expressed in the mouse spinal cord with diffuse STIM2 expression observed throughout the grey and white matter. STIM2 expression is also present within the dorsal root ganglion, albeit less strongly than STIM1. **(i-j)** Absence of fluorescence in the zero riboprobe control demonstrates specificity of the hybridisation reaction for STIM1 and STIM2 riboprobes in the cortex and spinal cord.

Scale bar denotes 200 µm for images (a), (b), (e) and (f), but 10 µm for (c), (d), (g) and (h). Abbreviations: DH = dorsal horn; DRG = dorsal root ganglion; GM = grey matter; VH = ventral horn; VZ = ventricular zone; WM = white matter.

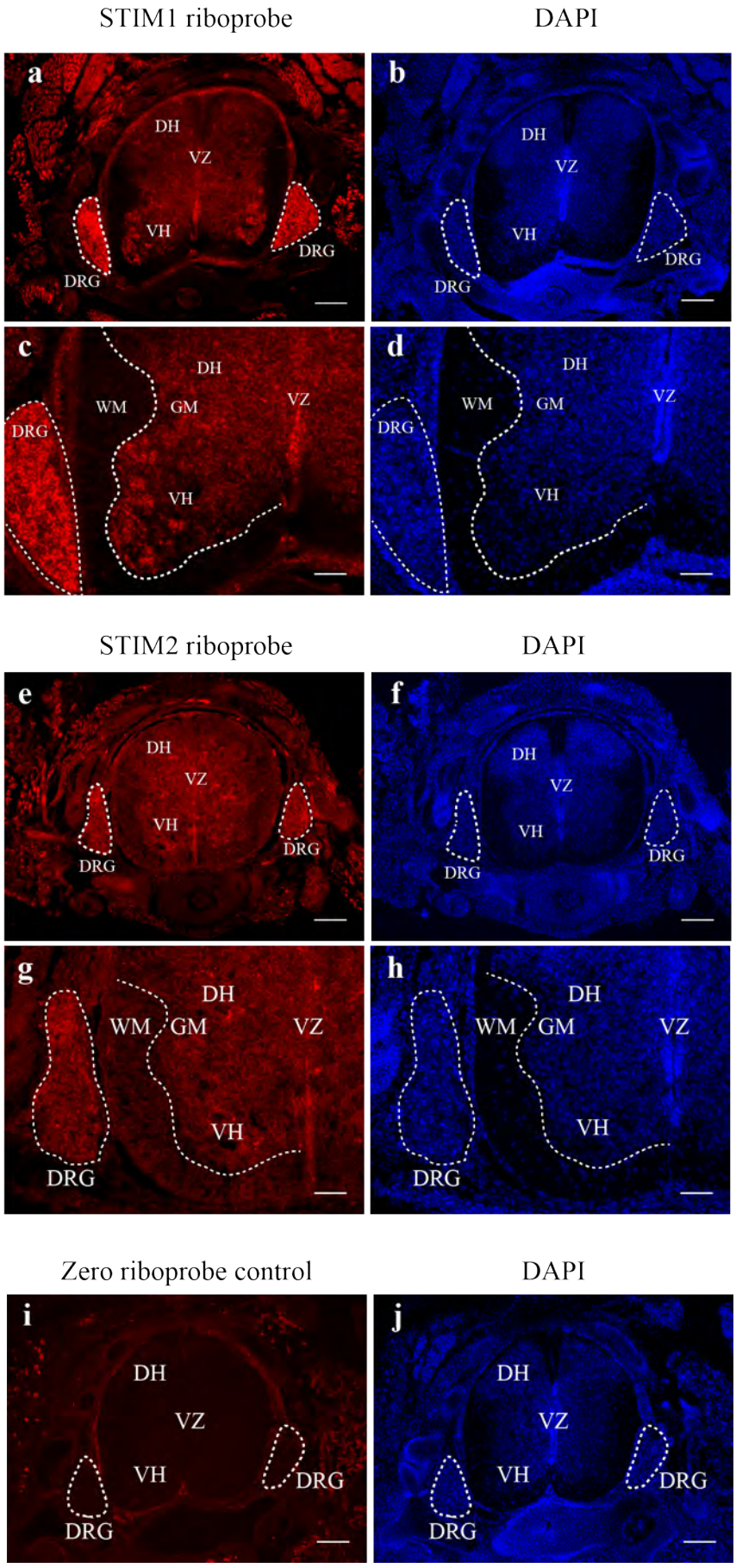
STIM1 riboprobe
DAPI
a
b
DH
VZ
VH
DRG
DRG
c
d
WM
GM
STIM2 riboprobe
e
f
g
h
Zero riboprobe control
i
j

2.3.2. STIM1 is the major neuronal STIM protein during development

Compared to STIM1 transcripts, STIM2 transcripts were detected at lower levels in the cortical plate and its expression was more diffuse within the spinal cord. The expression of STIM1 and STIM2 proteins in neurons is contentious, with some reports suggesting that STIM2 is the neuronal STIM protein in the embryonic and adult nervous systems (Berna-Erro et al., 2009; Skibinska-Kijek et al., 2009; Gruszczynska-Biegala et al., 2011), while other studies suggest that STIM1 and STIM2 are ubiquitously expressed, albeit at different levels, in the adult nervous system (Dziadek and Johnstone, 2007; Steinbeck et al., 2011; Xia et al., 2014). To determine whether STIM1 and STIM2 proteins are differentially expressed during development, immunohistochemistry was used to examine the pattern of expression for STIM1 and STIM2 in the cortex at E13, E15 and P5 to encompass early, mid and late stage corticogenesis (Sances et al., 2016).

STIM1 was widely expressed in the mouse cortex at E13, E15 and P5 (Fig. 2.4). At E13, STIM1 protein was widely expressed in the brain, with robust STIM1- immunoreactivity (IR) detected in both the dorsal pallium and the retrosplenial neocortex, with an enrichment of STIM1 expression observed in the ventricular zone (Fig. 2.4a-b). STIM1 protein expression remained high throughout the cortex at E15, with intense STIM1-IR detected in the ventricular zone and cortical plate (Fig. 2.4g-i). At P5, STIM1-IR was diffuse in all cortical layers, with diffuse cellular expression shown for layer IV-V (Fig 2.4o-p), which contains the first born, mature neurons of the cortex (Rakic et al., 2009). STIM2 protein was also expressed in the mouse cortex at E13, E15 and P5 (Fig. 2.4). Significantly, in contrast to STIM1, STIM2-IR at E13 and E15 was observed in process-like structures extending from the ventricular zone to the marginal zone of the developing cortex (Fig. 2.4c-d and j-l). However, by P5, STIM2-IR was no longer observed in process-like structures, but was widely expressed in the cortex, with diffuse cellular expression shown for layer IV-V (Fig. 2.4q-r), which was similar to STIM1 expression at P5. This observation that STIM2-IR localises to process-like structures in the embryonic cortex, but not the post-natal cortex, is indicative of radial glial expression (Anthony et al., 2004; Walker et al., 2010). Hence, these data suggest that STIM proteins are developmentally regulated and exhibit distinct patterns of expression in the embryonic nervous system.

Figure 2.4: STIM1 and STIM2 proteins exhibit different patterns of expression in the mouse cortex over a time course of development.

Immunohistochemistry for STIM1 and STIM2 on coronal sections of the mouse brain at E13 (a-f), E15 (g-n), and P5 (o-t). STIM1 protein is expressed in the mouse cortex throughout nervous system development. **(a-b)** Coronal section through the caudal telencephalon at E13 showing that STIM1 is widely expressed in the brain, with the presence STIM1-IR in the dorsal pallium and retrosplenial neocortex illustrating expression of STIM1 in the early neocortex. **(g-i)** Coronal section through the rostral telencephalon at E15 illustrating that STIM1 is widely expressed in the brain, with the presence of STIM1-IR in the ventricular zone and cortical plate showing diffuse STIM1 expression in the developing cortex. **(o-p)** Coronal section through the piriform cortex at P5, showing that STIM1-IR is detected throughout the cortex, with higher magnification of layer IV-V of the cortex illustrating the diffuse cell labelling of STIM1-IR in the cortex. STIM2 protein is expressed in the mouse cortex throughout nervous system development, but is observed in process-like structures in the embryonic nervous system. **(c-d)** Coronal section through the caudal telencephalon at E13 showing that STIM2 is widely expressed in the brain, with STIM2-IR localising to process–like structures that radiate away from the ventricular zone in both the dorsal pallium and retrosplenial neocortex (denoted by arrows). **(j-l)** Coronal section through the rostral telencephalon at E15 illustrating that STIM2 is widely expressed in the brain, with STIM2-IR still observed in process-like structures that radiate way from the ventricular zone and into the cortical plate (arrows). **(q-r)** Coronal section through the piriform cortex at P5 showing that STIM2-IR is observed throughout the cortex, with higher magnification of layer IV-V of the cortex showing that STIM2 exhibits diffuse cell expression in the cortex. **(e, m, s)** Zero primary antibody control (1ºAb control) probed with AlexFluor-594 illustrates the specificity of STIM1-IR and STIM2-IR. **(f, n, t)** Corresponding DAPI-stained images confirming that images (e, m, s) are from similar brain regions probed for STIM1 and STIM2 expression. *Scale bar denotes 200 µm for (a), (c), (g) and (j), 20 µm for (o) and (q), and 10 µm for remaining images. Asterisks indicate the location of the ventricle. Abbreviations: Ctx = cortex; CP = cortical plate; DP = dorsal pallium; GE = ganglionic eminence; PT = pretectum; RS = retrosplenial neocortex; vTH = ventral thalamus; VZ ventricular zone.*

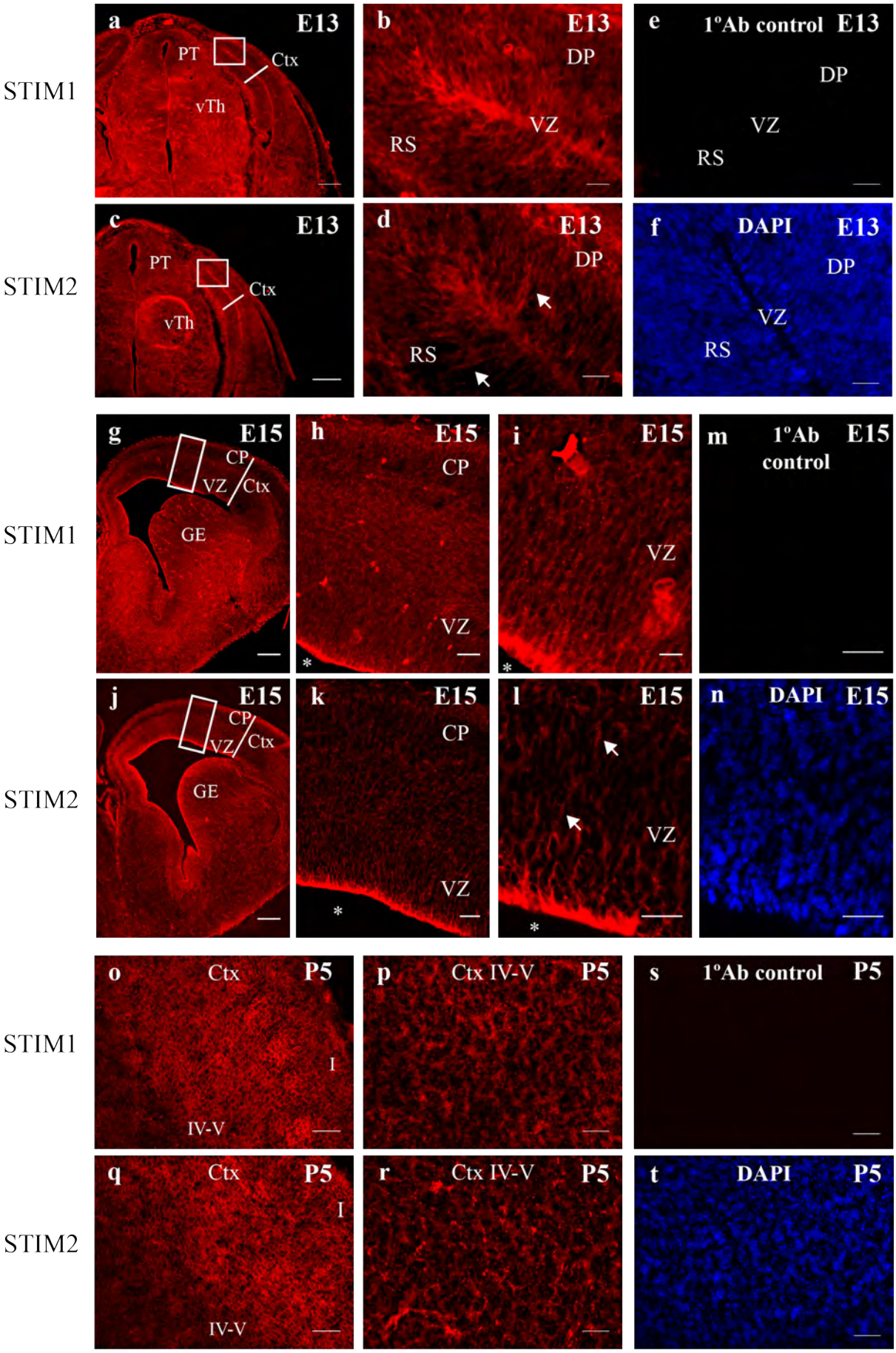
STIM1
STIM2
STIM1
STIM2
STIM1
STIM2
a E13
PT
Ctx
vTh
b E13
DP
VZ
RS
e 1°Ab control E13
DP
VZ
RS
c E13
PT
Ctx
vTh
d E13
DP
RS
f DAPI E13
DP
VZ
RS
g E15
CP
VZ
Ctx
GE
h E15
CP
VZ
i E15
VZ
m 1°Ab control E15
j E15
CP
VZ
Ctx
GE
k E15
CP
VZ
l E15
VZ
n DAPI E15
o Ctx P5
I
IV-V
p Ctx IV-V P5
s 1°Ab control P5
q Ctx P5
I
IV-V
r Ctx IV-V P5
t DAPI P5

To investigate whether STIM proteins are expressed in a cell-type specific manner in development, the expression of STIM1 and STIM2 proteins by NeuN-labelled neurons and nestin-labelled radial glial stem cells was examined in the E15 mouse spinal cord. Double immunolabelling for STIM1 with the neuronal nuclei marker NeuN showed that STIM1-IR is detected surrounding neuronal nuclei in the mouse spinal cord at E15 (Fig. 2.5a-h). An absence of co-localisation between STIM1-IR and nestin-IR revealed that STIM1 is not expressed by radial glia at E15 (Fig 2.6a-h). These findings suggest that STIM1 is expressed by neurons, but not radial glia, in the developing nervous system. In contrast, double immunolabelling for STIM2 with nestin revealed that STIM2-IR and nestin-IR are highly co-localised in the mouse spinal cord at E15 (Fig 2.7a-h). STIM2-IR was also observed in close proximity with NeuN-IR in the mouse spinal cord at E15 (Fig. 2.8a-h), albeit STIM2-IR was detected at lower levels than was observed for STIM1 (compare Fig. 2.8h with 2.4h).

Given that STIM2 co-localised with nestin-positive radial glia in the embryonic spinal cord, and STIM2-IR was localised to process-like structures in the embryonic cortex but not the post-natal cortex, it was reasoned that STIM2 is expressed by radial glia in the embryonic cortex. Double immunolabelling for STIM2 with nestin revealed that STIM2-IR is highly localised with nestin-IR within process like-structures (*arrows*) in the cortex at E15 (Fig. 2.9). In contrast, STIM1-IR and nestin-IR were not observed to co-localise in process-like structures in the embryonic cortex (Fig. 2.10). However, STIM1-IR and STIM2-IR were both highly co-localised with nestin-IR in cells lining the ventricle (Fig. 2.9 and Fig. 2.10), consistent with previous reports that STIM1 and STIM2 are co-expressed in neural progenitor cells (Li et al., 2012; Somasundaram et al., 2014). Moreover, previous work from this lab has also shown that STIM2 expression localises with glial fibrillary acidic protein (GFAP) positive astrocytes in the early post-natal rodent cortex (Hadrill et al., *in preperation*), as well as being localised to PDGFRα positive oligodendrocyte precursor cells in the embryonic mouse cortex (data not shown). However, STIM2 was not as strongly expressed in these cell types compared to radial glia. Taken together, these data suggest that STIM1 is more widely expressed in the nervous system compared with STIM2, with STIM2 expression largely restricted to radial glia in development. As such, it was concluded that STIM1 is the major neuronal STIM protein in development.

Figure 2.5: STIM1 is expressed by neurons in the mouse spinal cord at E15.

Immunolabelling for STIM1 (a,e), NeuN (b,f) and DAPI (c,g) on coronal sections of the mouse spinal cord at E15 illustrating STIM1-IR in neurons during nervous system development. **(a-d)** STIM1-IR is localised to neurons in the spinal cord at E15. Merged image (d) shows intense STIM1-IR (red) localised to the grey matter of the developing spinal cord and the accompanying DRG, which are indicated by NeuN-labelling of neurons (green). **(e-h)** Higher resolution images of the ventral horn, which is indicated by the box in (d). Merged image (h) illustrates that STIM1-IR (red) is localised to NeuN-positive neurons (green) within the spinal cord at E15. *Scale bar denotes 100 µm for images (a-d) and 10 µm for images (e-h). Abbreviations: DRG = dorsal root ganglion; GM = grey matter; VH = ventral horn; VZ = ventricular zone; WM = white matter.*

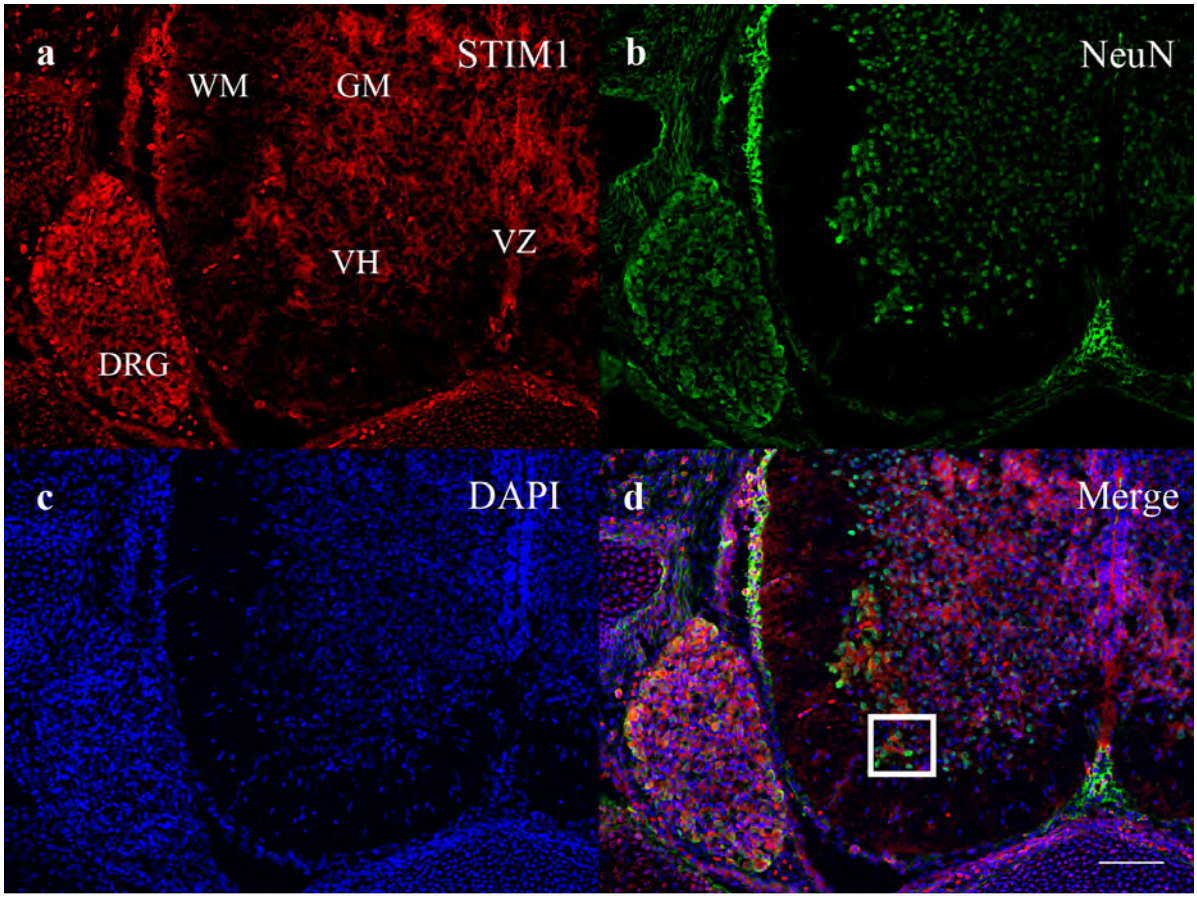
a
STIM1
WM
GM
VH
VZ
DRG
b
NeuN
c
DAPI
d
Merge

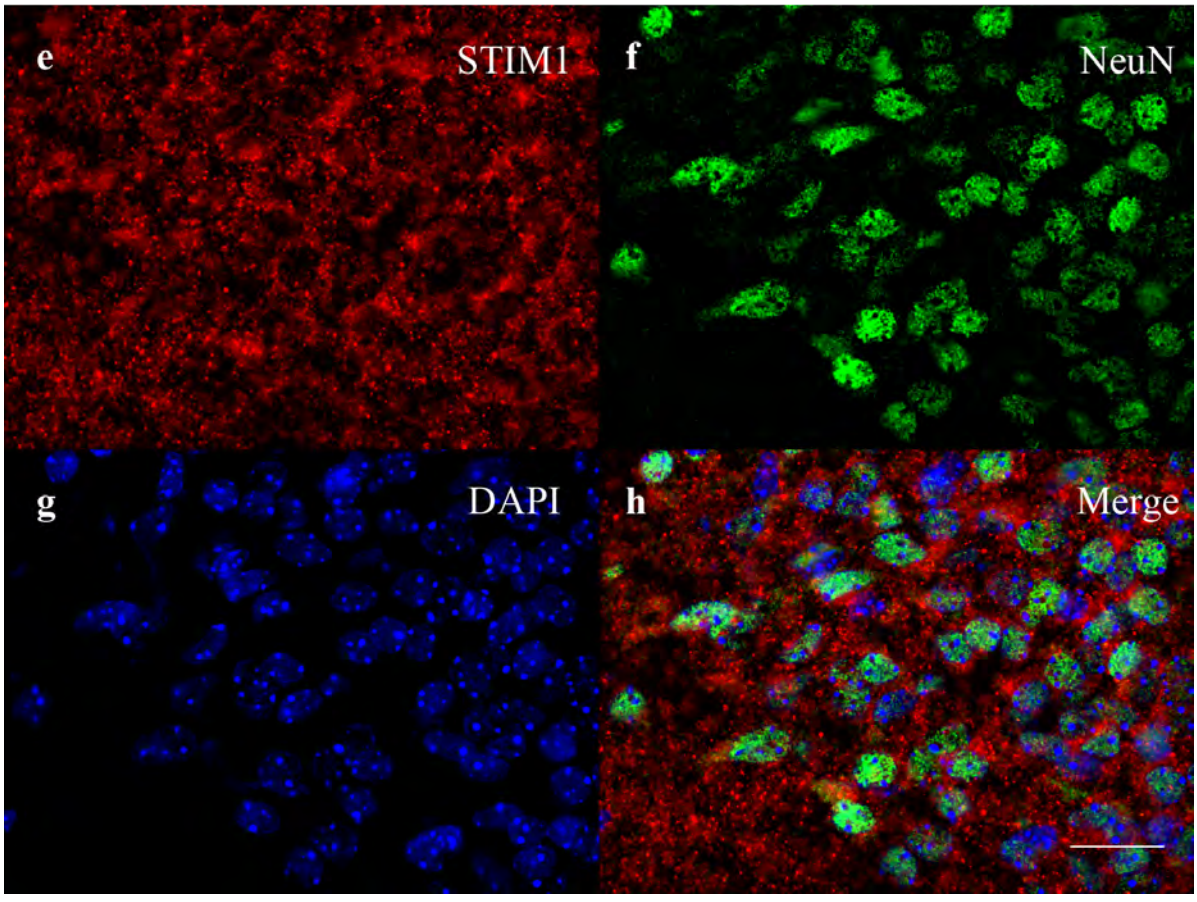
e
STIM1
f
NeuN
g
DAPI
h
Merge

Figure 2.6: STIM1 is not expressed by radial glia in the mouse spinal cord at E15.

Immunolabelling for STIM1 (a,e), nestin (b,f) and DAPI (c,g) on coronal sections of the mouse spinal cord at E15 illustrating that STIM1 is not expressed by radial glia in nervous system development. **(a-d)** STIM1-IR does not localise with radial glia in the spinal cord at E15. Merged image (d) shows that STIM1-IR (red) is present in the grey matter of the spinal cord at E15, while nestin-IR (green), a radial glia marker, is observed in process-like structures that traverse the spinal cord from the ventricular zone to the pial surface, indicative of radial glial processes. **(e-h)** Higher resolution images of the ventral horn, which is indicated by the box in (d). Merged image (h) illustrates that STIM1-IR (red) is not localised to nestin-positive radial glial processes (green) within the spinal cord at E15. *Scale bar denotes 100 µm for images (a-d) and 10 µm for images (e-h). Abbreviations: DRG = dorsal root ganglion; GM = grey matter; PS = Pial surface; VH = ventral horn; VZ = ventricular zone; WM = white matter.*

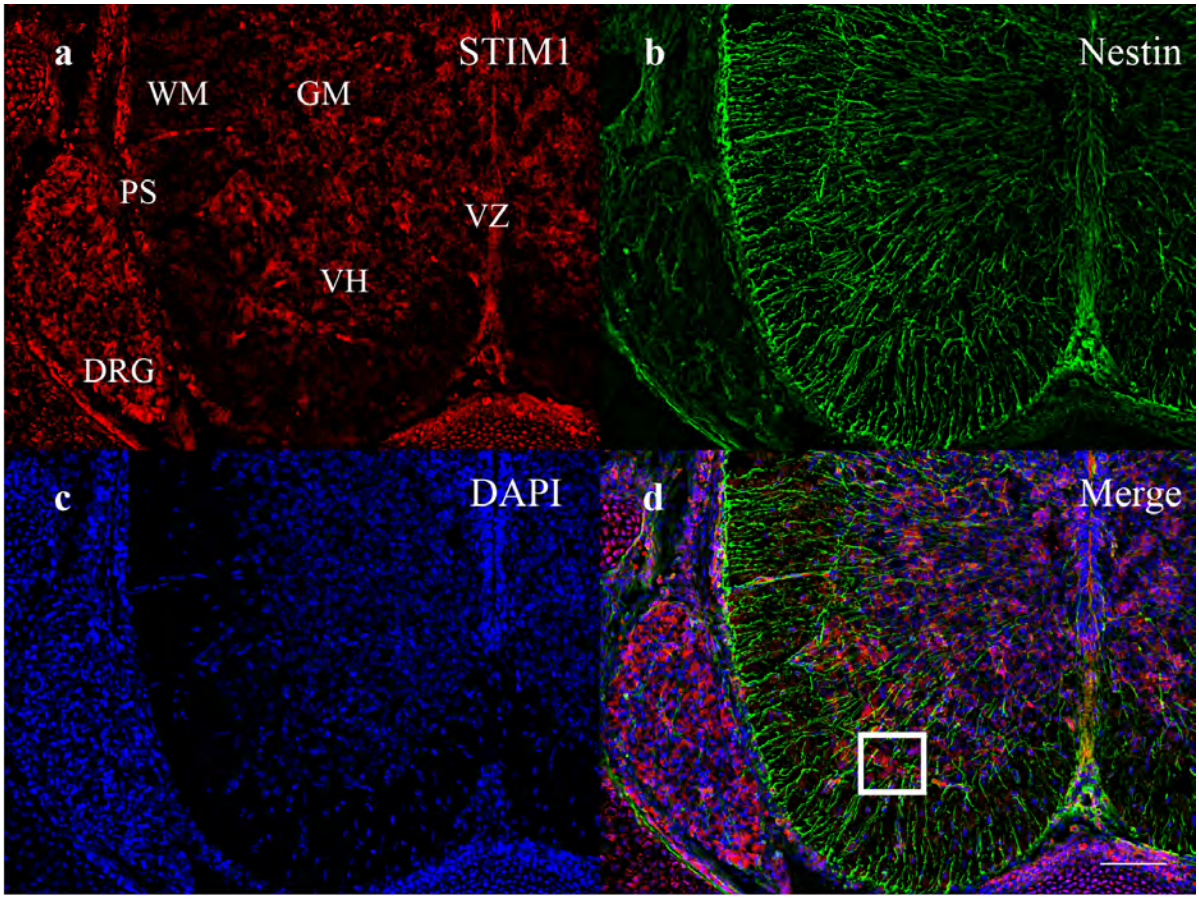
a
STIM1
WM
GM
PS
VZ
VH
DRG
b
Nestin
c
DAPI
d
Merge

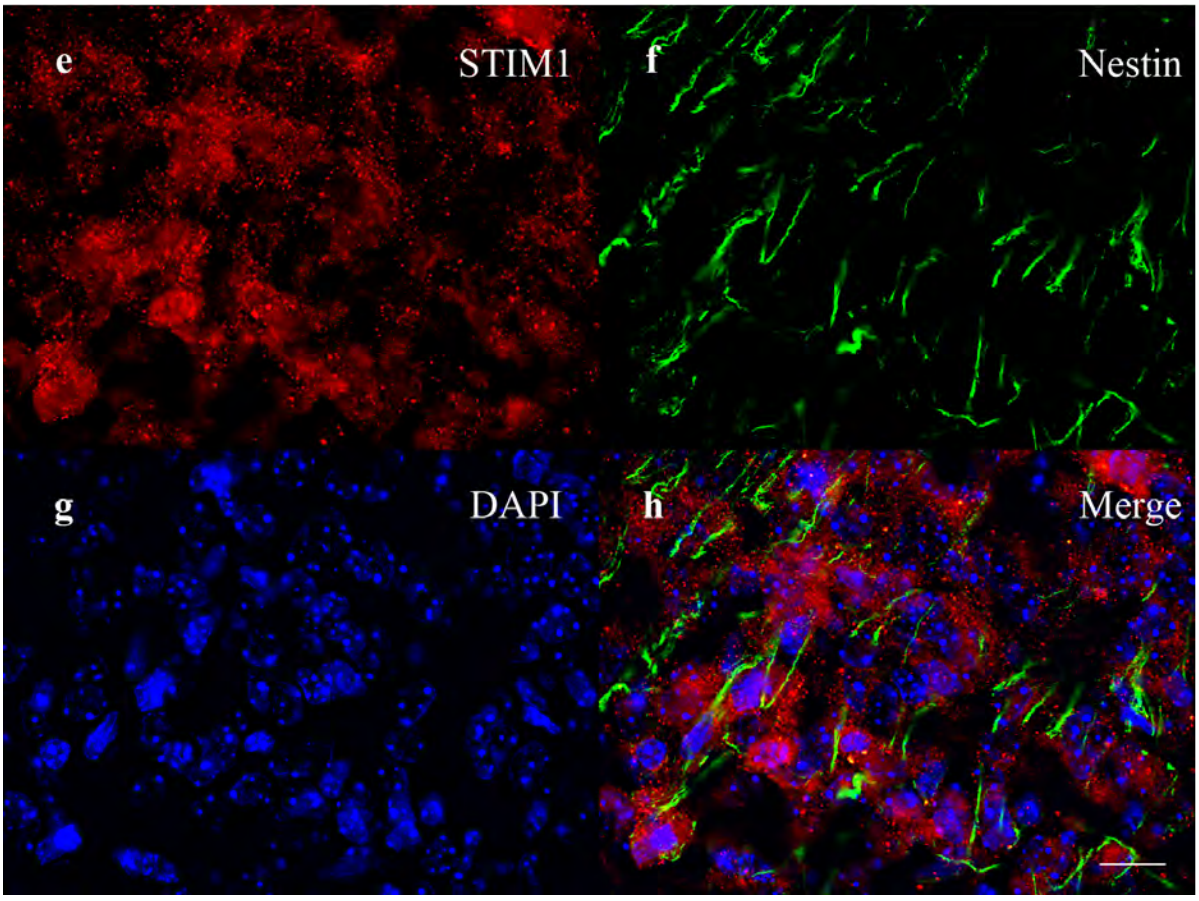
e
STIM1
f
Nestin
g
DAPI
h
Merge

Figure 2.7: STIM2 is expressed by radial glia in the mouse spinal cord at E15.

Immunolabelling for STIM2 (a,e), nestin (b,f) and DAPI (c,g) on coronal sections of the mouse spinal cord at E15 illustrating that STIM2 expression co-localises with the radial glia marker nestin in nervous system development. **(a-d)** STIM2-IR is localised with nestin-IR in the spinal cord at E15. Merged image (d) shows that STIM2-IR (red) and nestin-IR (green) co-localise in process-like structures that traverse the spinal cord from the ventricular zone to the pial surface, which are indicative of radial glial processes. **(e-h)** Higher resolution images of the marginal zone, which is indicated by the box in (d). Merged image (h) illustrates that STIM2-IR (red) is localised with nestin-IR (green) in radial glial processes within the spinal cord at E15. *Scale bar denotes 100 µm for images (a-d) and 10 µm for images (e-h). Abbreviations: DRG = dorsal root ganglion; GM = grey matter; PS = Pial surface; VH = ventral horn; VZ = ventricular zone; WM = white matter.*

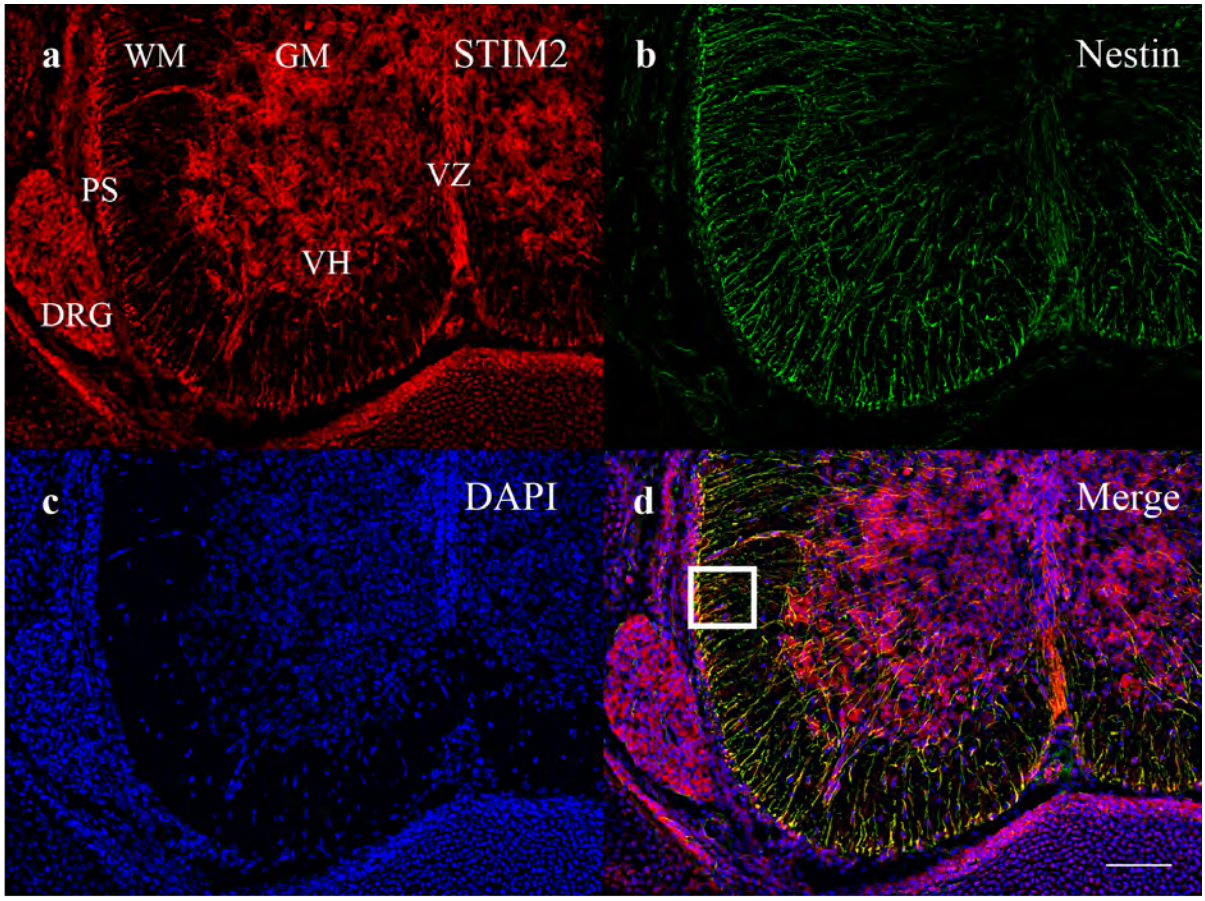
a
WM
GM
STIM2
PS
VZ
VH
DRG
b
Nestin
c
DAPI
d
Merge

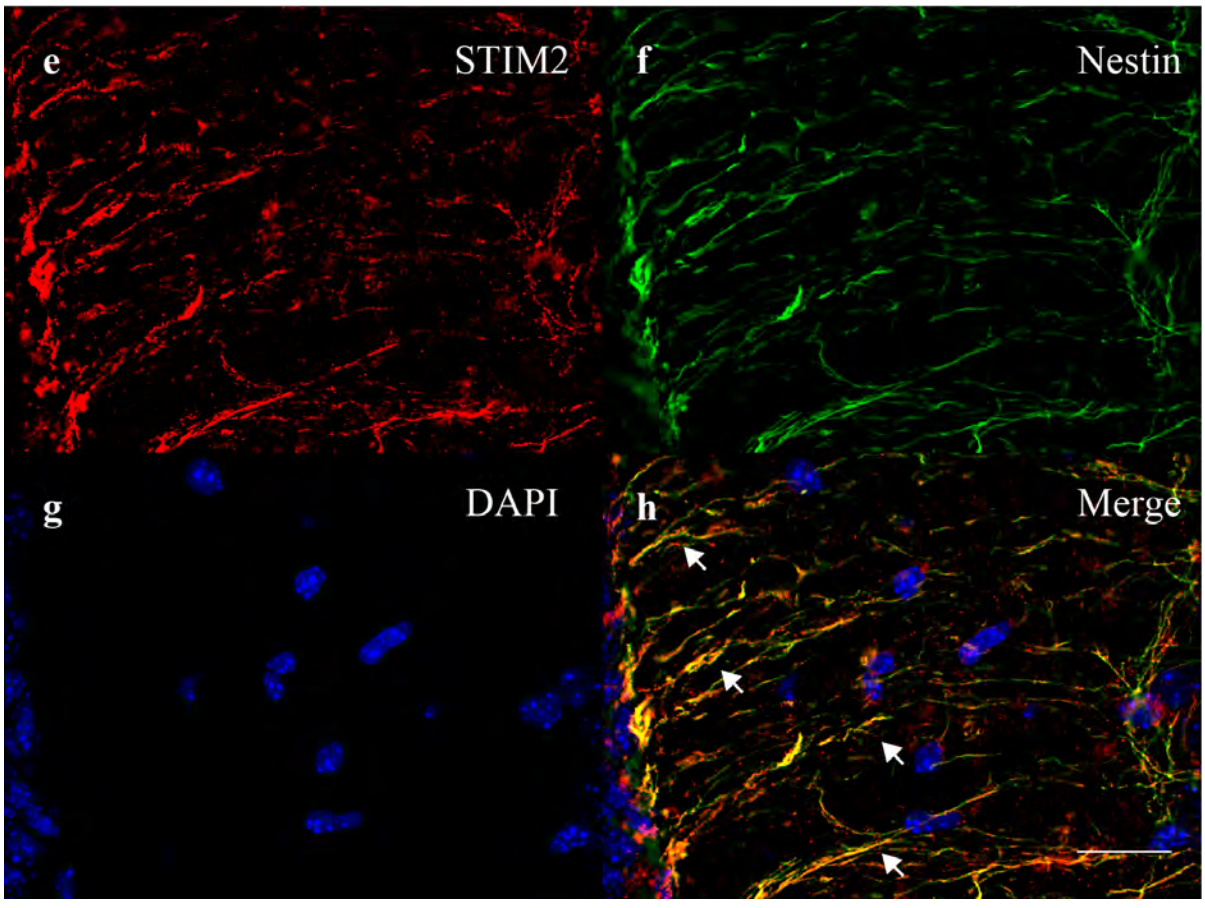
e
STIM2
f
Nestin
g
DAPI
h
Merge

Figure 2.8: STIM2 is expressed by neurons in the mouse spinal cord at E15, but at lower levels than STIM1.

Immunolabelling for STIM2 (a,e), NeuN (b,f) and DAPI (c,g) on coronal sections of the mouse spinal cord at E15 illustrating some STIM2 expression by neurons in nervous system development. **(a-d)** STIM2-IR is predominantly expressed in process-like structures clearly evident in the spinal cord white matter, but is also evident in the grey matter denoted by NeuN-IR. **(e-h)** Higher resolution images of the ventral horn area indicated in (d). Merged image (h) illustrates that STIM2-IR (red) is localised in process-like structures, but also weakly expressed in close proximity with neurons as denoted by NeuN-IR (green). *Scale bar denotes 100 µm for images (a-d) and 10 µm for images (e-h). Abbreviations: DRG = dorsal root ganglion; GM = grey matter; PS = Pial surface; VH = ventral horn; VZ = ventricular zone; WM = white matter.*

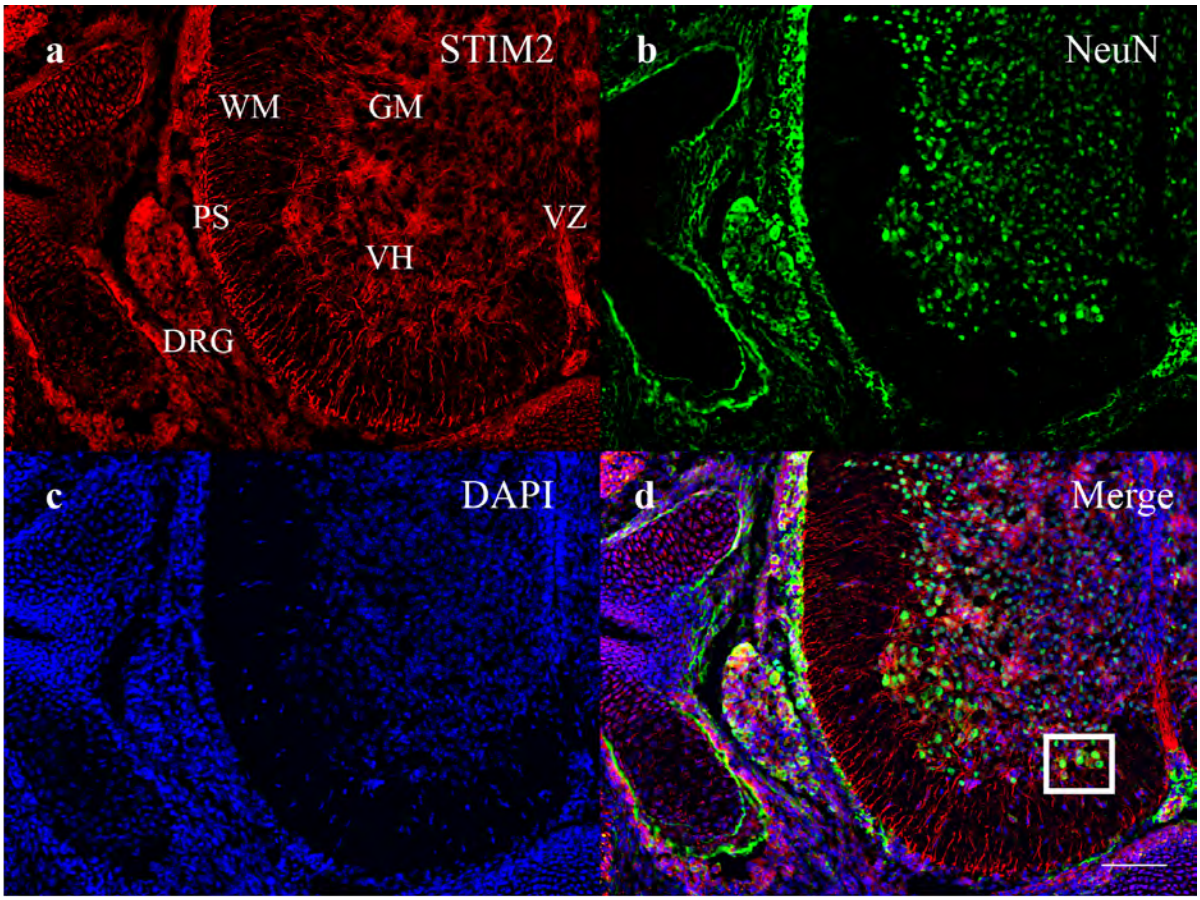
a
STIM2
WM
GM
PS
VZ
VH
DRG
b
NeuN
c
DAPI
d
Merge

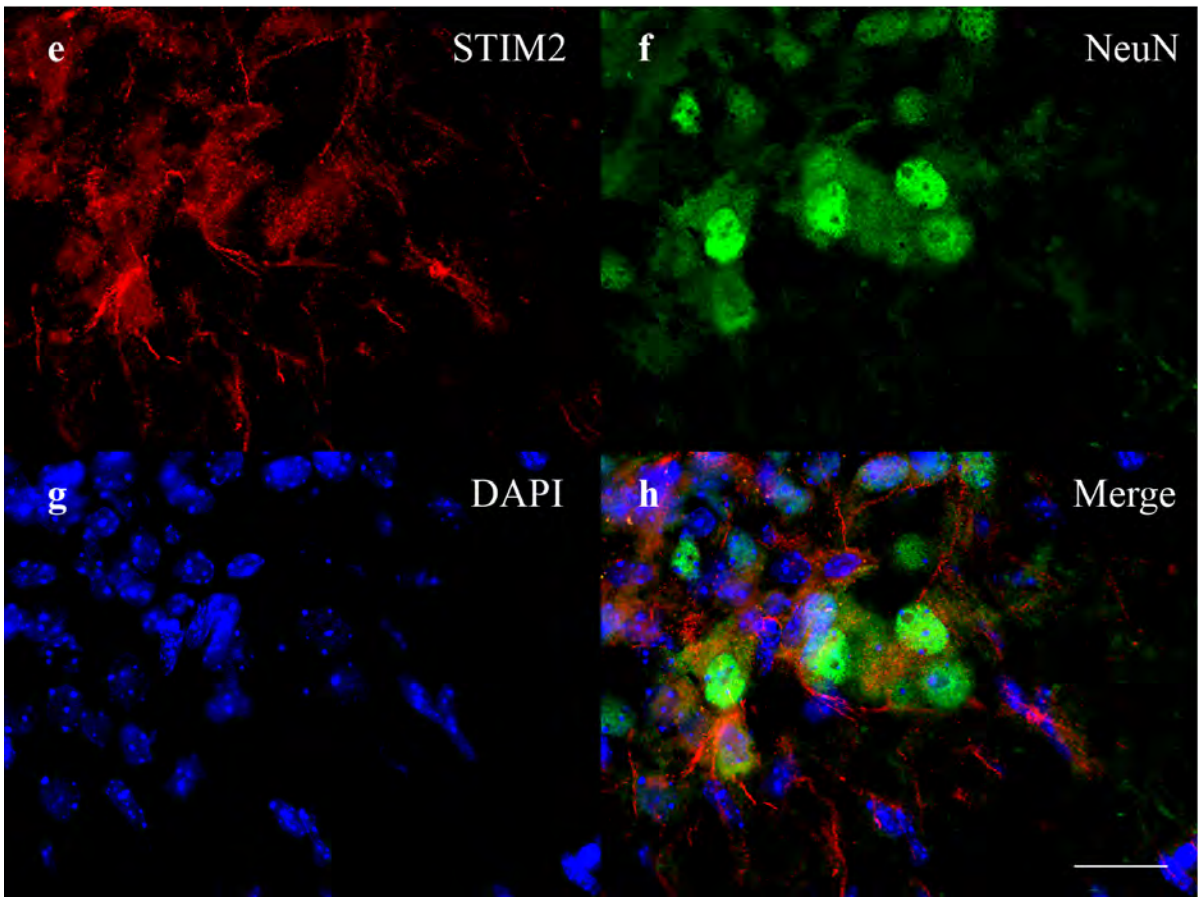
e
STIM2
f
NeuN
g
DAPI
h
Merge

Figure 2.9: STIM2 is expressed by radial glia in the mouse cortex at E15.

Immunolabelling for STIM2 and Nestin on coronal sections through the mouse cortex at E15. STIM2-IR (a-c) and Nestin-IR (d-f) in the cortex at E15, with merged images (g-i) illustrating the localisation of STIM2-IR to radial glia in the embryonic cortex. *Scale bar denotes 200 µm for images (a), (d) and (g), 20 µm for images (b), (e) and (h), and 10 µm for images (c), (f) and (i). Abbreviations: CP = cortical plate; Ctx = cortex; GE = ganglionic eminence; VZ = ventricular zone.*

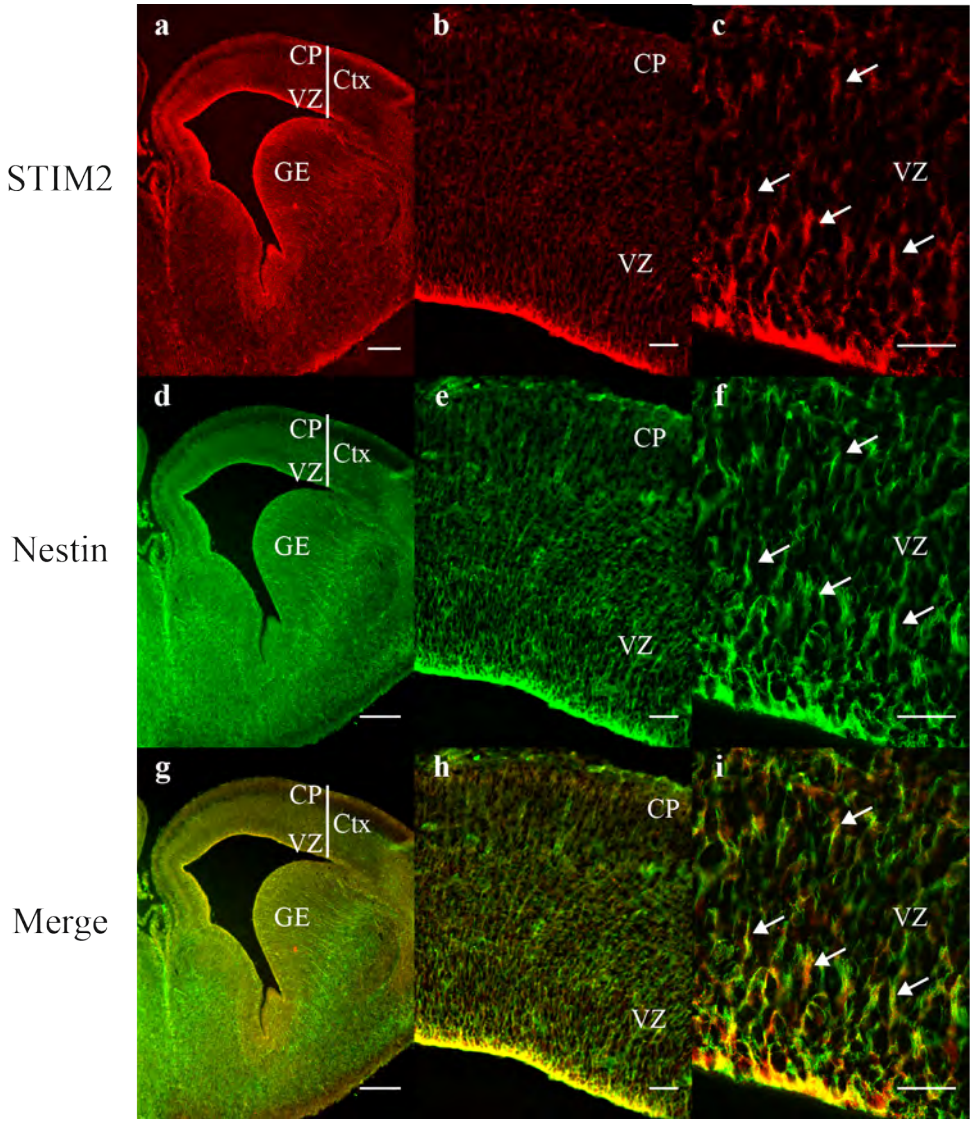
STIM2
Nestin
Merge
a
b
c
d
e
f
g
h
i
CP
Ctx
VZ
GE

Figure 2.10: STIM1 is weakly expressed in radial glial processes in the mouse cortex at E15.

Immunolabelling for STIM1 and Nestin on coronal sections through the mouse cortex at E15. STIM1-IR (a-c) and Nestin-IR (d-f) in the cortex at E15, with merged images (g-i) illustrating that STIM1 and nestin do not colocalised in the embryonic cortex. *Scale bar denotes 200 µm for images (a), (d) and (g), 20 µm for images (b), (e) and (h), and 10 µm for images (c), (f) and (i). Abbreviations: CP = cortical plate; Ctx = cortex; GE = ganglionic eminence; VZ = ventricular zone.*

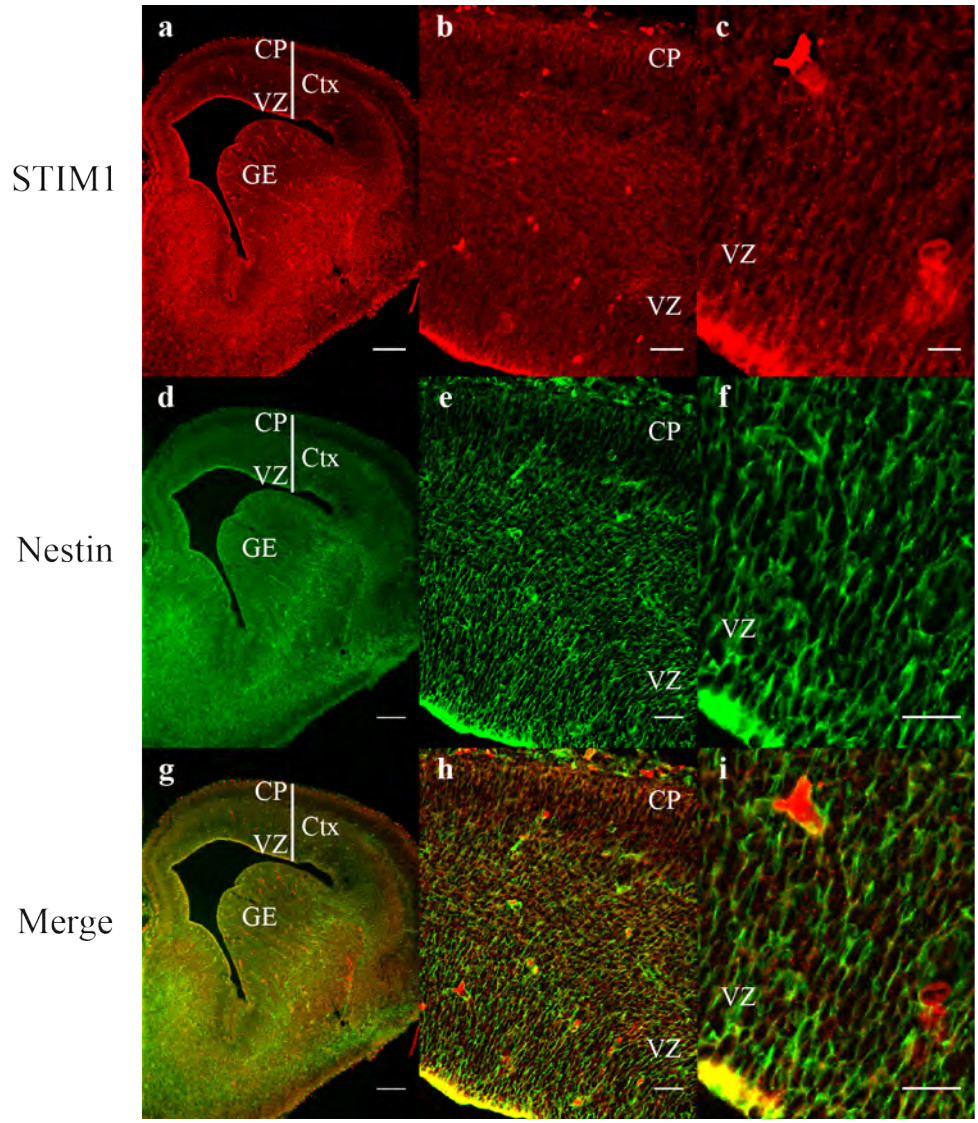
STIM1
Nestin
Merge
a
b
c
d
e
f
g
h
i
CP
Ctx
VZ
GE

2.3.3. Two STIM1 orthologs exist in zebrafish: identification of zSTIM1a and zSTIM1b

Data presented in this chapter suggest that STIM1 is the major neuronal STIM protein during mammalian development. No data is available regarding STIM expression or function in the zebrafish nervous system. However, a previous phylogenic analysis of STIM proteins identified two predicted zSTIM1 proteins, termed zSTIM1a and zSTIM1b (Cai, 2007a). This study sought to confirm that STIM orthologs exists in zebrafish, and to determine the level of homology between zebrafish and human STIM proteins. Human STIM1 is alternatively spliced with a larger 4.4 kilobase transcript predominating in the embryonic human brain (Williams et al., 2001). Hence, the resulting 685 amino acid STIM1 protein product was used to identify potential zebrafish orthologs from a library of translated nucleotides using an established search tool (tblastn; NCBI). Two potential zSTIM1 proteins, zSTIM1a and zSTIM1b, were identified using this approach, and alignment of the protein sequences for zSTIM1a and zSTIM1b with human STIM1 (Fig. 2.11), illustrated the homology of zebrafish orthologs with human STIM1 (discussed in detail below). The specificity of this approach for identifying STIM1 orthologs was determined by using the same approach to detect STIM1 orthologs in mouse, rat, *Xenopus* and *Drosophila*, where STIM1 has previously been studied (Roos et al., 2005; Zhang et al., 2005; Dziadek and Johnstone, 2007; Eid et al., 2008; Klejman et al., 2009; Skibinska-Kijek et al., 2009; Shim et al., 2013). A single STIM1 ortholog was identified in each species (alignments not shown), confirming the specificity of this bioinformatic approach. Furthermore, when the human STIM2 protein sequence was used to identify potential zebrafish STIM2 (zSTIM2) orthologs, two predicted zSTIM2 proteins termed zSTIM2a and zSTIM2b were identified (alignments not shown), suggesting that zSTIM1a and zSTIM1b are STIM1 orthologs, and do not represent STIM2 orthologs. Therefore, it was concluded that two zSTIM1 proteins exist in zebrafish. As data suggested that STIM1 is the major neuronal STIM protein in mammalian development, zSTIM2 proteins were not investigated further.

Figure 2.11: zSTIM1a and zSTIM1b are orthologs of human STIM1.

Sequence alignment of predicted zebrafish STIM1 (zSTIM1) proteins, zSTIM1a and zSTIM1b, with human STIM1 protein. Dark grey shading denotes residues conserved with human STIM1, light grey shading indicates residues conserved between zSTIM1 proteins alone. Red bars above sequences indicate described protein domains in the human STIM1 protein sequence to illustrate the homology between zebrafish and human STIM1 proteins.

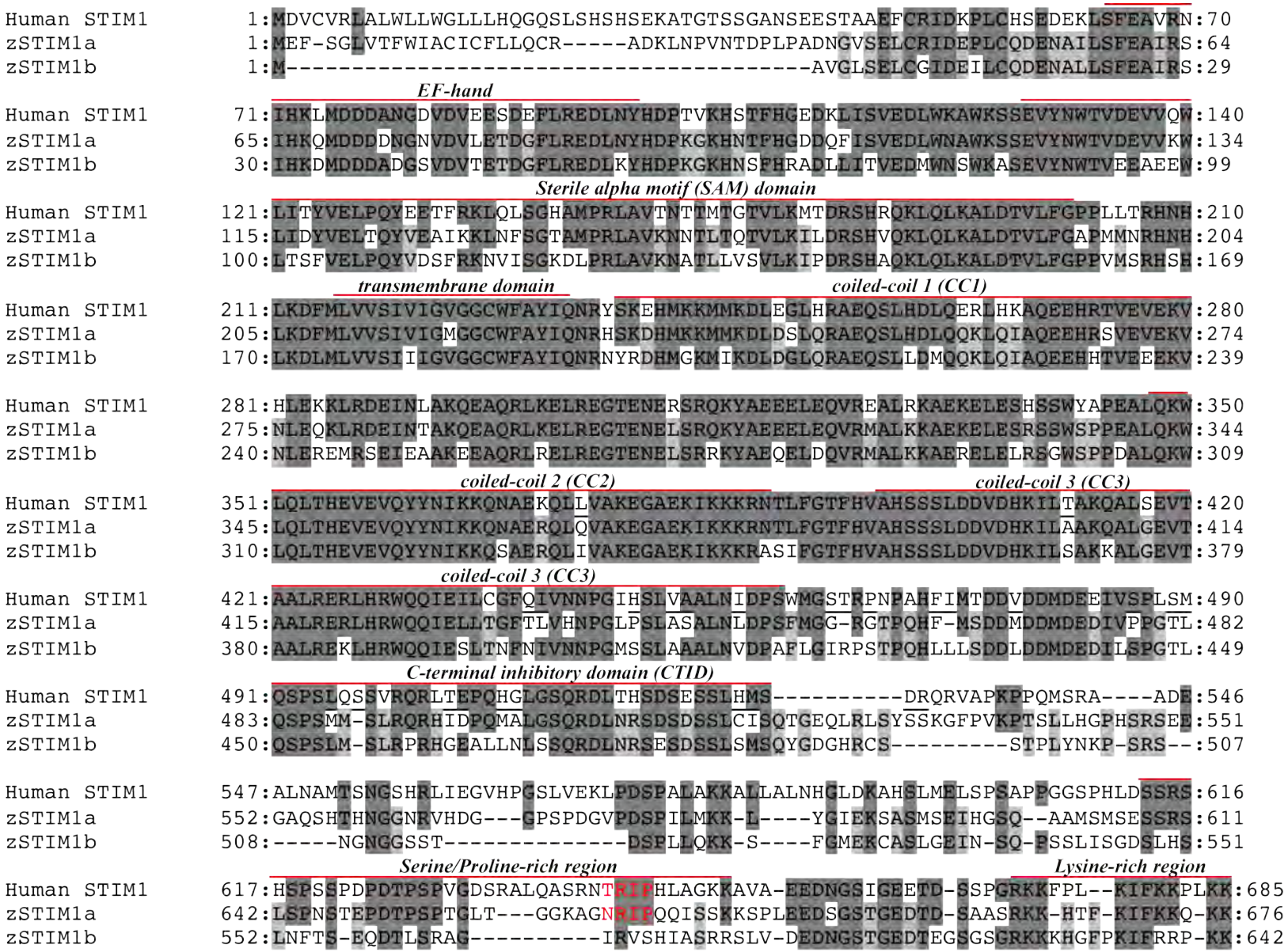
EF-hand
Sterile alpha motif (SAM) domain
transmembrane domain
coiled-coil 1 (CC1)
coiled-coil 2 (CC2)
coiled-coil 3 (CC3)
coiled-coil 3 (CC3)
C-terminal inhibitory domain (CTID)
Serine/Proline-rich region
Lysine-rich region

To investigate whether zSTIM1a and zSTIM1b are homologous to human STIM1, protein sequence homology was assessed by calculating protein sequence coverage and conservation. Protein sequence coverage was defined as the percentage of each STIM1 ortholog protein sequence that aligned to human STIM1, with protein sequence conservation defined as the percentage of amino acids identical to human STIM1 across the aligned protein sequence. Given that STIM1 proteins identified in mouse, rat, *Xenopus* and *Drosophila* are reported to be functionally similar to human STIM1 (Roos et al., 2005; Zhang et al., 2005; Stathopulos et al., 2006; Eid et al., 2008), STIM1 from these species served as controls for this analysis. The high degree of homology between human STIM1 and other mammalian STIM1 proteins was confirmed, with mouse and rat STIM1 proteins found to share a very high degree of sequence homology with human STIM1 (both exhibited 86% protein sequence coverage and 98% protein sequence conservation; Table 2.3). Moreover, *Xenopus* STIM1 exhibited 85% protein sequence coverage and 82% protein sequence conservations (Table 2.3), while *Drosophila* STIM displayed only 39% protein sequence coverage and 68% protein sequence conservation (Table 2.3). In comparison, zSTIM1a exhibited 80% protein sequence coverage and 78% proteins sequence conservation (Table 2.3), with zSTIM1b found to be less homologous, sharing only 59% protein sequence coverage and 68% proteins sequence conservation (Table 2.3). These data indicate that zSTIM1a and zSTIM1b share protein sequence homology that is comparable with *Xenopus* STIM1 and *Drosophila* STIM. Given that *Xenopus* STIM1 and *Drosophila* STIM perform functions similar to STIM1 (Roos et al., 2005; Zhang et al., 2005; Eid et al., 2008; Venkiteswaran and Hasan, 2009; Shim et al., 2013), these findings suggest that zSTIM1 will function in a comparable fashion to mammalian STIM1.

Homology of function can be predicted by the conservation of protein domains that mediate specific functions of a protein (Gu, 2001). Therefore, protein sequence homology was determined for protein domains known to be required for STIM1 functions (Fig. 2.12). Protein domains were selected based on previous evidence illustrating their importance for STIM1 function (Muik et al., 2008; Stathopulos et al., 2008; Frischauf et al., 2009; Zheng et al., 2011; Fahrner et al., 2014; Palty and Isacoff, 2015), with protein sequence conservation calculated for the N-terminal EF-hand/sterile alpha motif (EF-SAM) domain, the C-terminal coil-coiled 1 (CC1) domain, the coil-coiled 2/3 (CC2/CC3) domain, the C-terminal inhibitory domain (CTID), and the C-terminal unstructured

region (domains are denoted in Fig. 2.11 and represented diagrammatically in Fig. 2.12a-b). zSTIM1 proteins exhibited a large degree of protein sequence conservation in protein domains required for the calcium regulatory EF-SAM domain (76% and 64% for zSTIM1a and zSTIM1b respectively), for CRAC channel interactions via the CC1 domain (85%, 68%) and CC2-CC3 domain (88%, 83%; Fig. 2.12 c). However, both zSTIM1 proteins exhibited less homology in the CTID (59%, 48%) and the C-terminal unstructured region (40%, 39%; Fig. 2.12c). This reduced homology in C-terminal protein domains is consistent with reduced sequence homology in the C-terminus of *Xenopus* and *Drosophila* STIM1 proteins (Williams et al., 2001; Dziadek and Johnstone, 2007), which function in a similar manner to human STIM1 (Eid et al., 2008; Oh-Hora et al., 2008; Stiber et al., 2008; Venkiteswaran and Hasan, 2009). Therefore, these findings predict that calcium sensing and CRAC channel regulatory functions of STIM1 are conserved in zSTIM1 proteins.

	Chromosome	Protein size (# amino acids)	Protein coverage (%)*	Protein sequence conservation (%)*
Human STIM1	11	791	-	-
Mouse STIM1	7	685	86	98
Rat STIM1	1	685	86	98
***Xenopus* STIM1**	2	668	85	82
***Drosophila* STIM**	X	561	39	68
Zebrafish STIM1a	15	676	80	78
Zebrafish STIM1b	21	642	59	68

Table 2.3: STIM1 is conserved across vertebrate and invertebrate species.

Protein sequence conservation and coverage were calculated by alignment of protein sequences against the human STIM1 protein sequence using the BLAST® tool (blastp, NCBI). *Protein coverage: percentage of sequences of STIM1 orthologs aligned to human STIM1 protein sequence. Protein sequence conservation: the percentage of identical amino acids to human STIM1 across the full protein sequence.*

** Compared with human STIM1.*

Figure 2.12: zSTIM1a and zSTIM1b share a high degree of protein sequence homology with human STIM1.

The homology between human and zebrafish STIM1 proteins was assessed by calculating protein sequence conservation within protein domains known to be crucial for the function of STIM1. **(a-b)** Diagrammatic representation of (a) human STIM1 and (b) zebrafish STIM1a illustrating protein domains known to be required for STIM1 function. STIM1 protein domains were identified in the zSTIM1a protein sequence using the sequence alignment shown in Fig. 2.8 (numbers below each domain refer to the amino acid residues comprising each domain). Diagrams illustrate the EF-hand, hidden EF-hand, sterile-alpha motif (SAM), transmembrane domain, coiled-coil 1 (CC1), CC2, and CC3 domains, C-terminal inhibitory domain (CTID), serine/proline (S/P)-rich region and lysine (K)-rich region. The EF-SAM domain, STIM1 Orai1-activating region (SOAR, or CC2/CC3), and the C-terminal unstructured region are also specified. **(c)** zSTIM1a and zSTIM1b exhibit protein sequence conservation with human STIM1 in protein domains required for STIM1 function. Protein domains analysed included the EF-SAM domain (amino acids 57-196 of zSTIM1a), CC1 domain (232-336), CC2/CC3 (328-436), CTID (454-538) and the C-terminal unstructured region (539-676).
Domain conservation: percentage of identical amino acids to human STIM1 across the aligned zebrafish protein domain sequence. Domain coverage: percentage of human STIM1 protein domain matched with the aligned zebrafish protein domain sequence.

a Human STIM1

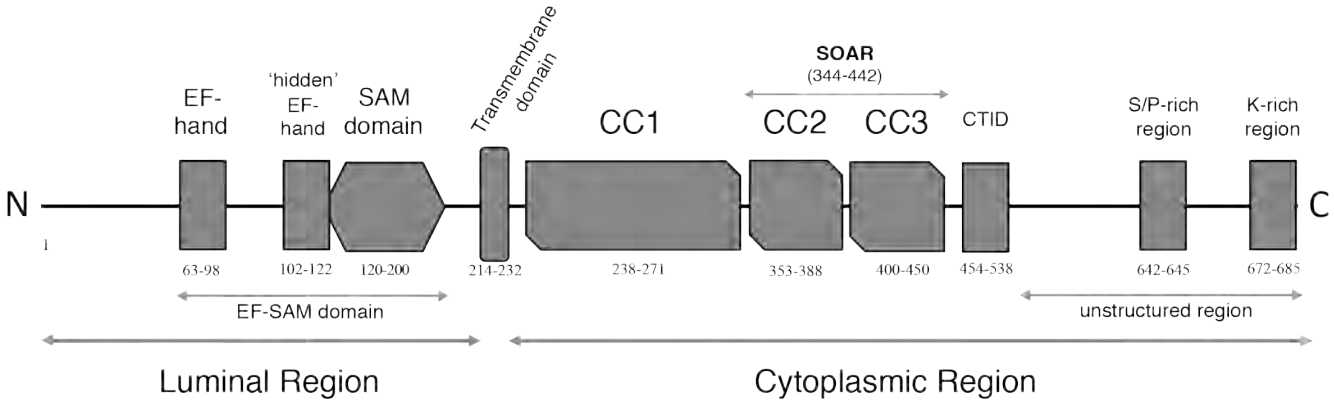

b Zebrafish STIM1a

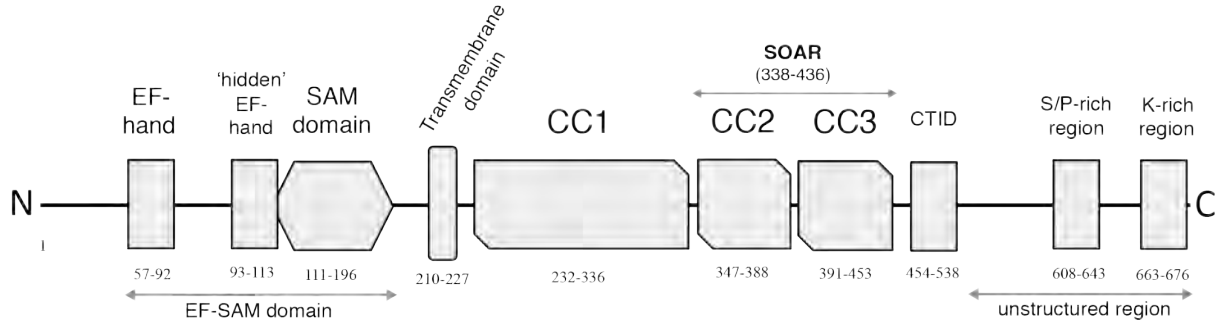

c Conservation of identified protein domains in zebrafish STIM1 orthologs compared with human STIM1

	EF-SAM domain		CC1 domain		CC2-CC3 domain		C-terminal inhibitory region		C-terminal unstructured region	
	Domain coverage (%)*	Domain conservation (%)*	Domain coverage (%)*	Domain conservation (%)*	Domain coverage (%)*	Domain conservation (%)*	Domain coverage (%)*	Domain conservation (%)*	Domain coverage (%)*	Domain conservation (%)*
zSTIM1a	100	76	100	85	100	88	89	59	94	44
zSTIM1b	100	64	100	68	100	83	75	48	74	34

* compared to human STIM1

2.3.4. zSTIM1a is the most conserved zebrafish STIM1 ortholog

zSTIM1a exhibited a higher degree of protein sequence homology with human STIM compared to zSTIM1b. Hence, it was reasoned that zSTIM1a and zSTIM1b could exhibit protein specific functions. When protein sequence homology was calculated between zSTIM1 proteins, it was found that zSTIM1b exhibits 98% protein sequence coverage and 65% protein sequence conservation compared with zSTIM1a (see Fig. 2.11 for protein sequence alignment), suggesting that zSTIM1a and zSTIM1b are functionally distinct proteins. To investigate whether zSTIM1a and zSTIM1b are functionally distinct proteins, the conservation of sequence motifs required for the calcium binding, CRAC channel activation, and microtubule plus-end tracking functions of STIM1 were investigated.

The calcium binding residues of the EF-hand (denoted by X, Y, Z, -Y, -X and -Z in Fig. 2.11a) are highly conserved in STIM1 orthologs (Cai, 2007a), as illustrated by alignment of human and mouse STIM1 EF-hands (Fig. 2.13a). The EF-hand of zSTIM1a and zSTIM1b exhibited a high degree of conservation with human STIM1 EF-hand (Fig. 2.13a), suggesting that the ability of zSTIM1 proteins to bind calcium is similar to human STIM1. However, zSTIM1a and zSTIM1b exhibit a substitution at a single calcium-binding residue (denoted by -Y in Fig. 2.13a). This calcium-binding residue has previously been shown to be the cause of divergent calcium binding properties of STIM1 and STIM2, where a glycine is present at the -Y residue of the EF-hand (Soboloff et al., 2006b; Brandman et al., 2007; Stathopulos et al., 2008; Thiel et al., 2013). However, in zSTIM1a and zSTIM1b aspartate is substituted with an asparagine and a serine respectively, which maintains a polar residue at -Y. The presence of a similar substitution in *Drosophila* STIM (dSTIM; Fig. 2.13a), which functions in a similar manner to human STIM1 (Roos et al., 2005; Zhang et al., 2005), would suggest that zSTIM1a and zSTIM1b retain the capacity to detect changes in the concentration of ER calcium.

The SOAR domain (amino acids 344-442 of human STIM1; denoted in Fig. 2.13b) is sufficient to activate Orai1 and trigger SOCE (Yuan et al., 2009; Kim and Muallem, 2011; Zhou et al., 2014). zSTIM1a shared 92% protein sequence conservation with human STIM1, while zSTIM1b was found to exhibit 85% protein sequence conservation (Fig.

2.13b). Therefore, it would be predicted that both zSTIM1a and zSTIM1b retain the ability to trigger CRAC channel formation and calcium influx SOCE.

STIM1 interacts with End-Binding (EB) proteins, which are a family of microtubule plus-end tracking proteins (+TIP) that bind to growing ends of microtubules (Stepanova et al., 2003; Honnappa et al., 2009). The binding of STIM1 to EB proteins is mediated by a TRIP motif (denoted green in Fig. 2.13c), which is located in the c-terminus of STIM1 (Grigoriev et al., 2008; Honnappa et al., 2009). Protein sequence analysis revealed that zSTIM1a exhibits a similar motif (NRIP, denoted green in Fig. 2.13c). Whilst the asparagine substitution at the first position of the TRIP motif in zSTIM1a may decrease the affinity of zSTIM1a to EB (Wen et al., 2004a; Honnappa et al., 2009; Buey et al., 2012), the hydrophobicity of the preceding residues likely compensates for this substitution (Buey et al., 2012). Therefore, these data predict that zSTIM1a retains the capacity to function as a +TIP protein. In contrast, there was an absence of a TRIP motif in the entire zSTIM1b sequence, with an IRVS sequence located at the predicted site of the TRIP motif (Fig. 2.13c). Whilst the effect of an isoleucine substitution at the first position of the TRIP motif is unknown, substitution of the final proline residue is not tolerated, and results in the abrogation of EB binding (Honnappa et al., 2009; Buey et al., 2012; Jiang et al., 2012). These data predict that zSTIM1a, but not zSTIM1b, retains the ability to function as a +TIP protein, suggesting that zSTIM1a is the more conserved zSTIM1 protein.

Phosphorylation of STIM1 by extracellular regulated kinases 1 and 2 (ERK1/2) regulates the dissociation of STIM1 from EB and the activation of SOCE (Pozo-Guisado et al., 2010; 2013; Casas-Rua et al., 2015; Tomas-Martin et al., 2015). ERK1/2 phosphorylates serine residues S575, S608 and S621 (denoted by # above sequence alignment Fig. 2.13c) and threonine at T626 (^ in Fig. 2.13c). Furthermore, phosphorylation at S628 (denoted by Δ above sequence alignment in Fig. 2.13c) occurs in response to thapsigargin-mediated activation of SOCE (Pozo-Guisado et al., 2010), and is important for ER exclusion during mitosis (Smyth et al., 2012). Therefore, to further explore whether zSTIM1a and zSTIM1b are distinct proteins, the presence of key phosphorylated residues in zSTIM1a and zSTIM1b was investigated. Consistent with the high degree of conserved function between mammalian STIM1 proteins, mouse STIM1 exhibits complete conservation of all phosphorylated residues (Fig. 2.13c-d). zSTIM1a retained the specific ERK1/2

phosphorylation sites corresponding to S575 and T626 in human STIM1, and the thapsigargin-induced phosphorylation site corresponding to S628 of human STIM1 (underlined in Fig. 2.13c). However, zSTIM1a does not exhibit the phosphorylation sites corresponding to S608 and S621 of human STIM1 (Fig. 2.13c-d). In contrast, zSTIM1b does not retain any of the specific ERK1/2 consensus sequences corresponding to S575, S608, S621 or T626, or the consensus sequence for phosphorylation of S628 (Fig. 2.13c-d), suggesting that zSTIM1a and zSTIM1b are not regulated by the same intracellular signaling pathways. In particular, these findings predict that zSTIM1b does not interact with microtubules by binding EB proteins, and would therefore not be predicted to retain the ER remodeling functions of STIM1. As such, further studies conducted in this thesis focuses on zSTIM1a.

Figure 2.13: STIM1a is the most functionally conserved STIM1 ortholog in zebrafish.

Protein sequence alignments illustrating the conservation of residues crucial for STIM1 protein function in zebrafish STIM1 (zSTIM1) proteins. **(a)** Sequence alignment for the EF-hand domain between human STIM1, mouse STIM1, zSTIM1a, zSTIM1b and *Drosophila* STIM (dSTIM). EF-hands are comprised of six negatively charged residues located within a calcium-binding loop between two α-helices (Bhattacharya et al., 2004; Grabarek, 2006; Zheng et al., 2008), as denoted below EF-hand sequences. Calcium binding residues are denoted by X, Y, Z, -Y, -X and -Z above protein sequences (Liou et al., 2005; Stathopulos et al., 2006; Cai, 2007a; Zheng et al., 2008). Black denotes residues conserved to human STIM1 proteins, with grey indicating residues not conserved to human STIM1 proteins. Red denotes aspartate residues corresponding to D70 in human STIM1. Mutation at this residue prevents calcium binding, resulting in a constitutively active STIM1 protein (Liou et al., 2005; Shim et al., 2013). Green illustrates glycine in human STIM2, illustrating polar to non-polar substitution at the -Y residue associated with the reduced affinity of the EF-hand for calcium in STIM2 (Zheng et al., 2008). **(b)** Sequence alignment for the STIM1 Orai1 activating region (SOAR) between human STIM1, zSTIM1a and zSTIM1b. Black denotes residues conserved with human STIM1 proteins, and grey indicating residues not conserved with human STIM1 proteins. **(c)** Sequence alignment for the serine/proline-rich region, illustrating conservation of the end-binding protein interaction motif (TRIP – denoted green) and phosphorylated residues (red) that regulate STIM1 function. ERK1/2 phosphorylated serine residues are indicated by # above the sequence alignment, whilst a serine phosphorylated in response to thapsigargin is denoted by Δ. **(d)** Table presenting the conservation of phosphorylated residues presented in (c) that are important for the trafficking of STIM1 within the cell and activation of SOCE. This table illustrates that zSTIM1a, but not zSTIM1b, retains crucial residues phosphorylated when STIM1 is activated and trafficked to ER-PM junction to initiate SOCE.

a EF-hand domain

```
                                        x  y  z  -y -x   -z
Human STIM1  63:LSFEAVRNIHKLMDDDANGDVDVEESDEFLREDLNY:98
Human STIM2  70:FSLEALQTIHKQMDDDKDGGIEVEESDEFIREDMKY:105
Mouse STIM1  63:LSFEAVRNIHKLMDDDANGDVDVEESDEFLREDLNY:98
zSTIM1a      57:LSFEAIRSIHKQMDDDDNGNVDVLETDGFLREDLNY:92
zSTIM1b      57:LSFEAIRSIHKDMDDDADGSVDVTETDGFLREDLKY:92
dSTIM       142:FGMEAIASLHRQLDDDDNGNIDLSESDDFLREELKY:168
                α-helix      Ca2+-binding loop    α-helix
```

b STIM1 Orai activating region (SOAR)

```
Human STIM1  344:PEALQKWLQLTHEVEVQYYNIKKQNAEKQLLVA:376
zSTIM1a      338:PEALQKWLQLTHEVEVQYYNIKKQNAERQLQVA:370
zSTIM1b      303:PDALQKWLQLTHEVEVQYYNIKKQSAERQLIVA:335

Human STIM1  377:KEGAEKIKKKRNTLFGTFHVAHSSSLDDVDHKI:410
zSTIM1a      371:KEGAEKIKKKRNTLFGTFHVAHSSSLDDVDHKI:404
zSTIM1b      336:KEGAEKIKKKRASIFGTFHVAHSSSLDDVDHKI:368

Human STIM1  411:LTAKQALSEVTAALRERLHRWQQIEILCGFQIV:442
zSTIM1a      405:LAAKQALGEVTAALRERLHRWQQIELLTGFTLV:436
zSTIM1b      369:LSAKKALGEVTAALREKLHRWQQIESLTNFNIV:403
```

c STIM1 serine/proline-rich region

```
                    #                                                  #
Human STIM1  573:PDSPALAKKALLALNHGLDKAHSLMELSPSAPPGGSPHLD:612
Mouse STIM1  573:PDSPALAKKTFMALNHGLDKAHSLMELNPSVPPGGSPLLD:612
zSTIM1a      575:PDSPILMKKLY-----GIEKSASMSEIHGS--QAAMSMSE:607
zSTIM1b      548:TDSPLLQKKSF-----GMEKCASLGEINSQ--PSSLISGD:579

                      #       ^  Λ                      * * * *
Human STIM1  613:SSRSHSPSSPDPDTPSPVGDSRALQASRNTRIPHLAGKK:650
Mouse STIM1  613:SSHSLSPSSPDPDTPSPVGDNRALQGSRNTRIPHLAGKK:650
zSTIM1a      608:SSRSLSPNSTEPDTPSPTG---LTGGKAGNRIPQISSKK:643
zSTIM1b      580:SLHSLNFTS-EQDTLSRAG----------IRVSHIASRR:616
```

d Conservation of phosphorylated residues

Phosphorylation site	Enzyme	Consensus sequence	Human STIM1	Mouse STIM1	Zebrafish STIM1a	Zebrafish STIM1b
Serine575	ERK1/2	PxS/TP	✓	✓	✓	✗
Serine608	ERK1/2	PxS/TP	✓	✓	✗	✗
Serine621	ERK1/2	PxS/TP	✓	✓	✗	✗
Threonine626	ERK1/2	PxS/TP	✓	✓	✓	✗
Serine628	unknown	unknown	✓	✓	✓	✗

2.3.5. zSTIM1a is expressed during zebrafish embryonic development, including throughout the nervous system.

As zSTIM1a was identified as the more highly conserved zSTIM1 protein, it was hypothesised that zSTIM1a would be expressed during zebrafish nervous system development. Whole mount *in situ* hybridisation was performed to determine the pattern of zSTIM1a transcript distribution over a time course from 12 to 96 hpf, encompassing key stages of nervous system development (Kimmel et al., 1995). zSTIM1a transcripts were detected throughout the embryo at 12 hpf, with zSTIM1a transcripts highly expressed in the eye primordium at this developmental stage (denoted by arrow; Fig. 2.14a). By 24 hpf, zSTIM1a was enriched in the eye (arrow), brain (left arrowhead), and in somites (right arrowhead) located along the developing tail (Fig. 2.14b,c). Viewed at higher power (Fig. 2.14c), the intense zSTIM1a expression was evident in the somites along the developing tail is obvious (arrow in Fig. 2.14b, and Fig. 2.14c). At 48 hpf, zSTIM1a transcripts remained enriched in the brain and somites (Fig. 2.14d), as well as being detected in the developing heart (denoted by arrowhead in Fig. 2.14d-f), correlating with zOrai1b expression at the same developmental stage (Volkers et al., 2012). By 72 hpf, zSTIM1a transcripts remained enriched in the brain and heart (Fig. 2.14e). However, the intensity of zSTIM1a transcripts in the somites appeared to decrease (Fig. 2.14e), which correlates with the known decrease in STIM1 expression by mammalian skeletal muscle with development (Stiber et al., 2008). At 72 hpf, zSTIM1a transcripts were also enriched in the heart (arrowhead) and swim bladder (arrow). At 96 hpf, zSTIM1a transcripts remained evident in the brain and somites at similar levels to 72 hpf (Fig. 2.14e). zSTIM1a also remained enriched in the heart (lower arrowhead), swim bladder (arrow) and the otic vesicle (upper arrowhead; Fig. 2.14e). A zero riboprobe control confirmed the specificity of the hybridisation reactions in 96 hpf tissue (Fig 2.14g). Therefore, zSTIM1a is expressed in zebrafish throughout a time course of nervous system development.

Figure 2.14: zSTIM1a is expressed throughout a time course of nervous system development.

(a-h) Whole mount *in situ* hybridisation demonstrates zSTIM1a transcript expression in zebrafish embryos from 12 to 96 hpf. (a) At 12 hpf zSTIM1a transcripts are enriched in in the eye primordium (arrow), and are present throughout the embryo. (b) At 24 hpf zSTIM1a transcripts showed intense staining within the forebrain (arrow), throughout the hindbrain (arrowhead), and in somites located along the developing trunk (upper arrow). (c) Higher power view at 24 hpf shows the intense zSTIM1a transcript expression within somites. (d) At 48 hpf zSTIM1a transcripts remained present in the brain and somites. (e) At 72 hpf, zSTIM1a transcripts remained enriched in the brain, but were less intense in the somites. (f) At 96 hpf, zSTIM1a transcripts were observed in the brain, somites, heart, otic vesicle and swim bladder. (g) A zero riboprobe control at 96 hpf illustrates specificity of hybridisation reaction.

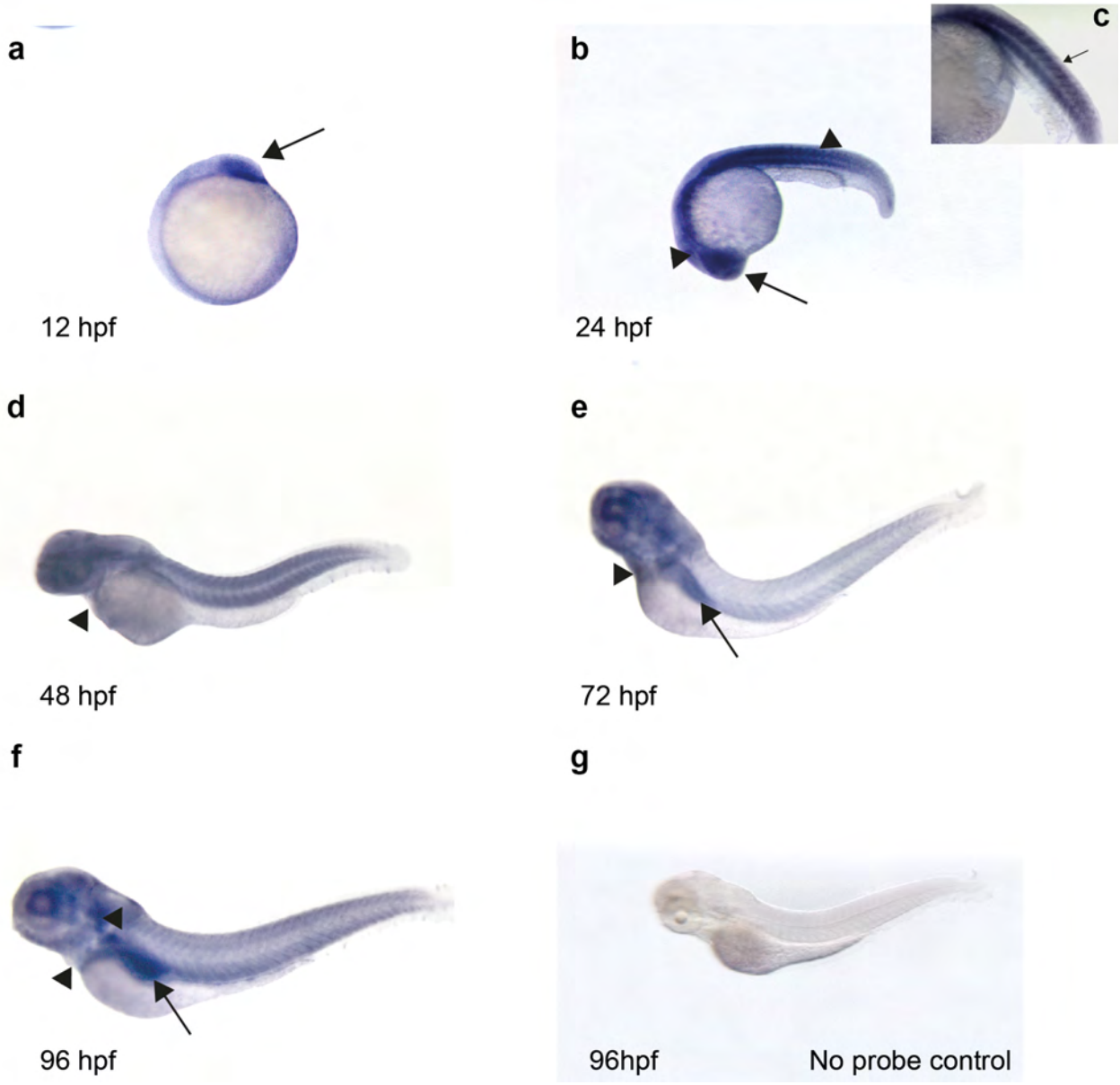
a
12 hpf
b
c
24 hpf
d
48 hpf
e
72 hpf
f
96 hpf
g
96hpf
No probe control

To confirm that zSTIM1a transcripts are expressed in the nervous system, *in situ* hybridisation was performed on coronal sections through the zebrafish nervous system at 96 hpf. zSTIM1a transcripts were detected throughout the forebrain, including in the pallium and subpallium (Fig. 2.15a). zSTIM1a transcripts were also present within the cellular layers of the retina (Fig. 2.15a-b), and in the midbrain, signified by expression in the optic tectum and the caudal tuberculum (Fig. 2.15b). In the hindbrain, zSTIM1a transcripts were present in the medulla oblongata (Fig. 2.15c). However, zSTIM1a was less intense in surrounding myotomes (Fig. 2.15c), which correlates with the decrease in zSTIM1a transcripts observed in somites at 96 hpf (see Fig. 2.15e). zSTIM1a transcripts were also present within the cells of the spinal cord at 96 hpf, again more strongly than the overlying myotomes (Fig. 2.15d). As zSTIM1a transcripts appeared to be ubiquitously expressed within the nervous system at 96 hpf, it was concluded that zSTIM1a is widely expressed in the zebrafish nervous system. This finding is consistent with the previous observation that STIM1 is widely expressed in the developing rodent nervous system, suggesting that expression of STIM1 in the developing nervous system is conserved across vertebrate species.

To further investigate the finding that zSTIM1a is expressed in the developing zebrafish nervous system, zSTIM1 protein expression was examined using immunoblotting and immunohistochemistry. However, commercially available anti-STIM1 antibodies raised against both the N- and C-terminal segments of the human STIM1 protein proved unreliable for detecting STIM1 proteins in zebrafish (data not shown).

Figure 2.15: zSTIM1a is expressed throughout the zebrafish nervous system.

(a-d) zSTIM1a transcripts are present throughout the developing zebrafish nervous system at 96 hpf. (a) Coronal section through the telencephalon and diencephalon illustrate zSTIM1a transcripts are present throughout the pallium, subpallium and preoptic hypothalamus. (b) Coronal section through the mesencephalon confirm that zSTIM1a transcripts are evident in the optic tectum and caudal tuberculum. (c) Coronal section through the myelencephalon illustrate that zSTIM1a transcripts are present in the medulla oblongata. (d) Coronal section through the rostral spinal cord showing that zSTIM1a transcripts are present in the spinal cord, as well as being present at a lower level in the surrounding myotome. *Scale bar illustrates 100 μm for all images*.

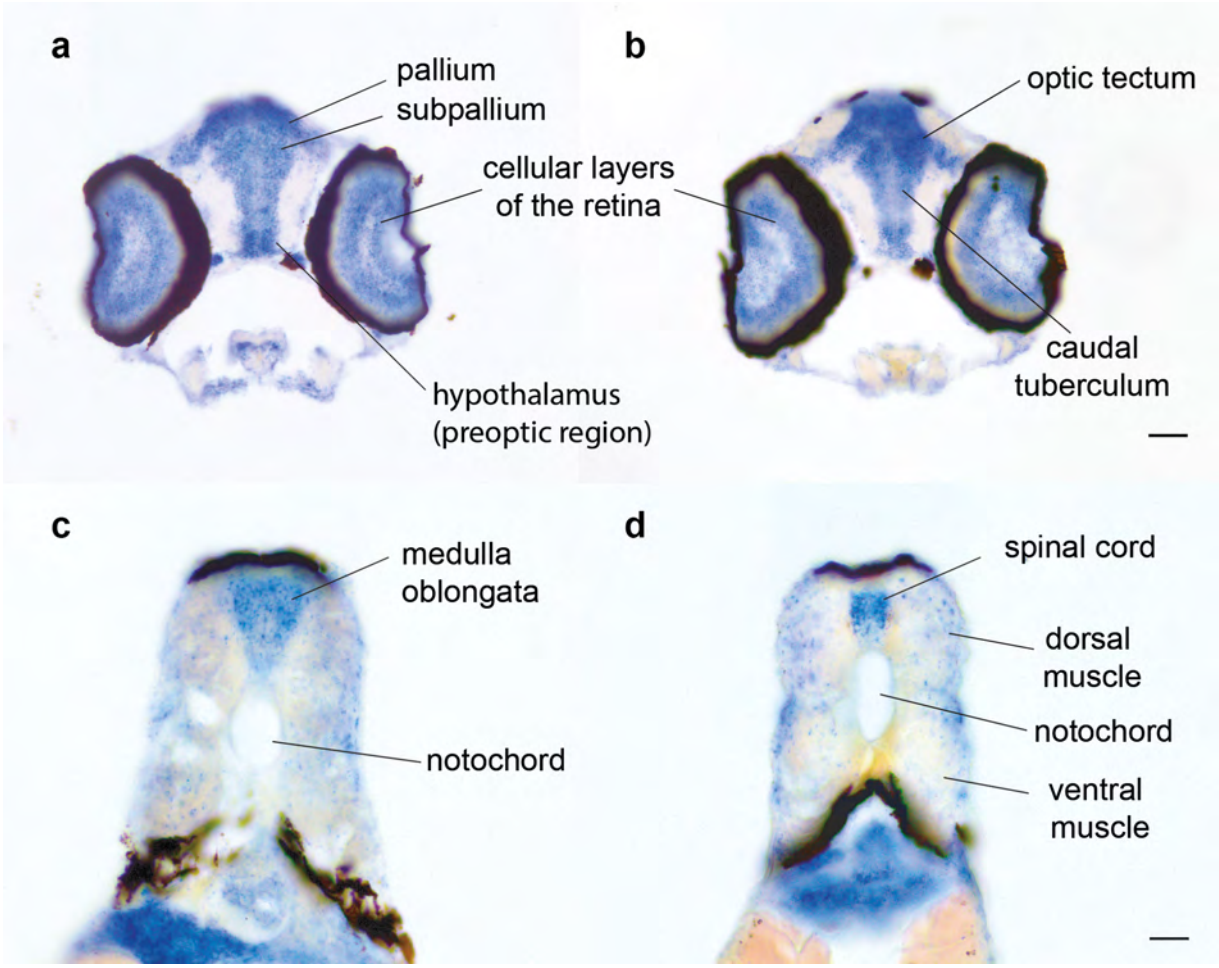
a
pallium
subpallium
cellular layers
of the retina
hypothalamus
(preoptic region)
b
optic tectum
caudal
tuberculum
c
medulla
oblongata
notochord
d
spinal cord
dorsal
muscle
notochord
ventral
muscle

2.4. Discussion

Findings presented in this chapter provide evidence that the molecular machinery for SOCE (STIM1, STIM2 and Orai1-3), are expressed in the developing mouse nervous system, exhibiting both overlapping and discrete patterns of expression. Distinct patterns of calcium signaling, such as waves and spikes, are required to properly pattern the developing nervous system (Bezprozvanny et al., 1991; Spitzer et al., 1994; Oancea and Meyer, 1996; Bito et al., 1997; Buonanno and Fields, 1999; Carey and Matsumoto, 1999; Hirota et al., 1999), and these calcium transients are reliant on calcium release from the ER (Bezprozvanny et al., 1991; Oancea and Meyer, 1996; Bito et al., 1997; Carey and Matsumoto, 1999; Hirota et al., 1999). Therefore, it is predicted that SOCE regulates calcium signaling events during nervous system development. STIM1 expression was observed to localise with the neuronal marker NeuN, whilst STIM2 expression was largely co-localised with the radial glia marker Nestin. These data support the hypotheses that STIM1 is the major neuronal STIM protein in development, and provide evidence to suggest that STIM1-mediated SOCE is important for neurogenesis.

STIM1 expression in the nervous system is highly conserved between vertebrate species. Data presented in this chapter demonstrate that two STIM1 orthologs exist in zebrafish, with zSTIM1a the more highly conserved STIM1 ortholog. zSTIM1a was found to be expressed during zebrafish development, including throughout the nervous system in a pattern of expression that correlates with mammalian STIM1 expression. Together, these studies reveal that STIM1 is the major neuronal STIM protein and that STIM1 is expressed during vertebrate nervous system development. As such, zebrafish will be used in subsequent chapters as an experimental model to investigate the function of STIM1 in nervous system development *in vivo*.

The molecular constituents of SOCE are expressed in the developing mammalian nervous system

Despite a wealth of knowledge regarding the expression of STIM proteins in the adult nervous system (Klejman et al., 2009; Skibinska-Kijek et al., 2009), the ontogeny of STIM proteins in the embryonic nervous system is not well understood. Data presented in this chapter reveals the pattern of STIM1 and STIM2 expression in the embryonic

mouse nervous system, which is consistent with findings obtained from embryonic and neonatal brain/spinal cord lysates (Williams et al., 2001; Dziadek and Johnstone, 2007; Xia et al., 2014). Significantly, STIM1 and STIM2 strongly co-localised with nestin in the ventricular zone of the cortex at E15, indicating that STIM proteins are highly expressed in progenitor cells that proliferate and differentiate to give rise most of the neurons and glial cells (Davis and Temple, 1994; Qian et al., 2000). At this developmental stage, spontaneous calcium transients generated in cells of the ventricular zone occur independent of electrical activity, glutamate or GABA signaling, and require release of calcium from the ER (Owens and Kriegstein, 1998; Owens et al., 2000). Given that STIM proteins trigger SOCE in response to ER calcium depletion (Soboloff et al., 2006b; Muik et al., 2008), and SOCE has been shown to be crucial for neural progenitor cell proliferation and differentiation (Li et al., 2012; Somasundaram et al., 2014; Hao et al., 2016), these findings suggest that STIM1 and STIM2 are appropriately expressed to control calcium signaling events during neuronal development.

As STIM proteins regulate calcium influxes by interacting with Orai proteins to trigger SOCE (Peinelt et al., 2006; Soboloff et al., 2006b; Zhou et al., 2014), it was predicted that STIM and Orai proteins are co-expressed in development. All three Orai proteins were present in the embryonic mouse brain and spinal cord at E15, and expression of Orai1-3 overlapped with STIM1 and STIM2 at this developmental stage. These observations correlate with data at both the transcript and protein level that shows STIM and Orai protein co-expression in neonatal and adult spinal cords (Xia et al., 2014), and cultured neurons (Klejman et al., 2009; Gruszczynska-Biegala et al., 2011; Mitchell et al., 2012). These observations also correlate with the SOCE occurring in both neurons and glia (Bouron, 2000; Emptage et al., 2000; Michaelis et al., 2014; Müller et al., 2014). *In vitro* studies have shown that SOCE is required for neural precursor cell proliferation and differentiation (Li et al., 2012; Somasundaram et al., 2014; Hao et al., 2016), the regulation of gene expression (Lalonde et al., 2014; Somasundaram et al., 2014), as well as cell motility (Tsai et al., 2014), which are essential for corticogenesis [for reviews see (Luhmann et al., 2016; Toth et al., 2016)]. Hence, the pattern of expression for STIM and Orai proteins observed in this study is consistent with SOCE being involved in the generation of calcium oscillations that regulate multiple aspects of neural development. Furthermore, the observation that STIM and Orai proteins are enriched in DRG sensory neurons correlates with data from this lab that suggests STIM1 is necessary for axon

pathfinding by DRG neurons (Mitchell et al., 2012). Taken together, these data confirm that the molecular constituents of SOCE are expressed in the developing mouse nervous system, providing further evidence to suggest that calcium influx via SOCE contributes to the regulation of neuronal function during development.

Shaping calcium signals by regulating expression of the molecular constituents of SOCE

It has been hypothesised that the spatial and temporal properties of calcium influx via SOCE can be altered by expressing different molecular constituents of SOCE, and that by regulating expression of STIM and Orai proteins, cells can modulate calcium influx via SOCE (Moccia et al., 2015). Orai1-3 have been shown to heteromultimerise to form CRAC channels (Inayama et al., 2015), with each Orai protein differentially affecting calcium conductance and calcium-dependent deactivation kinetics of the resulting CRAC channel (DeHaven et al., 2007; Lis et al., 2007; Moccia et al., 2015). Likewise, differential expression of STIM1 and STIM2 may act as a regulatory mechanism to shape calcium signaling, with STIM2-mediated SOCE characterised by slower activation kinetics and smaller oscillations in intracellular calcium (Brandman et al., 2007; Thiel et al., 2013; Moccia et al., 2015), while STIM1 mediates larger amplitude increases in intracellular calcium that lead to the activation of downstream signaling pathways (Venkiteswaran and Hasan, 2009; Ng et al., 2011; Mitchell et al., 2012; Hartmann et al., 2014; Tsai et al., 2014; Zhang et al., 2014; Pathak et al., 2015). Therefore, the observation that STIM1-2 and Orai1-3 exhibit distinct expression patterns in the developing nervous system may suggest that expression of the molecular components of SOCE is a regulatory mechanism to shape calcium signaling in the nervous system.

Fine-tuning of calcium signals by regulation STIM and Orai protein expression is likely to be highly complex. Recent studies have revealed that splice variants of mammalian STIM2, STIM2.1 and STIM2.2, inhibit and promote SOCE respectively (Graham et al., 2011; Miederer et al., 2015; Rana et al., 2015). Whilst a longer splice variant of mammalian STIM1, known as STIM1L, is reported to be expressed in the adult nervous system (Darbellay et al., 2011), and forms stable STIM1-Orai interactions for fast, repeated, calcium influx via SOCE (Darbellay et al., 2011; Sauc et al., 2015). As such, future studies should investigate whether splice variants of STIM proteins are present in

the developing nervous system, their ontogeny in development, as well as their contribution to calcium dynamics in neurons should be addressed.

STIM2 is expressed by radial glia in the embryonic rodent nervous system

STIM2 localised strongly with process-like structures that were positive for nestin in both the brain and spinal cord at E15. In the mouse cortex and spinal cord at E15, nestin labels radial glia processes that extend from the ventricular zone to the pial surface (Shibata et al., 1997; Choi et al., 2009; Walker et al., 2010). This finding is supported by the observation that STIM2 expression is restricted to radial glia in the embryonic rat nervous system and GFAP expressing astrocytes in the early post-natal nervous system (Hadrill et al., *in preparation*). Although STIM2 was also evident in neurons, expression was less intense compared with STIM1 expression. Moreover, STIM2 was present in the cortical plate at a lower level than in the ventricular zone, suggesting that STIM2 is downregulated as neurogenesis proceeds. This downregulation of STIM2 with neurogenesis provides support for a model whereby SOCE is decreased in neurons in concert with an upregulation of voltage-dependent and ligand-gated calcium channels [reviewed in (Toth et al., 2016)]. Indeed, downregulation of SOCE is associated with the progression of neural precursor cells to mature neurons, with a decrease in Orai expression (or calcium influx via SOCE) observed in most neural precursor cells that have acquired the mature neuronal marker doublecortin *in vitro* (Somasundaram et al., 2014). Therefore, STIM2 expression data presented here is consistent with STIM2 being predominating localised to radial glia in the embryonic nervous system.

STIM1 is the major neuronal STIM protein expressed in embryonic development

As neurogenesis progresses, immature cortical neurons migrate from the ventricular zone to the cortical plate before beginning the process of axon pathfinding to form neuronal circuitry (Rakic, 1988; Gomez et al., 1995; Noctor et al., 2004). Unlike STIM2, STIM1 expression remained high in the cortical plate. This data provides evidence to suggest that STIM proteins are differentially expressed in development, with STIM1 expression maintained in immature neurons. This observation was supported by the finding that STIM1 localised to neurons in the embryonic nervous system, while STIM2 was enriched in radial glia. Likewise, *in vitro* studies have shown that STIM1-mediated SOCE is

required for correct cell motility and growth cone motility (Mitchell et al., 2012; Shim et al., 2013; Tsai et al., 2014), while STIM1 expression is also necessary for correct axon pathfinding by *Xenopus* spinal interneurons (Shim et al., 2013). Significantly, immature neurons exhibit higher frequency calcium spikes associated with the regulation of cell motility, axon pathfinding, neurotransmitter specification and synaptogenesis (Gomez et al., 1995; Gu and Spitzer, 1995; Borodinsky et al., 2004; Torborg et al., 2004; Kirkby et al., 2013). While STIM1 mediates fast ER refilling in Purkinje neurons following synaptic calcium transients, which is required for higher frequency calcium transients (Hartmann et al., 2014). Taken together, these data provide evidence for STIM1-mediated SOCE being required for the generation of higher frequency spikes that regulate distinct processes during neuronal development, in particular the wiring of the nervous system.

STIM proteins exhibit similar expression patterns in the post-natal nervous system

In the post-natal nervous system, STIM1 and STIM2 were observed to be similarly expressed within the cortex. This observation is consistent with neurons expressing both STIM proteins in the mature nervous system (Klejman et al., 2009; Skibinska-Kijek et al., 2009; Steinbeck et al., 2011), and calcium influx via SOCE regulating synaptic calcium signaling (Emptage et al., 2000; Bouron et al., 2005; Hartmann et al., 2014; Kyung et al., 2015). As neurons develop, there is an upregulation of activity dependent ion channels, while the expression of STIM proteins and store-operated channels decreases (Toth et al., 2016). However, the small conductance of CRAC channels (Hoth and Penner, 1993), coupled with their high selectivity for calcium and spatial localisation to ER-PM junctions (Luik et al., 2006; DeHaven et al., 2007; Lis et al., 2007), confers SOCE with the ability to be a highly efficient and selective calcium influx mechanism that is uniquely poised to create calcium microdomains for the activation of specific calcium signaling pathway, providing a model for STIM function whereby SOCE is required for spatially localised calcium signals in mature neurons.

Taken together, these data suggest that STIM proteins are differentially expressed during neuronal development, with STIM1 being the major neuronal STIM protein throughout all stages of embryonic development, but that STIM2 is expressed in neurons of the post-natal nervous system.

Two zSTIM1 orthologs exist in zebrafish: zSTIM1a and zSTIM1b

Expression of STIM1 has been shown to be necessary for correct growth cone motility (Mitchell et al., 2012; Shim et al., 2013). Findings presented in this chapter suggest that STIM1 is the major STIM protein in neurons during development, which is consistent with STIM1 regulating axon pathfinding *in vivo*. To decipher the role of STIM in axon guidance *in vivo*, the zebrafish was chosen as an animal model of development. For zebrafish to be used as a model, STIM1 must be expressed during zebrafish nervous system development. Accordingly, these studies confirmed that STIM1 proteins exist in zebrafish, determined the degree of homology between mammalian and zebrafish STIM proteins, and established whether STIM1 is expressed in a similar fashion to mammalian STIM1 during nervous system development in zebrafish.

Bioinformatic analysis revealed that the zebrafish genome encodes two STIM1 proteins, known as STIM1a and STIM1b. This finding supports a previous phylogenic analysis of STIM1 that suggested two STIM1 orthologs are present in zebrafish (Cai, 2007a), and is consistent with the known duplication event that occurred in the cephalochordate genome following evolutionary divergence from other vertebrates (Holland et al., 1994; Postlethwait et al., 1998; Soshnikova et al., 2013). Moreover, protein sequence analysis revealed that zSTIM1a and zSTIM1b share a high degree of protein sequence homology with human STIM1. Taken together, these data suggest that two STIM1 orthologs exist in zebrafish.

zSTIM1a, and not zSTIM1b, is the more highly conserved STIM1 ortholog in zebrafish

To investigate the homology between zSTIM1 proteins and human STIM1, protein sequence conservation was calculated for protein domains of STIM1 that are required for STIM1 functions. STIM1 proteins activate SOCE in response to decreased calcium in the ER lumen, which is sensed by the N-terminal EF-hand (Zhang et al., 2005; Zheng et al., 2008). zSTIM1a and zSTIM1b both exhibited substitution at calcium binding residues within the EF-hand. However, the substitution were similar to substitutions present in *Drosophila* STIM, which retains the ability to regulate SOCE in response to changes in ER calcium (Roos et al., 2005; Zhang et al., 2005). Furthermore, the CC1/CC2 domain (or STIM1 Orai1-activating region) is known to be required for STIM1 to trigger

SOCE (Kawasaki et al., 2009; Yuan et al., 2009; Kim and Muallem, 2011; Zhou et al., 2014), and zSTIM1a and zSTIM1b both retain a high degree of homology within the coiled-coil domains. As such, zSTIM1a and zSTIM1b were both predicted to respond to similar changes in ER calcium and bind and activate Orai proteins, meaning that both zSTIM1 proteins are predicted to regulate SOCE in response to similar changes in ER calcium levels, providing evidence for conservation of function between zSTIM1 proteins. However, regulation of SOCE by STIM1 is also reported to require interactions between STIM1 and the +TIP protein EB1 (Grigoriev et al., 2008; Pozo-Guisado et al., 2010; Smyth et al., 2012; Yang et al., 2012; Asanov et al., 2013; Pozo-Guisado et al., 2013; Casas-Rua et al., 2015; Tomas-Martin et al., 2015). Significantly, zSTIM1a, but not zSTIM1b, was observed to retain the C-terminal TRIP motif responsible for conferring EB1 binding. Although a threonine to aspartate substitution in the zSTIM1a EB1-binding motif may decrease the affinity of zSTIM1a for EB1 (Wen et al., 2004a; Honnappa et al., 2009; Buey et al., 2012), the hydrophobicity of the preceding residues likely compensates for this substitution (Buey et al., 2012). Therefore, zSTIM1a, but not zSTIM1b, is predicted to be transported by the microtubule cytoskeleton to ER-PM junctions and activate SOCE, providing evidence to suggest that zSTIM1a is the more highly conserved zSTIM1 protein.

In addition to the TRIP motif, phosphorylation of residues in the C-terminus of STIM1 regulates STIM1-EB1 interactions and, therefore, SOCE. ERK1/2 phosphorylation of serine/threonine residues within the unstructured serine/proline-rich region of STIM1 is vital for STIM1-mediated SOCE, as well as the exclusion of the ER during cell division (Pozo-Guisado et al., 2010; Smyth et al., 2012; Pozo-Guisado et al., 2013; Casas-Rua et al., 2015; Tomas-Martin et al., 2015), suggesting that phosphorylation of these residues is important for STIM1 trafficking within the cell. ERK1/2 phosphorylates serine and threonine residues designated by a motif containing proline residues at the +1 and -2 positions (PxS/TP), or by a less specific phosphorylation motif containing a proline residue only at the +1 position (S/TP) (Lawrence et al., 2008; Fernandes and Allbritton, 2009; Pozo-Guisado et al., 2010). As such, to investigate the homology between zSTIM proteins and human STIM1, the conservation of phosphorylated residues was investigated. Whilst zSTIM1a contained the phosphorylated residues S575, T626 and S628, zSTIM1b did not retain consensus sequences for known phosphorylated residues.

This data provides further evidence that zSTIM1a is the more highly conserved zSTIM1 protein.

zSTIM1a is expressed throughout nervous system development in the zebrafish.

As STIM1 was expressed during mouse nervous system development, it was expected that zSTIM1a would be present in a similar pattern of expression in the zebrafish nervous system during development. Using whole mount *in situ* hybridisation, zSTIM1a expressed was confirmed in the developing zebrafish nervous system, with zSTIM1a also highly upregulated in the somites and the heart. These observations are consistent with the described pattern of zebrafish Orai1b (zOrai1b) transcripts in development (Volkers et al., 2012), suggesting that SOCE is important for zebrafish development. When the cellular expression of zSTIM1a transcripts was examined at 96 hpf, zSTIM1a was shown to be expressed throughout the developing nervous system, similar to the pattern of expression observed for STIM1 in the developing mouse nervous system. Taken together, data presented in this chapter provides evidence to suggest that STIM1 is the major neuronal STIM protein in development, and that expression of STIM1 in development is conserved across vertebrate nervous systems. Hence, it was concluded that zebrafish are an appropriate model to study the function of STIM1 in development.

Chapter 3:
STIM1 regulates axon pathfinding by motor neurons *in vivo*

Chapter 3: STIM1 regulates axon pathfinding by motor neurons *in vivo*

3.1. Introduction

STIM1 is necessary for correct growth cone motility *in vitro*. Reduced expression of STIM1 in rodent DRG sensory neurons causes a switch in growth cone turning response to BDNF from attraction to repulsion (Mitchell et al., 2012). Similarly, perturbing STIM1 function by overexpressing a dominant-negative or constitutively-active from of STIM1 in *Xenopus* spinal neurons results in a switch in the turning response to netrin-1 from attraction to repulsion (Shim et al., 2013). Importantly, attractive growth cone turning in response to both BDNF and netrin-1 requires spatially-restricted, sustained elevations in intracellular calcium, which is reliant on calcium release from the ER (Gomez and Spitzer, 1999; Zheng, 2000; Gomez et al., 2001; Wen et al., 2004b; Gasperini et al., 2009). Therefore, given that the ER is a finite source of calcium, it has been hypothesised that STIM1-mediated SOCE is required for the large amplitude increases in calcium required for growth cone attraction (Li et al., 2005; Gasperini et al., 2009; Mitchell et al., 2012). STIM1 is also necessary for sema3a-mediated growth cone repulsion (Mitchell et al., 2012), and sema3a is considered a largely calcium-independent guidance cue that does not elicit calcium release from the ER (Togashi et al., 2008), suggesting that SOCE-independent functions of STIM1 also contribute to the regulation of axon guidance.

The zebrafish spinal motor system is an excellent model in which to study the mechanisms that regulate axon pathfinding *in vivo*. Similar to other vertebrate species, zebrafish spinal motor neurons are classified into subtypes that exhibit distinct axon trajectories that enable each subtype to innervate the correct target (Eisen et al., 1986; Myers et al., 1986; Westerfield et al., 1986). In the zebrafish embryo, each somite is initially innervated by three primary motor neurons: the rostral primary (RoP), middle primary (MiP), and caudal primary (CaP) motor neurons, which are identified by their combinatorial expression of LIM homoebox genes and their anatomical position within each spinal hemisegment (Eisen et al., 1986; Appel et al., 1995). Primary motor neuron axogenesis begins with the CaP axon exiting the spinal cord via the ventral root at approximately 17 hpf (Eisen et al., 1986; Zeller et al., 2002; Hilario et al., 2010; Plazas et al., 2013). Approximately 2 hr later, the MiP, then the RoP, begin axon pathfinding within the spinal cord, growing caudally to contact the CaP axon before also exiting the

spinal cord at the ventral root (Eisen et al., 1986; 1989; Pike et al., 1992; Bernhardt et al., 1998).

Axon pathfinding by primary spinal motor neurons is highly stereotypic (Fig. 3.1). All three primary motor neurons extend away from the spinal cord along the common pathway (Eisen et al., 1986; Myers et al., 1986; Westerfield et al., 1986), which is a ventral projection from the spinal cord to the nascent horizontal myoseptum between the medial surface of the myotome and the notochord (Bernhardt et al., 1998). Once each primary motor neuron axon reaches the horizontal myoseptum, they pause for up to 1 hr, before making vastly different pathfinding decisions (Eisen et al., 1986; Myers et al., 1986; Melancon et al., 1997; Beattie et al., 2000; Plazas et al., 2013). The CaP axon extends distal to the horizontal myoseptum to reach the ventral aspect of the notochord, before continuing towards the ventral muscle boundary. By 48 hpf, the CaP axon has branched at the ventral muscle boundary, with one prominent branch extending in a dorsal-rostral direction to innervate the rostral myotome, and the other prominent branch extending dorsal-caudal direction to innervate the dorsal myotome (Myers et al., 1986). In contrast, once the MiP axon reaches the horizontal myoseptum, it sprouts a dorsal collateral growth cone, retracts the initial ventral axon, and grows dorsally to innervate the dorsal myotome (Eisen et al., 1986; Myers et al., 1986; Westerfield et al., 1986). Whilst the RoP axon branches at the horizontal myoseptum, with branches extending laterally to innervate the regions of the myotome located proximal to the horizontal myoseptum (Eisen et al., 1986; Myers et al., 1986; Westerfield et al., 1986). Hence, CaP axons represent an isolated *in vivo* model of axon pathfinding in which to study the importance of STIM1 for axon guidance.

Many of the cellular mechanisms underlying axon pathfinding by CaP axons have been elucidated, including motility at intermediate choice points, with a myriad of overlapping guidance cues and receptors identified to date (for reviews see (Beattie, 2000; Lewis and Eisen, 2003; Schneider and Granato, 2003; Fetcho et al., 2008; Bonanomi and Pfaff, 2010)). Consistent with *Xenopus* and mammalian models of growth cone guidance (Davies et al., 1986; Li et al., 2005; Gasperini et al., 2009), where the role of STIM1 in growth cone motility has previously been investigated (Mitchell et al., 2012; Shim et al., 2013), cultured zebrafish motor neurons express the BDNF receptor TrkB and exhibit growth cone attraction towards a source of BDNF (Chen et al., 2013). Furthermore,

Figure 3.1: Axon pathfinding by spinal primary motor neurons in highly stereotypic.

Schematic illustrating the stereotypic axon pathfinding decisions made by the rostral (RoP), middle (MiP) and caudal (CaP) primary motor neurons of the zebrafish spinal cord to reach their distinct muscle targets.

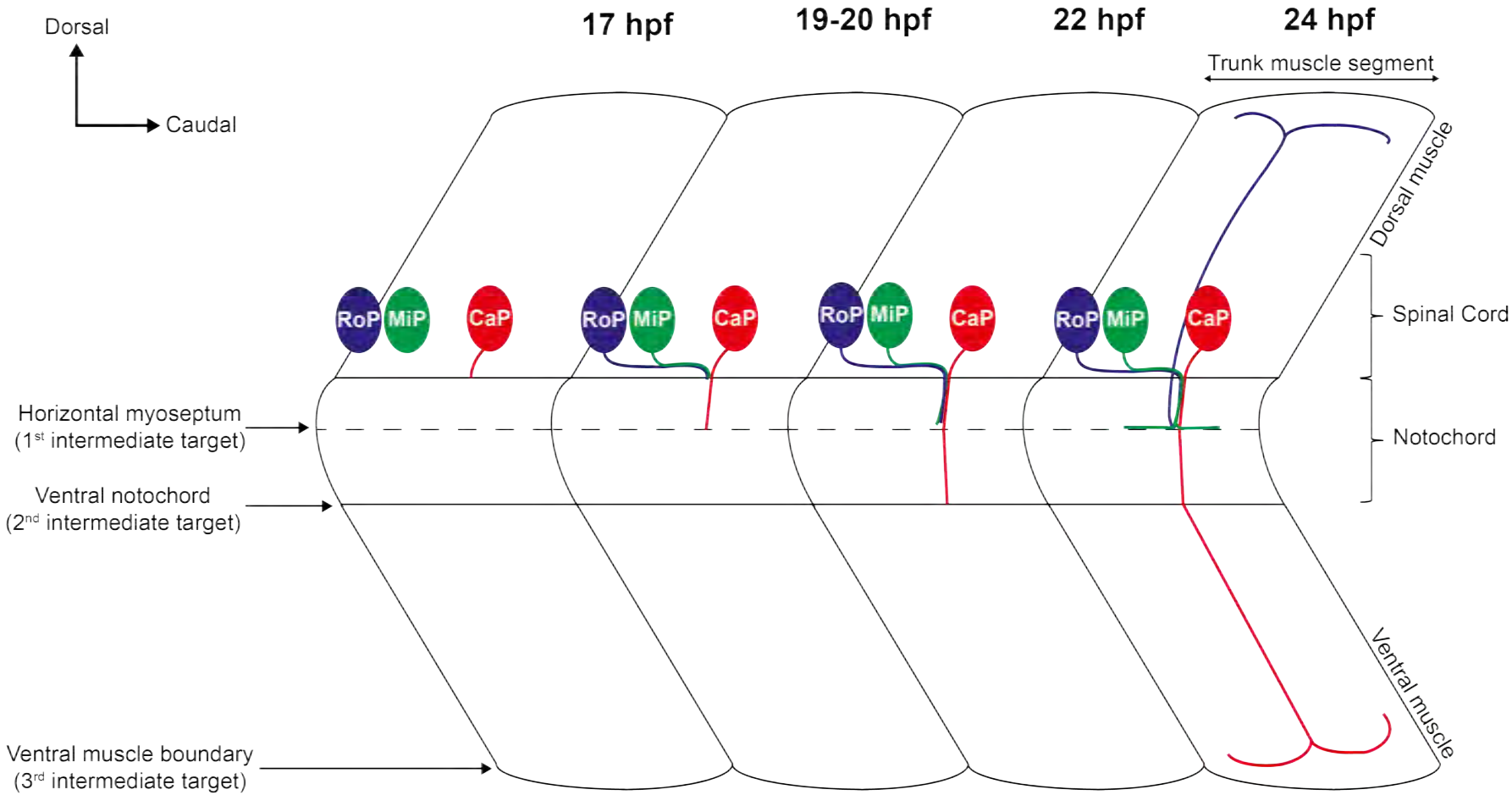
Dorsal
Caudal
17 hpf
19-20 hpf
22 hpf
24 hpf
Trunk muscle segment
Dorsal muscle
RoP
MiP
CaP
Spinal Cord
Notochord
Horizontal myoseptum
(1st intermediate target)
Ventral notochord
(2nd intermediate target)
Ventral muscle boundary
(3rd intermediate target)
Ventral muscle

zebrafish netrin-1 and sema3a orthologs, which exhibit a high degree of homology with mammalian proteins (Chen et al., 2013), are required for axon pathfinding by CaP neurons *in vivo* (Lauderdale et al., 1997; Shoji et al., 1998; Zeller and Granato, 1999; Sato-Maeda et al., 2006; Plazas et al., 2013). As STIM1 is necessary for correct growth cone motility in response to BDNF, netrin-1 and sema3a *in vitro* (Mitchell et al., 2012; Shim et al., 2013), axon pathfinding by CaP axons represent an excellent model to study the importance of STIM1 for axon guidance *in vivo*.

This chapter addresses the hypothesis that STIM1 is required for correct axon pathfinding *in vivo* by examining the effect of reduced zSTIM1a expression on axon pathfinding by zebrafish spinal motor neurons *in vivo*. STIM1 was previously shown to be necessary for vertebrate and invertebrate development (Eid et al., 2008; Oh-Hora et al., 2008; Stiber et al., 2008). However, no study has described the importance of zSTIM1a expression or function for zebrafish nervous system development or motor axon pathfinding. Therefore, the effect of reduced zSTIM1a expression on embryogenesis and axon pathfinding by spinal motor neurons was investigated.

3.2. Methods

3.2.1. Animals

Zebrafish embryos were obtained from natural spawning events and staged by external morphology according to established guidelines (Kimmel et al., 1995). The Gal4^{s1020t}/UAS:mCherry transgenic line utilised in these studies (Scott et al., 2007), was a kind gift of Dr Ethan Scott (University of Queensland).

3.2.2. Morpholino knockdown of zSTIM1a expression during development

zSTIM1a expression was reduced during development using specific zSTIM1a translation blocking morpholino antisense oligonucleotides (morpholinos), which were designed and synthesised by GeneTools LLC (GeneTools, OR, USA). zSTIM1a morpholino sequence (25mer) was complimentary to the translation start site (-19 to +6 of zSTIM1a, ATG is indicated by parentheses below). The control morpholino had 5 bases mismatched (mismatched sites are italicised and in lower case within the sequence below). Control and zSTIM1a morpholino were solubilised at 1 mM in MilliQ-water.

zSTIM1a morpholino: 5'-TCACCAATCCGCTGAACTC(CAT)AGT-3'
Control morpholino: 5'-TC*t*C*g*AATC*g*GCT*c*AACTC(CAT)A*c*T-3'

For morpholino knockdown experiments, zebrafish embryos were injected at the 1-4 cell stage with zSTIM1a or control morpholino. Glass capillaries (1.0 mm OD; Harvard Apparatus, Cambridge, UK) were pulled to a fine tip (P-97 Flaming/Brown Micropipette Puller; Sutter instruments, CA, USA) and backfilled with morpholino solution. Under an Olympus SZX16 zoom stereo-microscope, the pipette tip was broken using fine forceps and the ejection volume was calibrated such that 1-2 nL, or 1.0 pmol of morpholino, was injected with each pressure ejection (PLI-10 pico-liter injector; Harvard Apparatus). Morpholinos were injected into the yolk at the 1-4 cell stage, proximal to the cells, allowing morpholinos to be incorporated by cytoplasmic streaming. To control for the microinjection procedure, embryos were injected at the 1-4 cell stage with 1-2 nL of MilliQ-water alone (sham injection).

3.2.3. Assessing the effect of reduced zSTIM1a expression on zebrafish embryonic development

The effect of reduced zSTIM1a expression on zebrafish development was assessed by measuring embryo survival, size, and the presence of gross anatomical defects. Embryo survival was assessed at 8, 24, 48, 72 and 96 hpf, with embryo survival normalised to wild type controls. The occurrence of anatomical defects was quantified at 24, 48, 72 and 96 hpf. To calculate embryo survival and the frequency of anatomical defects, embryos were observed using an SZX16 zoom stereo-microscope (Olympus) equipped with a DFC295 CMOS camera (Leica Microsystems). Embryo size was assessed by measuring embryo length at 24 hpf, as well as measuring the height and width of trunk muscle segments. Images were acquired at 24 hpf in brightfield using an UltraView Vox spinning disk confocal microscope equipped with Volocity software (PerkinElmer). Embryo length was measured by tracing a line from the primordial mouth along the notochord to the tip of the tail. Muscle segment height was calculated by tracing a vertical line from the dorsal muscle boundary to the ventral muscle boundary, and muscle segment width was calculated by drawing a horizontal line from the rostral to caudal boundaries of the muscle at the level of the spinal cord. Measurements were performed in ImageJ (NIH). Images were prepared using ImageJ (NIH) and Adobe Illustrator CS6 (Adobe). All statistical tests were performed in GraphPad Prism6.0e (GraphPad Software).

To examine the development of skeletal muscle, myosin heavy chain was expression was examined by whole mount immunohistochemistry at 30 hpf. Embryos were fixed in 4% PFA at room temperature, permeabilised by dehydration in ascending concentrations of methanol (50-100%), and stored overnight in 100% methanol at -20°C. To aid the entry of antibodies, embryos were permeabilised by digestion in Proteinase K (PK, 10 μg/mL in PBS; ThermoFisher Scientific, CA, USA) for 15 min. To stop PK activity, embryos were rinsed in glycine (26.6 μM) and post-fixed for 20 min in 4% PFA. Embryos were incubated for 48 hr with anti-myosin heavy chain (1:200; mouse monoclonal, clone A4.1025; Merck Millipore, VIC, Australaia) in blocking solution (10% goat serum, 0.4% Triton X-100, 0.1% dimethyl sulfoxide (DMSO) in PBS pH 7.4), and subsequently detected using AlexaFlour® 488-conjugated secondary antibodies [1:500; IgG (H+L) highly cross absorbed antibody, Invitrogen]. Confocal stacks were acquired with 1 μm optical sections using an Eclipse TiE microscope (Nikon) equipped with a Revolution®

DSD2 spinning disk (Andor, Belfast, UK), and NIS elements software (Nikon). Images were prepared using ImageJ (NIH) and Adobe illustrator CS6 (Adobe).

3.2.4. Imaging and analysis of CaP axon pathfinding *in vivo*

The effect of reduced zSTIM1a expression on axon pathfinding *in vivo*, was assessed by visualising CaP axons in Gal4^{s1020t}/UAS:mCherry embryos. For imaging, embryos were anaesthetised [0.004% MS-222 (Sigma-Aldrich) dissolved in 0.5X E2 media] and immobilised in 1.5% low melt agarose (Promega, WI, USA). Images were acquired with an UltraView Vox spinning disk confocal microscope equipped with Volocity software (PerkinElmer). Imaging was restricted to CaP axons located in somites 6-9, with confocal stacks acquired with 1 μm increments using a 525 laser line and 568 emission filter or brightfield illumination.

Pathfinding by CaP axons was assessed by measuring axon length at 20 hpf and 24 hpf, the location of the CaP axon at 24 hpf, the trajectory of the CaP axon away from key pathfinding choice points, the number of filopodia at the growth cone, and the presence of axonal branching events by 24 hpf. Axon length was determined in ImageJ (NIH) by tracing a line through a z-projection of CaP axons from the point at which the axon exits the spinal cord to the most distal tip of the axon. Given that zSTIM1a morphants were smaller than control morphants at 24 hpf, axon length at 24 hpf was normalised to muscle segment height. The location of CaP axons was scored based on the position of their most distal point, with axons observed at the horizontal myoseptum, ventral notochord (which represent intermediate targets for the CaP axons) or within the ventral myotome.

The effect of reduced zSTIM1a expression on CaP axon guidance at choice points was assessed by measuring the angle of axon outgrowth away from choice points. The spinal cord, horizontal myoseptum and ventral notochord, were identified in brightfield. These structures were then used as fiducial marks from which angles of CaP axon outgrowth were calculated. Angles greater than 90° denoted a rostral angle of outgrowth, whilst an angle less than 90° signified a caudal angle of axon outgrowth.

The number of filopodia on CaP axons was quantified at 20 hpf and 24 hpf. At 24 hpf, filopodia were counted in the distal 20 μm of the CaP axon, which includes the growth cone. However, as a large percentage of CaP axons at 20 hpf were less than 20 μm in length, the total number of filopodia on CaP axons was measured. Filopodia were defined as projections that extended greater or equal to 10 μm away from the shaft of the CaP axon.

The number of branching events on each CaP axon was calculated at 24 hpf. A branch of the CaP axon was defined as a projection from the CaP axon that was equal or greater than 10 μm in length with at least one subsequent filopodia. To ensure branches were from the CaP axon, branches were only counted if they originated ventral from the myoseptum, but more than 20 μm from the distal tip.

Images were prepared using ImageJ (NIH) and Adobe illustrator CS6 (Adobe). All statistical tests were performed in GraphPad Prism6.0e (GraphPad Software). As no significant difference was observed between control morphants and wild type embryos for any measure, data presented will compare zSTIM1a morphants to control morphants alone. The absence of an effect of control morpholino injection on zebrafish development compared to wild type embryos is demonstrated in Figs. 3.2-3.4, and then not shown.

3.3. Results

3.3.1. zSTIM1a is important for survival of zebrafish embryos

To investigate the role of zSTIM1a in axon guidance, expression of zSTIM1a was reduced by morpholino microinjection at the 1-4 cell stage of development. STIM1 and SOCE have been described to be important for embryonic survival in mice, with STIM1 or Orai1 knockout mice dying in the late embryonic or early post-natal period (Gwack et al., 2008; Oh-Hora et al., 2008; Stiber et al., 2008; Vig et al., 2008). Similarly, STIM1 function is essential for *Drosophila* survival past the 2nd or 3rd instar stage of development (Eid et al., 2008), suggesting that the requirement of STIM1 for survival is conserved across invertebrate and vertebrate species. Therefore, it was reasoned that reducing zSTIM1a expression during zebrafish development would cause a decrease in embryo survival.

Reduced zSTIM1a expression caused a decrease in embryo survival (Fig. 3.2). Embryo survival at 96 hpf was reduced in zSTIM1a morphants (46.7% ± 4.8%, n=8 experiments of 50-150 embryos; $p<0.0001$), compared to both control morphants (87.5% ± 2.7%, n=8; $p<0.001$) and sham injected controls (98.5% ± 3.5%, n=5; $p<0.001$). No significant difference was observed between control morphants and sham injected controls ($p=0.0524$). The effect of zSTIM1a knockdown on embryo survival was evident by 8 hpf, with the survival of zSTIM1a morphants remained significantly decreased compared to control morphants at all stages of development (8 hpf $p<0.002$; 24 hpf $p<0.001$; 48 hpf, $p<0.001$; 72 hpf $p<0.001$). These data suggest that zSTIM1a expression is important for a critical event in early zebrafish development and, as such, zSTIM1a is vital for the survival of zebrafish embryos.

Figure 3.2: Reduction of zSTIM1a expression decreased the survival of zebrafish embryos.

The importance of zSTIM1a for embryonic development was investigated by assessing the effect of zSTIM1a knockdown on embryo survival. The percent of embryos surviving (normalised to wild type) at 0, 8, 24, 48, 72 and 96 hpf is shown for sham injected embryos (solid black circles), control morphants (light grey circles) and zSTIM1a morphants (empty black circles). Error bars represent SEM, with n values located in the legend correspond to the number of experiments, each of which included 50-150 embryos. Groups were compared using repeated One-way ANOVA with a Holm-Sidak correction for multiple comparisons ($^{****}p<0.0001$ is correct for comparing zSTIM1a morphants to control morphants and sham injected controls).

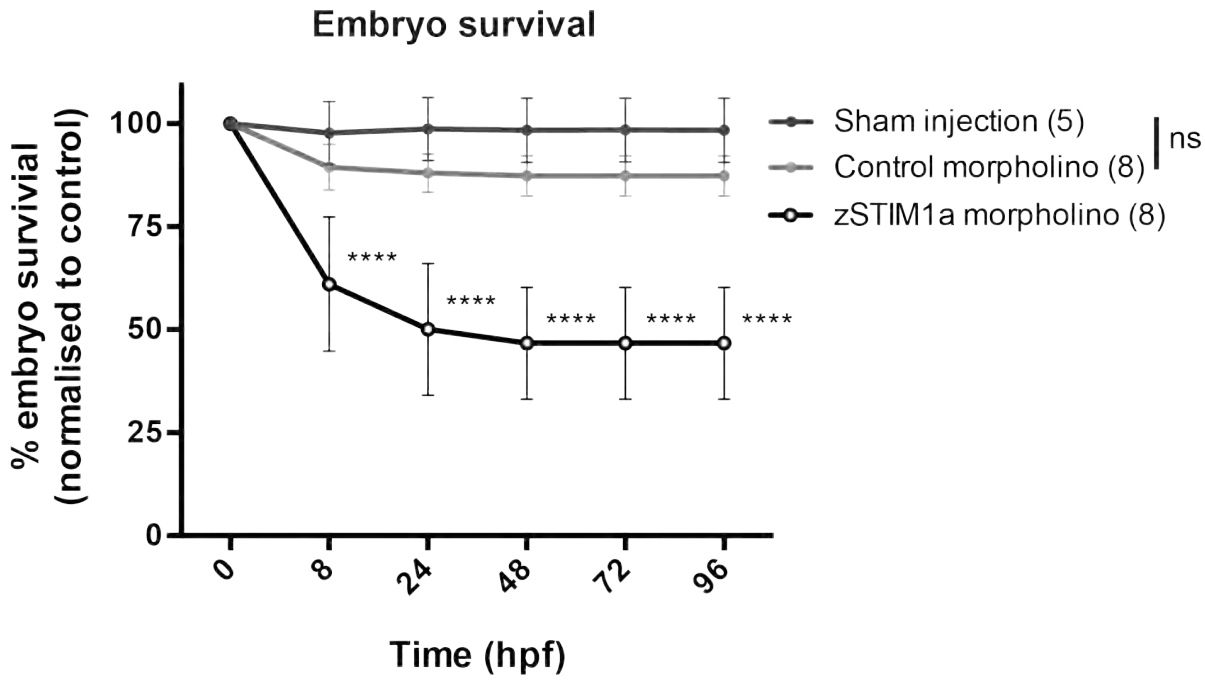
Embryo survival
% embryo survivial (normalised to control)
100
75
50
25
0
0
8
24
48
72
96
Time (hpf)
****
****
****
****
****
Sham injection (5)
Control morpholino (8)
zSTIM1a morpholino (8)
ns

3.3.2. Reduction of zSTIM1a expression in development decreases embryo size

STIM1$^{-/-}$ mice are smaller than their STIM1$^{+/-}$ litter mates (Stiber et al., 2008). To test whether reducing zSTIM1a expression in development similarly affects zebrafish embryo size, embryo length was measured at 24 hpf. Reduced expression of zSTIM1a during development caused a decrease in the size of zebrafish embryos (Fig. 3.3a-c). The length of zSTIM1a morphants (2.16 mm ± 0.026 mm, n=27 embryos) was reduced compared with both control morphants (2.56 mm ± 0.036 mm, n=14 embryos; $p<0.05$), and wild types (2.44 mm ± 0.026 mm, n=27 embryos; $p<0.0005$). However, no change was observed between control morphants and wild types ($p>0.9999$). These data support the hypothesis that zSTIM1a, and therefore SOCE, are important for the growth and development of zebrafish embryos, potentially caused by defects in skeletal muscle development.

STIM1 is important for the development and function of skeletal muscles in mice and *Drosophila* (Eid et al., 2008; Stiber et al., 2008; Venkiteswaran and Hasan, 2009). Hence, it was reasoned that reduced zSTIM1a expression would affect muscle development in zebrafish. The effect of reduced zSTIM1a expression on the development of skeletal muscles was assessed at 24 hpf to coincide with the timing of spinal motor axon outgrowth. Reduced expression of zSTIM1a resulted in a decreased size of tail muscle segments at 24 hpf (Fig. 3.3d-h). The distance from the dorsal to ventral boundary of tail muscle segments was decreased in zSTIM1a morphants (154.0 µm ± 1.15 µm, n=81) compared with both control morphants (158.3 µm ± 1.18 µm, n=36; $p<0.05$) and wild types (159.7 µm ± 0.76 µm, n=66; $p<0.0001$). Similarly, the distance from the anterior to posterior boundary of trunk muscle segments was reduced in zSTIM1a morphants (61.31 µm ± 0.63 µm, n=81) compared with both control morphants (64.01 µm ± 1.24 µm, n=36; $p<0.05$) and wild types (65.07 µm ± 0.62 µm, n=66; $p<0.0001$). There was no difference in tail muscle height or width between control morphants and wild types ($p=0.31$ and $p=0.40$ respectively). Taken together, these data demonstrate that zSTIM1a morphants are smaller than controls at 24 hpf, which correlates with decreased tail muscles size at the same developmental stage. These findings are consistent with findings from STIM1 knockout mice (Stiber et al., 2008), suggesting that the importance of STIM1 for development of skeletal musculature is conserved across vertebrate species.

Figure 3.3: Reducing zSTIM1a expression in development decreases embryo size.

(a-c) Reduced expression of zSTIM1a decreased embryo length. Representative images of (a) control morphant and (b) zSTIM1a morphant embryos at 24 hpf. Embryo length was calculated by drawing a line from the primordial mouth, along the notochord, to the distal tip of the tail (illustrated by the dashed lines in (a) and (b)). Scale bars denote 0.5 mm. (c) embryo length, as measured from mouth to tail, at 24 hpf (in mm) is shown for wild type, control morphants and zSTIM1a morphants.

(d-h) Reducing the expression of zSTIM1a during development decreased trunk muscle size. (d) Schematic illustrates the architecture of a single trunk muscle segment along the zebrafish tail. Representative images of trunk muscles from (e) control and (f) zSTIM1a morphants at 24 hpf. Horizontal dashed yellow lines denote the dorsal and ventral muscle boundaries used to calculate muscle segment height, whilst the slanted vertical dashed yellow lines show the somite boundary used to calculate muscle segment width. White arrows represent the distances used to calculate trunk muscle height and width. Scale bars denote 50 μm. (g-h) The distance from the dorsal to ventral and anterior to posterior boundaries of trunk muscle segments (in μm) at 24 hpf is shown for control, control morphants and zSTIM1a morphants. Groups were compared using One-way ANOVA with a Holm-Sidak correction for multiple comparisons ($^{*}p<0.05$, $^{***}p<0.0002$).

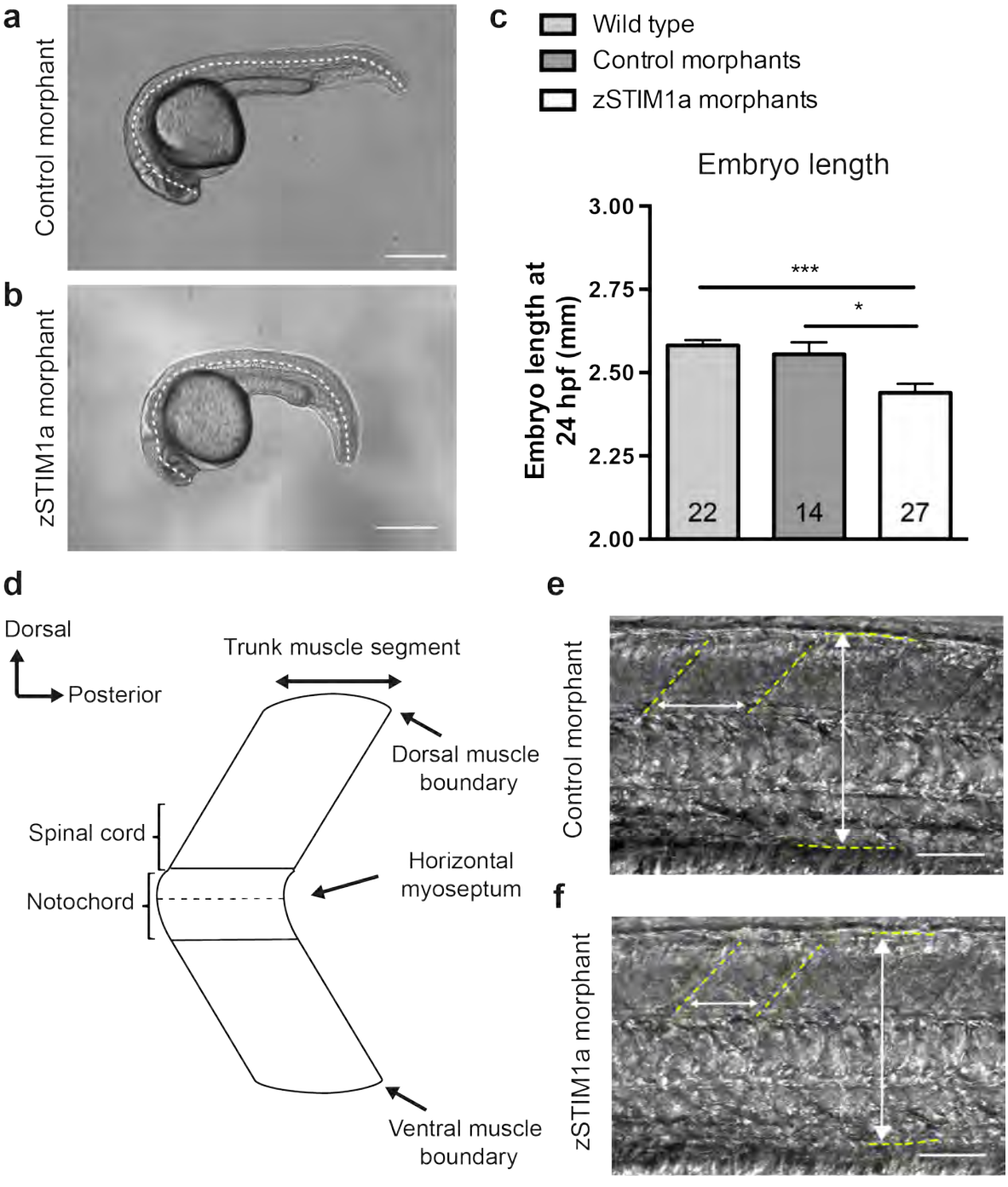
a
Control morphant
b
zSTIM1a morphant
c
Wild type
Control morphants
zSTIM1a morphants
Embryo length
Embryo length at 24 hpf (mm)
3.00
2.75
2.50
2.25
2.00
***
*
22
14
27
d
Dorsal
Posterior
Trunk muscle segment
Dorsal muscle boundary
Spinal cord
Notochord
Horizontal myoseptum
Ventral muscle boundary
e
Control morphant
f
zSTIM1a morphant
g
Muscle segment height
Muscle segment height (µm)
200
180
160
140
120
100
****
*
66
36
81
h
Muscle segment width
Muscle segment width (µm)
80
60
40
20
0
***
*
66
36
81

As muscle length and height were reduced in zSTIM1a morphants, skeletal muscle development was assessed. When zOrai1b expression was reduced in zebrafish, skeletal muscle development was perturbed, with distorted somite boundaries, detachment of myofilaments from the vertical myospeta and thinner myofibrils observed (Volkers et al., 2012). However, when myofilament structure was assessed in zSTIM1a morphants by immunolabelling for myosin heavy chain, no significant defects in skeletal cell development were observed (Fig. 3.4). Somite boundaries were intact, myofilaments extended the length of each myotome (dashed lines), and the thickness of myofibrils appeared unchanged (Fig. 3.4d-e). While no overt defects were found, a subtle change in myofibril shape was observed in zSTIM1a morphants, with myofibrils exhibiting a wavier appearance compared control morphants. These data are consistent with a function of zSTIM1a in skeletal muscle cell development and function in zebrafish.

3.3.3. Reduction of zSTIM1a expression causes anatomical defects in zebrafish embryos

To further investigate the effect of reduced zSTIM1a expression on zebrafish development, the prevalence of anatomical defects in surviving zSTIM1a morphant and control embryos was assessed. Anatomical defects observed in zSTIM1a morphants included bent/curled and/or shortened tails, and the presence of pericardial oedema and/or congestion of blood at the sinus venosus/caudal vein (Fig. 3.5a-b). The number of zSTIM1a morphants with an anatomic defect (40.1% ± 4.9%; n=7 experiments; Fig. 3.5c) was increased compared with wild type, sham injected controls and control morphant embryos ($p<0.0001$ against all treatment groups). Moreover, sham injected controls (8.6% ± 1.8%; n=4 experiments) and control morphants (11.7% ± 1.5%; n=7 experiments) showed no significant increase in the number of embryos with an anatomic defect compared with wild type (2.2% ± 1.0%, n=5 experiments; $p>0.9999$ and $p>0.2$ respectively). These data provide evidence for a zSTIM1a phenotype whereby both cardiac and skeletal muscle function is perturbed during development. These findings are consistent with cardiac defects observed in zOrai1b knockdown (Volkers et al., 2012), and skeletal myopathies in zebrafish and mice (Stiber et al., 2008; Volkers et al., 2012). Taken together, these data suggest that the importance of SOCE for cardiac and skeletal muscle development is conserved across species.

Figure 3.4: Reducing the expression of zSTIM1a during zebrafish embryogenesis does not cause overt defects in skeletal muscle anatomy.

(a) Diagram depicts zebrafish skeletal muscle anatomy at 30 hpf. Adaxial/muscle pioneer cells migrate superficially and generate slow muscle fibres. Subsequently, fast muscle cells differentiate more medially. **(b-c)** Transverse view of confocal stacks acquired at 30 hpf from representative (b) control and (c) zSTIM1a morphant $Gal4^{s1020t}$/UAS:mCherry embryos. Spinal motor neurons (red) denote the spinal cord. Immunolabelling for myosin heavy chain (green) demonstrates normal skeletal muscle architecture in zSTIM1a morphant embryos. Scale bars illustrate 10 µm. **(d-e)** Maximum intensity projections of the lateral view of confocal stacks shown in (b-c), illustrating muscle cell development in control and zSTIM1a morphant embryos at 30 hpf. Dotted lines denote a single myotome. Scale bars illustrate 10 µm for (b) and (c) and 20 µm for (d) and (e). Abbreviations: *hm = horizontal myoseptum; n = notochord*; *sc = spinal cord.*

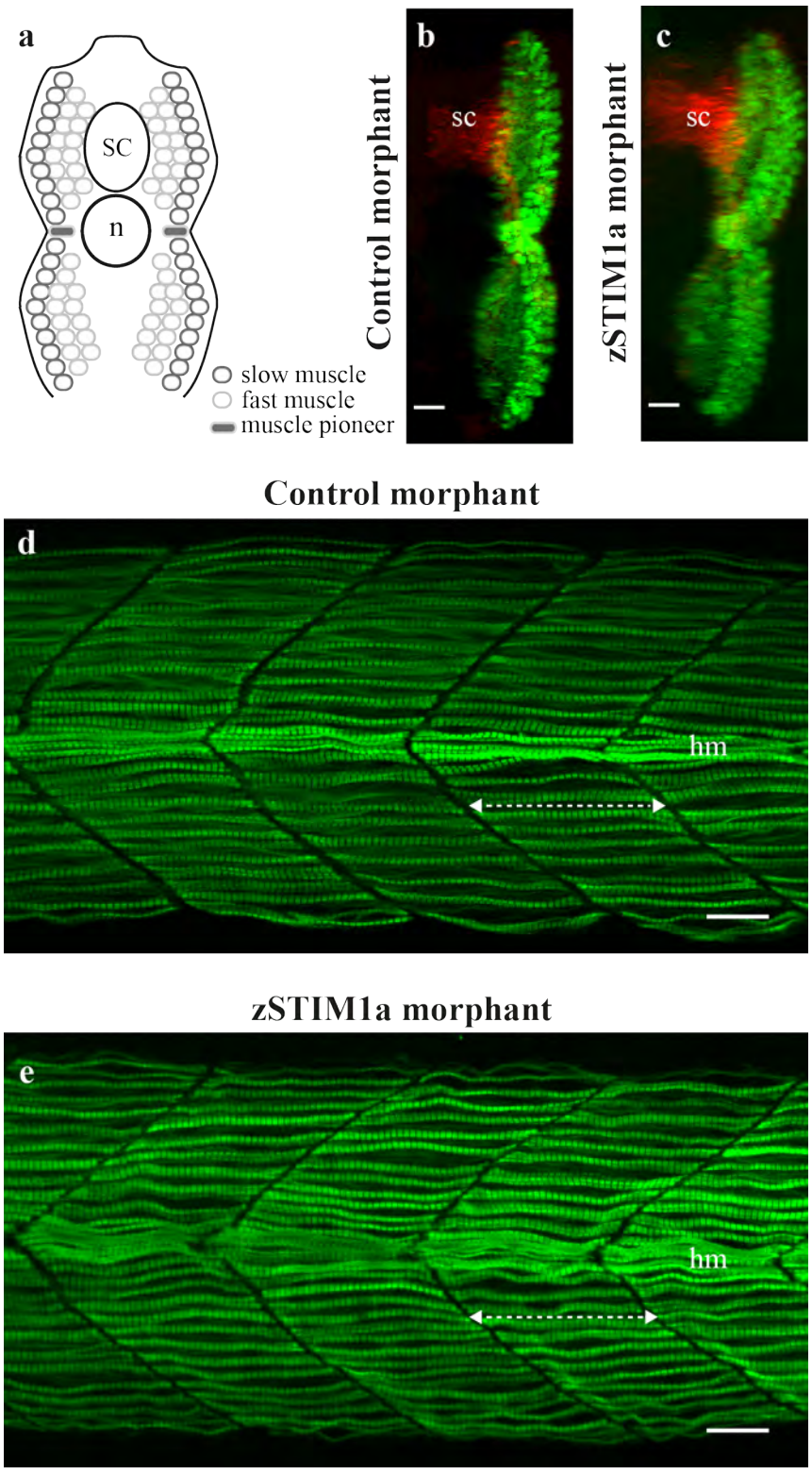
a
SC
n
slow muscle
fast muscle
muscle pioneer
b
sc
Control morphant
c
sc
zSTIM1a morphant
Control morphant
d
hm
zSTIM1a morphant
e
hm

Figure 3.5: Reducing the expression of zSTIM1a during zebrafish embryogenesis causes anatomical defects by 96 hpf.

Reduction of zSTIM1a expression caused anatomical defects. **(a-b)** Representative images of (a) control morphant and (b) zSTIM1a morphant embryos. Anatomic defects included bent/curled (*arrowhead*) or shortened tails, as well as defective cardiac function (*arrow*; pericardial oedema and blood congestion in the sinus venous and/or caudal vein). **(c)** The percent of embryos with an anatomic defect by 96 hpf is shown for wild type, sham injection, control morpholino and zSTIM1a morpholino treatment groups. Error bars represent SD. n values correspond to the number of experiments with at least 50 embryos per experiment. Treatment groups were compared using One-way ANOVA with a Holm-Sidak correction for multiple comparisons ($^{****}p<0.0001$).

a


Control morphant

b


zSTIM1a morphant

c

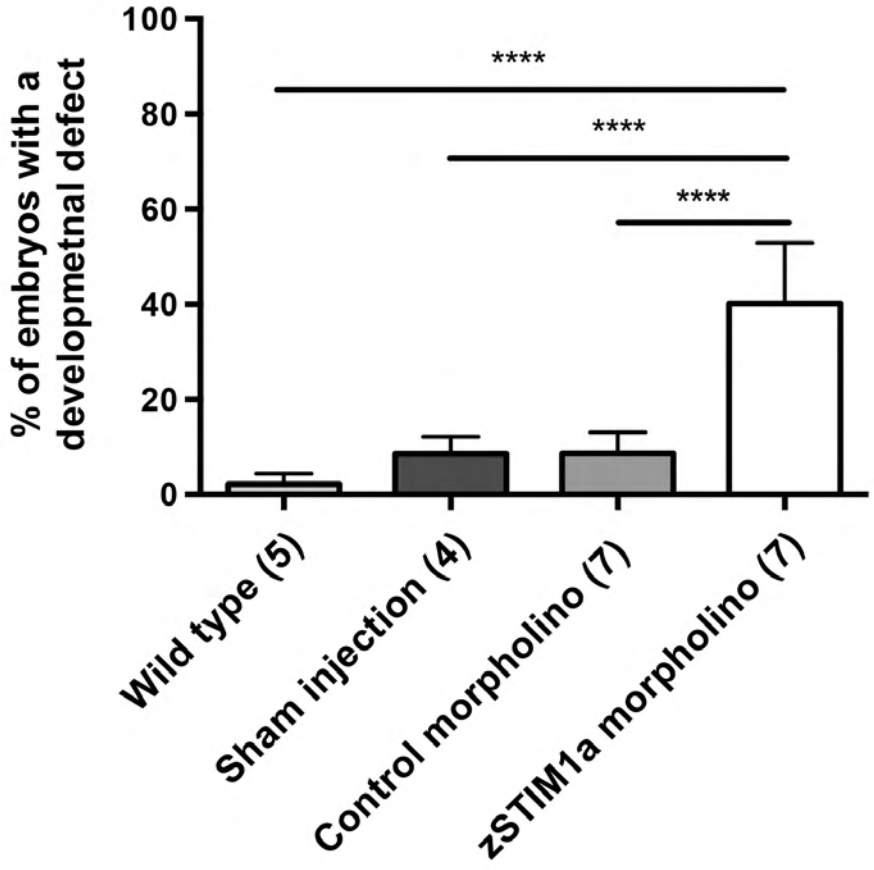
% of embryos with a developmetnal defect
100
80
60
40
20
0
****
****
****
Wild type (5)
Sham injection (4)
Control morpholino (7)
zSTIM1a morpholino (7)

3.3.4. zSTIM1a regulates axon pathfinding by caudal primary (CaP) motor neurons *in vivo*

No overt defects in nervous system development were observed in zSTIM1a morphants, however STIM1 has previously been shown to be necessary for growth cone motility (Mitchell et al., 2012; Shim et al., 2013). As such, the effect of reduced zSTIM1a expression on axon pathfinding was investigated. Perturbed CaP axon outgrowth has been attributed to CaP axons failing to exit the spinal cord and navigate the common pathway (Zeller and Granato, 1999; Zhang and Granato, 2000; Zeller et al., 2002; Feldner et al., 2005; 2007; Jing et al., 2009), or stalling/responding inappropriately at intermediate choice points, including the horizontal myoseptum and ventral notochord (Beattie et al., 2000; Halloran et al., 2000; Hilario et al., 2010; Guillon et al., 2016). If zSTIM1a expression is important for the outgrowth of CaP axons along the common pathway, then CaP axon length should be decreased at 20 hpf. However, zSTIM1a was found to be dispensable for CaP axons to exit the spinal cord and traverse the common pathway (Fig. 3.6), with no difference observed in CaP axon length at 20 hpf between zSTIM1a morphants (25.4 μm [min-max: 3.02 μm–43.99 μm], n=26 axons from 9 animals) and control morphants (25.4 μm [min-max: 8.44 μm–47.56 μm], n=29 axons from 10 animals; p=0.49), with both control and zSTIM1a morphant CaP axons extending along the common pathway towards the nascent horizontal myoseptum. These data suggest that STIM1 function is not required for CaP axons to exit the spinal cord and traverse the common pathway.

As CaP axon outgrowth along the common pathway was unperturbed in zSTIM1a morphants, next the effect of reduced zSTIM1a expression on the ability of CaP axons to navigate from the horizontal myoseptum (via the ventral notochord) to the ventral myotome was assessed by measuring CaP axon length at 24 hpf. zSTIM1a was found to be important for the ventral outgrowth of CaP axons away from the horizontal myoseptum (Fig. 3.6). At 24 hpf, normalised CaP axon length was decreased in zSTIM1a morphants (0.434 [min-max: 0.130–0.710], n=77 axons from 27 animals) compared with control morphants (0.546 [min-max: 0.340–0.770], n=32 axons from 12 animals; p<0.0001). This finding demonstrated that zSTIM1a is required for the appropriate outgrowth of CaP axons ventral to the horizontal myoseptum.

Figure 3.6: zSTIM1a is important for the outgrowth of CaP axons *in vivo*.

(a) Schematic illustrating CaP axon trajectory. After exiting the spinal cord at the ventral root at 17 hpf, CaP axons extend along the surface of the myotome around the notochord, arriving at the nascent horizontal myoseptum (dashed line) at approximately 20 hpf. After pausing at the horizontal myoseptum, CaP axons extend via the ventral notochord (22-23 hpf) towards the ventral muscle boundary (25-26 hpf). CaP axons eventually arborize within the ventral myotome to form neuro-muscular junctions (original figure).

(b-c) Representative control and zSTIM1a morphant CaP axons illustrating the effect of reduced zSTIM1a expression on axon pathfinding *in vivo*. Images are maximum intensity projections of confocal z-stacks acquired at 20 hpf (insets) and 24 hpf. Scale bars denote 5 μm and 10 μm respectively.

(d-e) Cumulative frequency distributions demonstrate the length of CaP axons as measured at 20 hpf and 24 hpf. Groups were compared by Kolmogorov-Smirnov test ($^{***}p<0.0001$), with significance between groups indicated in the legends.

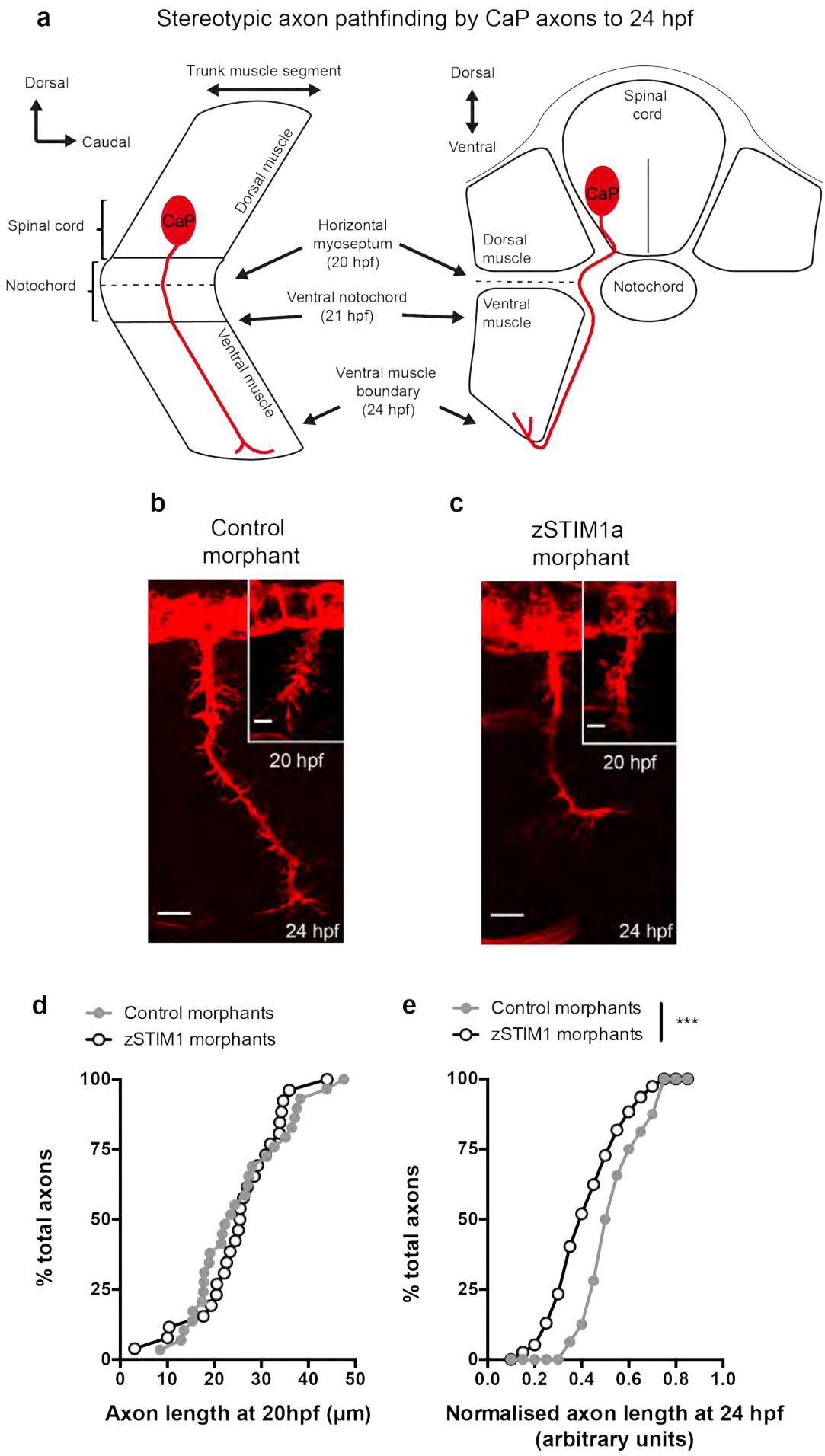
a
Stereotypic axon pathfinding by CaP axons to 24 hpf
Dorsal
Caudal
Trunk muscle segment
Dorsal muscle
Spinal cord
CaP
Notochord
Ventral muscle
Horizontal myoseptum (20 hpf)
Ventral notochord (21 hpf)
Ventral muscle boundary (24 hpf)
Dorsal
Ventral
Spinal cord
CaP
Dorsal muscle
Notochord
Ventral muscle
b
Control morphant
20 hpf
24 hpf
c
zSTIM1a morphant
20 hpf
24 hpf
d
Control morphants
zSTIM1 morphants
% total axons
100
75
50
25
0
0
10
20
30
40
50
Axon length at 20hpf (µm)
e
Control morphants
zSTIM1 morphants
***
% total axons
100
75
50
25
0
0.0
0.2
0.4
0.6
0.8
1.0
Normalised axon length at 24 hpf (arbitrary units)

As zSTIM1a morphant CaP axons failed to extend as far as control morphant CaP axons by 24 hpf, it was reasoned that zSTIM1a morphant CaP axons may stall at intermediate targets. To test this hypothesis, the location of CaP axons at 24 and 48 hpf in control or zSTIM1a morphants was categorised based on the location of their most distal aspect (Table 3.1). At 24 and 48 hpf, CaP axons are predicted to be located on the medial surface of the ventral myotome distal to the ventral notochord, or located on the superficial surface of the ventral myotome respectively (refer to Fig. 3.6a for a diagram depicting anatomic landmarks).

At 24 hpf, CaP axons of control morphants were predominantly located on the medial surface of the ventral myotome (93.7%), with the remainder located at the ventral notochord (6.3%). In contrast, CaP axons of zSTIM1a morphants at 24 hpf were located at the horizontal myoseptum (5.1%) and ventral notochord (32.1%), with only 62.8% of CaP axons located on the medial surface of the ventral myotome, which was significantly reduced compared to controls ($p<0.005$). Furthermore, 10.2% of zSTIM1a morphant axons located on the medial surface of the ventral myotome, but only 3.3% of control morphant axons, had bifurcated at the ventral notochord with both axon branches extending into distal aspect of the ventral myotome. These data suggest that zSTIM1a is important for axon pathfinding by CaP axons via intermediate targets, with CaP axons of zSTIM1a morphants stalling inappropriately at the horizontal myoseptum and ventral notochord, supporting the finding that the length of CaP axons is reduced at 24 hpf in zSTIM1a morphants.

By 48 hpf, 100% of control CaP axons were appropriately located on the superficial surface of the ventral myotome. However, a greater number of CaP axons of zSTIM1a morphants were located at the horizontal myoseptum (7.5%) and ventral notochord (10.0%), reducing the number of CaP axons located on the superficial surface of the ventral myotome (82.5%, $p<0.05$). Moreover, of the 82.5% of CaP axons of zSTIM1a morphants that reached superficial surface of the ventral myotome, 9% did so from an aberrant early branch. These data provide further evidence that zSTIM1a regulates axon pathfinding via intermediate choice points during CaP axon pathfinding, suggesting that STIM1 functions to regulate motile behaviours of axons *in vivo*.

	Location of CaP axons by 24 hpf **			Location of CaP axons by 48 hpf *		
	Horizontal myoseptum	**Ventral notochord**	**Ventral myotome**[±]	**Ventral notochord**	**Ventral myotome boundary**	**Superficial surface of the ventral myotome**
Control morphants	0/32 (0)	2/32 (6.3)	30/32 (93.7)[#]	0/44 (0)	0/44 (0)	44/44 (100)
zSTIM1a morphants	4/78 (5.1)	25/78 (32.1)	49/78 (62.8)[#]	3/40 (7.5)	4/40 (10.0)[†]	33/40 (82.5)[^]

Table 3.2: zSTIM1a morphant CaP axons exhibit axon guidance defects, with CaP axons inappropriately stalling at the horizontal myoseptum, ventral notochord or ventral myotome boundary.

CaP axons were visualised in Gal4^{s1020t}/UAS:mCherry embryos at 24 or 48 hpf, with axons scored on the position of the most distal aspect of the axon. The number of CaP axons at each location is represented as a fraction, with the corresponding percentage of total CaP axons shown in parentheses (n values represent the number of axons imaged in 27 zSTIM1a morphant and 12 control morphant embryos). Treatment groups were compared at 24 and 48 hpf using Chi squared analysis ($^{*}p<0.05$, $^{**}p<0.005$).

[±] *CaP axons located on the medial surface of the ventral myotome, distal to the notochord.*

[#] *One control morphant and five zSTIM1a morphant CaP axons bifurcated at the ventral notochord, with both axonal branches extending ventrally towards the distal region of the ventral myotome.*

[†] *Of the four zSTIM1a morphant axons stalled at the ventral myotome boundary, one axon exhibited an inappropriate caudal branch within the ventral myotome. Whilst another axon bifurcated inappropriately, with both axonal branches stalling at the ventral myotome boundary.*

[^] *Three zSTIM1a morphant CaP axons (9% of total axons) located at the superficial surface of the ventral myotome had extended from an aberrant branch point.*

As zSTIM1a morphant CaP axons stalled at the horizontal myoseptum or ventral notochord, it was reasoned that zSTIM1a expression is important for motility at pathfinding choice points. To further investigate the effect of zSTIM1a knockdown on axon guidance, the trajectory of axon outgrowth distal to the spinal cord, horizontal myoseptum and ventral notochord was assessed (Fig. 3.7). The angle of CaP axon outgrowth ventral from the spinal cord was shifted rostrally in zSTIM1a morphants (89.90° [min-max: 59.06°-127.30°], n=72 axons from 27 embryos) compared with control morphants (76.67° [min-max: 43.07°-99.60°], n=32 axons from 12 embryos, $p<0.0001$; Fig. 3.7d). Given the previous finding that zSTIM1a and control morphant CaP axons exhibit the same length by 20 hpf (see Fig. 3.7d), these data show that CaP axons with pathfinding defects as they extend distal to the spinal cord reach the horizontal myoseptum at an appropriate time, providing evidence for a subtle pathfinding defect in CaP axons extending to the horizontal myoseptum. CaP axon guidance distal to the horizontal myoseptum was also perturbed in zSTIM1a morphants (Fig. 3.7e), with the ventral extension of the CaP axon distal to the horizontal myoseptum found to occur at a more rostral angle in zSTIM1a morphants (79.53° [min-max: 51.91°-125.90°], n=58 axons) compared with control morphants (67.11° [min-max: 52.34°-84.82°], n=32 axons; $p<0.0001$). Furthermore, zSTIM1a morphants CaP axons were also observed to exhibit a greater variance in the range of axon outgrowth angles distal to the ventral notochord (60.34° [min-max: 1.99°-151.70°], n=64 axons) compared with control morphants (64.54° [min-max: 33.52°-70.36°], n=31 axons; $p<0.01$; Fig. 3.7f), suggesting that zSTIM1a is important for CaP axon extension distal to the ventral notochord. Together, these data suggest that zSTIM1a expression is important for the guidance of CaP axons away from intermediate choice points, supporting the previous observation that zSTIM1a morphant CaP axons stall inappropriately at intermediate choice points.

Figure 3.7: zSTIM1a expression regulates the trajectory of CaP axon outgrowth from intermediate pathfinding choice points.

(a-b) Representative images of (a) control and (b) zSTIM1a morphant CaP axons at 24 hpf. mCherry images are maximum intensity projections showing the trajectory of CaP axon outgrowth. Brightfield images are from a single confocal plane at the level that CaP axons exit the spinal cord and extend distal to the ventral notochord. Dashed white lines illustrate the spinal cord (sc), horizontal myoseptum (hm), and ventral notochord (nc) from which angles of axon outgrowth were measured. The dashed line indicates the horizontal myoseptum and has been superimposed from a different z-plane.

(c-e) Cumulative frequency distributions show the angle of axon outgrowth from the (c) spinal cord, (d) horizontal myoseptum and (e) ventral notochord for control and zSTIM1a morphants. The angles of axon outgrowth distal to the spinal cord, horizontal myoseptum and ventral notochord were compared by Kolmogorov-Smironov test ($^{**}p<0.005$, $^{***}p<0.001$, $^{****}p<0.0001$).

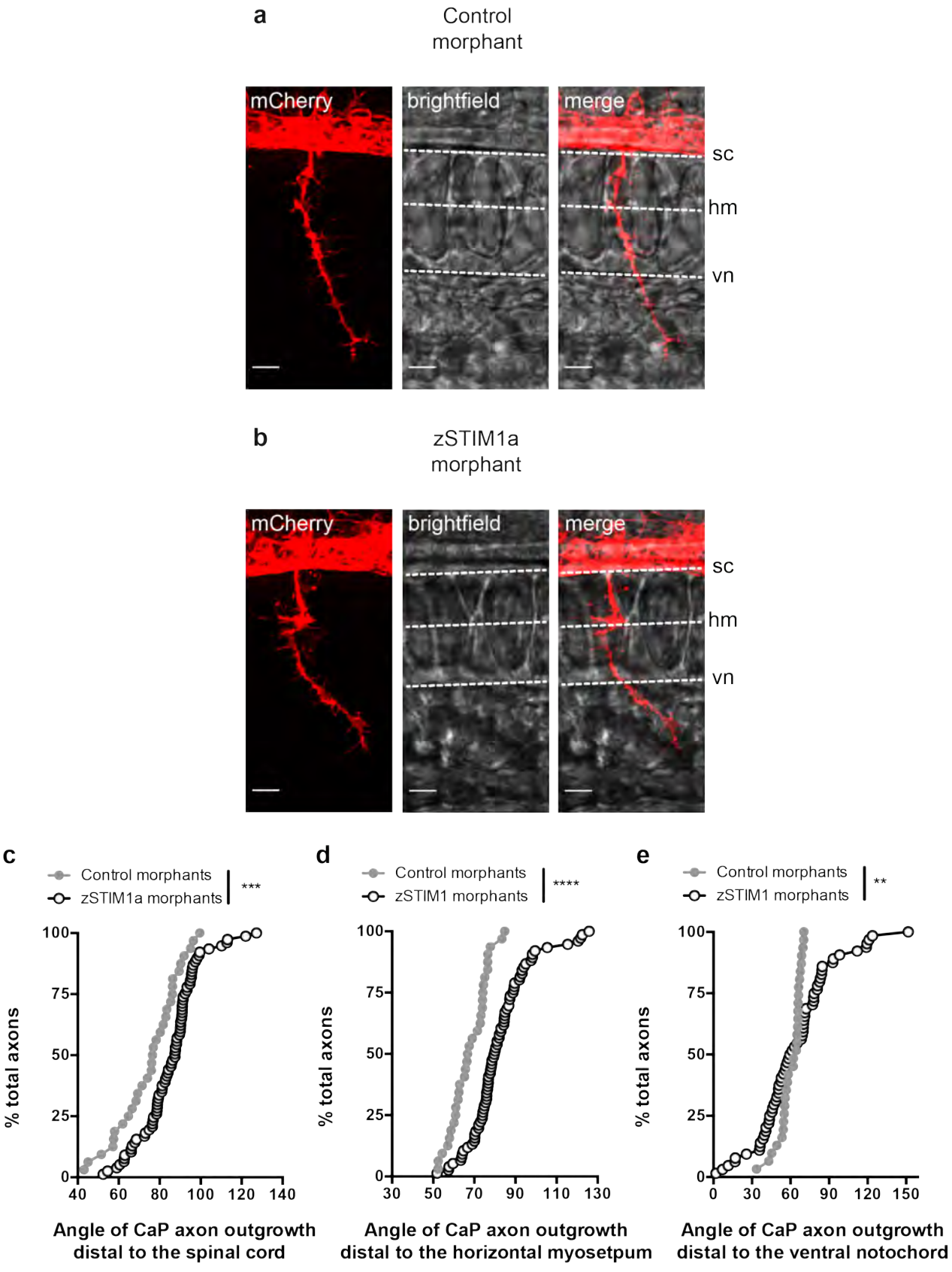
a
Control morphant
mCherry
brightfield
merge
sc
hm
vn
b
zSTIM1a morphant
mCherry
brightfield
merge
sc
hm
vn
c
Control morphants
zSTIM1a morphants
***
% total axons
100
75
50
25
0
40
60
80
100
120
140
Angle of CaP axon outgrowth distal to the spinal cord
d
Control morphants
zSTIM1 morphants
****
% total axons
100
75
50
25
0
30
50
70
90
110
130
Angle of CaP axon outgrowth distal to the horizontal myosetpum
e
Control morphants
zSTIM1 morphants
**
% total axons
100
75
50
25
0
0
30
60
90
120
150
Angle of CaP axon outgrowth distal to the ventral notochord

3.3.5. zSTIM1a regulates filopodial number and is important for axonal branching by CaP axons *in vivo*.

Calcium signaling, by acting on the actin and microtubule cytoskeleton, regulates filopodial protrusion, motility and stabilisation (Davenport et al., 1996; Lau et al., 1999; Gomez et al., 2001; Cheng et al., 2002; Robles et al., 2003; Dent et al., 2004; McVicker et al., 2014). STIM1 has previously been shown to be required for the generation of filopodial calcium signals in response to netrin-1 (Shim et al., 2013). Therefore, it was hypothesised that the formation and/or stabilisation of growth cone filopodia would be reduced in zSTIM1a morphant CaP axons. To assess whether zSTIM1a is important for the formation or stabilisation of filopodia in pathfinding axons, the number of filopodia on CaP axons was assessed at 20 and 24 hpf (Fig. 3.8). The number of filopodia observed on CaP axons at 20 hpf was reduced in zSTIM1a morphants (15.31 ± 1.21, n=26 axons), compared with control morphants (24.66 ± 1.16, n=29 axons; $p<0.0001$; Fig. 3.8c). Similarly, fewer filopodia were present on the distal 20 μm of zSTIM1a morphant CaP axons at 24 hpf (12.25 ± 0.54, n=53 axons) compared with control morphants (15.35 ± 0.67, n=31 axons; $p<0.001$; Fig. 3.8f). These data suggest that STIM1 is required for the generation or stabilisation of filopodial during CaP axon pathfinding.

Since zSTIM1a morphant CaP axons exhibit fewer filopodia, and filopodia are precursors of axonal branches (Szebenyi et al., 1998; Kalil et al., 2000; Dent and Gertler, 2003), it was reasoned that zSTIM1a morphant CaP axons would exhibit less branching. In zSTIM1a morphants, fewer CaP axons exhibited branching by 24 hpf (43.04%, n=78 axons), compared with control morphants (65.63%, n=32 axons; $p=0.0012$; Fig. 3.9c). Taken together, these data suggest that zSTIM1a is important for the regulation of the number of filopodia as well as axonal branching in CaP axons.

Figure 3.8: Reduced zSTIM1a expression decreases the number of filopodia on CaP axons during axon pathfinding.

CaP axons of zSTIM1a morphants exhibited perturbed filopodial dynamics during axon pathfinding *in vivo*. **(a-b)** Representative control and zSTIM1a morphant CaP axons at 20 hpf. **(c)** the total number of filopodia present on CaP axons at 20 hpf. **(d-e)** Representative control and zSTIM1a morphant CaP axons at 24 hpf. **(f)** the number of filopodia present in the distal 20 μm of CaP axons at 20 hpf. Groups were compared by Mann-Whitney *U*-test ($^{****}p<0.0001$, $^{***}p<0.001$). Scale bars illustrate 5 μm.

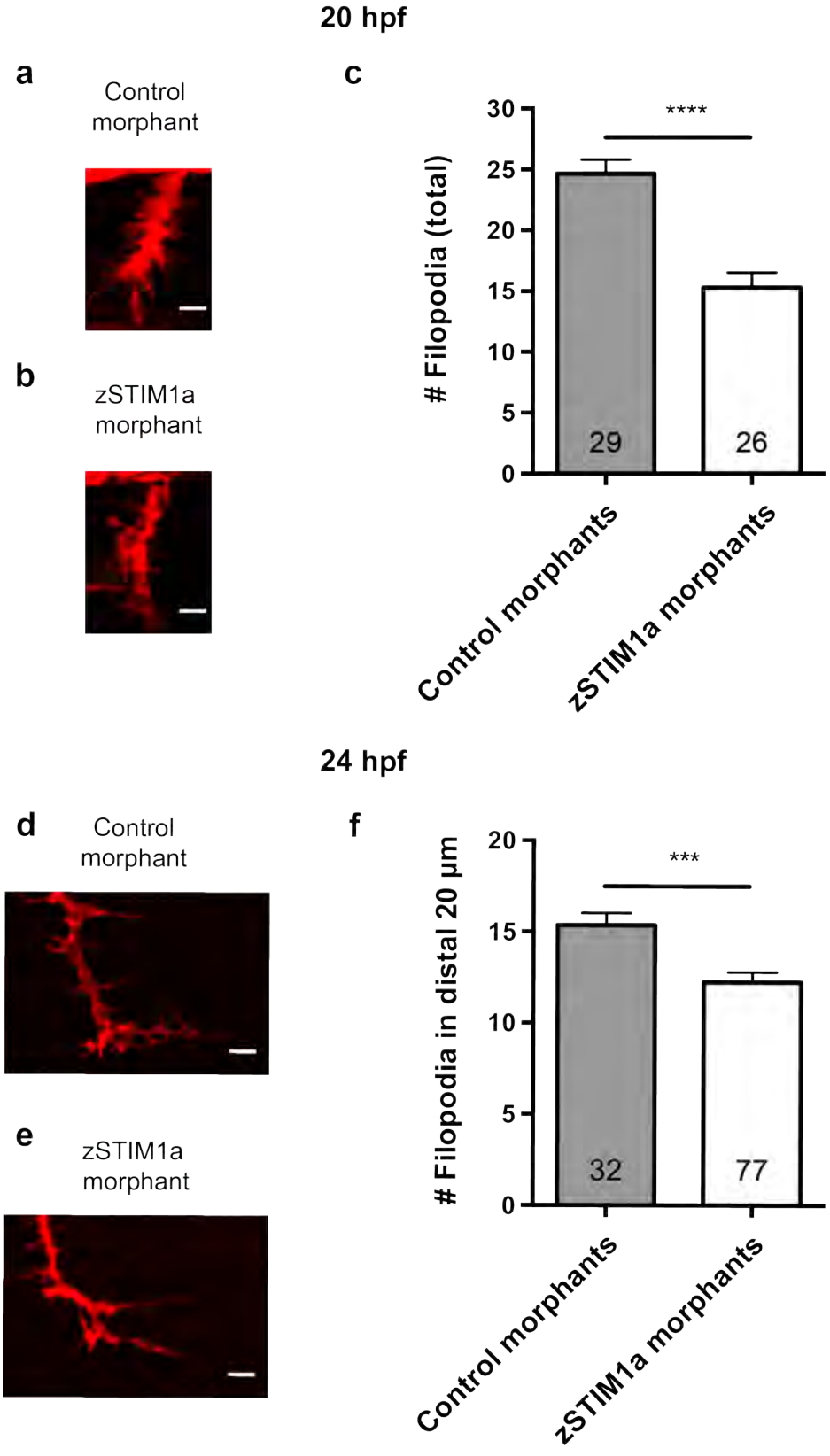
20 hpf
a
Control morphant
b
zSTIM1a morphant
c
Filopodia (total)
30
25
20
15
10
5
0
****
29
26
Control morphants
zSTIM1a morphants
24 hpf
d
Control morphant
e
zSTIM1a morphant
f
Filopodia in distal 20 µm
20
15
10
5
0
***
32
77
Control morphants
zSTIM1a morphants

Figure 3.9: Reduced expression of zSTIM1a decreases the number of CaP axons with a branch by 24 hpf.

(a-b) Representative images of CaP axons at 24 hpf, illustrating axonal branches present in control morphants axons, but absent in zSTIM1a morphants. Scale bar denotes 5 μm. **(c)** Percent of CaP axons with an axonal branch by 24 hpf for control morphants and zSTIM1a morphants. Groups were compared by Fisher's exact tests ($^{*}p<0.05$).

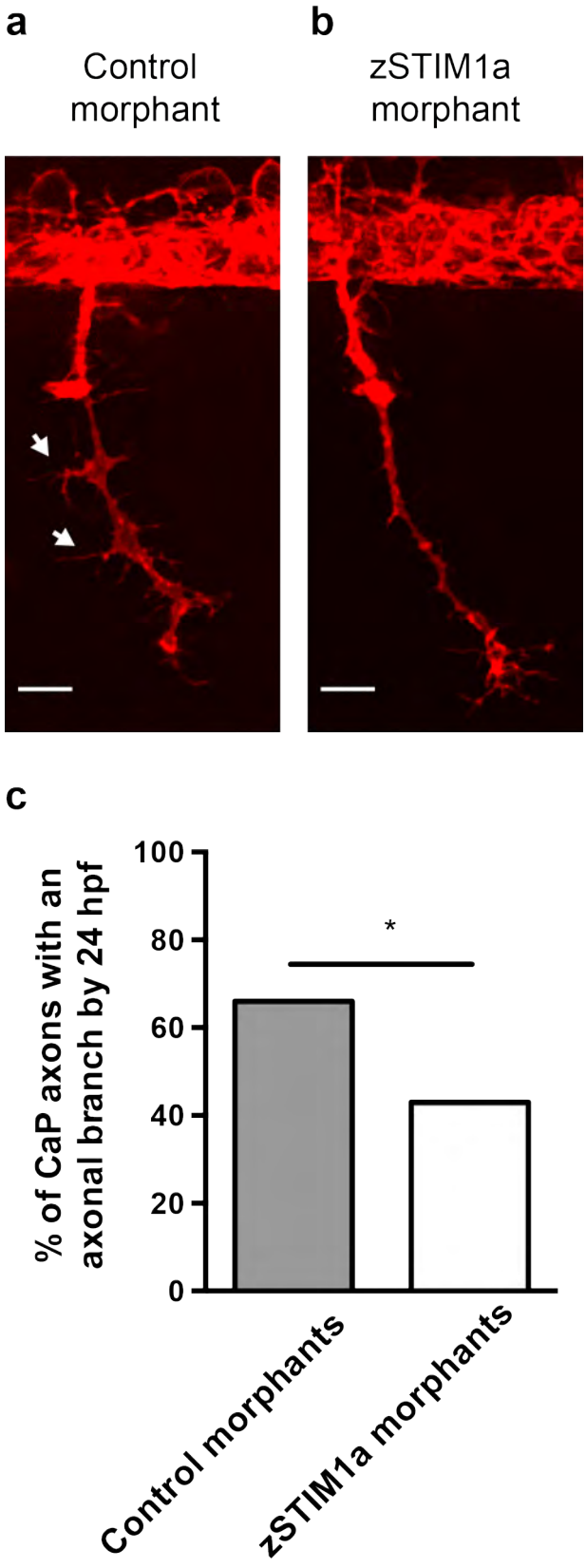
a
Control morphant
b
zSTIM1a morphant
c
% of CaP axons with an axonal branch by 24 hpf
100
80
60
40
20
0
*
Control morphants
zSTIM1a morphants

3.4. Discussion

Data presented in this chapter demonstrate the importance of STIM1 for nervous system development, in particular as a regulator of axon pathfinding by motor neurons *in vivo*. These studies provide evidence to suggest that zSTIM1a expression is crucial for zebrafish embryo survival and development, with gross defects were observed in cardiac and skeletal muscle development. Moreover, reduced zSTIM1a expressed also resulted in subtle defects in the wiring of the nervous system, with CaP axons observed to be stalled at intermediate choice points, exhibited fewer filopodia, and reduced axonal branching. Taken together, these data suggest that STIM1 is required for normal development, including nervous system development, and provide evidence that STIM1 is required for correct axon pathfinding by motor neurons *in vivo*.

zSTIM1a morphant embryos have a decreased rate of survival, are smaller than controls, and exhibit anatomic defects.

zSTIM1a is important for the survival and correct development of zebrafish embryos, with zSTIM1a morphant embryos exhibiting reduced survival and smaller size, impaired cardiac function, as well as bent, curled or shortened tails. The reduced survival of zSTIM1a morphants is consistent with vertebrate and invertebrate animal models in which STIM1 or SOCE have been perturbed in development (Eid et al., 2008; Gwack et al., 2008; Oh-Hora et al., 2008; Stiber et al., 2008; Vig et al., 2008; Pathak et al., 2017), with STIM1$^{-/-}$ and Orai1$^{-/-}$ mice dying in the late embryonic or early post-natal stage of development (Gwack et al., 2008; Oh-Hora et al., 2008; Stiber et al., 2008; Vig et al., 2008). Likewise, expression of dSTIM-specific RNAi, or overexpression of dSTIM, is embryonic lethal in *Drosophila* at the 2nd to 3rd instar stage of development (Eid et al., 2008). Recent work has shown that dSTIM knockout is lethal in *Drosophila* at the 2nd to 3rd instar stage of development (Pathak et al., 2017), with dOrai knockout also lethal, but to a lesser extent than dSTIM (Pathak et al., 2017), suggesting that STIM1 is more important than Orai for survival, most likely reflecting the multiple functions of STIM1. Interestingly, pan-neuronal dSTIM knockout, or dSTIM knockout in dopaminergic neurons only, is lethal at the 3rd instar stage of development (Pathak et al., 2017). Although lethality was decreased compared to global knockout (Pathak et al., 2017), these results illustrate the necessity of STIM1 for nervous system development. Therefore, the

observation that reduced expression of zSTIM1a causes reduced survival is consistent with a developmentally crucial function of STIM1.

Likewise, the observation that zSTIM1a morphants are smaller than controls, and display cardiac and skeletal muscle defects, is consistent with findings from mice, *Drosophila* and zebrafish. STIM1$^{-/-}$ and Orai1$^{-/-}$ mice are 25-30% smaller than heterozygous litter mates (Gwack et al., 2008; Stiber et al., 2008; Vig et al., 2008), and exhibit skeletal myopathy and defects in cardiac function (Gwack et al., 2008; Stiber et al., 2008; Vig et al., 2008). zOrai1b morphant zebrafish embryos exhibit defects in skeletal and cardiac muscle function, with disruption of myofilaments and detachment of myofibrils from vertical myosepta observed in skeletal muscle from 48 hpf (Volkers et al., 2012). dSTIM and dOrai knockout *Drosophila* also exhibit delayed development and are smaller than controls (Pathak et al., 2017). Given the similarities between the zSTIM1a morphant phenotype and the effect of perturbing STIM1 or SOCE in other animal models, these findings suggest that STIM1 function in development is highly conserved between vertebrate and invertebrate species.

Compared with mice and *Drosophila*, embryonic lethality resulting from reduced zSTIM1a expression in zebrafish occurred early in development. The majority of deaths in zSTIM1a morphants occurred by 8 hpf, corresponding to gastrulation stage of development (Kimmel et al., 1995). In contrast, STIM1$^{-/-}$ mice survive until post-natal day 1-2 (Oh-Hora et al., 2008; Stiber et al., 2008), and *Drosophila* with perturbed dSTIM function survive until the 2nd-3rd instar stage (Eid et al., 2008). However, a recent study conducted in zebrafish has shown that STIM1-mediated SOCE regulates sustained calcium signals that drive cytokinesis and daughter cell apposition during the first cell divisions post fertilisation in zebrafish embryos (Chan et al., 2015; 2016), supporting a crucial role for STIM1 in the regulation of cell division in early embryogenesis.

The observed pattern of zSTIM1a expression in development (*described in Chapter 2*), parallels zOrai1b expression in development (Volkers et al., 2012), and zSTIM1a morphants exhibit highly similar defects in cardiac and skeletal function when compared to zOrai1b morphants (Volkers et al., 2012). This correlation provides further evidence to suggest that zSTIM1a regulates SOCE, and that zSTIM1a-mediated SOCE is required for zebrafish development. However, in contradiction to data presented here, zOrai1b

morphants do not show reduced survival, with zOrai1b morphants described as indistinguishable from controls at 24 hpf (Volkers et al., 2012). Several models can explain this phenotypic difference between zSTIM1a and zOrai1b morphants.

Firstly, given that STIM1 initiates SOCE (Liou et al., 2005; Roos et al., 2005; Zhang et al., 2005), it would be predicted that zSTIM1a is more important than zOrai1b for SOCE. This prediction is consistent with the greater requirement of dSTIM compared with dOrai for *Drosophila* development (Pathak et al., 2015). Furthermore, zebrafish have two zOrai1 isoforms (zOrai1a and zOrai1b), as well as a second family member zOrai2 (Cai, 2007b), and calcium influx by SOCE can also be achieved via the activity of TRPC channels (Yuan et al., 2007; Alicia et al., 2008), as illustrated by STIM1-TRPC1 interactions being necessary for SOCE in *Xenopus* spinal neurons *in vitro* (Shim et al., 2013). Hence, compensation by zOrai1a, zOrai2, or TRPC channels may be responsible for ameliorating the effect of zOrai1b knockdown on zebrafish survival, leading to a less severe phenotype compared with the zSTIM1a phenotype described herein.

Secondly, SOCE-independent functions zSTIM1a could be required for zebrafish development. STIM1 functions in a non-SOCE dependent manner to regulate cAMP signaling via a store-operated cAMP pathway (Lefkimmiatis et al., 2009), and ER localisation within the cell via interactions with the microtubule cytoskeleton (Grigoriev et al., 2008; Smyth et al., 2012; Asanov et al., 2013). Indeed, STIM1 regulates ER remodeling and calcium signaling events required for the exclusion of ER from the mitotic spindle during cell division in HeLa cells *in vitro* (Smyth et al., 2012). Hence, non-SOCE dependent functions of zSTIM1a may also be required for zebrafish development, leading to decreased rate of survival when zSTIM1a expression was reduced. Therefore, it is plausible that zSTIM1a could exhibit both SOCE-dependent and SOCE-independent functions in embryonic development, illustrating the importance of STIM1 for zebrafish development.

As the zSTIM1a morphant phenotype closely resembles observed effects of STIM1 dysfunction in other vertebrate and invertebrate animal models, this data corroborates findings from Chapter 2 that zSTIM1a, and not zSTIM1b, is the most conserved STIM1 ortholog in zebrafish. Moreover, given that endogenous zSTIM1b expression did not appear to compensate for the effect of reduced zSTIM1a expression on development,

these data would argue that that zSTIM1a and zSTIM1b have distinct functions. zSTIM1b was shown in Chapter 2 to lack the TRIP motif that regulates STIM1-EB interactions at microtubule tips, which is required for the ER remodeling function of STIM1 that has been shown in non-neuronal cells (Grigoriev et al., 2008; Asanov et al., 2013). If the ER remodeling function of zSTIM1a is crucial for zebrafish development, then knockdown of zSTIM1b should not recapitulates the effect of zSTIM1a knockdown. Therefore, data presented here may also suggest that the non-canonical function of STIM1 are important for development.

An important limitation of this study is that a single translation blocking morpholino was used, and exogenous expression of STIM1 was not used to rescue zSTIM1a knockdown. Although a recent study has revealed a poor correlation between morpholino induced phenotypes and gene knockout phenotypes (Kok et al., 2015), this correlation does not hold true for all morpholino-induced phenotypes (Robu et al., 2007; Eisen and Smith, 2008; Bill et al., 2009). Furthermore, the strong similarities between the zSTIM1a morphant phenotype and other animal models of abolished or perturbed STIM1 function, and the lack of an effect of the mispaired control morpholino on development, would both argue for a specific effect of zSTIM1a knockdown on zebrafish development. Nevertheless, to validate the results presented herein future studies should utilize a second translation-blocking morpholino, a splice site targeted morpholino, or co-inject mRNA for human STIM1in an attempt to resuce the zSTIM1a morphant phenotype. One technical limitation to the co-injection of human STIM1 is that overexpression of STIM1 causes the aberrant activation of SOCE (Xu et al., 2006; Soboloff et al., 2006b), and results in perturbed cell function (Hewavitharana et al., 2008; Hajkova et al., 2011; Henke et al., 2012; Gwozdz et al., 2012a; 2012b; Henke et al., 2013; Wang et al., 2014; Vigont et al., 2015). Consistent with these findings, attempts made to rescue the zSTIM1a knockdown by co-injecting DNA encoding for a YFP-tagged human STIM1 (Liou et al., 2007) were unsuccessful, with injection of YFP-tagged human STIM1 alone affecting zebrafish development (data not shown). While the lack of rescue experiment is an important limitation of these experiments, these findings presented herein are consistent with the known effect of perturbed STIM1 function in other animal models, while being distinct from generalized defects in convergent extension associated with morpholino toxicity (Robu et al., 2007; Eisen and Smith, 2008). As such, a dominant-negative

zSTIM1a was synthesised to address the cell-autonomous effect of perturbed zSTIM1a function on axon pathfinding (see discussion below).

Another important limitation of this study is that zSTIM1a knockdown could not be assessed due to a lack of antibodies capable of detecting zSTIM1a protein by immunoblotting (Chapter 2). Hence the degree of protein knockdown induced by the zSTIM1a morpholino could not be measured. However, injection of fluorescently tagged morpholinos at the 1-4 cell stage has been shown to result in an even distribution of morpholinos throughout the embryo by 4 hpf, which persists to at least 28 hpf (Nasevicius and Ekker, 2000). While morpholinos targeted to green fluorescent protein (GFP) in GFP expressing zebrafish can effectively reduce GFP expression to 20% of control expression (Nasevicius and Ekker, 2000). Therefore, given that the zSTIM1a morphant phenotype is consistent with other animal models of perturbed STIM1 function, it can be reasoned that zSTIM1a expression was reduced by injection of the zSTIM1a morpholino.

zSTIM1a regulates axon pathfinding by zebrafish spinal motor neurons

Although no gross morphological defects were observed in the nervous system when zSTIM1a expression was reduced, it has been well characterised that subtle defects in the wiring of the nervous system lead to severe neurodevelopmental disease (Lewis and Levitt, 2002; Powell et al., 2003; Fromer et al., 2014). Hence, a hallmark of nervous system development is the fidelity with which each axon finds and synapses with its correct target (Dodd and Jessell, 1988; Catela et al., 2015). Vital to this process is the way in which axons navigate via intermediate targets, which function as guideposts to ensure that each axons reaches an appropriate target (Lance-Jones and Landmesser, 1981; Bentley and Keshishian, 1982; Bentley and Caudy, 1983; Bastiani et al., 1984). Indeed, axons that innervate distinct regions, such as the three primary motor neurons of each spinal cord hemisegment in zebrafish, can navigate via the same intermediate target (Eisen et al., 1986; Myers et al., 1986; Westerfield et al., 1986), highlighting how pathfinding decisions made by axons at intermediate choice points are crucial for the wiring of the nervous system in development (Beattie et al., 2000; Lieberam et al., 2005; Sato-Maeda et al., 2006; Hilario et al., 2010; Poliak et al., 2014). Although CaP axons of zSTIM1a morphants exhibited subtle axon pathfinding defects as they exit the spinal cord, they could extend along the common pathway to reach the horizontal myoseptum

at the same time as CaP axons of control morphants. These data suggest that zSTIM1a regulates axon pathfinding by CaP, but that zSTIM1a is ultimately dispensable for CaP axons to reach the horizontal myoseptum. However, once the CaP axons of zSTIM1a morphants reach the horizontal myoseptum, they are more likely to stall inappropriately at the myoseptum or ventral notochord, two key intermediate targets for the CaP axon (Beattie et al., 2000). One interpretation of this data is that zSTIM1a is important for axon guidance events at intermediate choice points during axon outgrowth. Consistent with this interpretation, CaP axons were observed to be stalled inappropriately at intermediate choice points at 24 and 48 hpf, and the trajectory of axon outgrowth distal to the spinal cord, horizontal myoseptum and ventral notochord were perturbed. Thus, zSTIM1a appears to be important for axon guidance throughout CaP axon outgrowth, with zSTIM1a knockdown causing a subtle pathfinding defect as CaP axons exit the spinal cord and navigate along the common pathway, but causing more overt defects as CaP navigate via intermediate targets. Therefore, these findings are consistent with a role for STIM1 in the regulation of axon guidance *in vivo*, supporting previous studies that found STIM1 to be necessary for growth cone motility in mammalian DRG sensory neurons (Mitchell et al., 2012), and midline crossing by axons of commissural interneurons in the *Xenopus* spinal cord (Shim et al., 2013).

Data presented here illustrate that zSTIM1a expression is important for axon pathfinding by CaP neurons, however it does not identify the mechanism by which CaP axon pathfinding is perturbed. STIM1 has been described to exhibit both SOCE-dependent and SOCE-independent functions (Roos et al., 2005; Zhang et al., 2005; Mercer, 2006; Peinelt et al., 2006; Grigoriev et al., 2008; Lefkimmiatis et al., 2009; Smyth et al., 2012; Asanov et al., 2013), both of which have been implicated in growth cone motility (Mitchell et al., 2012; Shim et al., 2013). In the work presented here, reducing the expression zSTIM1a decreased the number of filopodia present on CaP axons. Filopodia are crucial for axon guidance, with growth cones reoriented in response to single filopodial contacts with substrate-bound or diffusible guidance cues (O'Connor et al., 1990; Gomez and Letourneau, 1994; Zheng et al., 1996), and a lack of filopodia associated with errors as axons navigate via intermediate choice points (Chien et al., 1993). Calcium is a crucial modulator of filopodial motility (Gomez et al., 2001; Robles et al., 2003), with STIM1 and SOCE shown to mediate filopodial calcium transients in *Xenopus* spinal neurons *in vitro* (Shim et al., 2013). As ER calcium release contributes

to localised calcium signals in growth cones (Ooashi et al., 2005; Tojima et al., 2007; Gasperini et al., 2009), and localisation of ER to filopodia is proposed to be a mechanism to spatially restrict calcium signals (Davenport et al., 1996), the observed decrease in filopodial number in CaP axons of zSTIM1a morphants provides support for both a SOCE-dependent function of zSTIM1a in CaP axons, as well as a role for zSTIM1a as a +TIP protein that regulates ER remodeling in CaP axons enable localised calcium singling. As discussed, examining the function of zSTIM1b in motor axon guidance, which is not predicted to retain the capacity to mediate ER remodeling (*Chapter 2*), should provide evidence as to whether the ER remodeling function of STIM1 is required for axon pathfinding. Moreover, data presented cannot rule out that zSTIM1a functions to regulate store-operated cAMP signaling during axon pathfinding. As such, future studies should aim to decipher the contributions of these diverse function of STIM1during axons guidance.

Branching by the CaP axons has been well characterised (Eisen et al., 1986; Westerfield et al., 1986), with branches observed proximal to the CaP growth cone when the CaP axon is extending into the ventral myotome (Sainath and Granato, 2013). Consistent with a role for zSTIM1a in the regulation of CaP axon guidance, zSTIM1a morphant CaP axons were less likely to exhibit an axonal branching event. As filopodia are often the site of axonal branching events (Kalil et al., 2000; Szebenyi et al., 2001; Dent and Gertler, 2003), and fewer filopodia were observed in zSTIM1a morphant CaP axons, it is not surprising that zSTIM1a morphant CaP axons possessed fewer branches. Moreover, a calcium dependent process whereby axonal branches are promoted by localised, high frequency calcium transients has previously been described (Tang and Kalil, 2005). Interestingly, axonal branching was promoted by the local application of netrin-1 (Tang and Kalil, 2005), which has previously been shown to require STIM1-medaited SOCE to generate localised calcium signals in the growth cones of *Xenopus* neurons (Shim et al., 2013). Hence, decreased branching observed in CaP axons could be a direct result of perturbed zSTIM1a-mediated SOCE.

Although defects in calcium signaling, cAMP signaling or ER remodeling can explain perturbed axon pathfinding by CaP neurons of zSTIM1a morphants, it should be noted that CaP axon pathfinding is not purely a cell autonomous process, with many myotome-derived guidance cues known to inform motor axon outgrowth (Pike et al., 1992;

Lauderdale et al., 1997; Zeller and Granato, 1999; Beattie et al., 2000; Zhang and Granato, 2000; Zeller et al., 2002; Rodino-Klapac and Beattie, 2004; Birely et al., 2005; Schneider and Granato, 2006). In the experiments presented here, zSTIM1a expression was reduced throughout the entire animal. Therefore, the impact of reduced zSTIM1a expression on axon pathfinding may not be a cell-autonomous effect. Given the myriad of guidance cues and receptors implicated in the control of motor neuron axon guidance (Dodd and Jessell, 1988; Beattie, 2000; Schneider and Granato, 2003; Bonanomi and Pfaff, 2010; Alaynick et al., 2011), the effect of zSTIM1a knockdown on axon guidance *in vivo* is likely to be highly complex, with zSTIM1a likely to be involved in the regulation of axon guidance via multiple autonomous and non-autonomous guidance mechanisms.

Zebrafish sema3A1 and sema3A2 are crucial for CaP axon guidance (Roos et al., 1999; Halloran et al., 2000; Feldner et al., 2005; Sato-Maeda et al., 2006; Feldner et al., 2007; Palaisa and Granato, 2007; Plazas et al., 2013), with sema3A1 and sema3A2 acting via neuropillin-1a/PlexinA3 to trigger repulsion (Roos et al., 1999; Feldner et al., 2005; 2007; Palaisa and Granato, 2007; Plazas et al., 2013). Knockdown experiments have demonstrated that sema3A1/2 signaling is important for the refinement of axon outgrowth along the common pathway (Feldner et al., 2005; 2007). Interestingly, CaP axons downregulate neuropillin-1a (NP1a) after reaching the horizontal myoseptum (Sato-Maeda et al., 2006), presumably to permit the ventral targeting of CaP axons into the sema3A1-expressing ventral myotome (Bernhardt et al., 1998; Shoji et al., 2003; Feldner et al., 2005; Sato-Maeda et al., 2006). STIM1 is necessary for correct growth cone motility in response to sema3a (Mitchell et al., 2012). Consistent with a role for STIM1 in regulating axon guidance in response to sema3a, CaP axons of zSTIM1a morphants showed subtle pathfinding defects when traversing the common pathway, with a perturbed angle of extension distal to the spinal cord observed. Interestingly, calcium signals are known to control gene expression (Jessell, 2000; Sharma et al., 2000; Groth and Mermelstein, 2003; Bonanomi and Pfaff, 2010; Somasundaram et al., 2014; Kar and Parekh, 2015; Kar et al., 2016), with guidance cue receptor expression regulated in a calcium dependent manner during axon outgrowth (Hanson and Landmesser, 2006). While calcium signals directly modulate sema3a-PlexinA3 signaling in pathfinding CaP axons (Plazas et al., 2013). Therefore, it could be theorised that STIM1 interacts with

sema3a signaling both upstream of sema3a by controlling receptor expression, as well as downstream of sema3a by modulating sema3a-NP1a-PlexinA3 signaling.

STIM1 has also been implicated in the regulation of axon pathfinding in response to netrin-1 (Shim et al., 2013). The regulation of motor axon guidance by netrin-1 is highly complex, with netrin-1 exhibiting both attractive and repulsive effects on motor neuron axon pathfinding (Hedgecock et al., 1990; Kolodziej et al., 1996; Mitchell et al., 1996; Winberg et al., 1998; Poliak et al., 2014). In zebrafish embryos, adaxial cells that are initially located on the medial surface of the myotome, and muscle pioneer cells located at the horizontal myoseptum, express netrin-1a concurrent with CaP axon outgrowth (Lauderdale et al., 1997). The proximity of CaP axons with adaxial cell during pathfinding (Melancon et al., 1997; Zeller and Granato, 1999), and the targeting of CaP axons to the horizontal myoseptum (Myers et al., 1986; Westerfield and Eisen, 1987; Eisen and Melancon, 2001), suggests that netrin-1a is important for CaP axon guidance. However, netrin-1a expression is not essential for CaP axon outgrowth, with axons projecting from the spinal cord in *no tail* mutants that lack muscle pioneer cells (Halpern et al., 1993), supporting the view that additional guidance mechanisms compensate for the loss of netrin-1 signaling in motor axon outgrowth (Poliak et al., 2014). When the finding that zSTIM1a is important for the distal extension of CaP axons from both the spinal cord and horizontal myoseptum is considered together with data indicating that STIM1 is required for netrin-1mediated growth cone attraction (Shim et al., 2013), perturbed CaP axon guidance in zSTIM1a morphants may be caused by dysfunction in netrin-1 mediated axon outgrowth, but would not be predicted to cause the complete abrogation of CaP axon pathfinding.

The observation that axon pathfinding by zSTIM1a morphant CaP axons is perturbed at the horizontal myoseptum and ventral notochord, but that CaP axons ultimately reach the ventral myotome, albeit late, is consistent with previous studies in which myotome-derived guidance cues were perturbed. Ablation of muscle pioneers located at the horizontal myoseptum causes CaP axons to stall at the presumptive myoseptum, however they eventually reach the ventral muscle (Melancon et al., 1997). Suggesting that guidance signals produced by muscle pioneer cells influence axon outgrowth, but are not essential for targeting of the CaP axon to the ventral myotome. Likewise, in *stumpy* mutants [mutation in collagen XIXa1 (Hilario et al., 2010)], CaP axons correctly navigate

to the horizontal myoseptum but stall at the myoseptum and/or ventral notochord before eventually extending distally towards the ventral myotome (Beattie et al., 2000; Hilario et al., 2010). Similarly, a loss of function in collagen XVb, which is laid down by adaxial cells in front of the CaP axon to regulate axon extension, results in truncated CaP axon outgrowth (Guillon et al., 2016). In the *topped* mutant, CaP axons navigate correctly along the common pathway, but stall at the horizontal myoseptum, delaying their extension into the ventral myotome (Rodino-Klapac and Beattie, 2004). Cell transplantation studies showed that *topped* expression in ventromedial fast muscle cells adjacent to the horizontal myoseptum, but not the CaP axon, is able to rescue ventral extension of the CaP axon (Rodino-Klapac and Beattie, 2004). Given that similar axon pathfinding defects are observed in zSTIM1a morphant CaP axons, it can be hypothesised that zSTIM1a functions in response to myotome-derived guidance cues to make appropriate guidance decisions during CaP axon outgrowth. Significantly, data presented here also showed that skeletal muscle cell anatomy is intact at 30 hpf, providing evidence to suggest that axon guidance defects observed in zSTIM1a morphants are not caused by an underlying defect in the development of skeletal muscle cells.

These studies demonstrate the complexity of axon guidance by the CaP axon, and illustrate how, even though zSTIM1a knockdown perturbs axon guidance, other molecular mechanisms can still compensate, leading to CaP axons eventually reaching the ventral myotome. They also illustrate the importance of myotome-derived guidance cues for CaP axon pathfinding. In experiments presented here, zSTIM1a expression was reduced globally. Given that STIM1 has previously been shown to be required for skeletal muscle development (Stiber et al., 2008), and zSTIM1a morphants exhibit perturbed tail development, it is probable that the effect of reduced zSTIM1a expression on CaP axon pathfinding is due to myotome dysfunction. In *unplugged* mutants (mutation in the muscle specific receptor tyrosine kinase MuSK), CaP axons are not restricted to the centre of the myotome and stall at the horizontal myoseptum, yet CaP axons can still navigate into the ventral myotome (Zhang and Granato, 2000; Zhang et al., 2004; Flanagan-Steet, 2005; Panzer et al., 2005; Kim et al., 2006; Kim and Burden, 2007; Jing et al., 2009). Wnt signalling via *unplugged*/MuSK pre-patterns acetylcholine receptors (AChR) along the medial aspect of the myotome (Jing et al., 2009), and axons navigating via AChR clusters (Flanagan-Steet, 2005; Kim and Burden, 2007), forming *en passant* synapses (Westerfield et al., 1986; Jontes et al., 2000; Flanagan-Steet, 2005; Panzer et

al., 2005), which establish the earliest movements of the embryo (Saint-Amant and Drapeau, 1998; 2000). Furthermore, *unplugged*/MuSK signaling may also mediate CaP axon guidance by triggering deposition of extracellular matrix components by adaxial cells, such as tenascin-C and chondroitin sulfate proteoglycans (Zhang et al., 2004; Schweitzer et al., 2005). Therefore, given that STIM1 has previously been implicated in regulation of signaling at neuromuscular junctions (Venkiteswaran and Hasan, 2009), it is plausible that perturbed zSTIM1a function leads to axon pathfinding errors due to perturbed formation or signaling at neuromuscular junctions.

Deciphering the cell-autonomous function of zSTIM1a for axon pathfinding

Given that the morpholino knockdown approach raised questions as to the cell-autonomous effect of zSTIM1a knockdown, significant attempts were made to address whether perturbed zSTIM1a function in motor neurons is responsible for the defects in motor axon pathfinding in vivo (data not shown). Based on previous studies that utilised dominant negative versions of STIM1 to perturb STIM1 function in mammalian or *Xenopus* models (Liou et al., 2005; Shim et al., 2013), a dominant negative version of zSTIM1a (DN-zSTIM1a) was generated. To construct DN-zSTIM1a, an aspartate to alanine substitution was introduced at residue 70 of the calcium binding EF-hand (D70A), abolishing the ability of zSTIM1a to bind calcium, which produces a STIM1 protein that is constitutively active (Liou et al., 2005). Next, zSTIM1a was truncated at amino acid 233, abrogating the capacity of STIM1 to bind and activate Orai (Muik et al., 2009; Jha et al., 2013; Zhou et al., 2014), which produced DN-zSTIM1a. Furthermore, to permit the visualisation of DN-zSTIM1a, mCherry was inserted between residues 23 and 24 of zSTIM1a. Several strategies were used to express DN-zSTIM1a in zebrafish spinal motor neurons. The first strategy involved the generation of a promotor sequence using triplicate repeat of a 125bp minimal sequence of the mnx1 enhancer region, based on a previously described method (Zelenchuk and Brusés, 2011). This enhancer region regulates expression of the transcription factor mnx1 (also known as Hb9), which is expressed by post-mitotic spinal motor neurons (Tanabe et al., 1998; Arber et al., 1999). However, injection of the DN-zSTIM1a could not be detected in motor neurons. Hence, a second strategy utilising the Tol2 transposase system (Kwan et al., 2007; Asakawa and Kawakami, 2009; Don et al., 2017), was formulated. In collaboration with Dr Emily Don and Dr Nick Cole (Macquarie University, Sydney, Australia), the synthesised DN-

zSTIM1a sequence was inserted into the Tol2p2A destination vector (Kwan et al., 2007), downstream of the mnx1 enhancer sequence as recently described (Don et al., 2017). Co-injection of pTol2p2A-mnx1-DN-zSTIM1a with Tol2 transposase mRNA (synthesised from pCS2+-zT_2TP (Suster et al., 2011)), lead to chimeric expression of DN-zSTIM1a in zebrafish spinal motor neurons (data not shown). However, due to time constraints, the effect of DN-zSTIM1a expression for axon pathfinding by spinal motor neurons was not investigated for this thesis. Therefore, to validate data presented herein, future studies should utilise the Tol2 strategy to investigate the cell-autonomous role of zSTIM1a in the regulation of CaP axon pathfinding.

In summary, the data presented in this chapter suggest that zSTIM1a is important for zebrafish survival, muscle development, as well as the fine control of the wiring of the nervous system. Crucially, these data provide evidence to suggest that zSTIM1a regulates axon pathfinding by CaP axons, and provides evidence to suggest that STIM1 regulates has multiple functions and regulates multiple aspects of axon pathfinding *in vivo*, including axonal motility at intermediate choice points, as well as filopodial dynamics and axon branching.

Chapter 4:
STIM1 regulates calcium signaling in navigating motor axons *in vivo*

Chapter 4: STIM1 regulates calcium signaling by navigating motor axons *in vivo*

4.1. Introduction

Spatial and temporal patterns of calcium signaling exhibited by growth cones are a product of the source of calcium used to generate the calcium signaling event. (Tojima et al., 2011). Localised calcium signals are sufficient to 'steer' axon outgrowth (Zheng, 2000), with growth cone attraction or repulsion triggered by the activation of alternate downstream pathways, such as the CaMKII-CaN molecular switch, which ultimately act on the cytoskeleton to inform growth cone motility (Robles et al., 2003; Henley et al., 2004; Wen et al., 2004b; Forbes et al., 2012). Hence, the selectivity by which calcium activates intracellular signaling pathways is determined by the amplitude, frequency and spatial localisation of the calcium signals, which is a function of the source of calcium used to generate the calcium signal (Zheng, 2000; Wen et al., 2004b; Rizzuto and Pozzan, 2006; Cheng et al., 2011; Tojima et al., 2011; Kar and Parekh, 2015). For example, higher amplitude calcium signals generated by release of ER calcium via IICR and CICR activates CaMKII and are sufficient to induce turning towards the side of the growth cone with elevated in intracellular calcium (Höpker et al., 1999; Hong et al., 2000; Jin et al., 2005; Ooashi et al., 2005; Akiyama et al., 2009). While lower amplitude calcium signals generated by calcium influx without release of ER calcium activates CaN to trigger turning away from the side of the growth cone with elevated in intracellular calcium (Hong et al., 2000; Wen et al., 2004b; Ooashi et al., 2005; Akiyama et al., 2009). These studies illustrate the importance of the ER as a source of calcium during axon guidance.

The ER is a crucial source of intracellular calcium for axon extension, with ER calcium release vital for the generation of spontaneous calcium transients. Although calcium influx via L-type VDCC has been implicated in the regulation of spontaneous calcium transients in cortical neurons (Tang et al., 2003), inhibition of VDCC does not suppress spontaneous calcium spikes in growth cones of *Xenopus* spinal neurons (Gomez et al., 1995) or rodent DRG sensory neurons (Gasperini et al., 2009), suggesting that calcium influx via non-voltage dependent calcium channels regulates spontaneous calcium transients in pathfinding axons. Consistent with ER calcium playing a crucial role in the formation of spontaneous calcium transients, release of ER calcium potentiates calcium spikes in *Xenopus* spinal growth cones *in vitro* (Gomez et al., 1995), and depletion of ER

calcium with thapsigargin inducing robust spiking in previously quiet growth cones (Gomez et al., 1995). Furthermore, release of calcium from the ER is required for axons to steer towards a source of guidance cue (Hong et al., 2000; Li et al., 2005; Ooashi et al., 2005; Akiyama et al., 2009; Gasperini et al., 2009), with ER calcium release underpinning the sustained rise in intracellular calcium within growth cones in response to guidance cue signaling (Gasperini et al., 2009). To produce higher amplitude calcium signals, calcium influx via plasma membrane channels is amplified by the release of calcium from the ER, which is sufficient to induce axons to turn towards a source of guidance cue (Hong et al., 2000; Akiyama et al., 2009; Tojima, 2012). In contrast, repulsion occurs if an influx of extracellular calcium occurs without subsequent amplification by ER calcium (Ooashi et al., 2005; Gasperini et al., 2009; Mitchell et al., 2012). As the ER is a finite store of calcium that must be replenished by SOCE to sustain increased intracellular calcium, it has been suggested that calcium influx via SOCE is required to sustain intracellular calcium during attractive growth cone turning (Gasperini et al., 2009; Mitchell et al., 2012; Shim et al., 2013). Consistent with this prediction, STIM1 knockdown causes an attenuation of elevated intracellular calcium within growth cones in response to BDNF and netrin-1 (Mitchell et al., 2012; Shim et al., 2013), which correlates with perturbed growth cone turning to these guidance cues (Mitchell et al., 2012; Shim et al., 2013). However, it is not known whether STIM1 participates in the regulation of calcium signaling during axon pathfinding in the intact nervous system. As previous results demonstrated that reduced zSTIM1a expression perturbs axon pathfinding by CaP neurons at intermediate targets, it would be predicted that zSTIM1a is important for the regulation of calcium signaling as CaP axons navigate via intermediate targets.

Primary motor neurons of the zebrafish spinal cord exhibit two types of calcium transients: calcium waves and calcium spikes (Saint-Amant and Drapeau, 2000; Muto et al., 2011; Warp et al., 2012; Plazas et al., 2013). Calcium waves are initiated by a central pattern generator located within the zebrafish spinal cord (Saint-Amant and Drapeau, 1998; 2000), propagated via gap junctions (Saint-Amant and Drapeau, 2001; Plazas et al., 2013), and are present in axon-less neurons of the spinal cord prior to axon pathfinding (Ashworth and Bolsover, 2002; Plazas et al., 2013). In contrast, between 18 and 24 hpf, calcium spikes are observed in zebrafish primary motor neurons alone, and then only once the axon pathfinding has been initiated (Plazas et al., 2013). In CaP neurons, calcium

spikes are initiated in the distal axon and propagate to the soma, with a delay of less than a second in axons located both proximal and distal to the horizontal myoseptum (Plazas et al., 2013), illustrating the fast kinetics of calcium spiking in CaP axons. The frequency of calcium spikes increases with axon outgrowth, with low frequency spikes detected in CaP soma as axogenesis begins and the CaP axon extends along the common pathway towards the horizontal myoseptum (Plazas et al., 2013), and higher frequency spikes and bursting spikes observed as CaP axons reach and navigate distal to the horizontal myoseptum (Plazas et al., 2013). These observations are consistent with higher frequency calcium transients regulate pausing of *Xenopus* spinal neurons at intermediate choice points (Gomez and Spitzer, 1999). However, to determine whether zSTIM1a-mediated SOCE is involved in the regulation of motor neuron pathfinding, first the presence and regulation of SOCE by zSTIM1a in zebrafish motor neurons needed to be established. The role of zSTIM1a-mediated SOCE in axon pathfinding was then assessed by measuring calcium transients in CaP axons navigating via selected intermediate targets *in vivo*.

4.2. Methods

4.2.1. Animals

Gal4^{s1020t}/UAS:mCherry and Gal4^{s1020t}/UAS:GCaMP5 transgenic lines (Scott et al., 2007) were a kind gift of Dr Ethan Scott (University of Queensland). Embryos were obtained from natural spawning events and staged by external morphology according to established guidelines (Kimmel et al., 1995).

4.2.2. Morpholino knockdown of zSTIM1a expression

Knockdown of zSTIM1a expression at the 1-4 stage was performed as previously described (*see Chapter 3 2.1*).

4.2.3. Zebrafish spinal motor neuron cultures

Spinal motor neuron cultures were generated from Gal4^{s1020t}/UAS:mCherry embryos staged at 14 to 18 hpf using a protocol modified from previous reports (Andersen, 2001; Chen et al., 2013). To isolate spinal cords, embryos were rinsed in 70% ethanol, washed in 0.5X E2 media, dechorionated, and all structures located anterior to the first somite, and distal from the tail bud, were removed with sharp forceps. The yolk sac and Kupffer's vesicle were then removed from the remaining tail, with the developing skin gently peeled away from the underlying tissue. To generate dissociated cell cultures, tail segments containing spinal cords were removed from three embryos an placed into *dissection media* [in mM: 115 NaCL, 2.5 KCl, 0.4 EDTA, 8 HEPES, 0.025 % (m/v) trypsin, pH 7.5], and were incubated for 10 min at room temperature before being transferred into *culture media* [Leibovitz's L-15 media (Invitrogen) supplemented with 2% fetal calf serum (Invitrogen), 1.25 D-glucose, 0.625 sodium pyruvate, 2.5 $CaCl_2$, 4 HEPES, Penicillin/Streptomycin, 10 ng/mL ciliary neurotrophic factor (CNTF), 500 pg/mL basic fibroblast growth factor (bFGF), pH 7.5] and gently triturated 20 times. Dissociated cells were plated onto glass coverslips that were pre-treated with poly-l-ornithine (1 mg/mL)

and Laminin (1 mg/mL), with cultures incubated at 28°C for 4 hr prior to commencing experiments.

For imaging, cultures were maintained in *culture media* at 28°C in a humidified chamber. Images were acquired using a Nikon Eclipse TiE microscope, equipped with a 40X Fluor-S oil-immersion objective with DIC optics (Nikon), and NIS Elements 6D software (Nikon). Spinal motor neurons were identified by their morphology and expression of mCherry. Images of navigating axons were acquired at 0.33 Hz for 25 min. Images were prepared using ImageJ (NIH) and Adobe illustrator CS6 (Adobe).

4.2.4. Immunocytochemistry

Zebrafish spinal motor neuron cultures were fixed in 4% PFA at room temperature for 1 hr before being incubated overnight at 4°C with antibodies for the homeobox genes Islet1/2 [39.4D5, Developmental Studies Hybridoma Bank (DSHB), University of Iowa (deposited by Jessell, T.M. and Brenner-Morton S.); 1:500]. Islet1/2 antibodies were detected using AlexaFlour® 488-conjugated secondary antibodies [IgG (H+L) highly cross absorbed antibody, Invitrogen; 1:1,000]. Images were acquired with an Olympus BX50 microscope equipped with a UPlanSApo 60x-1.35 water immersion lens (Nikon), CoolSNAP HQ^2 CCD camera (Photometrics), and NIS elements software (Nikon). Images were prepared using ImageJ (NIH) and Adobe Illustrator CS6 (Adobe).

4.2.5. Characterisation of SOCE in zebrafish spinal motor neurons *in vitro*

To measure the concentration of intracellular calcium in zebrafish spinal motor neurons, cultures were loaded with Fura-2 AM (1 μM) in *calcium-replete imaging media* [in mM: Hanks Buffered Saline Solution (HBSS; Invitrogen) supplemented with 2.5 $CaCl_2$, 1 $MgCl_2$, 10 D-glucose, 15 HEPES] for 10 min at room temperature, washed with fresh *calcium-replete imaging media*, and incubated at 28°C for a further 20 min prior to imaging. Images were captured at 0.5 Hz for 25 min on an Eclipse TiE microscope (Nikon), equipped with a 40X Flour-S oil-immersion objective with DIC optics (Nikon) and NIS Elements 6D software (Nikon). Fura-2 was alternatively excited at 340 and 380

nm with an attenuated illumination source (33% transmission; Lambda DG-4, Sutter Instruments, CA USA). Images were acquired at 510 nm with an EMCCD digital camera (Evolve 512; Photometrics) using regions of interest (ROI) defined by NIS Elements (Nikon). After subtracting background fluorescence, a ratio (R) of fluorescence at 340 nm to fluorescence at 380 nm was calculated in the soma of identified motor neurons.

To quantitate SOCE, cultures were maintained at 28°C in a humidified chamber, with a gravity flow exchange system used for media changes as appropriate. The imaging protocol was as follows: baseline intracellular calcium was acquired for 2 min in *calcium replete imaging media*, before calcium was removed from the media by incubating cells for 5 min with *calcium-free imaging media* (in mM: HBSS supplemented with 1 $MgCl_2$, 10 D-glucose, 15 HEPES and 0.3 EGTA). At 7 min, Thapsigargin (5 µM; Santa-Cruz Biotech, CA, USA), was added in *calcium-free imaging media* to induce depletion of ER calcium, and acquire minimal intracellular calcium (R_{min}). At 17 min, calcium was added with *calcium-replete imaging media* to trigger calcium influx via SOCE. At 22 min, Ionomycin (5 µM; Sigma-Aldrich, USA) was added to induce maximal intracellular calcium (R_{max}). The concentration of intracellular calcium ($[Ca^{2+}]_i$) was calculated in NIS elements (Nikon) according to the formula $[Ca^{2+}]_i = K_{eff} \times (R-R_{min})/(R_{max}-R)$, where K_{eff} represents the calcium binding constant of Fura-2 (Grynkiewicz et al., 1985). Traces of $[Ca^{2+}]_i$ (in nM) were generated in GraphPad Prism6.0e (GraphPad). Baseline $[Ca^{2+}]_i$ was calculated as the mean of the initial 2 min of imaging in calcium-replete conditions. Minimal calcium was an average of intracellular calcium acquired in *calcium-free imaging media* following depletion of ER calcium stores. SOCE was measured as the change in $[Ca^{2+}]_i$ from prior to re-addition of extracellular calcium to the peak $[Ca^{2+}]_i$ upon re-addition of extracellular calcium. Statistical tests were performed using GraphPad Prism6.0e (GraphPad), with images prepared using NIS elements (Nikon) and Adobe Illustrator CS6 (Adobe Systems, USA).

4.2.6. Characterisation of calcium transients in CaP axons during axon pathfinding in vivo

To image calcium transients in CaP axons, embryos were obtained from crosses between $Gal4^{s1020t}$/UAS:mCherry and $Gal4^{s1020t}$/UAS:GCaMP5 lines. Embryos were raised to 17-

18 hpf at 26°C, with Gal4^{s1020t}/UAS:mCherry::GCaMP5 embryos selected for *in vivo* calcium imaging. Prior to imaging, embryos were paralysed by yolk injection of α-bungarotoxin (α-BT, Abcam, Cambridge, UK; 1-2 ηL of 0.25 mM α-BT in 0.1 M PBS, pH 7.4) and mounted in 1.5% low melt agarose (Promega, WI, USA). Embryos were imaged from 18 to 25 hpf to acquire CaP axons (of somites 6-9) located proximal to the horizontal myoseptum, at the horizontal myoseptum, and distal to the horizontal myoseptum; which was defined by observing the most distal aspect of the CaP axon using mCherry expression. Calcium imaging was performed with a Zeiss LSM 510 confocal imaging system equipped with a water-emersion 20x W-PLAN Achromatic lens (Zeiss). For calcium imaging, images were collected at 5 Hz for 5 min focusing on the distal aspect of CaP axons with the 488 laser line and 500-550 bandpass filter, with 2.5x digital zoom.

Calcium transients were analysed by defining regions of interest in the distal axon shaft of CaP neurons in ImageJ (NIH). Raw cumulative pixel intensity (fluorescence, F) were converted into a change in fluorescence from baseline fluorescence ($\Delta F/F_0$) using Microsoft Excel (Microsoft, CA, USA), and exported to MATLAB (MATLAB_R2016a, MathWorks, USA) for peak analysis. Minimum $\Delta F/F_0$ was normalized to zero and calcium transients were identified as fluorescence peaks greater than two times the standard deviation of noise, greater than 10% of the maximum fluorescent signal, and lasting ≥0.2 sec (measured as peak width at half maxima). Calcium transients were categorised as low frequency spikes (<7.5 spikes min^{-1}), high frequency spikes (≥7.5 spikes min^{-1}), and bursting spikes (≥15 spikes min^{-1}) measured as peak interval. Statistical tests were performed in GraphPad Prism6.0e (GraphPad).

4.3. Results

4.3.1. zSTIM1a regulates SOCE in zebrafish spinal motor neurons

To test whether zSTIM1a regulates SOCE in zebrafish spinal motor neurons, a protocol for the generation, maintenance and identification of zebrafish spinal motor neurons *in vitro* was developed. Motor neuron cultures were generated from spinal cords of 14-18 hpf Gal4^{s1020t}/UAS:mCherry embryos (Fig. 4.1a). By 4 hr after plating, spinal neurons were polarised with long axon extensions (Fig. 4.1b), that were actively extending (Fig. 4.1c). Spinal neurons identified by neuronal morphology (polarised with extending neurites) and mCherry expression were also positive for the primary motor neuron marker Islet1/2 (Fig. 4.1d). These data suggest that identified neurons are primary motor neurons, illustrating the utility of this protocol to isolate, maintain and identify spinal motor neurons for calcium imaging studies.

zSTIM1a regulates calcium homeostasis and SOCE in zebrafish spinal motor neurons *in vitro* (Fig. 4.2). Spinal motor neurons isolated from zSTIM1a morphants exhibited reduced concentration of calcium at baseline (63.2 nM ± 3.7 nM, n=42 cells from 6 cultures) compared with control morphants (113.2 nM ± 7.2 nM, n=25 cells from 3 cultures; $p<0.0001$), suggesting that zSTIM1a regulates calcium homeostasis in spinal motor neurons. When calcium was added to the media following ER calcium depletion in zero calcium media with thapsigargin, the magnitude of calcium influx (denoting calcium influx via SOCE) was reduced in motor neurons of zSTIM1a morphants (81.6 nM ± 8.8 nM, n=42 cells from 6 cultures) compared with motor neurons of control morphants (184.3 nM ± 40.4 nM, n=25 cells from 3 cultures; $p<0.005$). Taken together, these data suggest that zSTIM1a regulates SOCE, and that zSTIM1a-mediated SOCE is important for calcium homeostasis in zebrafish spinal motor neurons.

Figure 4.1: Characterisation of zebrafish spinal motor neuron cultures.

(a) Diagram exhibiting the spinal cord dissection. Dashed white lines depict the cut sites on a representative Gal4^{s1020t}/UAS:mCherry embryo. **(b)** Representative spinal motor neuron 4 hr after plating (Arrows illustrate soma and arrowheads denote growth cones at the distal axon). **(c)** Exploratory behaviour of an identified motor neuron axon 4 hr after plating over a time course of 25 min. **(d)** Immunohistochemistry for the primary motor neuron marker Islet1/2 (green) in mCherry (red) expressing motor neurons fixed 4 hr after plating. *Scale bars denote 100 µm in (a), 10 µm in (b) and (d), and 5 µm in (c).*

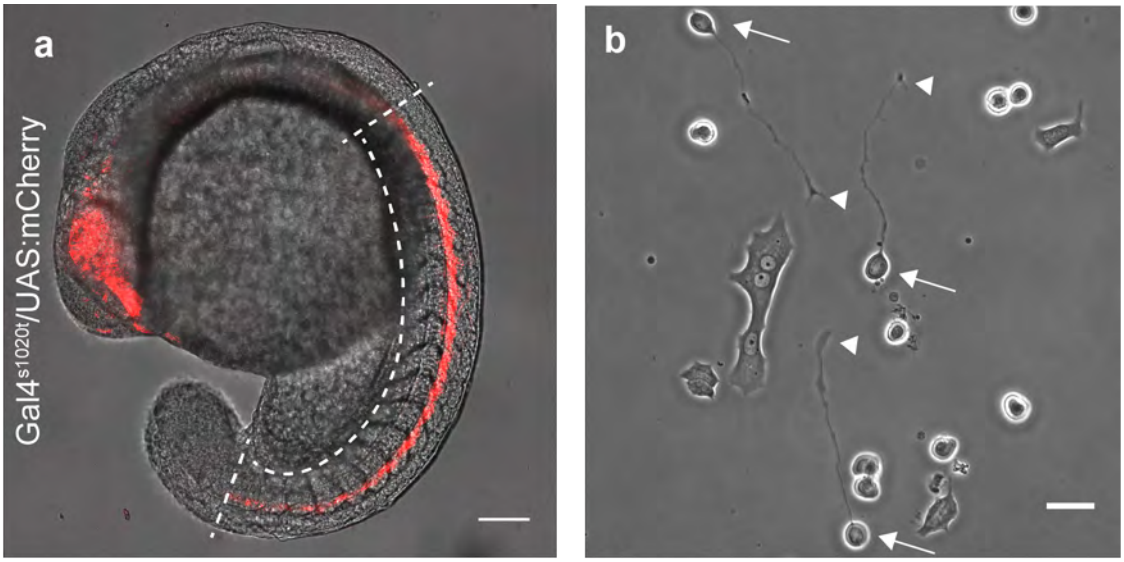
a
Gal4s1020t/UAS:mCherry
b

c

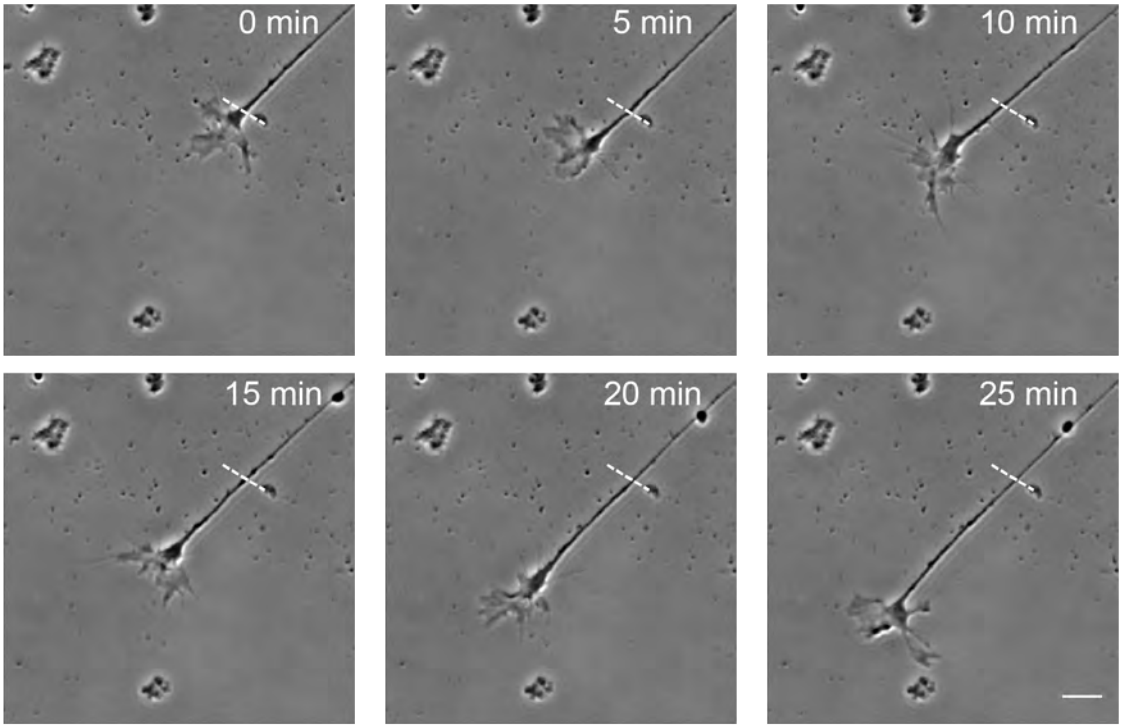
0 min
5 min
10 min
15 min
20 min
25 min

d

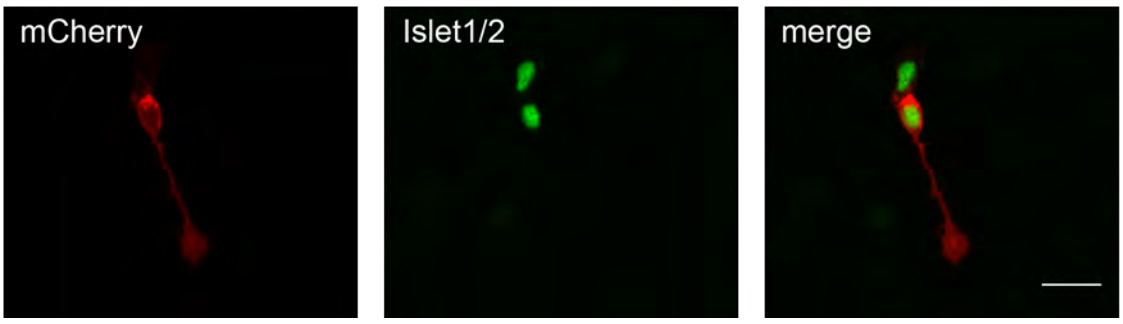
mCherry
Islet1/2
merge

Figure 4.2: Reduced zSTIM1a expression decreases basal calcium and attenuates evoked SOCE in zebrafish spinal motor neurons *in vitro*.

zSTIM1a is required for SOCE in zebrafish spinal motor neurons. **(a)** Representative phase and pseudocoloured Fura-2 images of spinal motor neurons isolated from control and zSTIM1a morphants. Fura-2 images were pseudocoloured according to the intracellular concentration of calcium ($[Ca^{2+}]_i$) in nM, with purple as lowest and red as highest. Images were acquired at baseline in calcium-replete conditions (2.5 mM Ca^{2+}), following store depletion with 5 μM thapsigargin (Tg) in zero calcium media (0 mM Ca^{2+} with Tg), and following the re-addition of extracellular calcium (2.5 mM $[Ca^{2+}]$), representing the magnitude of calcium entry via SOCE. Scale bars in phase images illustrate 10 μm and are correct for pseudocoloured Fura-2 images. **(b-c)** Average $[Ca^{2+}]_i$ in (b) baseline and (c) store depleted conditions was calculated for spinal motor neurons isolated from control and zSTIM1a morphant embryos. **(d-e)** The capacity of spinal motor neurons to trigger calcium influx via SOCE was assessed by determining the magnitude change in $[Ca^{2+}]_i$ upon the re-addition of extracellular calcium following store-depletion in zero extracellular calcium. (d) Graph illustrates the change in $[Ca^{2+}]_i$ within spinal motor neurons isolated from control and zSTIM1a morphants upon the re-addition of extracellular calcium. Scale bar denotes 50 nM $[Ca^{2+}]_i$ and 5 min. (e) Average magnitude of calcium influx in spinal motor neurons from control and zSTIM1a morphants. Treatment groups were compared by Student's *t*-test ($^{**}p<0.005$, $^{****}p<0.0001$).

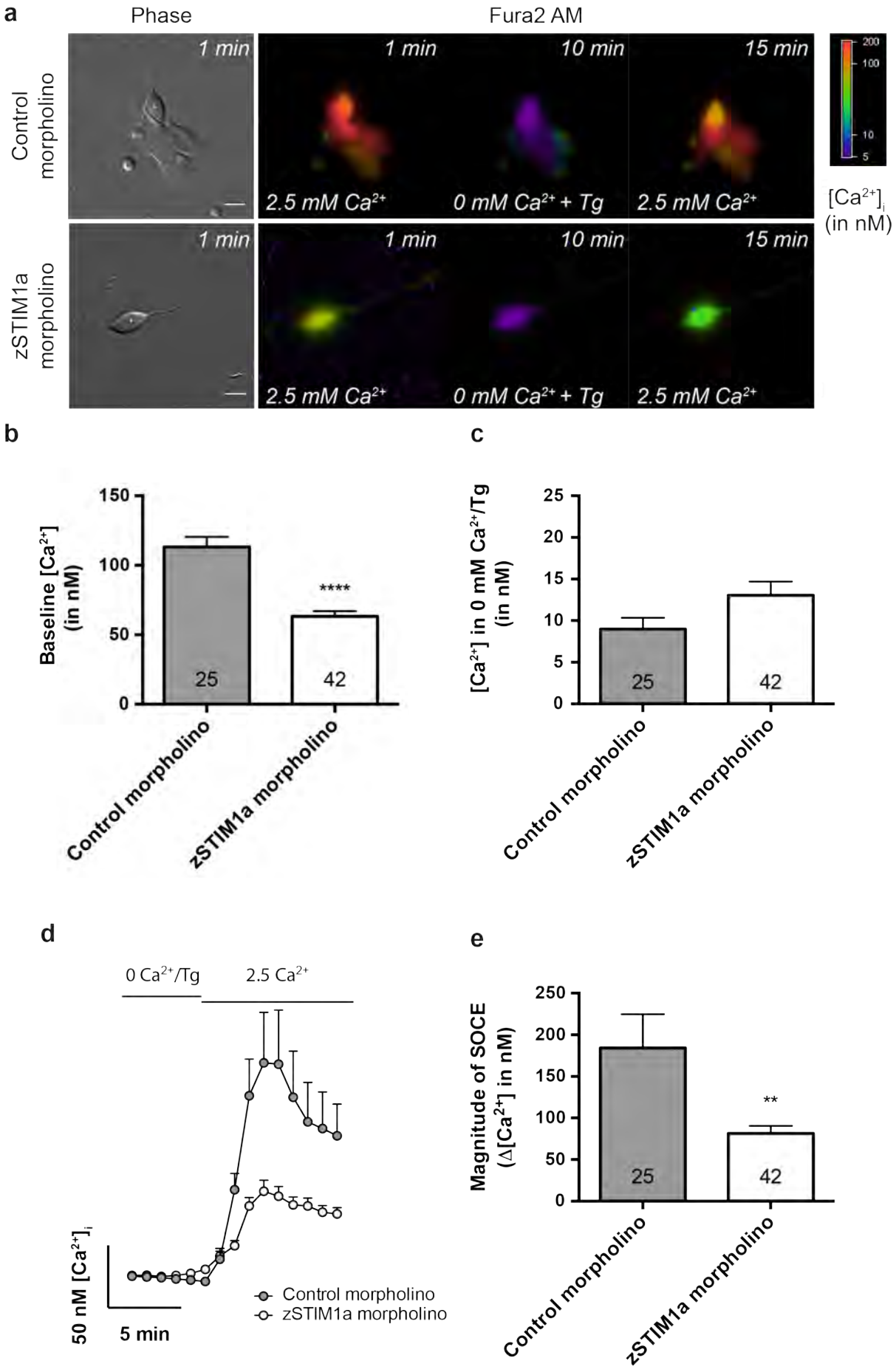
a
Phase
Fura2 AM
Control morpholino
zSTIM1a morpholino
1 min
1 min
10 min
15 min
2.5 mM Ca2+
0 mM Ca2+ + Tg
2.5 mM Ca2+
200
100
10
5
[Ca2+]i (in nM)
b
Baseline [Ca2+] (in nM)
150
100
50
0
****
25
42
Control morpholino
zSTIM1a morpholino
c
[Ca2+] in 0 mM Ca2+/Tg (in nM)
25
20
15
10
5
0
25
42
Control morpholino
zSTIM1a morpholino
d
0 Ca2+/Tg
2.5 Ca2+
50 nM [Ca2+]i
5 min
Control morpholino
zSTIM1a morpholino
e
Magnitude of SOCE (Δ[Ca2+] in nM)
250
200
150
100
50
0
**
25
42
Control morpholino
zSTIM1a morpholino

4.3.2. zSTIM1a regulates calcium transients in CaP axons during axon pathfinding *in vivo*

To determine the effect of reduced zSTIM1a expression on calcium dynamics in CaP axons, spontaneous calcium transients were characterised in CaP axons of control morphants located proximal to the horizontal myoseptum (pre-myoseptum), at the horizontal myoseptum (myoseptum), and distal to the horizontal myoseptum (post-myoseptum; Fig. 4.3a). CaP axons of control morphants exhibited spontaneous calcium transients that increased in frequency when CaP axons were located at the myoseptum (0.11 ± 0.02 Hz, n=11), or post-myoseptum (0.11 ± 0.02 Hz, n=17;), compared to CaP axons located pre-myoseptum (0.05 ± 0.01 Hz, n=11; $p<0.005$ and $p<0.0005$ respectively; Fig. 4.3b). However, no difference in transient frequency was detected between CaP axons of control morphants located at the myoseptum and post-myoseptum ($p=0.85$). These finding are consistent with previous observations of spontaneous calcium transients in CaP soma (Plazas et al., 2013), and suggest that the frequency of calcium transients increases as CaP axons reach the horizontal myoseptum, and remains high as CaP axons extend distal to the horizontal myoseptum.

Three types of calcium transients were observed in CaP axons of control morphants (Fig. 4.3c): low frequency spikes (<7.5 spikes min^{-1}), high frequency spikes (≥7.5 spikes min^{-1}), and bursting spikes (≥15 spikes min^{-1}), consistent with previous observations of spontaneous calcium transients in CaP soma (Plazas et al., 2013). Importantly, CaP axons of control morphants expressed defined patterns of calcium transients depending on the stage of axon outgrowth. Control CaP axons located pre-myoseptum predominantly expressed low frequency spikes (11.45 ± 1.35, n=11), with fewer high frequency spikes (3.00 ± 0.94, n=11; $p<0.0001$) or bursting spikes (1.27 ± 0.67, n=11; $p<0.0001$) observed (Fig. 4.3d). In contrast, control CaP axons located at the myoseptum exhibited an increased number of high frequency spikes (11.35 ± 2.65, n=17), and bursting spikes (12.88 ± 2.44, n=17), compared with control CaP axons located pre-myoseptum ($p<0.05$ and $p<0.001$ respectively). However, the number of low frequency spikes in CaP axons located at the myoseptum (10.18 ± 1.73, n=17) was unchanged from pre-myoseptum ($p=0.49$). Similarly, control CaP axons located post-myoseptum exhibited an increased number of high frequency spikes (17.55 ± 6.78, n=11) and bursting spikes (6.46 ± 2.31, n=11) compared with control CaP axons located pre-myoseptum ($p<0.05$ and $p<0.001$

respectively). The number of low frequency spikes (9.91 ± 2.14, n=11) remained unchanged from pre myoseptum (p=0.55). Comparing control CaP axons located post-myoseptum with control CaP axons at the myoseptum revealed that the number of high frequency spikes was unchanged in CaP axons located post-myoseptum (p=0.30), however the number of bursting spikes trended towards being decreased (p<0.051). Taken together, these data demonstrate that the number of low frequency spikes remains unchanged with axon outgrowth, with high frequency spikes and bursting spikes increased when CaP axons are located at, or distal to, the horizontal myoseptum. Furthermore, these data also reveal that bursting spikes are highest at the myoseptum stage of axon outgrowth, which is consistent with axons pausing at the horizontal myoseptum (Gomez and Spitzer, 1999; Plazas et al., 2013).

Figure 4.3: CaP axons generate spontaneous calcium transients that increase in frequency with axon outgrowth.

(a) Schematic depicts the localisation of CaP axons during calcium imaging. CaP axons were located proximal to the horizontal myoseptum (pre-myoseptum), at the horizontal myoseptum (myoseptum), or distal to the horizontal myoseptum (post-myoseptum). The horizontal myoseptum (hm) is denoted by a dashed line. **(b)** Average frequency of calcium transients (in Hz) in CaP axons of control morphants at the pre-myoseptum, myoseptum, and post-myoseptum stage of axon outgrowth. Calcium transient frequencies were compared between stages of axon outgrowth using One-way ANOVA with Holm-Sidak correction for multiple comparisons ($^{**}p<0.005$). **(c)** Example calcium traces from CaP axons of control morphants illustrating low frequency spikes (top; <7.5 spikes min^{-1}), high frequency spikes (middle; ≥7.5 spikes min^{-1}), and bursting spikes (bottom; ≥15 spikes min^{-1}; bursting spikes are denoted by lines above traces). Scale bar illustrates 25% of maximum change in fluorescence and 10 sec. **(d)** The average number of low frequency, high frequency, and bursting spikes observed in the 5 min imaging period in CaP axons of control morphants at the pre-myoseptum, myoseptum, and post-myoseptum stages of axon outgrowth. The number of low, high and bursting spikes at each stage of axon outgrowth were compared using One-way ANOVA with Holm-Sidak correction for multiple comparisons ($^{****}p<0.0001$). The number of low high and bursting spikes were also compared between stages of axon outgrowth using One-way ANOVA with Holm-Sidak correction for multiple comparisons ($^{\#}p<0.05$; $^{\#\#\#}p<0.005$).

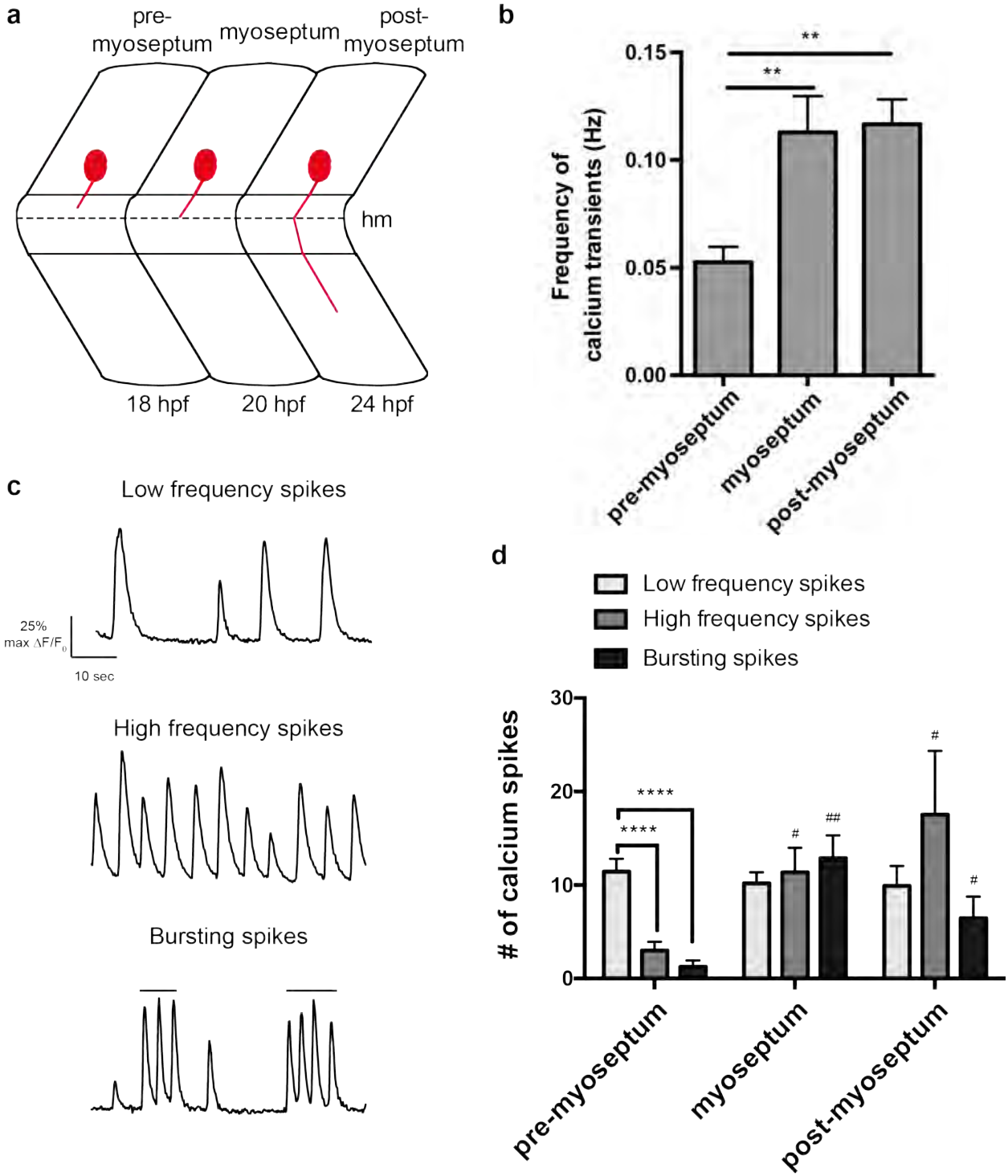
a
pre-
myoseptum
myoseptum
post-
myoseptum
hm
18 hpf
20 hpf
24 hpf
b
Frequency of
calcium transients (Hz)
0.15
0.10
0.05
0.00
**
**
pre-myoseptum
myoseptum
post-myoseptum
c
Low frequency spikes
25%
max ΔF/F0
10 sec
High frequency spikes
Bursting spikes
d
Low frequency spikes
High frequency spikes
Bursting spikes
# of calcium spikes
30
20
10
0
****
****
#
##
#
#
pre-myoseptum
myoseptum
post-myoseptum

CaP axons of zSTIM1a morphants exhibit perturbed axon pathfinding (*Chapter 3*), and SOCE is attenuated in motor neurons cultured from zSTIM1a morphant embryos. Therefore, it was hypothesised that zSTIM1a-mediated calcium signaling would be perturbed in CaP axons during axon outgrowth *in vivo*. To test this hypothesis, the effect of reduced zSTIM1a expression on the generation of spontaneous calcium transients in CaP axons was investigated. CaP axons normally express spontaneous calcium transients (as shown in Fig. 4.3), however only 73.8% of CaP axons of zSTIM1a morphants were active within the same imaging period (Fig. 4.4b). That is, 26.2% of CaP axons of zSTIM1a morphants exhibited zero calcium transients in 5-min, a phenomenon not observed in control morphants. Importantly, zSTIM1a morphant embryos that contained CaP axons exhibiting zero calcium transients were alive following imaging, with a heartbeat and strong peripheral circulation observed. In zSTIM1a morphants, 73.8% of CaP axons exhibited calcium transients, however in these axons the frequency of calcium transients was reduced at all stages of axon outgrowth. Compared to control morphants, the frequency of calcium transients was decreased in CaP axons of zSTIM1a morphants pre-myoseptum (0.025 ± 0.011 Hz, n=7; $p<0.05$), at the myoseptum (0.069 ± 0.018 Hz, n=13; $p<0.05$), and post-horizontal myoseptum (0.073 ± 0.011 Hz, n=22; $p<0.05$). Together, these data suggest that zSTIM1a is required for the generation of spontaneous calcium transients by CaP axons.

The frequency of calcium transients in CaP axons normally increases as CaP axons reach and extend distal to the myoseptum (see Fig. 4.3). However, there was no increase in frequency of calcium transients between CaP axons located pre-myoseptum and CaP axons at the myoseptum in zSTIM1a morphants (Fig. 4.4c; $p=0.12$). While there was an increase in calcium transient frequency in CaP axons located post-myoseptum when compared to CaP axons located pre-myoseptum in zSTIM1a morphants ($p<0.05$), the frequency of calcium transients was decreased compared to control morphants at the same stage of axon outgrowth (Fig. 4.4c).

Based on the hypothesis that SOCE is required for sustained elevated intracellular calcium associated with higher frequency calcium transients, it was predicted that zSTIM1a was required for bursting spikes in CaP axons. To test this hypothesis, the effect of reduced zSTIM1a expression on the types of calcium transients generated by CaP axons was assessed at each stage of axon outgrowth. Reducing the expression of

zSTIM1a had no effect on the number of low frequency calcium spikes at any stage of axon outgrowth (Fig. 4.4d). The number of low frequency spikes observed in CaP axons of zSTIM1a morphants located proximal to the horizontal myoseptum (6.43 ± 2.55, n=7), at the horizontal myoseptum (7.85 ± 2.55, n=13), and distal to the horizontal myoseptum (11.86 ± 2.13, n=22), was unchanged from CaP axons of control morphants (p=0.07, p=0.38 and p=0.57). Reduced expression of zSTIM1a had no effect on the generation of high frequency spikes, with the number of high frequency spikes observed in CaP axons of zSTIM1a morphants located pre-myoseptum (1.14 ± 1.14, n=7), at the myoseptum (10.38 ± 4.58, n=13), and post-myoseptum (9.14 ± 3.00, n=22), unchanged from CaP axons of control morphants (p=0.23, p=0.85 and p=0.17). In contrast, zSTIM1a was required for the generation of bursting spikes in CaP axons located at, and distal to, the horizontal myoseptum (Fig. 4.4d). CaP axons of zSTIM1a morphant exhibited fewer bursting spikes compared to CaP axons of control morphants when located at the myoseptum (2.61 ± 1.56, N=13; p<0.005), or located post-myoseptum (1.55 ± 0.56, N=22; p<0.01). Although bursting spikes were absent in CaP axons of zSTIM1a morphants located proximal to the horizontal myoseptum (0.00 ± 0.00, n=7), this was not significantly decreased when compared with control morphants (p=0.15). Consistent with the hypothesis that zSTIM1a regulates high frequency transients, these data suggest that zSTIM1a plays a crucial role in the generation of bursting calcium spikes, but not high or low frequency spikes, in CaP axons during axon pathfinding.

Figure 4.4: Reduced expression of zSTIM1a perturbs calcium transients in navigating CaP axons *in vivo*.

(a) Representative calcium responses observed in CaP axons of control and zSTIM1a morphants located proximal to the horizontal myoseptum (pre-myoseptum), at the horizontal myoseptum (myoseptum), or distal to the horizontal myoseptum (post-myoseptum). Scale bar applies to all traces.

(b) The percent of control and zSTIM1a morphant CaP axons exhibiting ≥1 calcium transients within a 5 min imaging period. Groups were compared by Fisher's exact test ($^{***}p<0.0005$).

(c) The average frequency of calcium transients (Hz) observed in CaP axons of control and zSTIM1a morphants located at the pre-myoseptum, myoseptum, or post-myoseptum stage of axon outgrowth. Groups and stages of axon outgrowth were compared by Two-way ANOVA with Holm-Sidak correction for multiple comparisons ($^{*}p<0.05$).

(d-f) The average number of low frequency spikes (<7.5 spikes min^{-1}), high frequency spikes (≥7.5 spikes min^{-1}), and bursting spikes (≥15 spikes min^{-1}) observed in CaP axons of control and zSTIM1a morphants at the (d) pre-myoseptum, (e) myoseptum, or (f) post-myoseptum stage of axon outgrowth. Groups were compared by Two-way ANOVA with Holm-Sidak correction for multiple comparisons ($^{*}p<0.05$, $^{**}p<0.005$, $^{***}p<0.0005$). Legend in (c) applies to (d-f).

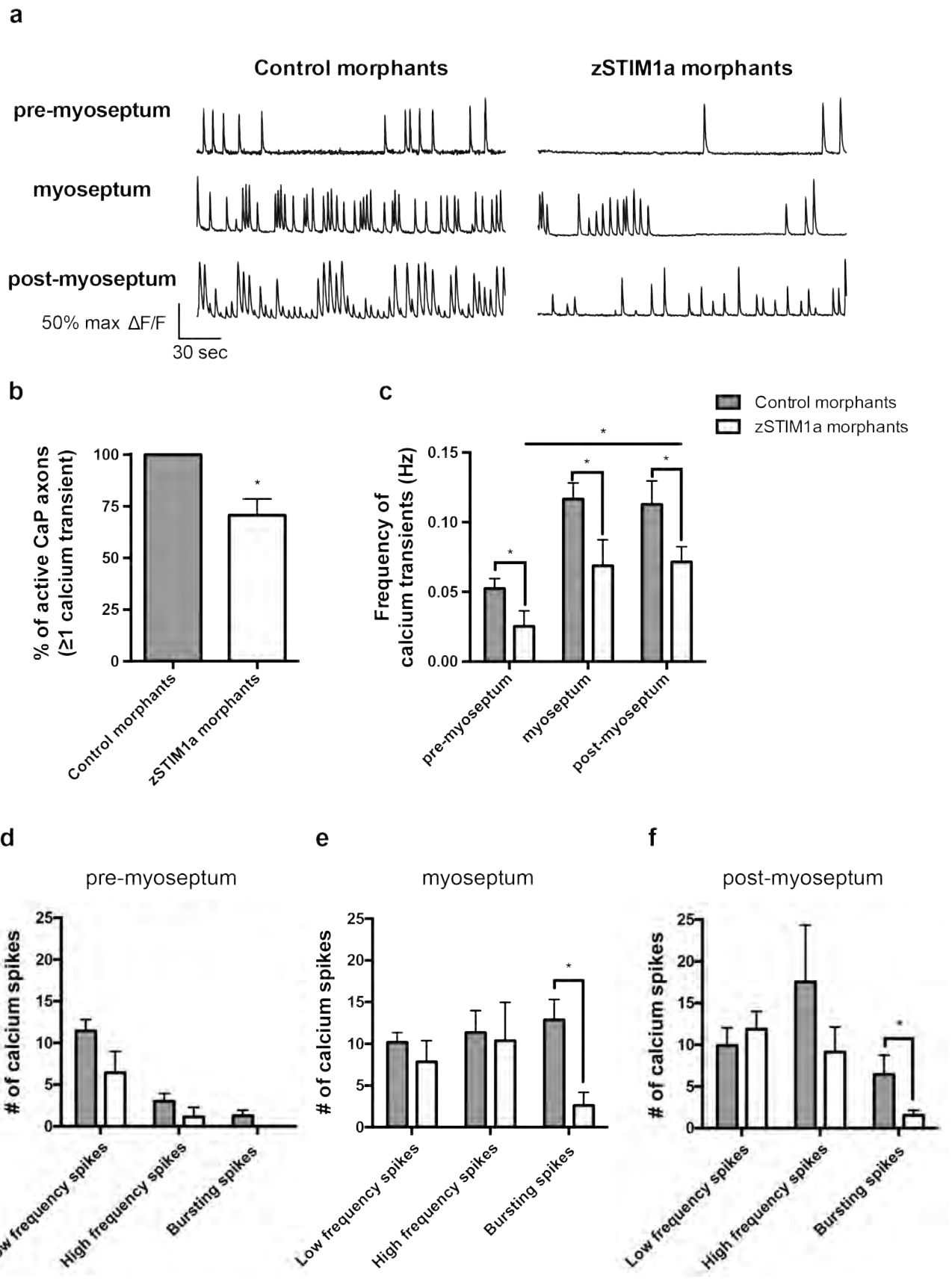
a
Control morphants
zSTIM1a morphants
pre-myoseptum
myoseptum
post-myoseptum
50% max ΔF/F
30 sec
b
% of active CaP axons (≥1 calcium transient)
100
75
50
25
0
*
Control morphants
zSTIM1a morphants
c
Control morphants
zSTIM1a morphants
Frequency of calcium transients (Hz)
0.15
0.10
0.05
0.00
*
*
*
*
pre-myoseptum
myoseptum
post-myoseptum
d
pre-myoseptum
# of calcium spikes
25
20
15
10
5
0
Low frequency spikes
High frequency spikes
Bursting spikes
e
myoseptum
# of calcium spikes
*
Low frequency spikes
High frequency spikes
Bursting spikes
f
post-myoseptum
# of calcium spikes
*
Low frequency spikes
High frequency spikes
Bursting spikes

4.4. Discussion

In this chapter, the function of STIM1 as a regulator of calcium signaling in pathfinding motor neurons was examined *in vivo*. Findings from these studies provide evidence to suggest that zSTIM1a mediates SOCE in zebrafish spinal motor neurons *in vitro*, and that zSTIM1a contributes to the regulation of calcium signaling in navigating axons *in vivo*. Taken together, these data suggest that motor neurons harness STIM1-mediated SOCE to generate intracellular calcium signals that, in turn, inform axon pathfinding.

zSTIM1a regulates SOCE in zebrafish spinal motor neurons.

In neurons, the ER calcium store is partially emptied at rest, and requires constant replenishment in a voltage-independent process (Garaschuk et al., 1997; Usachev and Thayer, 1997; 1999; Verkhratsky, 2005), with evidence suggesting that SOCE is responsible for store refilling (Berna-Erro et al., 2009; Hartmann et al., 2014; Sun et al., 2014a; Moccia et al., 2015; Samtleben et al., 2015). Indeed, SOCE is required to maintain basal ER calcium homeostasis in rodent hippocampal neurons, with inhibition of SOCE causing a rapid decrease in ER calcium (Samtleben et al., 2015). In the present study, SOCE was detected in zebrafish motor neurons, with reduced zSTIM1a expression attenuating calcium influx via SOCE and decreasing basal cytosolic calcium levels. These finding are consistent with previous reports of SOCE in hippocampal, cortical, cerebellar and DRG sensory neurons cultured from rodents (Baba et al., 2003; Gemes et al., 2011; Gruszczynska-Biegala et al., 2011; Steinbeck et al., 2011; Mitchell et al., 2012; Kyung et al., 2015); *Drosophila* neurons (Venkiteswaran and Hasan, 2009; Pathak et al., 2015); *Xenopus* spinal neurons (Shim et al., 2013); and bag cell neurons of *Aplysia* (Kachoei et al., 2006). Therefore, findings presented in this chapter provide evidence to suggest that STIM1-mediated SOCE is a conserved mechanism of calcium influx in neurons, and that calcium influx via SOCE regulates basal calcium homeostasis. These data also support the observation that STIM1 is the major neuronal STIM protein in development (*Chapter 2*), providing further evidence to suggest that STIM1-mediated SOCE is important for neuronal development.

Calcium transients regulate axon pathfinding in a frequency-dependent manner

Navigating axons exhibit spontaneous calcium transients *in vitro* and *in vivo* (Gu et al., 1994; Gomez et al., 1995; Gu and Spitzer, 1995; Gomez and Spitzer, 1999; Tang et al., 2003; Gasperini et al., 2009), which modulate axon extension in a frequency-dependent manner (for reviews see (Goldberg and Grabham, 1999; Gomez and Spitzer, 2000; Spitzer, 2006)). Zebrafish spinal motor neurons primarily exhibit two types of spontaneous calcium transients, waves and spikes (Ashworth and Bolsover, 2002; Saint-Amant, 2005; Plazas et al., 2013). Calcium waves predominate in axon-less neurons prior to the onset of axon pathfinding (Ashworth and Bolsover, 2002; Plazas et al., 2013), while calcium spikes, which originate in the distal axon before spreading to the soma, predominate in actively navigating neurons (Saint-Amant and Drapeau, 2000; Plazas et al., 2013). The spontaneous calcium spikes observed in CaP axons in this study are consistent with spontaneous spikes detected in the soma of navigating zebrafish motor neurons (Saint-Amant and Drapeau, 2001; Plazas et al., 2013), as well as being consistent with spontaneous activity observed in pathfinding chick and mouse motor neurons *in vivo* (Milner and Landmesser, 1999; Hanson and Landmesser, 2003; 2004). These results provide evidence to support the hypothesis that spontaneous calcium transients have a crucial function in the regulation of axon pathfinding *in vivo*.

The role of intermediate targets as choice points for navigating axons is a highly conserved process, with guidepost cells directing grasshopper neurons (Bentley and Keshishian, 1982; Bentley and Caudy, 1983; Bastiani et al., 1984), the limb plexus influencing motor axon outgrowth in chick and mice (Lance-Jones and Landmesser, 1981; Tosney and Landmesser, 1985; Kania and Jessell, 2003; Poliak et al., 2014), and the horizontal myoseptum informing axon pathfinding by zebrafish motor neurons (Eisen et al., 1986; Myers et al., 1986; Westerfield et al., 1986; Beattie et al., 2000; Eisen and Melancon, 2001). As precise spatiotemporal patterns of calcium signaling correlates with specific axon motility behaviours, it is hypothesised that axon motility at intermediate targets is regulated by calcium transients in a frequency-dependent manner (Gomez and Spitzer, 1999; Tang et al., 2003; Hutchins and Kalil, 2008; Plazas et al., 2013). As calcium transient frequency is dependent on the location of the growth cone, the environment of the growth cone was suggested to be a key determinate of calcium transient frequency (Gomez and Spitzer, 1999). This suggestion is consistent with data

presented in this chapter, with calcium transient frequency correlating with the position of the growth cone. During the formation of the zebrafish motor circuit, CaP axons extend rapidly along the common pathway from the spinal cord to the horizontal myoseptum (Eisen et al., 1986; Myers et al., 1986; Plazas et al., 2013), which correlates with the observation here that CaP axons predominantly expressed low frequency calcium spikes during this time. When CaP axons were located at the horizontal myoseptum, the frequency of calcium transients was increased, with an increased number of high frequency calcium spikes and bursting calcium spikes observed. Moreover, as CaP axons extended distal to the horizontal myoseptum, high frequency and bursting spikes were unchanged, consistent with CaP axons interacting with a second intermediate target, the ventral notochord (Beattie et al., 2000). Therefore, results presented in this chapter provide evidence to support the hypothesis that spontaneous calcium transients regulate axon motility behaviour *in vivo* in a frequency dependent manner, with higher frequency transients associated with slowing and pausing behaviours as the CaP axon interacts with intermediate targets.

zSTIM1a regulates the frequency of calcium transient in pathfinding axons in vivo

Given the importance of spontaneous calcium transients for controlling axon pathfinding at intermediate targets (Gomez and Spitzer, 1999; Plazas et al., 2013), the reduced frequency of spontaneous calcium transients observed in CaP axons of zSTIM1a morphants provide a likely molecular mechanism to describe the perturbed axon pathfinding by CaP axons of zSTIM1a morphant embryos (*Chapter 3*). Spontaneous calcium spikes are generated by local release of calcium from the ER via IICR, which is subsequently amplified and propagated through the neuron via release of ER calcium by CICR (Berridge, 2006; Rizzuto and Pozzan, 2006; Pani and Singh, 2009; Yang et al., 2010). Therefore, two interconnected mechanisms are proposed to mediate the reduced frequency of calcium transients in pathfinding CaP axons of zSTIM1a morphants: a decreased baseline concentration of ER calcium, and a reduced capacity to refill the ER calcium store between calcium transients. Spontaneous calcium spikes rely on ER calcium release (Holliday et al., 1991; Clapham, 1995; Berridge, 1998), with calcium release from the ER potentiating calcium spikes, as well as triggering spikes in growth cones not previously spiking (Gomez et al., 1995). SOCE is necessary for neurons to maintain ER calcium homeostasis, with inhibition of SOCE decreasing the concentration

of calcium in the ER (Samtleben et al., 2015). Hence, it is likely that STIM1-deficient motor neurons have a decreased amount of ER calcium available to be released, thereby decreasing the capacity of motor neurons to elicit calcium spikes.

Calcium spiking activity relies on refilling of the ER calcium store between calcium transients. Extracellular calcium is required for spontaneous calcium spikes, as removal of extracellular calcium attenuates spontaneous calcium spikes (Holliday et al., 1991; Gomez et al., 1995; Gasperini et al., 2009). When STIM1 expression was abolished in cerebellar Purkinje neurons, repetitive mGluR1-mediated synaptic calcium transients were strongly attenuated (Hartmann et al., 2014). Given that mGluR1-mediated calcium transients rely on calcium release from the ER (Takechi et al., 1998; Hartmann et al., 2008), and a key role of STIM1 is to trigger SOCE to replenish depleted ER calcium stores (Peinelt et al., 2006; Soboloff et al., 2006b), it was reasoned that a deficit in store refilling between synaptic calcium transients underlies the attenuation of synaptic calcium signals (Hartmann et al., 2014). In zSTIM1a-deficient motor neurons, bursting spikes were selectively reduced without a commensurate decrease in the number of low or high frequency spikes. Given that bursting spikes would deplete ER calcium stores more rapidly, the specificity of bursting spikes being decreased suggests an attenuation of the capacity of CaP neurons to refill the ER calcium store between calcium spikes.

In this study, zSTIM1a expression was reduced using morpholino oligonucleotides, which abolished or attenuated calcium transients expressed by CaP axons. As zSTIM1a expression was reduced, but not abolished, in these studies, it is predicted that some zSTIM1a is available to participate in SOCE. Therefore, the finding that 26% of CaP axons of zSTIM1a morphants exhibited zero calcium transients during the imaging period may indicate that zSTIM1a expression was reduced to a greater extent in these neurons. However, a lack of appropriate STIM1 antibodies (see Chapter 2), prevented the quantification of zSTIM1a knockdown. Given that reduced zSTIM1a expression also caused a decrease in the frequency of calcium transients at all stages of axon outgrowth, it can be reasoned that eliminating zSTIM1a expression may further attenuate, or even abolish, calcium spiking in all CaP axons. However, further experiments are required to demonstrate whether zSTIM1a is necessary for the generation of spontaneous calcium transients in navigating axons *in vivo*. Ablation of zSTIM1a expression in cell type specific manner, using gene editing technology such as the clustered regularly interspaced

short palindromic repeats (CRISPR)-Cas9 or transcription activator-like effector nucleases (TALEN) systems (Ekker, 2008; Bedell et al., 2012; Hwang et al., 2013; Peng et al., 2014; Kok et al., 2015), or expression of a dominant negative form of STIM1 (Liou et al., 2005; Shim et al., 2013), could be used to determine whether zSTIM1a is required for spontaneous calcium transients in pathfinding axons *in vivo*. Furthermore, if calcium influx via SOCE is required for the generation of bursting spikes, then an attenuation of bursting spikes should be present in CaP axons lacking TRPC channels or CRAC channels (Orai proteins). While significant progress was made to express of a dominant negative version of zSTIM1a (DN-zSTIM1a) in motor neurons (*Chapter 3*), time constraints meant that the effect of DN-zSTIM1a expression on the capacity of CaP axons to generate calcium spikes could not be investigated. However, these experiments should be performed to validate results presented in this chapter.

zSTIM1a is a regulator of axon guidance at intermediate targets

As discussed, axon outgrowth is regulated by calcium transients in a frequency dependent manner (Gomez and Spitzer, 1999; Tang and Kalil, 2005; Hutchins and Kalil, 2008). Therefore, given that CaP axons exhibit a decrease in the frequency of calcium spikes at all stages of axon outgrowth when zSTIM1a expression was reduced, it would be predicted that axon outgrowth would occur more rapidly in zSTIM1a morphant CaP axons, perhaps decreasing the time spent at intermediate choice points. However, this prediction is not supported by data presented in Chapter 3, where CaP axons of zSTIM1a morphants reached the horizontal myoseptum at the same time as control axons, but stalled inappropriately at this and subsequent intermediate targets.

The observation that CaP axons of control and zSTIM1a morphants reach the horizontal myoseptum at the same time (*Chapter 3*), can be explained by analyzing the type of calcium spikes expressed in CaP axons located proximal to the myoseptum. Low frequency spikes were expressed at similar levels in CaP axons of control and zSTIM1a morphants, even though the overall frequency of calcium transients was reduced. Thus, it appears that axon extension *in vivo* occurs at a similar rate over a wide range of low frequency transients. This finding is also consistent with the observation that CaP axons exhibit no defects in axon outgrowth when calcium spiking is suppressed by the stochastic expression of an inward rectifying potassium channel, or by exposure to the voltage-

dependent sodium channel blocker tricaine (Plazas et al., 2013). These data suggest that there is a wide range of calcium spike frequency that will enable CaP axons to navigate the common pathway. However, these data do not explain why CaP axons of zSTIM1a morphants stall for longer at intermediate targets.

The frequency of calcium transients was decreased in CaP axons of zSTIM1a morphants located at the myoseptum, with the number of bursting spikes selectively reduced. These data suggest that high frequency spikes are sufficient to slow axon extension, consistent with both control and zSTIM1a morphants axons pausing at intermediate targets. However, bursting spikes were selectively reduced, suggesting that bursting spikes are required for the pathfinding decisions that allow the CaP axons to extend away from intermediate targets. This suggestion correlates with the finding that CaP axons of zSTIM1a morphants are stalled at intermediate targets and exhibit perturbed angles of axon outgrowth as they extend away from intermediate targets (Chapter 3). Therefore, these data provide evidence to suggest that the generation of bursting calcium spikes is required for correct axon pathfinding via intermediate targets, and that STIM1 plays a key role in the regulation of bursting calcium spikes. Given that calcium spikes rely on calcium release from the ER (Meyer and Stryer, 1991; Berridge, 1998), these data support a model whereby STIM1 is required for the refilling of ER calcium store between calcium spikes to regulate axon pathfinding via intermediate targets.

Directional motility, or 'steering' of pathfinding axons, is dependent on spatially and temporally localised calcium signals in the growth cone, which mediate both attraction and repulsion to extracellular guidance cues (Zheng, 2000; Gomez et al., 2001; Henley et al., 2004; Wen et al., 2004b; Ooashi et al., 2005). In principle, growth cone motility is biased towards the side of the growth cone in which sustained, localised elevations in intracellular calcium occur, with both calcium release from the ER and calcium influx via STIM1-mediated SOCE necessary for attractive axon guidance (Ooashi et al., 2005; Gasperini et al., 2009; Mitchell et al., 2012). Hence, a cogent argument can be made that SOCE, by refilling ER calcium stores, also mediates sustained, localised rises in intracellular calcium that potentiate the calcium-dependent remodeling of the growth cone in the direction of the attractive guidance cue (Gasperini et al., 2009; Mitchell et al., 2012). Consistent with this hypothesis, reduced STIM1 expression, or inhibition of STIM1 function, results in a switching in the motility response of growth cones from

attraction to repulsion upon BDNF or netrin-1 signaling (Mitchell et al., 2012; Shim et al., 2013). In studies presented here, CaP axons stalled at intermediate targets and exhibited subtle defects in axon guidance when extending from intermediate targets (Chapter 3), which is associated with a specific reduction in bursting calcium spikes. This data is consistent with previous studies the requirement of spontaneous activity for correct axon pathfinding (Hanson and Landmesser, 2006; Hanson et al., 2008; Kastanenka and Landmesser, 2010; 2013; Plazas et al., 2013).

There are likely multiple mechanisms by which axon pathfinding is perturbed when bursting calcium spikes are attenuated. One possibility is that reduced activity decreases the expression of guidance cue receptors on navigating axons. In chick spinal neurons, inhibition of bursting activity prevents the normal expression of the Ephrin receptor EphA4 and the adhesion molecule polysialylated neural cell adhesion molecule (NCAM), leading to errors in motor axon pathfinding (Hanson and Landmesser, 2004). Interestingly, CaP axons downregulate the sema3A receptor neuropillin-1a once they reach the horizontal myoseptum (Sato-Maeda et al., 2006), which coincides with increased bursting activity. Downregulation of neuropillin-1a permits CaP axons to extend into the sema3A1 expressing ventral myotome (Sato-Maeda et al., 2006; Feldner et al., 2007). Therefore, in CaP axons of zSTIM1a morphants, a mechanism may exist whereby the attenuation of bursting calcium spikes prevents the downregulation of neuropillin-1a, leading to the stalling of CaP axons at the horizontal myoseptum observed in *Chapter 3* as the CaP axons remains sensitive to sema3a in the ventral myotome.

A second possibility is that activity based competition between axons underlies defects in axon pathfinding when activity is perturbed (Yu et al., 2004; Plazas et al., 2013). However, given that CaP axons navigate in the absence of interactions with other motor neurons (Myers et al., 1986; Westerfield et al., 1986), competition between axons is unlikely to explain errors in CaP axon pathfinding. Indeed, previous studies have shown that if activity is abolished stochastically in the spinal cord, then CaP axon pathfinding is not perturbed (Plazas et al., 2013). As such, competition between neurons is unlikely to explain defects in CaP axons of zSTIM1a morphants.

Signaling between navigating axons and the underlying myotome may also regulate axon pathfinding by CaP neurons. CaP axons navigate via pre-patterned AChR clusters

(Flanagan-Steet, 2005; Panzer et al., 2005), with signaling from the navigating CaP axons to the myotome inducing the earliest behavioral events observed in zebrafish embryos (Saint-Amant and Drapeau, 1998; 2000), suggesting that signaling between navigating CaP axons and the myoseptum may participate in the regulation of axon outgrowth. During axon outgrowth, motor neuron-derived agrin, as well as wnt signaling from the notochord, promote signaling via the kinase MuSK/*unplugged*, which leads to the stabilisation of pre-patterned AChR clusters (Sanes and Lichtman, 2001; Kim et al., 2006; Jing et al., 2009). Studies have shown that axon pathfinding by CaP neurons is defective if the MuSK/*unplugged* signaling pathway is perturbed (Zhang and Granato, 2000; Zhang et al., 2004; Xu et al., 2005; Kim and Burden, 2007; Jing et al., 2009), suggested that signaling between pathfinding motor axons and the developing myotome regulate axon pathfinding (Panzer et al., 2005; Jing et al., 2009). Inhibition of all synaptic activity with tetanus-toxin has no effect on axon pathfinding (Plazas et al., 2013), with AChR expression not required for CaP axons outgrowth (Westerfield et al., 1990), suggesting that the signaling between the navigating axon and the myotome is not essential for axon outgrowth. However, reduced STIM1 function has previously been shown to strongly attenuate, but not abolish, synaptic activity at neuromuscular junctions (Venkiteswaran and Hasan, 2009). Hence, signaling between navigating CaP axons and the myotome is likely to be perturbed in zSTIM1a morphants. Given that defects in the MUSK/*unplugged* pathway causes perturbed axon outfought (Zhang and Granato, 2000; Zhang et al., 2004; Xu et al., 2005; Kim and Burden, 2007; Jing et al., 2009), defective signaling at AChR clusters cannot be ruled out as a mechanism that underlies perturbed axon pathfinding in zSTIM1a morphant embryos. Future studies on this question could employ electrophysiology techniques to measure post-synaptic activity in the myotome, or measure the coiling behaviour of zSTIM1a morphant embryos, as both approaches could be used to investigate whether signaling between CaP axons and AChR clusters on the myotome is perturbed in zSTIM1a morphants.

Taken together, these studies illustrate the complexity with which calcium regulates axon guidance. Defects in axon pathfinding observed in CaP axons of zSTIM1a morphants are likely the result of complex interactions between spontaneous calcium transients, the regulation of guidance cue receptor expression and interactions between the pathfinding axon and the myotome. Deciphering the cell-autonomous role of STIM1 in regulating axon pathfinding will be key to further understanding how STIM1 and SOCE regulate

axon guidance *in vivo*. However, dissecting the role of zSTIM1a-mediated SOCE as a regulator of calcium signals that mediate axon pathfinding from STIM1 as a regulator of cell development, gene expression and cell motility, will prove challenging. Given the transparent nature of zebrafish, optogenetics techniques, such as a light activated STIM1 proteins (Kyung et al., 2015), and advances in calcium imaging, it may be possible to alter STIM1 function in pathfinding axons in a spatially and temporally restricted manner to dissect these functions.

A further explanation for why decreasing the number of bursting spikes causes CaP axons to stall at intermediate choice points is that calcium signaling pathways are activated by transients at different frequencies (Tomida et al., 2003). CaMKII is a spike frequency detector (Hudmon and Schulman, 2002), that promotes axon outgrowth (Borodinsky et al., 2003; Fink et al., 2003; Tang et al., 2003), increases filopodial dynamics (Lau et al., 1999; Fink et al., 2003), triggers branch formation (Tang and Kalil, 2005), and determines the polarity of axon outgrowth (Zheng, 2000; Wen et al., 2004b). CaMKII is activated by large amplitude, sustained rises in intracellular calcium (Wen et al., 2004b; McVicker et al., 2014), with STIM1 and calcium release from the ER both required for sustained rises in intracellular calcium in growth cones (Gasperini et al., 2009; Mitchell et al., 2012). Therefore, perhaps the sustained rise in intracellular calcium associated with bursting spikes are associated with CaMKII activation. Hence, lack of CaMKII activation could explain why CaP axons of zSTIM1a morphants stall at intermediate targets, have a decreased number of filopodia, and exhibit fewer axonal branches.

Likewise, calcium also activates the mitogen-activated protein kinases (MAPK)/ERK signaling pathway in pathfinding axons (Borodinsky et al., 2003; Tang and Kalil, 2005). The MAPK/ERK signaling pathway required for motor axon outgrowth in mice (Soundararajan et al., 2010). While phosphorylation of STIM1 by ERK, which is conserved in zSTIM1a but not zSTIM1b (*Chapter 2*), is required for STIM1 to dissociate from EB1 and trigger SOCE (Pozo-Guisado et al., 2010; 2013; Casas-Rua et al., 2015; Tomas-Martin et al., 2015). Therefore, activation of MAPK/ERK signaling pathway may represent a feedback mechanism to promote SOCE and replenish depleted calcium stores, thus facilitating high frequency calcium spikes. In zSTIM1a-deficient axons, this feedback mechanism would be expected to be reduced, further limiting the capacity of CaP axons to generate calcium spikes. Therefore, these studies argue for a more nuanced

view of the role of spontaneous calcium transients in regulating axon outgrowth at intermediate targets, and suggest that high and low frequency calcium transients regulate the rate of axon outgrowth, while bursting spikes are of particular importance for axon motility behaviours at intermediate targets.

In Chapter 3, CaP axons of zSTIM1a morphants were observed to exhibit fewer filopodia, which are regulated by calcium signaling, and play crucial structural and sensory roles in axon outgrowth. Axonal growth cones can be reoriented in response to a single filopodial contact (O'Connor et al., 1990; Oakley and Tosney, 1993; Gomez and Letourneau, 1994; Zheng et al., 1996), with growth cone motility biased in the direction of stabilised filopodia (reviewed in (Chilton, 2006; Dent et al., 2011)). Indeed, axons lacking filopodia exhibit errors in axon pathfinding *in vivo* (Chien et al., 1993), suggesting that filopodia are a key determinate of axon motility behaviour. Calcium signaling regulates filopodial dynamics, with a focal increase in intracellular calcium sufficient to induce filopodia formation (Davenport and Kater, 1992; Lau et al., 1999; Dent et al., 2004; Tang and Kalil, 2005), while filopodial motility is regulated in a calcium dependent manner (Chang et al., 1995; Szebenyi et al., 1998; Lau et al., 1999; Cheng et al., 2002; Tang et al., 2003; Tang and Kalil, 2005). Furthermore, spatially localised calcium transients within filopodia correlate with growth cone motility behaviours (Gomez et al., 2001; Nicol et al., 2011). Therefore, calcium transients are crucial for the formation and mobility of filopodia. Moreover, it has long been hypothesised that localisation of internal stores to filopodia is a mechanism to amplify calcium signaling in a spatially restricted manner to inform growth cone motility (Davenport et al., 1996).

Recent studies have shown that STIM1-mediated SOCE is required for filopodial calcium transients elicited by netrin-1 (Shim et al., 2013), and that STIM1 is localised to the turning side of the growth cone (Mitchell et al., 2012), and into filopodia (Shim et al., 2013), in response to depletion of ER calcium stores. By interacting with the microtubule cytoskeleton via EB1, STIM1 regulates remodeling of the ER in non-neuronal cells (Grigoriev et al., 2008; Smyth et al., 2012; Asanov et al., 2013). Therefore, it could also be hypothesised that the reduced number of filopodia observed on CaP axons of zSTIM1a morphants, and the perturbed axon pathfinding at intermediate choice points, is the result of defects in the spatial localisation of calcium signaling within the growth cone caused by perturbing ER remodeling, as well as temporal defects in calcium entry via SOCE.

These data are further supported by the lack of a compensatory response by zSTIM1b when zSITM1a expression was reduced. Given that zSTIM1b is not predicted to bind EB (Chapter 2), and therefore should not function to regulate ER remodeling, the finding that zSTIM1b does not compensate for zSTIM1a may suggest that STIM1-mediated ER remodeling is important for the regulation of filopodial dynamics, axon branching and correct navigational responses at intermediate targets.

The data presented in this chapter suggest that zSTIM1a-mediated SOCE is required to refill depleted ER calcium stores, allowing for sustained, repeated bursting calcium spikes that regulate axon pathfinding *in vivo*. Precise patterns of calcium signaling control multiple aspects of axon guidance, including the rate of axon extension, growth cone motility, filopodial dynamics, axonal branching, as well as regulating expression of guidance cue receptors and modulating intracellular signaling in response to guidance cues. These data suggest that STIM1 is necessary for correct calcium signaling, which would provide a cellular mechanism by which reduced zSTIM1a expression causes defects in axon pathfinding by CaP neurons *in vivo*. These findings suggest a novel mechanism by which calcium signaling is regulated by STIM1 during axon pathfinding *in vivo*.

Chapter 5:
Conclusions and future directions

Chapter 5: Conclusions and future directions

This work has characterised the ontogeny of STIM1 during development and, by providing evidence for a requirement of STIM1 for the precise patterns of calcium signaling that regulate axon pathfinding *in vivo*, suggest a critical role for STIM1-mediated calcium signaling for nervous system development. The conservation of STIM1 expression in developing vertebrate nervous systems was revealed, with STIM1 expressed in both mouse and zebrafish nervous systems, suggesting that STIM1 has a conserved function in nervous system development. By examining the cellular localisation of STIM proteins in the embryonic mouse nervous, STIM1 was found to be the major neuronal STIM protein during development, with the second STIM protein, STIM2, primarily localised to radial glia. Consistent with a critical function for STIM1 in embryonic development, the most conserved zebrafish ortholog of STIM1, zSTIM1a, was required for the survival, growth and correct development of zebrafish embryos. zSTIM1a was shown to regulate SOCE in zebrafish spinal motor neurons, and the precise patterns of spontaneous calcium spikes in motor axons *in vivo*. When zSTIM1a expression was reduced, bursting calcium spikes were specifically decreased in motor axons. This dysregulation of calcium signaling in navigating axons correlated with motor axons stalling at intermediate targets, expressing fewer filopodia, and exhibiting defects in axon extension away from intermediate targets, suggesting that STIM1-mediated calcium signaling is necessary for correct axon pathfinding. The findings presented in this thesis provide evidence that STIM1 function is vital for the normal regulation of calcium signaling and correct guidance of navigating axons *in vivo*, informing our understanding of the mechanisms that regulate calcium signaling during nervous system development.

STIM1-mediated bursting calcium spikes are necessary for correct axon pathfinding

Data presented here suggest that zSTIM1a regulates SOCE in zebrafish motor neurons *in vitro*, and that reduced zSTIM1a expression attenuates bursting calcium spikes in navigating CaP axons *in vivo*. Calcium spikes depend on calcium release from the ER (Barish, 1991; Holliday et al., 1991), with bursting calcium spikes rapidly depleting the ER and, hence, there is a requirement for rapid refilling of the ER between spikes for bursting activity to be sustained. Hence, this data indicates that STIM1-mediated SOCE

refills depleted ER calcium stores between calcium spikes in navigating axons, and is required to sustain elevated intracellular calcium for the regulation of axon pathfinding *in vivo*. A feature of bursting calcium spikes is that elevated intracellular calcium is sustained, potentiating calcium signaling pathways to mediate long-term changes that mediate processes such as growth cone motility (Gomez et al., 2001). These findings are consistent with previous reports showing that STIM1 is necessary to sustain elevated intracellular calcium in rodent growth cones turning towards BDNF (Mitchell et al., 2012), that STIM1 is required for netrin-1 triggered increases in the frequency of filopodial calcium transients in *Xenopus* growth cones (Shim et al., 2013). STIM1 also mediates store-refilling following fast mGluR-mediated synaptic calcium transients in Purkinje neurons (Hartmann et al., 2014). Therefore, this data provides evidence that STIM1-mediated SOCE is a conserved mechanism for the regulation of precise patterns of calcium signaling in neurons.

Calcium transients regulate axon pathfinding in a frequency-dependent manner. Low frequency transients elicit axon extension, while higher frequency transients cause slowing of axon extension and pausing of axons at intermediate targets (Gomez and Spitzer, 1999; Tang et al., 2003; Plazas et al., 2013). Data from control CaP axons supports this model, with low frequency calcium spikes predominating in axons extending along the common pathway to reach the horizontal myoseptum, while high frequency and bursting calcium spikes were increased in axons located at the horizontal myoseptum, a key choice point for CaP axon outgrowth. In CaP axons of zSTIM1a morphants located at the horizontal myoseptum, there was an attenuation of bursting spikes, but no significant decrease in high or low frequency spikes. This attenuation of bursting spikes produced a frequency of calcium transients that was so low that it was comparable to the frequency of calcium transients detected in control CaP axons extending along the common pathway. Therefore, if axon pathfinding occurs in a frequency-dependent manner, then it would be predicted that CaP axons of zSTIM1a morphants would not pause at the horizontal myoseptum but continue to extend. However, CaP axons of zSTIM1a morphants stalled at intermediate targets such as the horizontal myoseptum and the ventral notochord. These data suggest that it is not just the frequency of calcium transients that is important for determining axon outgrowth, but that the discrete spatiotemporal properties of bursting calcium spikes regulate distinct cellular processes that are important for axons to navigate away from intermediate targets.

These findings raise the question: what are the molecular mechanisms controlled by bursting calcium spikes that are required for correct axon pathfinding? The stalling of CaP axons of zSTIM1a morphants at intermediate targets when bursting calcium spikes are attenuated can be explained by several mechanisms, including the dysregulation of guidance cue receptor expression and reduced filopodial number. The onset of bursting activity in axons navigating via intermediate targets is known to trigger changes in guidance cue receptor expression that are required for correct axon pathfinding (Hanson and Landmesser, 2004). It is also known that CaP axons downregulate the sema3A receptor neuropillin-1 when paused at the horizontal myoseptum, which facilitates extension into the sema3A-expressing ventral myotome (Shoji et al., 2003; Feldner et al., 2005; Sato-Maeda et al., 2006). Therefore, it could be predicted that expression of guidance cue receptors, such as neuropillin-1, is dysregulated in CaP axons of zSTIM1a morphants, causing defects in axon pathfinding. Furthermore, for growth cones to make appropriate guidance decisions they must extend filopodia to sample their environment for guidance cues, which will inform the direction of growth cone motility by inducing either stabilisation or destabilisation of filopodia (Gomez and Letourneau, 1994; Zheng et al., 1996; Gomez et al., 2001). If guidance cue receptor expression is dysregulated, then CaP axons could be predicted to not respond correctly to environmental guidance cues that normally promote filopodial extension and stabilisation to mediate axon outgrowth away from intermediate targets. This prediction is supported the observation that CaP axons of zSTIM1a morphants are less likely to be branched, suggesting that CaP axons are not responding correctly to their environment. However, stalling at intermediate targets and reduced axonal branching may also be the direct result of a reduced number of filopodia caused by an attenuation of bursting spikes. One mechanism by which an attenuation of bursting calcium spikes could reduce the number of filopodia is via a decrease in the activity of CaMKII. CaMKII is activated in response to larger amplitude increases in intracellular calcium, and is therefore activated by higher frequency calcium transients, with the activation of CaMKII promoting filopodial generation and extension (Tang et al., 2003; Tang and Kalil, 2005). (Tang et al., 2003). Therefore, when bursting calcium spikes are attenuated in CaP axons of zSTIM1a morphants, it could be predicted that there are less filopodia as a direct result, and that therefore the CaP axon is no longer able to sense appropriate guidance cues to form axonal branches or navigate correctly via intermediate targets. Given that the expression

of guidance cue receptors and filopodial dynamics are so tightly interwoven in their regulation of axon pathfinding, it would be predicted that both mechanisms contribute axon pathfinding defects in response to an attenuation of bursting calcium spikes when zSTIM1a expression is reduced.

A limitation of these studies is that zSTIM1a expression was reduced throughout the embryo, and therefore it is not possible to distinguish the cell autonomous effects of reduced zSTIM1a expression on calcium signaling and axon pathfinding by CaP neurons. To address this significant limitation, a dominant-negative (DN)-zSTIM1a that was genetically expressed within spinal motor neurons using the Tol2 expression system was generated, however time limitations prevented the effect of DN-zSTIM1a expression on axon pathfinding from being investigated. Similar dominant-negative STIM1 proteins have been shown to disrupt SOCE (Liou et al., 2007), as well as cause defects in midline crossing by *Xenopus* spinal commissural axons (Shim et al., 2013). Therefore, future experiments expressing DN-zSTIM1a in zebrafish spinal motor axons would be predicted to validate data presented here, and provide evidence for a cell-autonomous function of STIM1 in regulating calcium signaling and axon pathfinding in CaP neurons. Furthermore, as studies focused on spinal motor neurons, whether the function of STIM1 as a regulator of axon pathfinding is a conserved process in other neural circuits remains to be determined. Expressing DN-zSTIM1a in other zebrafish circuits that also exhibit highly stereotypic axon pathfinding behaviours would provide insights into the conserved function of STIM1 in axon pathfinding *in vivo*. Candidate systems would include olfactory neurons (Celik et al., 2002; Arganda-Carreras et al., 2014), retinal ganglion cells (Karlstrom et al., 1996), Mauthner cells (Jontes et al., 2000), and neurons of the posterior lateral line (Shoji et al., 1998; Halloran et al., 2000). These neurons exhibit precise axon pathfinding events during development, and mediate distinct behavioral responses that could be used to test the functional relevance of any defects observed in axon pathfinding when zSTIM1a function is perturbed.

Data presented here suggests that STIM1-mediated bursting calcium spikes are crucial for axons to navigate via intermediate targets. If STIM1-mediated bursting activity is required for correct navigational responses when axons are paused at intermediate targets, then restoring bursting activity would be predicted to rescue axon pathfinding in zSTIM1a-deficient motor neurons. One approach would be to utilise optogenetic

techniques, such as expressing channelrhodopsin-2 (Nagel et al., 2003), in zebrafish spinal motor neurons to allow activity to be manipulated by light. Bursting activity could potentially then be restored in CaP axons with reduced zSTIM1a expression (or expressing DN-zSTIM1a as outlined above), as the CaP axon reaches the horizontal myoseptum. If the restoration of bursting activity rescues axon pathfinding by CaP axons, then these results would provide further evidence for a crucial role of bursting calcium spikes in regulating navigational decisions made by axons at intermediate targets. However, it has been hypothesised that the source of calcium used to generate a calcium signal is crucial for determining pathfinding decisions, with calcium release from the ER believed to provide distinct spatiotemporal patterns of calcium signaling within the growth cone (Tojima et al., 2011). Hence, it is important to dissect the role of STIM1 in facilitating localised calcium release from the ER from its role in refilling the ER calcium store to facilitate bursting calcium spikes. A light-activated STIM1 protein (Pham et al., 2011; Kyung et al., 2015), could be expressed in spinal motor neurons with reduced zSTIM1a expression. By activating the optically controlled STIM1 protein throughout the CaP neuron, or within the growth cone, would provide a mechanism to discriminate between the function of STIM1 as a global regulator SOCE and the function of STIM1 as a regulator of spatially restricted calcium signaling within growth cones.

Findings presented here confirm that low frequency calcium spikes promote axon extension, while high frequency calcium spikes slow axon extension and promote pausing. These findings may suggest a model of axon pathfinding whereby STIM1-mediated bursting calcium spikes are required for correct navigational responses of axons at intermediate targets (Fig. 5.1). However, these data do not rule out the possibility that STIM1 has additional functions in the regulation of axon pathfinding beyond the regulation of SOCE.

Figure 5.1: STIM1 is required for bursting calcium spikes, which mediate axon outgrowth from intermediate targets.

(a) Schematic depicting a proposed model for the role of distinct patterns of calcium signaling in the regulation of axon pathfinding by CaP axons via the horizontal myoseptum. At 20 hpf, the CaP axons predominately expresses low frequency spikes, producing a narrow growth cone with few filopodia that promotes axon extension, correlating with CaP axons rapidly extending along the common pathway to reach the horizontal myoseptum. At 20 hpf, expression of higher frequency spikes and bursting spikes promote filopodial formation, producing a larger, more complex growth cone that becomes paused at the horizontal myoseptum. Bursting spikes may also trigger changes in guidance cue receptor and adhesion molecule expression, allowing the CaP axon to extend away from the horizontal myoseptum. At 22 hpf, the CaP axon is extending away from the horizontal myoseptum, but spike frequency remains high as the CaP axon is navigating at a slower rate compared to pre-myoseptum towards a further intermediate target, the ventral notochord.

(b) The importance of zSTIM1a-mediated bursting calcium spikes for axon pathfinding by CaP axons via the horizontal myoseptum. At 20 hpf, the number of low frequency spikes generated in CaP axons of zSTIM1a morphants is comparable to control morphants. As a result, axons navigate to the horizontal myoseptum largely unperturbed, arriving at the same time as controls. At 22 hpf, CaP axons of zSTIM1a morphants located at the horizontal myoseptum exhibit a similar number of high frequency spikes, meaning that CaP axons of zSTIM1a morphants pause at the horizontal myoseptum. However, CaP axons of zSTIM1a morphants exhibit a significant attenuation of bursting spikes. This may cause defects in the generation of filopodia, expression of guidance cue receptors and adhesion molecules, and hence cause CaP axons becoming stalled for longer at the horizontal myoseptum.

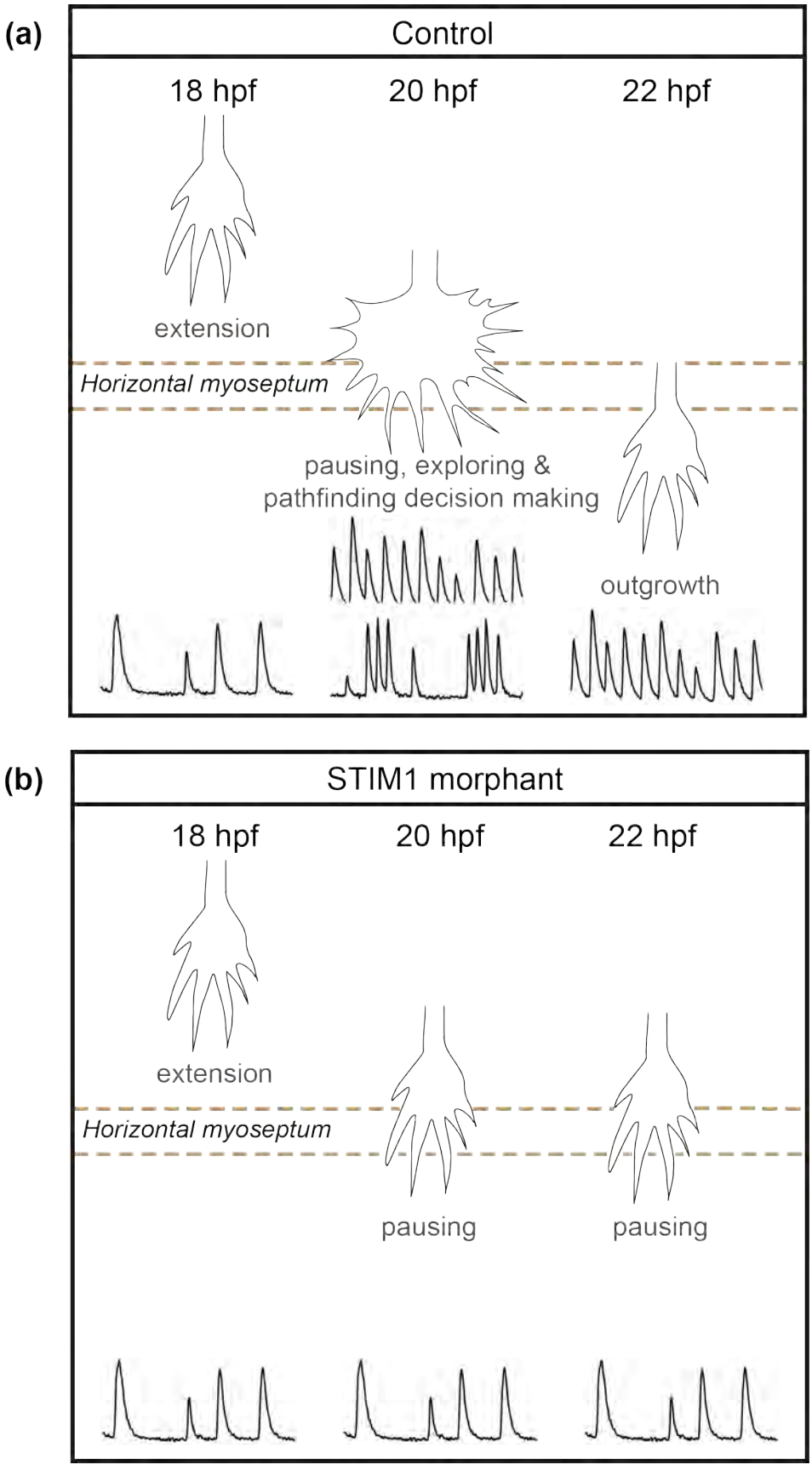
(a)
Control
18 hpf
20 hpf
22 hpf
extension
Horizontal myoseptum
pausing, exploring &
pathfinding decision making
outgrowth
(b)
STIM1 morphant
18 hpf
20 hpf
22 hpf
extension
Horizontal myoseptum
pausing
pausing

STIM1 is a multifaceted protein that regulates multiple aspects of axon pathfinding

A tenet of axon pathfinding is that growth cones extend in the direction of stabilised filopodia. Localised, larger amplitude calcium signals 'steer' axon outgrowth by triggering extension and stabilisation of microtubules into filopodia (Sabry et al., 1991; Davenport et al., 1993; Dent and Kalil, 2001; Schaefer et al., 2008; Zhang and Forscher, 2009). Calcium release from the ER is required for sustained, localised calcium signals that regulate growth cone motility (Hong et al., 2000; Ooashi et al., 2005; Akiyama et al., 2009). As such, remodeling of the ER into filopodia has been hypothesised to be a mechanism that localises calcium signals within the growth cone to facilitate growth cone motility (Davenport et al., 1996)

Previous studies have shown that calcium signals trigger microtubule extension and stabilisation towards the turning side of the growth cone (Guan and Rao, 2003; Jin et al., 2005; Zhang and Forscher, 2009), with ER remodeling to the periphery of the growth cone occurring in parallel with projecting microtubules in response to guidance cue mediated calcium signaling (Zhang and Forscher, 2009). Given the ER-localisation of STIM1, it is unsurprising that STIM1 is actively trafficked to the turning side of the growth cone, as well as into filopodia, in response to guidance cue signaling or store-depletion (Mitchell et al., 2012; Shim et al., 2013). However, in non-neuronal cells, STIM1 interacts with the microtubule cytoskeleton to regulate ER remodeling, and this function of STIM1 facilitates localisation of calcium signaling within cells (Grigoriev et al., 2008; Asanov et al., 2013; Tsai et al., 2014; Casas-Rua et al., 2015). Hence, it could be predicted that STIM1 functions to regulate spatial and temporal localisation of calcium signals within growth cones by controlling remodeling of the ER into filopodia, facilitating sustained calcium signals required for filopodial stabilisation.

In non-neuronal cells, the interaction between STIM1 and the microtubule cytoskeleton is mediated by STIM1 binding to the microtubule plus-end tracking protein EB (Grigoriev et al., 2008). EB proteins are present in the growth cone, and are necessary for correct growth cone motility (Stepanova et al., 2003). Hence, STIM1 and EB are appropriately expressed to regulate ER remodeling in the growth cone. However, it remains unknown whether STIM1 functions to regulate ER remodeling in the growth cone. In work presented here, CaP axons exhibited fewer filopodia, showed perturbed

axon pathfinding, were less likely to have branched. Given the critical role of spatially localised calcium signals for filopodial induction and motility (Tang and Kalil, 2005), branching (Hutchins and Kalil, 2008), and growth cone turning (Gomez et al., 2001), it is likely that defects in axon pathfinding observed in studies presented here could be caused by an inability of growth cones to produce spatially restricted calcium signals as a result of perturbed STIM1-mediated ER remodeling.

To investigate whether the function of STIM1 as a regulator of ER remodeling contributes to the defects in axon pathfinding in CaP axons of zSTIM1a morphants, the ability of STIM1 to interact with EB could be perturbed in navigating CaP axons. STIM1-EB interactions occur via a conserved TRIP motif (Honnappa et al., 2009), and are regulated by the phosphorylation of key residues in STIM1 (Pozo-Guisado et al., 2010; 2013; Tomas-Martin et al., 2015). zSTIM1a with a mutated TRIP motif, or mutations in the phosphorylated residues predicted to regulate STIM1-EB interactions, could be expressed in CaP axons using the Tol2 expression system outlined herein. If expression of mutant zSTIM1a results in defects in axon pathfinding, then these data would suggest that the function of STIM1 as a regulator of ER remodeling is crucial for axon pathfinding. A second approach to address this question would be to reduce expression of zSTIM1b. zSTIM1b was found to have no discernable TRIP motif and does not retain consensus sequences for phosphorylation predicted to regulate the ER remodeling function of STIM1. Hence, it could be predicted that reducing zSTIM1b expression would not impact the function of STIM1 in regulating ER remodeling. Therefore, if reduced expression of zSTIM1b does not affect axon pathfinding by CaP neurons, then these data would argue for a crucial role of the ER remodeling function of STIM1 during axon pathfinding. The fact that axon pathfinding defects are observed in zSTIM1a morphants, where endogenous zSTIM1b is still present, may suggest that the ER remodeling function of zSTIM1a is crucial for axon pathfinding.

STIM1 may also regulate axon pathfinding via interactions with the cAMP/PKA signaling pathway. In non-neuronal cells, STIM1 has been shown to trigger cAMP production via the store-operated cAMP signaling pathway (Lefkimmiatis et al., 2009), while Orai has also been shown to activate cAMP production (Willoughby et al., 2012). Induction of cAMP triggers the formation of STIM1 puncta (Tian et al., 2012), and potentiates ER calcium release via CICR (Tojima et al., 2011), suggesting that a positive

feedback mechanism exists to increase ER calcium release when SOCE is activated. Therefore, inhibition of the store-operated cAMP signaling pathway may also contribute to defects in calcium signaling and axon pathfinding observed in studies presented here. However, dissecting the role of the store-operated cAMP signaling pathway may be difficult due to the highly interconnected nature of cAMP signaling and calcium signaling in growth cone motility (Song et al., 1997; Nicol et al., 2011).

In conclusion, data presented in this thesis provide evidence to support the hypothesis that STIM1 regulates calcium signaling in pathfinding axons *in vivo*, and is required for correct axon pathfinding *in vivo*. These data suggest a role for STIM1-mediated SOCE in the refilling of ER calcium stores between calcium transients in navigating axons, and that STIM1 regulates calcium signaling required for correct axon pathfinding. However, it is likely that STIM1 has multiple roles in the regulation of axon pathfinding. As STIM1 was found to be the major neuronal protein in development, and given the crucial role that precise patterns of calcium signaling play at each stage of neuronal development, these results argue for a critical role for STIM1 during nervous system development.

References

References:

Ahrens MB, Li JM, Orger MB, Robson DN, Schier AF, Engert F, Portugues R (2012) Brain-wide neuronal dynamics during motor adaptation in zebrafish. Nature.

Ahrens MB, Orger MB, Robson DN, Li JM, Keller PJ (2013) Whole-brain functional imaging at cellular resolution using light-sheet microscopy. Nat Meth 10:413–420.

Akerboom J et al. (2012) Optimization of a GCaMP Calcium Indicator for Neural Activity Imaging. J Neurosci 32:13819–13840.

Akiyama H, Kamiguchi H (2013) Second messenger networks for accurate growth cone guidance Kamiguchi H, Borodinsky LN, eds. Developmental Neurobiology 75:411–422.

Akiyama H, Matsu-ura T, Mikoshiba K, Kamiguchi H (2009) Control of Neuronal Growth Cone Navigation by Asymmetric Inositol 1,4,5-Trisphosphate Signals. Science Signaling 2:ra34–ra34.

Alaynick WA, Jessell TM, Pfaff SL (2011) SnapShot: Spinal Cord Development. Cell 146:178–178.e1.

Albarran L, Lopez JJ, Woodard GE, Salido GM, Rosado JA (2016) Store-operated Ca 2+Entry-associated Regulatory factor (SARAF) Plays an Important Role in the Regulation of Arachidonate-regulated Ca 2+(ARC) Channels. Journal of Biological Chemistry 291:6982–6988.

Alicia S, Angélica Z, Carlos S, Alfonso S, Vaca L (2008) STIM1 converts TRPC1 from a receptor-operated to a store-operated channel: Moving TRPC1 in and out of lipid rafts. Cell Calcium 44:479–491.

Andersen SS (2001) Preparation of dissociated zebrafish spinal neuron cultures. Methods Cell Sci 23:205–209.

Anitha A et al. (2008) Genetic analyses of Roundabout(ROBO) axon guidance receptors in autism. Am J Med Genet 147B:1019–1027.

Anthony TE, Klein C, Fishell G, Heintz N (2004) Radial glia serve as neuronal progenitors in all regions of the central nervous system. Neuron 41:881–890.

Antigny F, Jousset H, Konig S, Frieden M (2011) Thapsigargin activates Ca(2)+ entry both by store-dependent, STIM1/Orai1-mediated, and store-independent, TRPC3/PLC/PKC-mediated pathways in human endothelial cells. Cell Calcium 49:115–127.

Appel B, Korzh V, Glasgow E, Thor S, Edlund T, Dawid IB, Eisen JS (1995) Motoneuron fate specification revealed by patterned LIM homeobox gene expression in embryonic zebrafish. Development 121:4117–4125.

Araki Y, Lin D-T, Huganir RL (2010) Plasma membrane insertion of the AMPA receptor GluA2 subunit is regulated by NSF binding and Q/R editing of the ion

pore. Proceedings of the National Academy of Sciences 107:11080–11085.

Arber S, Han B, Mendelsohn M, Smith M, Jessell TM, Sockanathan S (1999) Requirement for the homeobox gene Hb9 in the consolidation of motor neuron identity. Neuron 23:659–674.

Arganda-Carreras I, Wakisaka N, Masuda M, l USUMU, Seung HS, Miyasaka N, Yoshihara Y (2014) Olfactory projectome in the zebrafish forebrain revealed by genetic single-neuron labelling. Nature Communications 5:1–14.

Asakawa K, Kawakami K (2009) The Tol2-mediated Gal4-UAS method for gene and enhancer trapping in zebrafish. Methods 49:275–281.

Asanov A, Sherry R, Sampieri A, Vaca L (2013) A relay mechanism between EB1 and APC facilitate STIM1 puncta assembly at endoplasmic reticulum-plasma membrane junctions. Cell Calcium 54:246–256.

Ashworth R, Bolsover SR (2002) Spontaneous activity-independent intracellular calcium signals in the developing spinal cord of the zebrafish embryo. Developmental Brain Research 139:131–137.

Averaimo S, Nicol X (2014) Intermingled cAMP, cGMP and calcium spatiotemporal dynamics in developing neuronal circuits. Front Cell Neurosci 8:376.

Baba AA, Yasui TT, Fujisawa SS, Yamada RXR, Yamada MKM, Nishiyama NN, Matsuki NN, Ikegaya YY (2003) Activity-evoked capacitative Ca2+ entry: implications in synaptic plasticity. Journal of Neuroscience 23:7737–7741.

Barish ME (1991) Increases in intracellular calcium ion concentration during depolarization of cultured embryonic Xenopus spinal neurones. J Physiol 444:545–565.

Bastiani MJ, Raper JA, Goodman CS (1984) Pathfinding by Neuronal Growth Cones in Grasshopper Embryos .3. Selective Affinity of the G-Growth Cone for the P-Cells Within the a/P Fascicle. Journal of Neuroscience 4:2311–2328.

Bean BP (1989) Neurotransmitter inhibition of neuronal calcium currents by changes in channel voltage dependence. Nature 340:153–156.

Beattie CE (2000) Control of motor axon guidance in the zebrafish embryo. Brain Res Bull 53:489–500.

Beattie CE, Melancon E, Eisen JS (2000) Mutations in the stumpy gene reveal intermediate targets for zebrafish motor axons. Development 127:2653–2662.

Bedell VM, Wang Y, Campbell JM, Poshusta TL, Starker CG, Krug RG II, Tan W, Penheiter SG, Ma AC, Leung AYH, Fahrenkrug SC, Carlson DF, Voytas DF, Clark KJ, Essner JJ, Ekker SC (2012) In vivo genome editing using a high-efficiency TALEN system. Nature 491:114–118.

Bentley D, Caudy M (1983) Pioneer axons lose directed growth after selective killing of guidepost cells. Nature 304:62–65.

Bentley D, Keshishian H (1982) Pathfinding by peripheral pioneer neurons in grasshoppers. Science 218:1082–1088.

Berna-Erro A, Braun A, Kraft R, Kleinschnitz C, Schuhmann MK, Stegner D, Wultsch T, Eilers J, Meuth SG, Stoll G, Nieswandt B (2009) STIM2 Regulates Capacitive Ca2+ Entry in Neurons and Plays a Key Role in Hypoxic Neuronal Cell Death. Science Signaling 2:ra67–ra67.

Bernhardt RR, Goerlinger S, Roos M, Schachner M (1998) Anterior-posterior subdivision of the somite in embryonic zebrafish: implications for motor axon guidance. Dev Dyn 213:334–347.

Berridge MJ (1998) Neuronal calcium signaling. Neuron 21:13–26.

Berridge MJ (2002) The endoplasmic reticulum: a multifunctional signaling organelle. Cell Calcium 32:235–249.

Berridge MJ (2006) Calcium microdomains: Organization and function. Cell Calcium 40:405–412.

Berridge MJ, Bootman MD, Roderick HL (2003) Calcium signalling: dynamics, homeostasis and remodelling. Nat Rev Mol Cell Biol 4:517–529.

Berridge MJ, Irvine RF (1989) Inositol phosphates and cell signalling. Nature 341:197–205.

Bezprozvanny I, Watras J, Ehrlich BE (1991) Bell-shaped calcium-response curves of Ins(1,4,5)P3- and calcium-gated channels from endoplasmic reticulum of cerebellum. Nature 351:751–754.

Bhattacharya S, Bunick CG, Chazin WJ (2004) Target selectivity in EF-hand calcium binding proteins. Biochimica et Biophysica Acta (BBA) - Molecular Cell Research 1742:69–79.

Bill BR, Petzold AM, Clark KJ, Schimmenti LA, Ekker SC (2009) A primer for morpholino use in zebrafish. Zebrafish 6:69–77.

Birely J, Schneider VA, Santana E, Dosch R, Wagner DS, Mullins MC, Granato M (2005) Genetic screens for genes controlling motor nerve–muscle development and interactions. Developmental Neurobiology 280:162–176.

Bito H, Deisseroth K, Tsien RW (1997) Ca2+-dependent regulation in neuronal gene expression. Current Opinion in Neurobiology 7:419–429.

Blankenship AG, Feller MB (2009) Mechanisms underlying spontaneous patterned activity in developing neural circuits. Nat Rev Neurosci 11:18–29.

Bojarski L, Herms J, Kuznicki J (2008) Calcium dysregulation in Alzheimer's disease. Neurochemistry International 52:621–633.

Bonanomi D, Pfaff SL (2010) Motor Axon Pathfinding. Cold Spring Harbor Perspectives in Biology 2:a001735–a001735.

Bootman MD, Berridge MJ (1995) The elemental principles of calcium signaling. Cell 83:675–678.

Bootman MD, Lipp P, Berridge MJ (2001) The organisation and functions of local Ca(2+) signals. Journal of Cell Science 114:2213–2222.

Borodinsky LN, Belgacem YH, Swapna I, Visina O, Balashova OA, Sequerra EB, Tu MK, Levin JB, Spencer KA, Castro PA, Hamilton AM, Shim S (2014) Spatiotemporal integration of developmental cues in neural development Kamiguchi H, Borodinsky LN, eds. Developmental Neurobiology 75:349–359.

Borodinsky LN, O'Leary D, Neale JH, Vicini S, Coso OA, Fiszman ML (2003) GABA-induced neurite outgrowth of cerebellar granule cells is mediated by GABAAreceptor activation, calcium influx and CaMKII and erk1/2 pathways. Journal of Neurochemistry 84:1411–1420.

Borodinsky LN, Root CM, Cronin JA, Sann SB, Gu X, Spitzer NC (2004) Activity-dependent homeostatic specification of transmitter expression in embryonic neurons. Nature 429:523–530.

Bouron A, Altafaj X, Boisseau S, De Waard M (2005) A store-operated Ca2+ influx activated in response to the depletion of thapsigargin-sensitive Ca2+ stores is developmentally regulated in embryonic cortical neurons from mice. Developmental Brain Research 159:64–71.

Bouron AA (2000) Activation of a capacitative Ca(2+) entry pathway by store depletion in cultured hippocampal neurones. FEBS Lett 470:269–272.

Bovolenta P, Mason C (1987) Growth cone morphology varies with position in the developing mouse visual pathway from retina to first targets. Journal of Neuroscience 7:1447–1460.

Brandman O, Liou J, Park WS, Meyer T (2007) STIM2 Is a Feedback Regulator that Stabilizes Basal Cytosolic and Endoplasmic Reticulum Ca2+ Levels. Cell 131:1327–1339.

Bridgman PC, Kachar B, REESE TS (1986) The structure of cytoplasm in directly frozen cultured cells. II. Cytoplasmic domains associated with organelle movements. J Cell Biol 102:1510–1521.

Brini M, Calì T, Ottolini D, Carafoli E (2014) Neuronal calcium signaling: function and dysfunction. Cell Mol Life Sci 71:2787–2814.

Brose K, Bland KS, Wang KH, Arnott D, Henzel W, Goodman CS, Tessier-Lavigne M, Kidd T (1999) Slit proteins bind Robo receptors and have an evolutionarily conserved role in repulsive axon guidance. Cell 96:795–806.

Brown DA, Griffith WH (1983) Calcium-activated outward current in voltage-clamped hippocampal neurones of the guinea-pig. J Physiol 337:287–301.

Buck KB, Zheng JQ (2002) Growth cone turning induced by direct local modification of microtubule dynamics. J Neurosci 22:9358–9367.

Buey RM, Sen I, Kortt O, Mohan R, Gfeller D, Veprintsev D, Kretzschmar I, Scheuermann J, Neri D, Zoete V, Michielin O, de Pereda JM, Akhmanova A, Volkmer R, Steinmetz MO (2012) Sequence Determinants of a Microtubule Tip Localization Signal (MtLS). Journal of Biological Chemistry 287:28227–28242.

Buonanno A, Fields RD (1999) Gene regulation by patterned electrical activity during neural and skeletal muscle development. Current Opinion in Neurobiology.

Burgess GM, Godfrey PP, McKinney JS, Berridge MJ, Irvine RF, Putney JWJ (1984) The second messenger linking receptor activation to internal Ca release in liver. Nature 309:63–66.

Burnette DT, Ji L, Schaefer AW, Medeiros NA, Danuser G, Forscher P (2008) Myosin II Activity Facilitates Microtubule Bundling in the Neuronal Growth Cone Neck. Developmental Cell 15:163–169.

Cai X (2007a) Molecular Evolution and Functional Divergence of the Ca2+ Sensor Protein in Store-operated Ca2+ Entry: Stromal Interaction Molecule Cookson M, ed. PLoS ONE 2:e609.

Cai X (2007b) Molecular Evolution and Structural Analysis of the Ca2+ Release-Activated Ca2+ Channel Subunit, Orai. Journal of Molecular Biology 368:1284–1291.

Cai X, Zhou Y, Nwokonko RM, Loktionova NA, Wang X, Xin P, Trebak M, Wang Y, Gill DL (2016) The Orai1 Store-operated Calcium Channel Functions as a Hexamer. J Biol Chem:jbc.M116.758813–jbc.M116.758824.

Cajal SRY (1890) A quelle epoque apparaissent les expansions des cellules nerveuses de la moëlle épinière du poulet? Anat Anzerger:609–613.

Carey MB, Matsumoto SG (1999) Spontaneous calcium transients are required for neuronal differentiation of murine neural crest. Developmental Neurobiology.

Carlstrom LP, Hines JH, Henle SJ, Henley JR (2010) Bidirectional remodeling of β1-integrin adhesions during chemotropic regulation of nerve growth. BMC Biol 9:82–82.

Casas-Rua V, Tomas-Martin P, Lopez-Guerrero AM, Alvarez IS, Pozo-Guisado E, Martin-Romero FJ (2015) Biochimica et Biophysica Acta. BBA - Molecular Cell Research 1853:233–243.

Catela C, Shin MM, Dasen JS (2015) Assembly and Function of Spinal Circuits for Motor Control. Annu Rev Cell Dev Biol 31:669–698.

Celik A, Fuss SH, Korsching SI (2002) Selective targeting of zebrafish olfactory receptor neurons by the endogenous OMP promoter. Eur J Neurosci 15:798–806.

Chan CM, Aw JTM, Webb SE, Miller AL (2016) SOCE proteins, STIM1 and Orai1, are localized to the cleavage furrow during cytokinesis of the first and second cell division cycles in zebrafish embryos. Zygote:1–10.

Chan CM, Chen Y, Hung TS, Miller AL, Shipley AM, Webb SE (2015) Inhibition of SOCE disrupts cytokinesis in zebrafish embryos via inhibition of cleavage furrow deepening. Int J Dev Biol 59:289–301.

Chang HYH, Takei KK, Sydor AMA, Born TT, Rusnak FF, Jay DGD (1995) Asymmetric retraction of growth cone filopodia following focal inactivation of calcineurin. Nature 376:686–690.

Charles AC, Kodali SK, Tyndale RF (1996) Intercellular calcium waves in neurons. Molecular and Cellular Neuroscience 7:337–353.

Chen M, Van Hook MJ, Thoreson WB (2015) Ca2+ Diffusion through Endoplasmic Reticulum Supports Elevated Intraterminal Ca2+ Levels Needed to Sustain Synaptic Release from Rods in Darkness. J Neurosci 35:11364–11373.

Chen Z, Lee H, Henle SJ, Cheever TR, Ekker SC, Henley JR (2013) Primary Neuron Culture for Nerve Growth and Axon Guidance Studies in Zebrafish (Danio rerio) Hendricks M, ed. PLoS ONE 8:e57539.

Cheng KT, Liu X, Ong HL, Swaim W, Ambudkar IS (2011) Local Ca2+ Entry Via Orai1 Regulates Plasma Membrane Recruitment of TRPC1 and Controls Cytosolic Ca2+ Signals Required for Specific Cell Functions Aldrich RA, ed. PLoS Biol 9:e1001025.

Cheng S, Geddis MS, Rehder V (2002) Local calcium changes regulate the length of growth cone filopodia. J Neurobiol 50:263–275.

Chien CB, Rosenthal DE, Harris WA, Holt CE (1993) Navigational errors made by growth cones without filopodia in the embryonic Xenopus brain. Neuron 11:237–251.

Chilton JK (2006) Molecular mechanisms of axon guidance. Developmental Neurobiology 292:13–24.

Choi J-S, Lee J-H, Shin Y-J, Lee J-Y, Yun H, Chun M-H, Lee M-Y (2009) Transient expression of Bis protein in midline radial glia in developing rat brainstem and spinal cord. Cell Tissue Res 337:27–36.

Clapham DE (1995) Calcium signaling. Cell 80:259–268.

Connor JAJ, Kater SBS, Cohan CC, Fink LL (1990) Ca2+ dynamics in neuronal growth cones: regulation and changing patterns of Ca2+ entry. Cell Calcium 11:233–239.

Covington EDE, Wu MMM, Lewis RSR (2010) Essential role for the CRAC activation domain in store-dependent oligomerization of STIM1. Mol Biol Cell 21:1897–1907.

Craig EM, Van Goor D, Forscher P, Mogilner A (2012) Membrane Tension, Myosin Force, and Actin Turnover Maintain Actin Treadmill in the Nerve Growth Cone. Biophysj 102:1503–1513.

Cvetkovska V, Hibbert AD, Emran F, Chen BE (2013) Overexpression of Down

syndrome cell adhesion molecule impairs precise synaptic targeting. Nature Publishing Group 16:677–682.

Dailey MEM, Bridgman PCP (1989) Dynamics of the endoplasmic reticulum and other membranous organelles in growth cones of cultured neurons. Journal of Neuroscience 9:1897–1909.

Dailey MEM, Bridgman PCP (1991) Structure and organization of membrane organelles along distal microtubule segments in growth cones. J Neurosci Res 30:242–258.

Darbellay B, Arnaudeau S, Bader CR, Konig S, Bernheim L (2011) STIM1L is a new actin-binding splice variant involved in fast repetitive Ca2+ release. The Journal of Cell Biology 194:335–346.

Davenport RW, Dou P, Mills LR, Kater SB (1996) Distinct calcium signaling within neuronal growth cones and filopodia. J Neurobiol 31:1–15.

Davenport RW, Kater SB (1992) Local increases in intracellular calcium elicit local filopodial responses in Helisoma neuronal growth cones. Neuron 9:405–416.

Davenport RWR, Dou PP, Rehder VV, Kater SBS (1993) A sensory role for neuronal growth cone filopodia. Nature 361:721–724.

Davies AM, Thoenen H, Barde YA (1986) The response of chick sensory neurons to brain-derived neurotrophic factor. Journal of Neuroscience 6:1897–1904.

Davis AA, Temple S (1994) A self-renewing multipotential stem cell in embryonic rat cerebral cortex. Nature 372:263–266.

de Juan-Sanz J, Holt GT, Schreiter ER, de Juan F, Kim DS, Ryan TA (2017) Axonal Endoplasmic Reticulum Ca2+ Content Controls Release Probability in CNS Nerve Terminals. Neuron:1–22.

De Koninck P, Schulman H (1998) Sensitivity of CaM kinase II to the frequency of Ca2+ oscillations. Science 279:227–230.

Defer N, Best-Belpomme M, Hanoune J (2000) Tissue specificity and physiological relevance of various isoforms of adenylyl cyclase. Am J Physiol Renal Physiol 279:F400–F416.

DeHaven WI, Smyth JT, Boyles RR, Putney JW (2007) Calcium inhibition and calcium potentiation of Orai1, Orai2, and Orai3 calcium release-activated calcium channels. J Biol Chem 282:17548–17556.

Deisseroth K, Bito H, Schulman H, Tsien RW (1995) Synaptic plasticity: A molecular mechanism for metaplasticity. Curr Biol 5:1334–1338.

Del Bene F, Wyart C, Robles E, Tran A, Looger L, Scott EK, Isacoff EY, Baier H (2010) Filtering of Visual Information in the Tectum by an Identified Neural Circuit. Science 330:669–673.

Dent EW, Barnes AM, Tang F, Kalil K (2004) Netrin-1 and semaphorin 3A promote or inhibit cortical axon branching, respectively, by reorganization of the cytoskeleton. J Neurosci 24:3002–3012.

Dent EW, Gertler FB (2003) Cytoskeletal Dynamics and Transport in Growth Cone Motility and Axon Guidance. Neuron 40:209–227.

Dent EW, Gupton SL, Gertler FB (2011) The Growth Cone Cytoskeleton in Axon Outgrowth and Guidance. Cold Spring Harbor Perspectives in Biology 3:a001800–a001800.

Dent EW, Kalil K (2001) Axon branching requires interactions between dynamic microtubules and actin filaments. J Neurosci 21:9757–9769.

Derler I, Fahrner M, Muik M, Lackner B, Schindl R, Groschner K, Romanin C (2009) A Ca2(+)release-activated Ca2(+) (CRAC) modulatory domain (CMD) within STIM1 mediates fast Ca2(+)-dependent inactivation of ORAI1 channels. Journal of Biological Chemistry 284:24933–24938.

Dickson BJ (2002) Molecular mechanisms of axon guidance. Science 298:1959–1964.

Dodd J, Jessell TM (1988) Axon guidance and the patterning of neuronal projections in vertebrates. Science 242:692–699.

Don EK, Formella I, Badrock AP, Hall TE, Morsch M, Hortle E, Hogan A, Chow S, Gwee SSL, Stoddart JJ, Nicholson G, Chung R, Cole NJ (2017) A Tol2 Gateway-Compatible Toolbox for the Study of the Nervous System and Neurodegenerative Disease. Zebrafish 14:69–72.

Dziadek MA, Johnstone LS (2007) Biochemical properties and cellular localisation of STIM proteins. Cell Calcium 42:10–10.

Eid J-P, Arias A, Robertson H, Hime GR, Dziadek M (2008) The Drosophila STIM1 orthologue, dSTIM, has roles in cell fate specification and tissue patterning. BMC Dev Biol 8:104.

Eisen JS, Melancon E (2001) Interactions with identified muscle cells break motoneuron equivalence in embryonic zebrafish. Nat Neurosci 4:1065–1070.

Eisen JS, Myers PZ, Westerfield M (1986) Pathway selection by growth cones of identified motoneurones in live zebra fish embryos. Nature 320:269–271.

Eisen JS, Pike SH, Debu B (1989) The growth cones of identified motoneurons in embryonic zebrafish select appropriate pathways in the absence of specific cellular interactions. Neuron 2:1097–1104.

Eisen JS, Smith JC (2008) Controlling morpholino experiments: don't stop making antisense. Development 135:1735–1743.

Ekker SC (2008) Zinc Finger–Based Knockout Punches for Zebrafish Genes. Zebrafish 5:121–123.

Emptage NJN, Reid CAC, Fine AA (2000) Calcium Stores in Hippocampal Synaptic Boutons Mediate Short-Term Plasticity, Store-Operated Ca^2^+ Entry, and Spontaneous Transmitter Release. Neuron 29:12–12.

Faas GC, Raghavachari S, Lisman JE, Mody I (2011) Calmodulin as a direct detector of Ca2+ signals. Nat Neurosci 14:301–304.

Fahrner M, Muik M, Schindl R, Butorac C, Stathopulos P, Zheng L, Jardin I, Ikura M, Romanin C (2014) A Coiled-coil Clamp Controls Both Conformation and Clustering of Stromal Interaction Molecule 1 (STIM1). Journal of Biological Chemistry 289:33231–33244.

Fambrough D, Goodman CS (1996) The Drosophila beaten path gene encodes a novel secreted protein that regulates defasciculation at motor axon choice points. Cell 87:1049–1058.

Feldner J, Becker T, Goishi K, Schweitzer J, Lee P, Schachner M, Klagsbrun M, Becker CG (2005) Neuropilin-1a is involved in trunk motor axon outgrowth in embryonic zebrafish Chien C-B, Vetter ML, eds. Dev Dyn 234:535–549.

Feldner J, Reimer MM, Schweitzer J, Wendik B, Meyer D, Becker T, Becker CG (2007) PlexinA3 restricts spinal exit points and branching of trunk motor nerves in embryonic zebrafish. J Neurosci 27:4978–4983.

Feller MB (1999) Spontaneous correlated activity in developing neural circuits. Neuron 22:653–656.

Fernandes N, Allbritton NL (2009) Effect of the DEF motif on phosphorylation of peptide substrates by ERK. Biochemical and Biophysical Research Communications 387:414–418.

Feske S, Gwack Y, Prakriya M, Srikanth S, Puppel S-H, Tanasa B, Hogan PG, Lewis RS, Daly M, Rao A (2006) A mutation in Orai1 causes immune deficiency by abrogating CRAC channel function. Nature 441:179–185.

Feske S, Prakriya M, Rao A, Lewis RS (2005) A severe defect in CRAC Ca2+ channel activation and altered K+ channel gating in T cells from immunodeficient patients. J Exp Med 202:651–662.

Fetcho JR, Higashijima S-I, McLean DL (2008) Zebrafish and motor control over the last decade. Brain Res Rev 57:86–93.

Fields RDR, Guthrie PBP, Russell JTJ, Kater SBS, Malhotra BSB, Nelson PGP (1993) Accommodation of mouse DRG growth cones to electrically induced collapse: kinetic analysis of calcium transients and set-point theory. J Neurobiol 24:1080–1098.

Fink CC, Bayer K-U, Myers JW, Ferrell JE Jr., Schulman H, Meyer T (2003) Selective Regulation of Neurite Extension and Synapse Formation by the β but not the α Isoform of CaMKII. Neuron 39:283–297.

Flanagan-Steet H (2005) Neuromuscular synapses can form in vivo by incorporation of

initially aneural postsynaptic specializations. Development 132:4471–4481.

Forbes EM, Thompson AW, Yuan J, Goodhill GJ (2012) Calcium and cAMP Levels Interact to Determine Attraction versus Repulsion in Axon Guidance. Neuron 74:490–503.

Forscher PP, Kaczmarek LK, Buchanan J, Smith SJ (1987) Cyclic AMP induces changes in distribution and transport of organelles within growth cones of Aplysia bag cell neurons. Journal of Neuroscience 7:3600–3611.

Forscher PP, Smith SJS (1988) Actions of cytochalasins on the organization of actin filaments and microtubules in a neuronal growth cone. J Cell Biol 107:1505–1516.

Fox AP, Nowycky MC, Tsien RW (1987) Single-channel recordings of three types of calcium channels in chick sensory neurones. J Physiol.

Frischauf I, Muik M, Derler I, Bergsmann J, Fahrner M, Schindl R, Groschner K, Romanin C (2009) Molecular determinants of the coupling between STIM1 and Orai channels: differential activation of Orai1-3 channels by a STIM1 coiled-coil mutant. Journal of Biological Chemistry 284:21696–21706.

Fromer M et al. (2014) De novo mutations in schizophrenia implicate synaptic networks. Nature 506:179–184.

Gallarda BW, Bonanomi D, Müller D, Brown A, Alaynick WA, Andrews SE, Lemke G, Pfaff SL, Marquardt T (2008) Segregation of axial motor and sensory pathways via heterotypic trans-axonal signaling. Science 320:233–236.

Gallo G, Lefcort FB, Letourneau PC (1997) The trkA receptor mediates growth cone turning toward a localized source of nerve growth factor. Journal of Neuroscience 17:5445–5454.

Garaschuk O, Linn J, Eilers J, Konnerth A (2000) Large-scale oscillatory calcium waves in the immature cortex. Nat Neurosci 3:452–459.

Garaschuk O, Yaari Y, Konnerth A (1997) Release and sequestration of calcium by ryanodine-sensitive stores in rat hippocampal neurones. J Physiol 502 (Pt 1):13–30.

Garcia-Alvarez G, Shetty MS, Lu B, Yap KAF, Oh-Hora M, Sajikumar S, Bichler Z, Fivaz M (2015) Impaired spatial memory and enhanced long-term potentiation in mice with forebrain-specific ablation of the Stim genes. Front Behav Neurosci 9.

Gasperini R, Choi-Lundberg D, Thompson MJ, Mitchell CB, Foa L (2009) Homer regulates calcium signalling in growth cone turning. Neural Dev 4:29.

Gemes G, Bangaru MLY, Wu HE, Tang Q, Weihrauch D, Koopmeiners AS, Cruikshank JM, Kwok WM, Hogan QH (2011) Store-Operated Ca2+ Entry in Sensory Neurons: Functional Role and the Effect of Painful Nerve Injury. Journal of Neuroscience 31:3536–3549.

Goh EL, Young J, Kuwako K, Tessier-Lavigne M, He Z, Griffin JW, Ming G-L (2008) beta1-integrin mediates myelin-associated glycoprotein signaling in neuronal

growth cones. Molecular Brain 1:10.

Goldberg DJ, Grabham PW (1999) Braking news: calcium in the growth cone. Neuron 22:423–425.

Gomez TM, Letourneau PC (1994) Filopodia initiate choices made by sensory neuron growth cones at laminin/fibronectin borders in vitro. Journal of Neuroscience 14:5959–5972.

Gomez TM, Snow DM, Letourneau PC (1995) Characterization of spontaneous calcium transients in nerve growth cones and their effect on growth cone migration. Neuron 14:1233–1246.

Gomez TM, Zheng JQ (2006) The molecular basis for calcium-dependent axon pathfinding. Nat Rev Neurosci 7:115–125.

Gomez TMT, Robles EE, Poo MM, Spitzer NCN (2001) Filopodial calcium transients promote substrate-dependent growth cone turning. Science 291:1983–1987.

Gomez TMT, Spitzer NCN (1999) In vivo regulation of axon extension and pathfinding by growth-cone calcium transients. Nature 397:350–355.

Gomez TMT, Spitzer NCN (2000) Regulation of growth cone behavior by calcium: new dynamics to earlier perspectives. J Neurobiol 44:174–183.

Goodhill GJ (2016) Can Molecular Gradients Wirethe Brain? Trends in Neurosciences:1–10.

Goodhill GJ, Faville RA, Sutherland DJ, Bicknell BA, Thompson AW, Pujic Z, Sun B, Kita EM, Scott EK (2015) The dynamics of growth cone morphology. BMC Biol 13:10.

Gordon-Weeks PR (1987) The cytoskeletons of isolated, neuronal growth cones. Neuroscience 21:977–989.

Goswami C (2010) Structural and functional regulation of growth cone, filopodia and synaptic sites by TRPV1. Commun Integr Biol 3:614–618.

Goswami C, Schmidt H, Hucho F (2007) TRPV1 at nerve endings regulates growth cone morphology and movement through cytoskeleton reorganization. FEBS Journal 274:760–772.

Goto S, Yamamoto H, Fukunaga K, Iwasa T, Matsukado Y, Miyamoto E (1985) Dephosphorylation of Microtubule-Associated Protein 2, τ Factor, and Tubulin by Calcineurin. Journal of Neurochemistry 45:276–283.

Grabarek Z (2006) Structural Basis for Diversity of the EF-hand Calcium-binding Proteins. Journal of Molecular Biology 359:509–525.

Graham SJL, Dziadek MA, Johnstone LS (2011) A Cytosolic STIM2 Preprotein Created by Signal Peptide Inefficiency Activates ORAI1 in a Store-independent Manner. Journal of Biological Chemistry 286:16174–16185.

Greka AA, Navarro BB, Oancea EE, Duggan AA, Clapham DED (2003) TRPC5 is a regulator of hippocampal neurite length and growth cone morphology. Nat Neurosci 6:837–845.

Grigoriev I, Gouveia SM, van der Vaart B, Demmers J, Smyth JT, Honnappa S, Splinter D, Steinmetz MO, Putney JW Jr., Hoogenraad CC, Akhmanova A (2008) STIM1 Is a MT-Plus-End-Tracking Protein Involved in Remodeling of the ER. 18:177–182.

Gross SA, Wissenbach U, Philipp SE, Freichel M, Cavalié A, Flockerzi V (2007) Murine ORAI2 splice variants form functional Ca2+ release-activated Ca2+ (CRAC) channels. J Biol Chem 282:19375–19384.

Grosse J, Braun A, Varga-Szabo D, Beyersdorf N, Schneider B, Zeitlmann L, Hanke P, Schropp P, Mühlstedt S, Zorn C, Huber M, Schmittwolf C, Jagla W, Yu P, Kerkau T, Schulze H, Nehls M, Nieswandt B (2007) An EF hand mutation in Stim1 causes premature platelet activation and bleeding in mice. J Clin Invest 117:3540–3550.

Groth RD, Mermelstein PG (2003) Brain-derived neurotrophic factor activation of NFAT (nuclear factor of activated T-cells)-dependent transcription: A role for the transcription factor NFATc4 in neurotrophin-mediated gene expression. Journal of Neuroscience 23:8125–8134.

Gruszczynska-Biegala J, Kuznicki J (2013) Native STIM2 and ORAI1 proteins form a calcium-sensitive and thapsigargin-insensitive complex in cortical neurons. Journal of Neurochemistry 126:727–738.

Gruszczynska-Biegala J, Pomorski P, Wisniewska MB, Kuznicki J (2011) Differential Roles for STIM1 and STIM2 in Store-Operated Calcium Entry in Rat Neurons Holowka D, ed. PLoS ONE 6:e19285.

Grynkiewicz G, POENIE M, TSIEN RY (1985) A new generation of Ca2+ indicators with greatly improved fluorescence properties. J Biol Chem 260:3440–3450.

Gu X (2001) Maximum-likelihood approach for gene family evolution under functional divergence. Mol Biol Evol 18:453–464.

Gu X, Olson EC, Spitzer NC (1994) Spontaneous neuronal calcium spikes and waves during early differentiation. Journal of Neuroscience 14:6325–6335.

Gu X, Spitzer NC (1995) Distinct aspects of neuronal differentiation encoded by frequency of spontaneous Ca2 transients. Nature 375:784–787.

Guan K-L, Rao Y (2003) Signalling mechanisms mediating neuronal responses to guidance cues. Nat Rev Neurosci 4:941–956.

Guillon E, Bretaud S, Ruggiero F (2016) Slow Muscle Precursors Lay Down a Collagen XV Matrix Fingerprint to Guide Motor Axon Navigation. Journal of Neuroscience 36:2663–2676.

Gundersen RW, Barrett JN (1980) Characterization of the turning response of dorsal root neurites toward nerve growth factor. J Cell Biol 87:546–554.

Gwack Y, Srikanth S, Feske S, Cruz-Guilloty F, Oh-Hora M, Neems DS, Hogan PG, Rao A (2007) Biochemical and functional characterization of Orai proteins. J Biol Chem 282:16232–16243.

Gwack Y, Srikanth S, Oh-hora M, Hogan PG, Lamperti ED, Yamashita M, Gelinas C, Neems DS, Sasaki Y, Feske S, Prakriya M, Rajewsky K, Rao A (2008) Hair Loss and Defective T- and B-Cell Function in Mice Lacking ORAI1. Molecular and Cellular Biology 28:5209–5222.

Gwozdz T, Dutko-Gwozdz J, Aziz N, Bolotina VM (2012a) Overexpression of Orai1 and STIM1 can Change Some Properties of Endogenous SOCE. Biophysj 102:315a.

Gwozdz T, Dutko-Gwozdz J, Schafer C, Bolotina VM (2012b) Overexpression of Orai1 and STIM1 Proteins Alters Regulation of Store-operated Ca 2+Entry by Endogenous Mediators. J Biol Chem 287:22865–22872.

Hajkova Z, Bugajev V, Draberova E, Vinopal S, Draberova L, Janacek J, Draber P, Draber P (2011) STIM1-Directed Reorganization of Microtubules in Activated Mast Cells. The Journal of Immunology 186:913–923.

Halloran MC, Kalil K (1994) Dynamic behaviors of growth cones extending in the corpus callosum of living cortical brain slices observed with video microscopy. Journal of Neuroscience 14:2161–2177.

Halloran MC, Sato-Maeda M, Warren JT, Su F, Lele Z, Krone PH, Kuwada JY, Shoji W (2000) Laser-induced gene expression in specific cells of transgenic zebrafish. Development 127:1953–1960.

Hanson MG, Landmesser LT (2003) Characterization of the circuits that generate spontaneous episodes of activity in the early embryonic mouse spinal cord. J Neurosci 23:587–600.

Hanson MG, Landmesser LT (2004) Normal patterns of spontaneous activity are required for correct motor axon guidance and the expression of specific guidance molecules. Neuron.

Hanson MG, Landmesser LT (2006) Increasing the Frequency of Spontaneous Rhythmic Activity Disrupts Pool-Specific Axon Fasciculation and Pathfinding of Embryonic Spinal Motoneurons. J Neurosci 26:12769–12780.

Hanson MG, Milner LD, Landmesser LT (2008) Spontaneous rhythmic activity in early chick spinal cord influences distinct motor axon pathfinding decisions. Brain Res Rev 57:77–85.

Hao B, Lu Y, Wang Q, Guo W, Cheung K-H, Yue J (2014) Role of STIM1 in survival and neural differentiation of mouse embryonic stem cells independent of Orai1-mediated Ca. Stem Cell Research 12:452–466.

Hao B, Webb SE, Miller AL, Yue J (2016) The role of Ca(2+) signaling on the self-renewal and neural differentiation of embryonic stem cells (ESCs). Cell Calcium 59:67–74.

Hartmann J, Dragicevic E, Adelsberger H, Henning HA, Sumser M, Abramowitz J, Blum R, Dietrich A, Freichel M, Flockerzi V, Birnbaumer L, Konnerth A (2008) TRPC3 Channels Are Required for Synaptic Transmission and Motor Coordination. Neuron 59:392–398.

Hartmann J, Karl RM, Alexander RPD, Adelsberger H, Brill MS, Rühlmann C, Ansel A, Sakimura K, Baba Y, Kurosaki T, Misgeld T, Konnerth A (2014) STIM1 Controls Neuronal Ca. Neuron 82:635–644.

Heap LA, Goh CC, Kassahn KS, Scott EK (2013) Cerebellar output in zebrafish: an analysis of spatial patterns and topography in eurydendroid cell projections. Front Neural Circuits 7:–53.

Hedgecock EM, Culotti JG, Hall DH (1990) The unc-5, unc-6, and unc-40 genes guide circumferential migrations of pioneer axons and mesodermal cells on the epidermis in C. elegans. Neuron 4:61–85.

Henke N, Albrecht P, Bouchachia I, Ryazantseva M, Knoll K, Lewerenz J, Kaznacheyeva E, Maher P, Methner A (2013) The plasma membrane channel ORAI1 mediates detrimental calcium influx caused by endogenous oxidative stress. 4:e470–e479.

Henke N, Albrecht P, Pfeiffer A, Toutzaris D, Zanger K, Methner A (2012) Stromal Interaction Molecule 1 (STIM1) Is Involved in the Regulation of Mitochondrial Shape and Bioenergetics and Plays a Role in Oxidative Stress. J Biol Chem 287:42042–42052.

Henle SJ, Wang G, Liang E, Wu M, Poo MM, Henley JR (2011) Asymmetric PI(3,4,5)P3 and Akt Signaling Mediates Chemotaxis of Axonal Growth Cones. J Neurosci 31:7016–7027.

Henley J, Poo M-M (2004) Guiding neuronal growth cones using Ca2+ signals. Trends in Cell Biology 14:320–330.

Henley JR, Huang K-H, Wang D, Poo M-M (2004) Calcium Mediates Bidirectional Growth Cone Turning Induced by Myelin-Associated Glycoprotein. Neuron 44:909–916.

Hernandez-Fleming M, Rohrbach EW, Bashaw GJ (2017) Sema-1a Reverse Signaling Promotes Midline Crossing in Response to Secreted Semaphorins. CellReports 18:174–184.

Hewavitharana T, Deng X, Wang Y, Ritchie MF, Girish GV, Soboloff J, Gill DL (2008) Location and Function of STIM1 in the Activation of Ca2+ Entry Signals. J Biol Chem 283:26252–26262.

Hidalgo A, Brand AH (1997) Targeted neuronal ablation: the role of pioneer neurons in guidance and fasciculation in the CNS of Drosophila. Development 124:3253–3262.

Hilario JD, Wang C, Beattie CE (2010) Collagen XIXa1 is crucial for motor axon navigation at intermediate targets. Development 137:4261–4269.

Hines JH, Abu-Rub M, Henley JR (2010) Asymmetric endocytosis and remodeling of β1-integrin adhesions during growth cone chemorepulsion by MAG. Nat Neurosci 13:829–837.

Hirota J, Michikawa T, Natsume T, Furuichi T, Mikoshiba K (1999) Calmodulin inhibits inositol 1,4,5-trisphosphate-induced calcium release through the purified and reconstituted inositol 1,4,5-trisphosphate receptor type 1. FEBS Lett 456:322–326.

Hogan PG (2015) The STIM1-ORAI1 microdomain. Cell Calcium 58:357–367.

Hogan PG, Rao A (2015) Biochemical and Biophysical Research Communications. Biochemical and Biophysical Research Communications 460:40–49.

Holland PW, Garcia-Fernandez J, Williams NA, Sidow A (1994) Gene duplications and the origins of vertebrate development. Dev Suppl:125–133.

Holliday J, Adams RJ, Sejnowski TJ, Spitzer NC (1991) Calcium-induced release of calcium regulates differentiation of cultured spinal neurons. Neuron 7:787–796.

Hong KK, Nishiyama MM, Henley JJ, Tessier-Lavigne MM, Poo MM (2000) Calcium signalling in the guidance of nerve growth by netrin-1. Nature 403:93–98.

Honnappa S, Gouveia SM, Weisbrich A, Damberger FF, Bhavesh NS, Jawhari H, Grigoriev I, van Rijssel FJA, Buey RM, Lawera A, Jelesarov I, Winkler FK, WUthrich K, Akhmanova A, Steinmetz MO (2009) An EB1-Binding Motif Acts as a Microtubule Tip Localization Signal. Cell 138:366–376.

Hooper R, Rothberg BS, Soboloff J (2014) Neuronal STIMulation at Rest. Science Signaling 7:pe18–pe18.

Hoth MM, Penner RR (1992) Depletion of intracellular calcium stores activates a calcium current in mast cells. Nature 355:353–356.

Hoth MM, Penner RR (1993) Calcium release-activated calcium current in rat mast cells. 465:359–386.

Hou P-F, Liu Z-H, Li N, Cheng W-J, Guo S-W (2014) Knockdown of STIM1 Improves Neuronal Survival After Traumatic Neuronal Injury Through Regulating mGluR1-Dependent Ca2+ Signaling in Mouse Cortical Neurons. Cell Mol Neurobiol.

Hou X, Pedi L, Diver MM, Long SB (2012) Crystal Structure of the Calcium Release-Activated Calcium Channel Orai. Science 338:1308–1313.

Höpker VH, Shewan D, Tessier-Lavigne M, Poo M, Holt C (1999) Growth-cone attraction to netrin-1 is converted to repulsion by laminin-1. Nature 401:69–73.

Huang GN, Zeng W, Kim JY, Yuan JP, Han L, Muallem S, Worley PF (2006) STIM1 carboxyl-terminus activates native SOC, Icrac and TRPC1 channels. Nat Cell Biol 8:1003–1010.

Hudmon A, Schulman H (2002) Neuronal Ca 2+/Calmodulin-Dependent Protein Kinase

II: The Role of Structure and Autoregulation in Cellular Function. Annu Rev Biochem 71:473–510.

Hutchins BI, Kalil K (2008) Differential outgrowth of axons and their branches is regulated by localized calcium transients. J Neurosci 28:143–153.

Hwang WY, Fu Y, Reyon D, Maeder ML, Tsai SQ, Sander JD, Peterson RT, Yeh J-RJ, Joung JK (2013) Efficient genome editing in zebrafish using a CRISPR-Cas system. Nature Biotechnology 31:227–229.

Hyland C, Mertz AF, Forscher P, Dufresne E (2014) Dynamic peripheral traction forces balance stable neurite tension in regenerating Aplysia bag cell neurons. Sci Rep 4:1–8.

Inayama M, Suzuki Y, Yamada S, Kurita T, Yamamura H, Ohya S, Giles WR, Imaizumi Y (2015) Orai1–Orai2 complex is involved in store-operated calcium entry in chondrocyte cell lines. Cell Calcium 57:337–347.

Jaconi M, Pyle J, Bortolon R, Ou J, Clapham D (1997) Calcium release and influx colocalize to the endoplasmic reticulum. Curr Biol 7:599–602.

Jang H, Levy S, Flavell SW, Mende F, Latham R, Zimmer M, Bargmann CI (2017) Dissection of neuronal gap junction circuits that regulate social behavior in Caenorhabditis elegans. Proc Natl Acad Sci U S A:201621274–10.

Jessell TM (2000) Neuronal specification in the spinal cord: inductive signals and transcriptional codes. Nat Rev Genet 1:20–29.

Jha A, Ahuja M, Maléth J, Moreno CM, Yuan JP, Kim MS, Muallem S (2013) The STIM1 CTID domain determines access of SARAF to SOAR to regulate Orai1 channel function. The Journal of Cell Biology 202:71–79.

Jiang K, Toedt G, Montenegro Gouveia S, Davey NE, Hua S, van der Vaart B, Grigoriev I, Larsen J, Pedersen LB, Bezstarosti K, Lince-Faria M, Demmers J, Steinmetz MO, Gibson TJ, Akhmanova A (2012) A Proteome-wide screen for mammalian SxIP motif-containing microtubule plus-end tracking proteins. Curr Biol 22:1800–1807.

Jin M, Guan C-B, Jiang Y-A, Chen G, Zhao C-T, Cui K, Song Y-Q, Wu C-P, Poo M-M, Yuan X-B (2005) Ca2+-dependent regulation of rho GTPases triggers turning of nerve growth cones. J Neurosci 25:2338–2347.

Jing L, Lefebvre JL, Gordon LR, Granato M (2009) Wnt Signals Organize Synaptic Prepattern and Axon Guidance through the Zebrafish unplugged/MuSK Receptor. Neuron 61:721–733.

Jontes JD, Buchanan J, Smith SJ (2000) Growth cone and dendrite dynamics in zebrafish embryos: early events in synaptogenesis imaged in vivo. Nat Neurosci 3:231–237.

Kachoei BA, Knox RJ, Uthuza D, Levy S, Kaczmarek LK, Magoski NS (2006) A Store-Operated Ca2+ Influx Pathway in the Bag Cell Neurons of Aplysia. Journal

of Neurophysiology 96:2688–2698.

Kaethner RJ, Stuermer CA (1992) Dynamics of terminal arbor formation and target approach of retinotectal axons in living zebrafish embryos: a time-lapse study of single axons. Journal of Neuroscience 12:3257–3271.

Kahn OI, Baas PW (2016) Microtubules and GrowthCones: Motors Drive the Turn. Trends in Neurosciences 39:433–440.

Kalil K, Szebenyi G, Dent EW (2000) Common mechanisms underlying growth cone guidance and axon branching. Developmental Neurobiology 44:145–158.

Kania A, Jessell TM (2003) Topographic Motor Projections in the Limb Imposed by LIM Homeodomain Protein Regulation of Ephrin-A:EphA Interactions. Neuron 38:581–596.

Kaplan A, Kent CB, Charron F, Fournier AE (2013) Switching Responses: Spatial and Temporal Regulators of Axon Guidance. Mol Neurobiol.

Kar P, Mirams GR, Christian HC, Parekh AB (2016) Control of NFAT Isoform Activation and NFAT-Dependent Gene Expression through Two Coincident and Spatially Segregated Intracellular Ca2+ Signals. Molecular Cell 64:746–759.

Kar P, Parekh AB (2015) Distinct spatial Ca2+ signatures selectively activate different NFAT transcription factor isoforms. Molecular Cell 58:232–243.

Karlstrom RO, Trowe T, Klostermann S, Baier H, Brand M, Crawford AD, Grunewald B, Haffter P, Hoffmann H, Meyer SU, Müller BK, Richter S, van Eeden FJ, Nüsslein-Volhard C, Bonhoeffer F (1996) Zebrafish mutations affecting retinotectal axon pathfinding. Development 123:427–438.

Kastanenka KV, Landmesser LT (2010) In Vivo Activation of Channelrhodopsin-2 Reveals That Normal Patterns of Spontaneous Activity Are Required for Motoneuron Guidance and Maintenance of Guidance Molecules. J Neurosci 30:10575–10585.

Kastanenka KV, Landmesser LT (2013) Optogenetic-mediated increases in in vivo spontaneous activity disrupt pool-specific but not dorsal-ventral motoneuron pathfinding. Proceedings of the National Academy of Sciences 110:17528–17533.

Kater SB, Mills LR (1991) Regulation of growth cone behavior by calcium. Journal of Neuroscience 11:891–899.

Kawasaki T, Lange I, Feske S (2009) A minimal regulatory domain in the C terminus of STIM1 binds to and activates ORAI1 CRAC channels. Biochemical and Biophysical Research Communications 385:49–54.

Kennedy TE, Serafini T, la Torre de J, Tessier-Lavigne M (1994) Netrins are diffusible chemotropic factors for commissural axons in the embryonic spinal cord. Cell 78:425–435.

Kerstein PC, Nichol RH IV, Gomez TM (2015) Mechanochemical regulation of growth

cone motility. Front Cell Neurosci 9:1–16.

Keshishian H, Bentley D (1983) Embryogenesis of peripheral nerve pathways in grasshopper legs. Developmental Neurobiology 96:116–124.

Ketschek A, Spillane M, Dun X-P, Hardy H, Chilton J, Gallo G (2016) Drebrin coordinates the actin and microtubule cytoskeleton during the initiation of axon collateral branches. Developmental Neurobiology 76:1092–1110.

Killeen MT, Sybingco SS (2008) Netrin, Slit and Wnt receptors allow axons to choose the axis of migration. Developmental Neurobiology 323:143–151.

Kim JY, Muallem S (2011) Unlocking SOAR releases STIM. The EMBO Journal 30:1673–1675.

Kim MJ, Liu I-H, Song Y, Lee JA, Halfter W, Balice-Gordon RJ, Linney E, Cole GJ (2006) Agrin is required for posterior development and motor axon outgrowth and branching in embryonic zebrafish. Glycobiology 17:231–247.

Kim N, Burden SJ (2007) MuSK controls where motor axons grow and form synapses. Nat Neurosci 11:19–27.

Kim SJ, Kim YS, Yuan JP, Petralia RS, Worley PF, Linden DJ (2003) Activation of the TRPC1 cation channel by metabotropic glutamate receptor mGluR1. Nature 426:285–291.

Kimmel CB, Ballard WW, Kimmel SR, Ullmann B, Schilling TF (1995) Stages of embryonic development of the zebrafish. Dev Dyn 203:253–310.

Kirkby LA, Sack GS, Firl A, Feller MB (2013) A Role for Correlated Spontaneous Activity in the Assembly of Neural Circuits. Neuron 80:1129–1144.

Kirschner M, Mitchson T (1986) Microtubule dynamics. Nature 324:621–621.

Kiselyov KK, Xu XX, Mozhayeva GG, Kuo TT, Pessah II, Mignery GG, Zhu XX, Birnbaumer LL, Muallem SS (1998) Functional interaction between InsP3 receptors and store-operated Htrp3 channels. Nature 396:478–482.

Klejman ME, Gruszczynska-Biegala J, Skibinska-Kijek A, Wisniewska MB, Misztal K, Blazejczyk M, Bojarski L, Kuznicki J (2009) Expression of STIM1 in brain and puncta-like co-localization of STIM1 and ORAI1 upon depletion of Ca2+ store in neurons. Neurochemistry International 54:49–55.

Koester MP, Müller O, Pollerberg GE (2007) Adenomatous Polyposis Coli Is Differentially Distributed in Growth Cones and Modulates Their Steering. J Neurosci 27:12590–12600.

Kok FO, Shin M, Ni C-W, Gupta A, Grosse AS, van Impel A, Kirchmaier BC, Peterson-Maduro J, Kourkoulis G, Male I, DeSantis DF, Sheppard-Tindell S, Ebarasi L, Betsholtz C, Schulte-Merker S, Wolfe SA, Lawson ND (2015) Reverse Genetic Screening Reveals Poor Correlation between Morpholino-Induced and Mutant Phenotypes in Zebrafish. Developmental Cell 32:97–108.

Kolodziej PA, Timpe LC, Mitchell KJ, Fried SR, Goodman CS, Jan LY, Jan YN (1996) frazzled encodes a Drosophila member of the DCC immunoglobulin subfamily and is required for CNS and motor axon guidance. Cell 87:197–204.

Komuro H, Kumada T (2005) Ca2+ transients control CNS neuronal migration. Cell Calcium 37:387–393.

Komuro H, Rakic P (1996) Intracellular Ca2+ fluctuations modulate the rate of neuronal migration. Neuron 17:275–285.

Korzeniowski MK, Manjarres IM, Varnai P, Balla T (2010) Activation of STIM1-Orai1 Involves an Intramolecular Switching Mechanism. Science Signaling 3:ra82–ra82.

Koyama M, Minale F, Shum J, Nishimura N, Schaffer CB, Fetcho JR (2016) A circuit motif in the zebrafish hindbrain for a two alternative behavioral choice to turn left or right. Elife 5:451.

Kraft R (2015) STIM and ORAI proteins in the nervous system. Channels (Austin) 9:245–252.

Krause M, Gautreau A (2014) Steering cell migration: lamellipodium dynamics and the regulation of directional persistence. Nat Rev Mol Cell Biol 15:577–590.

Kuwada JY (1986) Cell Recognition by Neuronal Growth Cones in a Simple Vertebrate Embryo. Science 233:740–746.

Kwan KM, Fujimoto E, Grabher C, Mangum BD, Hardy ME, Campbell DS, Parant JM, Yost HJ, Kanki JP, Chien C-B (2007) The Tol2kit: a multisite gateway-based construction kit for Tol2 transposon transgenesis constructs. Dev Dyn 236:3088–3099.

Kyung T, Lee S, Kim JE, Cho T, Park H, Jeong Y-M, Kim D, Shin A, Kim S, Baek J, Kim J, Kim NY, Woo D, Chae S, Kim C-H, Shin H-S, Han Y-M, Kim D, Do Heo W (2015) Optogenetic control of endogenous Ca. Nature Biotechnology 33:1092–1096.

Lalonde J, Saia G, Gill G (2014) Store-Operated Calcium Entry Promotes the Degradation of the Transcription Factor Sp4 in Resting Neurons. Science Signaling 7:ra51–ra51.

Lance-Jones C, Landmesser L (1981) Pathway selection by chick lumbosacral motoneurons during normal development. Proc R Soc Lond, B, Biol Sci 214:1–18.

Lankford KLK, Letourneau PCP (1990) Roles of actin filaments and three second-messenger systems in short-term regulation of chick dorsal root ganglion neurite outgrowth. Cell Motil Cytoskeleton 20:7–29.

Lau PMP, Zucker RSR, Bentley DD (1999) Induction of filopodia by direct local elevation of intracellular calcium ion concentration. J Cell Biol 145:1265–1275.

Laude AJ, Simpson AWM (2009) Compartmentalized signalling: Ca2+ compartments, microdomains and the many facets of Ca2+ signalling. FEBS Journal 276:1800–

1816.

Lauderdale JD, Davis NM, Kuwada JY (1997) Axon tracts correlate with netrin-1a expression in the zebrafish embryo. Molecular and Cellular Neuroscience 9:293–313.

Lautermilch NJ, Spitzer NC (2000) Regulation of calcineurin by growth cone calcium waves controls neurite extension. J Neurosci 20:315–325.

Lawrence MC, Jivan A, Shao C, Duan L, Goad D, Zaganjor E, Osborne J, McGlynn K, Stippec S, Earnest S, Chen W, Cobb MH (2008) The roles of MAPKs in disease. Cell Res 18:436–442.

Lefkimmiatis K, Srikanthan M, Maiellaro I, Moyer MP, Curci S, Hofer AM (2009) Store-operated cyclic AMP signalling mediated by STIM1. Nat Cell Biol 11:433–442.

Lewis AK, Bridgman PC (1992) Nerve growth cone lamellipodia contain two populations of actin filaments that differ in organization and polarity. J Cell Biol 119:1219–1243.

Lewis DA, Levitt P (2002) Schizophrenia as a disorder of neurodevelopment. Annu Rev Neurosci 25:409–432.

Lewis KE, Eisen JS (2003) From cells to circuits: development of the zebrafish spinal cord. Progress in Neurobiology 69:419–449.

Li C, Bassell GJ, Sasaki Y (2009) Fragile X Mental Retardation Protein is Involved in Protein Synthesis-Dependent Collapse of Growth Cones Induced by Semaphorin-3A. Front Neural Circuits 3:11.

Li HS, Xu XZ, Montell C (1999) Activation of a TRPC3-dependent cation current through the neurotrophin BDNF. Neuron 24:261–273.

Li M, Chen C, Zhou Z, Xu S, Yu Z (2012) A TRPC1-mediated increase in store-operated Ca2+ entry is required for the proliferation of adult hippocampal neural progenitor cells. Cell Calcium 51:486–496.

Li Y, Jia Y-C, Cui K, Li N, Zheng Z-Y, Wang Y-Z, Yuan X-B (2005) Essential role of TRPC channels in the guidance of nerve growth cones by brain-derived neurotrophic factor. Nature 434:894–898.

Lieberam I, Agalliu D, Nagasawa T, Ericson J, Jessell TM (2005) A Cxcl12-Cxcr4 Chemokine Signaling Pathway Defines the Initial Trajectory of Mammalian Motor Axons. Neuron 47:667–679.

Lin CH, Forscher P (1995) Growth Cone Advance Is Inversely Proportional to Retrograde F-Actin Flow. Neuron 14:763–771.

Liou J, Kim ML, Heo WD, Jones JT, Myers JW, Ferrell JE, Meyer T (2005) STIM is a Ca2+ sensor essential for Ca2+-store-depletion-triggered Ca2+ influx. Curr Biol 15:1235–1241.

Liou JJ, Fivaz MM, Inoue TT, Meyer TT (2007) Live-cell imaging reveals sequential oligomerization and local plasma membrane targeting of stromal interaction molecule 1 after Ca2+ store depletion. Proc Natl Acad Sci U S A 104:9301–9306.

Lis A, Peinelt C, Beck A, Parvez S, Monteilh-Zoller M, Fleig A, Penner R (2007) CRACM1, CRACM2, and CRACM3 Are Store-Operated Ca2+ Channels with Distinct Functional Properties. 17:794–800.

Lohof AMA, Quillan MM, Dan YY, Poo MMM (1992) Asymmetric modulation of cytosolic cAMP activity induces growth cone turning. Journal of Neuroscience 12:1253–1261.

Lu B, Fivaz M (2016) Neuronal SOCE: Myth or Reality? Trends in Cell Biology:1–3.

Luhmann HJ, Sinning A, Yang J-W, Reyes-Puerta V, Stüttgen MC, Kirischuk S, Kilb W (2016) Spontaneous Neuronal Activity in Developing Neocortical Networks: From Single Cells to Large-Scale Interactions. Front Neural Circuits 10:166.

Luik RM, Wang B, Prakriya M, Wu MM, Lewis RS (2008) Oligomerization of STIM1 couples ER calcium depletion to CRAC channel activation. Nature 454:538–542.

Luik RM, Wu MM, Buchanan J, Lewis RS (2006) The elementary unit of store-operated Ca2+ entry: local activation of CRAC channels by STIM1 at ER-plasma membrane junctions. J Cell Biol 174:815–825.

Majewski L, Kuznicki J (2015) Biochimica et Biophysica Acta. BBA - Molecular Cell Research 1853:1940–1952.

Malinow R, Schulman H, Tsien RW (1989) Inhibition of postsynaptic PKC or CaMKII blocks induction but not expression of LTP. Science 245:862–866.

Mallavarapu A, Mitchison T (1999) Regulated actin cytoskeleton assembly at filopodium tips controls their extension and retraction. J Cell Biol 146:1097–1106.

Manji SSM, Parker NJ, Williams RT, Van Stekelenburg L, Pearson RB, Dziadek M, Smith PJ (2000) STIM1: a novel phosphoprotein located at the cell surface. Biochimica et Biophysica Acta (BBA) - Protein Structure and Molecular Enzymology 1481:147–155.

Marsick BM, Flynn KC, Santiago-Medina M, Bamburg JR, Letourneau PC (2010) Activation of ADF/cofilin mediates attractive growth cone turning toward nerve growth factor and netrin-1. Developmental Neurobiology 70:565–588.

Mason C, Erskine L (2000) Growth cone form, behavior, and interactions in vivo: retinal axon pathfinding as a model. J Neurobiol 44:260–270.

Mattson MP, LaFerla FM, Chan SL, Leissring MA, Shepel PN, Geiger JD (2000) Calcium signaling in the ER: its role in neuronal plasticity and neurodegenerative disorders. Trends in Neurosciences 23:222–229.

McKay RR, Szymeczek-Seay CL, Lievremont JP, Bird GS, Zitt C, Jüngling E, Lückhoff A, Putney JW (2000) Cloning and expression of the human transient

receptor potential 4 (TRP4) gene: localization and functional expression of human TRP4 and TRP3. Biochem J 351 Pt 3:735–746.

McVicker DP, Millette MM, Dent EW (2014) Signaling to the microtubule cytoskeleton: An unconventional role for CaMKII Kamiguchi H, Borodinsky LN, eds. Developmental Neurobiology 75:423–434.

Medeiros NA, Burnette DT, Forscher P (2006) Myosin II functions in actin-bundle turnover in neuronal growth cones. Nat Cell Biol 8:216–226.

Melancon E, Liu DW, Westerfield M, Eisen JS (1997) Pathfinding by identified zebrafish motoneurons in the absence of muscle pioneers. Journal of Neuroscience 17:7796–7804.

Mercer JC (2006) Large Store-operated Calcium Selective Currents Due to Co-expression of Orai1 or Orai2 with the Intracellular Calcium Sensor, Stim1. Journal of Biological Chemistry 281:24979–24990.

Meyer T, Stryer L (1991) Calcium Spiking. Annual Review of Biophysics and Biophysical Chemistry 20:153–174.

Michaelis M, Nieswandt B, Stegner D, Eilers J, Kraft R (2014) STIM1, STIM2, and Orai1 regulate store-operated calcium entry and purinergic activation of microglia. Glia 63:652–663.

Miederer A-M, Alansary D, Schwär G, Lee P-H, Jung M, Helms V, Niemeyer BA (2015) A STIM2 splice variant negatively regulates store-operated calcium entry. Nature Communications 6:6899.

Milner LD, Landmesser LT (1999) Cholinergic and GABAergic inputs drive patterned spontaneous motoneuron activity before target contact. Journal of Neuroscience 19:3007–3022.

Ming GI, Song HJ, Berninger B, Inagaki N, Tessier-Lavigne M, Poo MM (1999) Phospholipase C-gamma and phosphoinositide 3-kinase mediate cytoplasmic signaling in nerve growth cone guidance. Neuron 23:139–148.

Ming GL, Song HJ, Berninger B, Holt CE, Tessier-Lavigne M, Poo MM (1997) CAMP-dependent growth cone guidance by netrin-1. Neuron 19:1225–1235.

Mitchell CB, Gasperini RJ, Small DH, Foa L (2012) STIM1 is necessary for store-operated calcium entry in turning growth cones. Journal of Neurochemistry 122:1155–1166.

Mitchell KJ, Doyle JL, Serafini T, Kennedy TE, Tessier-Lavigne M, Goodman CS, Dickson BJ (1996) Genetic analysis of Netrin genes in Drosophila: Netrins guide CNS commissural axons and peripheral motor axons. Neuron 17:203–215.

Miyazaki K, Ross WN (2013) Ca2+ Sparks and Puffs Are Generated and Interact in Rat Hippocampal CA1 Pyramidal Neuron Dendrites. J Neurosci 33:17777–17788.

Moccia F, Zuccolo E, Soda T, Tanzi F, Guerra G, Mapelli L, Lodola F, D'Angelo E

(2015) Stim and Orai proteins in neuronal Ca2+ signaling and excitability. Front Cell Neurosci 9.

Montoro RJ, Yuste R (2004) Gap junctions in developing neocortex: a review. Brain Res Rev 47:216–226.

Moreno C, Sampieri A, Vivas O, Peña-Segura C, Vaca L (2012) STIM1 and Orai1 mediate thrombin-induced Ca2 influx in rat cortical astrocytes. Cell Calcium 52:457–467.

Mueller BK (1999) GROWTH CONE GUIDANCE: First Steps Towards a Deeper Understanding. Annu Rev Neurosci 22:351–388.

Muik M, Fahrner M, Derler I, Schindl R, Bergsmann J, Frischauf I, Groschner K, Romanin C (2009) A Cytosolic Homomerization and a Modulatory Domain within STIM1 C Terminus Determine Coupling to ORAI1 Channels. Journal of Biological Chemistry 284:8421–8426.

Muik M, Fahrner M, Schindl R, Stathopulos P, Frischauf I, Derler I, Plenk P, Lackner B, Groschner K, Ikura M, Romanin C (2011) STIM1 couples to ORAI1 via an intramolecular transition into an extended conformation. The EMBO Journal 30:1678–1689.

Muik M, Frischauf I, Derler I, Fahrner M, Bergsmann J, Eder P, Schindl R, Hesch C, Polzinger B, Fritsch R, Kahr H, Madl J, Gruber H, Groschner K, Romanin C (2008) Dynamic coupling of the putative coiled-coil domain of ORAI1 with STIM1 mediates ORAI1 channel activation. J Biol Chem 283:8014–8022.

Muto A, Ohkura M, Kotani T, Higashijima S-I, Nakai J, Kawakami K (2011) Genetic visualization with an improved GCaMP calcium indicator reveals spatiotemporal activation of the spinal motor neurons in zebrafish. Proceedings of the National Academy of Sciences 108:5425–5430.

Müller MS, Fox R, Schousboe A, Waagepetersen HS, Bak LK (2014) Astrocyte glycogenolysis is triggered by store-operated calcium entry and provides metabolic energy for cellular calcium homeostasis. Glia 62:526–534.

Myers PZ, Eisen JS, Westerfield M (1986) Development and axonal outgrowth of identified motoneurons in the zebrafish. Journal of Neuroscience 6:2278–2289.

Nagel G, Szellas T, Huhn W, Kateriya S, Adeishvili N, Berthold P, Ollig D, Hegemann P, Bamberg E (2003) Channelrhodopsin-2, a directly light-gated cation-selective membrane channel. Proc Natl Acad Sci U S A 100:13940–13945.

Nasevicius A, Ekker SC (2000) Effective targeted gene “knockdown” in zebrafish. Nat Genet 26:216–220.

National Health and Medical Research Council (Australia) (2013) Australian code for the care and use of animals for scienti c purposes. :1–96.

Ng AN, Krogh M, Toresson H (2011) Dendritic EGFP-STIM1 activation after type I metabotropic glutamate and muscarinic acetylcholine receptor stimulation in

hippocampal neuron. J Neurosci Res 89:1235–1244.

Niclou SP, Jia L, Raper JA (2000) Slit2 is a repellent for retinal ganglion cell axons. J Neurosci 20:4962–4974.

Nicol XX, Hong KPK, Spitzer NCN (2011) Spatial and temporal second messenger codes for growth cone turning. Proc Natl Acad Sci U S A 108:13776–13781.

Nilius B, Owsianik G (2011) The transient receptor potential family of ion channels. Genome Biol 12:218.

Nishiyama M, Hoshino A, Tsai L, Henley JR, Goshima Y, Tessier-Lavigne M, Poo M-M, Hong K (2003) Cyclic AMP/GMP-dependent modulation of Ca2+ channels sets the polarity of nerve growth-cone turning. Nature Publishing Group 423:990–995 Available at: http://eutils.ncbi.nlm.nih.gov/entrez/eutils/elink.fcgi?dbfrom=pubmed&id=12827203&retmode=ref&cmd=prlinks.

Noctor SC, Martínez-Cerdeño V, Ivic L, Kriegstein AR (2004) Cortical neurons arise in symmetric and asymmetric division zones and migrate through specific phases. Nat Neurosci 7:136–144.

O'Connor TP, Bentley D (1993) Accumulation of actin in subsets of pioneer growth cone filopodia in response to neural and epithelial guidance cues in situ. J Cell Biol 123:935–948.

O'Connor TP, Duerr JS, Bentley D (1990) Pioneer growth cone steering decisions mediated by single filopodial contacts in situ. Journal of Neuroscience 10:3935–3946.

Oakley RA, Tosney KW (1993) Contact-mediated mechanisms of motor axon segmentation. Journal of Neuroscience 13:3773–3792.

Oancea E, Meyer T (1996) Reversible desensitization of inositol trisphosphate-induced calcium release provides a mechanism for repetitive calcium spikes. J Biol Chem 271:17253–17260.

Oh-Hora MM, Yamashita MM, Hogan PGP, Sharma SS, Lamperti EE, Chung WW, Prakriya MM, Feske SS, Rao AA (2008) Dual functions for the endoplasmic reticulum calcium sensors STIM1 and STIM2 in T cell activation and tolerance. Nat Immunol 9:432–443.

Ohbayashi K, Fukura H, Inoue HK, Komiya Y, Igarashi M (1998) Stimulation of L-type Ca2+ channel in growth cones activates two independent signaling pathways. J Neurosci Res 51:682–696.

Ong HL, Ambudkar IS (2015) Molecular determinants of TRPC1 regulation within ER-PM junctions. Cell Calcium.

Ooashi N, Futatsugi A, Yoshihara F, Mikoshiba K, Kamiguchi H (2005) Cell adhesion molecules regulate Ca 2+-mediated steering of growth cones via cyclic AMP and ryanodine receptor type 3. The Journal of Cell Biology 170:1159–1167.

Ouyang K, Zheng H, Qin X, Zhang C, Yang D, Wang X, Wu C, Zhou Z, Cheng H (2005) Ca2+ sparks and secretion in dorsal root ganglion neurons. Proc Natl Acad Sci U S A 102:12259–12264.

Owens DF, Flint AC, Dammerman RS, Kriegstein AR (2000) Calcium dynamics of neocortical ventricular zone cells. Dev Neurosci 22:25–33.

Owens DF, Kriegstein AR (1998) Patterns of intracellular calcium fluctuation in precursor cells of the neocortical ventricular zone. The Journal of neuroscience.

Padayatti PS, Pattanaik P, Ma X, van den Akker F (2004) Structural insights into the regulation and the activation mechanism of mammalian guanylyl cyclases. Pharmacology & Therapeutics 104:83–99.

Palaisa KA, Granato M (2007) Analysis of zebrafish sidetracked mutants reveals a novel role for Plexin A3 in intraspinal motor axon guidance. Development 134:3251–3257.

Palty R, Isacoff EY (2015) Cooperative Binding of Stromal Interaction Molecule 1 (STIM1) to the N and C Termini of Calcium Release-Activated Calcium Modulator 1 (Orai1). Journal of Biological Chemistry:jbc.M115.685289.

Palty R, Raveh A, Kaminsky I, Meller R, Reuveny E (2012) SARAF Inactivates the Store Operated Calcium Entry Machinery to Prevent Excess Calcium Refilling. Cell 149:425–438.

Pani B, Singh BB (2009) Lipid rafts/caveolae as microdomains of calcium signaling. Cell Calcium 45:625–633.

Panzer JA, Gibbs SM, Dosch R, Wagner D, Mullins MC, Granato M, Balice-Gordon RJ (2005) Neuromuscular synaptogenesis in wild-type and mutant zebrafish. Developmental Neurobiology 285:340–357.

Park CY, Hoover PJ, Mullins FM, Bachhawat P, Covington ED, Raunser S, Walz T, Garcia KC, Dolmetsch RE, Lewis RS (2009) STIM1 Clusters and Activates CRAC Channels via Direct Binding of a Cytosolic Domain to Orai1. Cell 136:876–890.

Parker NJN, Begley CGC, Smith PJP, Fox RMR (1996) Molecular Cloning of a Novel Human Gene (D11S4896E) at Chromosomal Region 11p15.5. Genomics 37:4–4.

Parvez S, Beck A, Peinelt C, Soboloff J, Lis A, Monteilh-Zoller M, Gill DL, Fleig A, Penner R (2008) STIM2 protein mediates distinct store-dependent and store-independent modes of CRAC channel activation. FASEB J 22:752–761.

Pathak T, Agrawal T, Richhariya S, Sadaf S, Hasan G (2015) Store-Operated Calcium Entry through Orai Is Required for Transcriptional Maturation of the Flight Circuit in Drosophila. J Neurosci 35:13784–13799.

Pathak T, Trivedi D, Hasan G (2017) CRISPR-Cas Induced Mutants Identify a Requirement for dSTIM in Larval Dopaminergic Cells of Drosophila melanogaster. G3:g3.116.038539–g3.116.038542.

Peinelt C, Vig M, Koomoa DL, Beck A, Nadler MJS, Koblan-Huberson M, Lis A, Fleig A, Penner R, Kinet J-P (2006) Amplification of CRAC current by STIM1 and CRACM1 (Orai1). Nat Cell Biol 8:771–773.

Peng Y, Clark KJ, Campbell JM, Panetta MR, Guo Y, Ekker SC (2014) Making designer mutants in model organisms. Development 141:4042–4054.

Pham E, Mills E, Truong K (2011) A Synthetic Photoactivated Proteinto Generate Local or Global Ca. Chemistry & Biology 18:880–890.

Pike SH, Melancon EF, Eisen JS (1992) Pathfinding by zebrafish motoneurons in the absence of normal pioneer axons. Development 114:825–831.

Plazas PV, Nicol X, Spitzer NC (2013) Activity-dependent competition regulates motor neuron axon pathfinding via PlexinA3. Proc Natl Acad Sci U S A 110:1524–1529.

Poliak S, Morales D, Croteau L-P, Krawchuk D, Palmesino E, Morton S, Cloutier J-F, Charron F, Dalva MB, Ackerman SL, Kao T-J, Kania A (2014) Synergistic integration of Netrin and ephrin axon guidance signals by spinal motor neurons. Elife 4:–.

Portugues R, Severi KE, Wyart C, Ahrens MB (2013) Optogenetics in a transparent animal: circuit function in the larval zebrafish. Current Opinion in Neurobiology 23:119–126.

Postlethwait JH et al. (1998) Vertebrate genome evolution and the zebrafish gene map. Nat Genet 18:345–349.

Powell EME, Campbell DBD, Stanwood GDG, Davis CC, Noebels JLJ, Levitt PP (2003) Genetic disruption of cortical interneuron development causes region- and GABA cell type-specific deficits, epilepsy, and behavioral dysfunction. Journal of Neuroscience 23:622–631.

Pozo-Guisado E, Campbell DG, Deak M, Alvarez-Barrientos A, Morrice NA, Alvarez IS, Alessi DR, Martin-Romero FJ (2010) Phosphorylation of STIM1 at ERK1/2 target sites modulates store-operated calcium entry. Journal of Cell Science 123:3084–3093.

Pozo-Guisado E, Casas-Rua V, Tomas-Martin P, Lopez-Guerrero AM, Alvarez-Barrientos A, Martin-Romero FJ (2013) Phosphorylation of STIM1 at ERK1/2 target sites regulates interaction with the microtubule plus-end binding protein EB1. Journal of Cell Science 126:3170–3180.

Prakriya M, Feske S, Gwack Y, Srikanth S, Rao A, Hogan PG (2006) Orai1 is an essential pore subunit of the CRAC channel. Nature 443:230–233.

Putney JW Jr. (1986) A model for receptor-regulated calcium entry. Cell Calcium 7:1–12.

Putney JW Jr. (2003) Capacitative calcium entry in the nervous system. Cell Calcium 34:339–344.

Putney JW Jr. (2007) Recent breakthroughs in the molecular mechanism of capacitative calcium entry (with thoughts on how we got here). Cell Calcium 42:103–110.

Putney JW, Broad LM, Braun FJ, Lievremont JP, Bird G (2001) Mechanisms of capacitative calcium entry. Journal of Cell Science 114:2223–2229.

Qian X, Shen Q, Goderie SK, He W, Capela A, Davis AA, Temple S (2000) Timing of CNS cell generation: a programmed sequence of neuron and glial cell production from isolated murine cortical stem cells. Neuron 28:69–80.

Rakic P (1988) Specification of cerebral cortical areas. Science 241:170–176.

Rakic P, Ayoub AE, Breunig JJ, Dominguez MH (2009) Decision by division: making cortical maps. Trends in Neurosciences 32:291–301.

Ramsey IS, Delling M, Clapham DE (2006) An introduction to TRP channels. Annu Rev Physiol 68:619–647.

Rana A, Yen M, Sadaghiani AM, Malmersjo S, Park CY, Dolmetsch RE, Lewis RS (2015) Alternative splicing converts STIM2 from an activator to an inhibitor of store-operated calcium channels. The Journal of Cell Biology 209:653–670.

Rao W, Zhang L, Peng C, Hui H, Wang K, Su N, Wang L, Dai S-H, Yang Y-F, Chen T, Luo P, Fei Z (2015) Biochimica et Biophysica Acta. BBA - Molecular Basis of Disease 1852:2402–2413.

Raper JA, Bastiani MJ, Goodman CS (1984) Pathfinding by Neuronal Growth Cones in Grasshopper Embryos .4. the Effects of Ablating the a-Axon and P-Axon Upon the Behavior of the G-Growth Cone. Journal of Neuroscience 4:2329–2345.

Ren Y, Suter DM (2016) Research Article. Neural Plasticity:1–13.

Rizzuto R, Pozzan T (2006) Microdomains of intracellular Ca2+: molecular determinants and functional consequences. Physiol Rev 86:369–408.

Robles E, Huttenlocher A, Gomez TM (2003) Filopodial calcium transients regulate growth cone motility and guidance through local activation of calpain. Neuron 38:597–609.

Robu ME, Larson JD, Nasevicius A, Beiraghi S, Brenner C, Farber SA, Ekker SC (2007) p53 activation by knockdown technologies. PLoS Genet 3:e78.

Rodino-Klapac LR, Beattie CE (2004) Zebrafish topped is required for ventral motor axon guidance. Developmental Neurobiology 273:308–320.

Roos J, DiGregorio PJ, Yeromin AV, Ohlsen K, Lioudyno M, Zhang S, Safrina O, Kozak JA, Wagner SL, Cahalan MD, Veliçelebi G, Stauderman KA (2005) STIM1, an essential and conserved component of store-operated Ca2+ channel function. J Cell Biol 169:435–445.

Roos M, Schachner M, Bernhardt RR (1999) Zebrafish semaphorin Z1b inhibits growing motor axons in vivo. Mech Dev 87:103–117.

Ros O, Cotrufo T, Martinez-Marmol R, Soriano E (2015) Regulation of Patterned Dynamics of Local Exocytosis in Growth Cones by Netrin-1. J Neurosci 35:5156–5170.

Rosenberg SS, Spitzer NC (2011) Calcium Signaling in Neuronal Development. Cold Spring Harbor Perspectives in Biology 3:a004259–a004259.

Ross WN (2012) Understanding calcium waves and sparks in central neurons. :1–12.

Sabbioni SS, Barbanti-Brodano GG, Croce CMC, Negrini MM (1997) GOK: a gene at 11p15 involved in rhabdomyosarcoma and rhabdoid tumor development. Cancer Res 57:4493–4497.

Sabry JH, O'Connor TP, Evans L, Toroian-Raymond A, Kirschner M, Bentley D (1991) Microtubule behavior during guidance of pioneer neuron growth cones in situ. J Cell Biol 115:381–395.

Sainath R, Granato M (2013) Plexin A3 and turnout regulate motor axonal branch morphogenesis in zebrafish. Giniger E, ed. PLoS ONE 8:e54071.

Saint-Amant L (2005) Development of motor networks in zebrafish embryos. Zebrafish 3:173–190.

Saint-Amant L, Drapeau P (1998) Time course of the development of motor behaviors in the zebrafish embryo. J Neurobiol 37:622–632.

Saint-Amant L, Drapeau P (2000) Motoneuron activity patterns related to the earliest behavior of the zebrafish embryo. Journal of Neuroscience 20:3964–3972.

Saint-Amant L, Drapeau P (2001) Synchronization of an embryonic network of identified spinal interneurons solely by electrical coupling. Neuron 31:1035–1046.

Sampieri A, Zepeda A, Asanov A, Vaca L (2009) Visualizing the store-operated channel complex assembly in real time: Identification of SERCA2 as a new member. Cell Calcium 45:439–446.

Samtleben S, Wachter B, Blum R (2015) Cell Calcium. Cell Calcium 58:147–159.

Sances S, Bruijn LI, Chandran S, Eggan K, Ho R, Klim JR, Livesey MR, Lowry E, Macklis JD, Rushton D, Sadegh C, Sareen D, Wichterle H, Zhang S-C, Svendsen CN (2016) Modeling ALS with motor neurons derived from human induced pluripotent stem cells. Nat Neurosci 16:542–553.

Sanes JR, Lichtman JW (2001) Induction, assembly, maturation and maintenance of a postsynaptic apparatus. Nat Rev Neurosci 2:791–805.

Satin LS, Adams PR (1987) Spontaneous miniature outward currents in cultured bullfrog neurons. Brain Res 401:331–339.

Sato-Maeda M, Tawarayama H, Obinata M, Kuwada JY, Shoji W (2006) Sema3a1 guides spinal motor axons in a cell- and stage-specific manner in zebrafish. Development 133:937–947.

Sauc S, Bulla M, Nunes P, Orci L, Marchetti A, Antigny F, Bernheim L, Cosson P, Frieden M, Demaurex N (2015) STIM1L traps and gates Orai1 channels without remodeling the cortical ER. Journal of Cell Science 128:1568–1579.

Sbacchi S, Acquadro F, Calo I, Cali F, Romano V (2010) Functional Annotation of Genes Overlapping Copy Number Variants in Autistic Patients: Focus on Axon Pathfinding. Audio, Transactions of the IRE Professional Group on 11:136–145.

Schaefer AW, Kabir N, Forscher P (2002) Filopodia and actin arcs guide the assembly and transport of two populations of microtubules with unique dynamic parameters in neuronal growth cones. J Cell Biol 158:139–152.

Schaefer AW, Schoonderwoert VTG, Ji L, Mederios N, Danuser G, Forscher P (2008) Coordination of Actin Filament and Microtubule Dynamics during Neurite Outgrowth. Developmental Cell 15:146–162.

Schindl R, Bergsmann J, Frischauf I, Derler I (2008) 2-aminoethoxydiphenyl borate alters selectivity of Orai3 channels by increasing their pore size. Journal of Biological ….

Schindl R, Frischauf I, Bergsmann J, Muik M, Derler I, Lackner B, Groschner K, Romanin C (2009) Plasticity in Ca^{2+} Selectivity of Orai1/Orai3 Heteromeric Channel. Proceedings of the National Academy of Sciences of the United States of America 106:19623–19628.

Schneider VA, Granato M (2003) Motor axon migration: a long way to go. Developmental Neurobiology 263:1–11.

Schneider VA, Granato M (2006) The Myotomal diwanka (lh3) Glycosyltransferase and Type XVIII Collagen Are Critical for Motor Growth Cone Migration. Neuron 50:683–695.

Schweitzer J, Becker T, Lefebvre J, Granato M, Schachner M, Becker CG (2005) Tenascin-C is involved in motor axon outgrowth in the trunk of developing zebrafish Chien C-B, Vetter ML, eds. Dev Dyn 234:550–566.

Scott EK, Mason L, Arrenberg AB, Ziv L, Gosse NJ, Xiao T, Chi NC, Asakawa K, Kawakami K, Baier H (2007) Targeting neural circuitry in zebrafish using GAL4 enhancer trapping. Nat Meth.

Serafini T, Colamarino SA, Leonardo ED, Wang H, Beddington R, Skarnes WC, Tessier-Lavigne M (1996) Netrin-1 is required for commissural axon guidance in the developing vertebrate nervous system. Cell 87:1001–1014.

Serafini T, Kennedy TE, Gaiko MJ, Mirzayan C, Jessell TM, Tessier-Lavigne M (1994) The netrins define a family of axon outgrowth-promoting proteins homologous to C. elegans UNC-6. Cell 78:409–424.

Seredick SD, Van Ryswyk L, Hutchinson SA, Eisen JS (2012) Zebrafish Mnx proteins specify one motoneuron subtype and suppress acquisition of interneuron characteristics. Neural Dev 7:1–1.

Sharma K, Leonard AE, Lettieri K, Pfaff SL (2000) Genetic and epigenetic mechanisms contribute to motor neuron pathfinding. Nature 406:515–519.

Shelly M, Lim BK, Cancedda L, Heilshorn SC, Gao H, Poo MM (2010) Local and Long-Range Reciprocal Regulation of cAMP and cGMP in Axon/Dendrite Formation. Science 327:547–552.

Shibasaki K, Murayama N, Ono K, Ishizaki Y, Tominaga M (2010) TRPV2 Enhances Axon Outgrowth through Its Activation by Membrane Stretch in Developing Sensory and Motor Neurons. J Neurosci 30:4601–4612.

Shibata T, Yamada K, Watanabe M, Ikenaka K, Wada K, Tanaka K, Inoue Y (1997) Glutamate transporter GLAST is expressed in the radial glia-astrocyte lineage of developing mouse spinal cord. Journal of Neuroscience 17:9212–9219.

Shim AH-R, Tirado-Lee L, Prakriya M (2014) ACCEPTED MANUSCRIPT. Journal of Molecular Biology:1–55.

Shim S, Goh EL, Ge S, Sailor K, Yuan JP, Roderick HL, Bootman MD, Worley PF, Song H, Ming G-L (2005) XTRPC1-dependent chemotropic guidance of neuronal growth cones. Nat Neurosci 8:730–735.

Shim S, Zheng JQ, Ming G-L (2013) A critical role for STIM1 in filopodial calcium entry and axon guidance. Molecular Brain 6:51.

Shirasaki R, Lewcock JW, Lettieri K, Pfaff SL (2006) FGF as a Target-Derived Chemoattractant for Developing Motor Axons Genetically Programmed by the LIM Code. Neuron 50:841–853.

Shoji W, Isogai S, Sato-Maeda M, Obinata M, Kuwada JY (2003) Semaphorin3a1 regulates angioblast migration and vascular development in zebrafish embryos. Development 130:3227–3236.

Shoji W, Yee CS, Kuwada JY (1998) Zebrafish semaphorin Z1a collapses specific growth cones and alters their pathway in vivo. Development 125:1275–1283.

Singh BB, Lockwich TP, Bandyopadhyay BC, Liu X (2004) VAMP2-dependent exocytosis regulates plasma membrane insertion of TRPC3 channels and contributes to agonist-stimulated Ca 2+ influx. Molecular Cell.

Skibinska-Kijek A, Wisniewska MB, Gruszczynska-Biegala J, Methner A, Kuznicki J (2009) Immunolocalization of STIM1 in the mouse brain. Acta Neurobiol Exp (Wars) 69:413–428.

Smyth JT, Beg AM, Wu S, Putney JW Jr., Rusan NM (2012) Phosphoregulation of STIM1 Leads to Exclusion of the Endoplasmic Reticulum from the Mitotic Spindle. 22:1487–1493.

Soboloff J, Spassova MA, Hewavitharana T, He L-P, Xu W, Johnstone LS, Dziadek MA, Gill DL (2006a) STIM2 Is an Inhibitor of STIM1-Mediated Store-Operated Ca2+ Entry. 16:1465–1470.

Soboloff J, Spassova MA, Tang XD, Hewavitharana T, Xu W, Gill DL (2006b) Orai1 and STIM reconstitute store-operated calcium channel function. J Biol Chem 281:20661–20665.

Sobue KK (1993) Actin-based cytoskeleton in growth cone activity. Neurosci Res 18:91–102.

Somasundaram A, Shum AK, McBride HJ, Kessler JA, Feske S, Miller RJ, Prakriya M (2014) Store-Operated CRAC Channels Regulate Gene Expression and Proliferation in Neural Progenitor Cells. J Neurosci 34:9107–9123.

Song H-J, Ming G-L, He Z, Lehmann M, McKerracher L, Tessier-Lavigne M, Poo M-M (1998) Conversion of Neuronal Growth Cone Responses from Repulsion to Attraction by Cyclic Nucleotides. Science 281:1515.

Song HJH, Ming GLG, Poo MMM (1997) cAMP-induced switching in turning direction of nerve growth cones. Nature 388:275–279.

Song HJH, Poo MMM (1999) Signal transduction underlying growth cone guidance by diffusible factors. Current Opinion in Neurobiology 9:9–9.

Soshnikova N, Dewaele R, Janvier P, Krumlauf R, Duboule D (2013) Developmental Biology. Developmental Neurobiology 378:194–199.

Soundararajan P, Fawcett JP, Rafuse VF (2010) Guidance of Postural Motoneurons Requires MAPK/ERK Signaling Downstream of Fibroblast Growth Factor Receptor 1. J Neurosci 30:6595–6606.

Spitzer NC (2004) Coincidence detection enhances appropriate wiring of the nervous system. Proc Natl Acad Sci U S A 101:5311–5312.

Spitzer NC (2006) Electrical activity in early neuronal development. Nature 444:707–712.

Spitzer NC, Gu X (1997) Purposeful patterns of spontaneous calcium transients in embryonic spinal neurons. Semin Cell Dev Biol 8:13–19.

Spitzer NC, Gu X, Olson E (1994) Action potentials, calcium transients and the control of differentiation of excitable cells. Current Opinion in Neurobiology 4:70–77.

Stathopulos PB, Zheng L, Li G-Y, Plevin MJ, Ikura M (2008) Structural and Mechanistic Insights into STIM1-Mediated Initiation of Store-Operated Calcium Entry. Cell 135:110–122.

Stathopulos PBP, Li G-YG, Plevin MJM, Ames JBJ, Ikura MM (2006) Stored Ca2+ depletion-induced oligomerization of stromal interaction molecule 1 (STIM1) via the EF-SAM region: An initiation mechanism for capacitive Ca2+ entry. Journal of Biological Chemistry 281:35855–35862.

Stein E, Tessier-Lavigne M (2001) Hierarchical Organization of Guidance Receptors: Silencing of Netrin Attraction by Slit Through a Robo/DCC Receptor Complex. Science 291:1928–1938.

Steinbeck JA, Henke N, Opatz J, Gruszczynska-Biegala J, Schneider L, Theiss S, Hamacher N, Steinfarz B, Golz S, Brüstle O, Kuznicki J, Methner A (2011) Store-operated calcium entry modulates neuronal network activity in a model of chronic epilepsy. Experimental Neurology 232:185–194.

Stepanova T, Slemmer J, Hoogenraad CC, Lansbergen G, Dortland B, De Zeeuw CI, Grosveld F, van Cappellen G, Akhmanova A, Galjart N (2003) Visualization of microtubule growth in cultured neurons via the use of EB3-GFP (end-binding protein 3-green fluorescent protein). J Neurosci 23:2655–2664.

Stiber J, Hawkins A, Zhang Z-S, Wang S, Burch J, Graham V, Ward CC, Seth M, Finch E, Malouf N, Williams RS, Eu JP, Rosenberg P (2008) STIM1 signalling controls store-operated calcium entry required for development and contractile function in skeletal muscle. Nat Cell Biol 10:688–697.

Stoeckli E, Zou Y (2009) How are neurons wired to form functional and plastic circuits? Meeting on Axon Guidance, Synaptogenesis & Neural Plasticity. EMBO Rep 10:326–330.

Strasser GA, Rahim NA, VanderWaal KE, Gertler FB, Lanier LM (2004) Arp2/3 Is a Negative Regulator of Growth Cone Translocation. Neuron 43:81–94.

Sun S, Zhang H, Liu J, Popugaeva E, Xu N-J, Feske S, White CL III, Bezprozvanny I (2014a) Reduced Synaptic STIM2 Expression and Impaired Store-Operated Calcium Entry Cause Destabilization of Mature Spines in Mutant Presenilin Mice. Neuron 82:79–93.

Sun Y, Chauhan A, Sukumaran P, Sharma J, Singh BB, Mishra BB (2014b) Inhibition of store-operated calcium entry in microglia by helminth factors: implications for immune suppression in neurocysticercosis. J Neuroinflammation 11:1120.

Suster ML, Abe G, Schouw A, Kawakami K (2011) Transposon-mediated BAC transgenesis in zebrafish. Nat Protoc 6:1998–2021.

Suter DM, Forscher P (2001) Transmission of growth cone traction force through apCAM–cytoskeletal linkages is regulated by Src family tyrosine kinase activity. The Journal of Cell Biology 155:427–438.

Sutherland DJ, Goodhill GJ (2013) The interdependent roles of Ca2+ and cAMP in axon guidance. Developmental Neurobiology.

Sutherland DJ, Pujic Z, Goodhill GJ (2014) Calcium signaling in axon guidance. Trends in Neurosciences 37:424–432.

Szebenyi G, Callaway JL, Dent EW, Kalil K (1998) Interstitial branches develop from active regions of the axon demarcated by the primary growth cone during pausing behaviors. Journal of Neuroscience 18:7930–7940.

Szebenyi G, Dent EW, Callaway JL, Seys C, Lueth H, Kalil K (2001) Fibroblast growth factor-2 promotes axon branching of cortical neurons by influencing morphology and behavior of the primary growth cone. Journal of Neuroscience 21:3932–3941.

Takahashi Y, Murakami M, Watanabe H, Hasegawa H, Ohba T, Munehisa Y, Nobori K, Ono K, Iijima T, Ito H (2007) Essential role of the N-terminus of murine Orai1 in store-operated Ca2+ entry. Biochemical and Biophysical Research Communications 356:45–52.

Takechi H, Eilers J, Konnerth A (1998) A new class of synaptic response involving calcium release in dendritic spines. Nature 396:757–760.

Takei K, Shin R-M, Inoue T, Kato K, Mikoshiba K (1998) Regulation of Nerve Growth Mediated by Inositol 1,4,5-Trisphosphate Receptors in Growth Cones. Science 282:1705–.

Tanabe Y, William C, Jessell TM (1998) Specification of motor neuron identity by the MNR2 homeodomain protein. Cell 95:67–80.

Tanaka E, Kirschner MW (1995) The role of microtubules in growth cone turning at substrate boundaries. J Cell Biol 128:127–137.

Tang F, Dent EW, Kalil K (2003) Spontaneous calcium transients in developing cortical neurons regulate axon outgrowth. J Neurosci 23:927–936.

Tang F, Kalil K (2005) Netrin-1 induces axon branching in developing cortical neurons by frequency-dependent calcium signaling pathways. J Neurosci 25:6702–6715.

Tedeschi A, Dupraz S, Laskowski CJ, Xue J, Ulas T, Beyer M, Schultze JL, Bradke F (2016) The Calcium Channel Subunit Alpha2delta2 Suppresses Axon Regeneration in the Adult CNS. Neuron 92:419–434.

Terasaki M, Slater NT, Fein A (1994) Continuous network of endoplasmic reticulum in cerebellar Purkinje neurons.

Tessier-Lavigne M, Goodman CS (1996) The molecular biology of axon guidance. Science 274:1123–1133.

Thiel M, Lis A, Penner R (2013) STIM2 drives Ca2+ oscillations through store-operated Ca2+ entry caused by mild store depletion. 591:1433–1445.

Tian G, Tepikin AV, Tengholm A, Gylfe E (2012) cAMP Induces Stromal Interaction Molecule 1 (STIM1) Puncta but neither Orai1 Protein Clustering nor Store-operated Ca2+ Entry (SOCE) in Islet Cells. Journal of Biological Chemistry 287:9862–9872.

Togashi K, Schimmelmann von MJ, Nishiyama M, Lim C-S, Yoshida N, Yun B, Molday RS, Goshima Y, Hong K (2008) Cyclic GMP-Gated CNG Channels Function in Sema3A-Induced Growth Cone Repulsion. Neuron 58:694–707.

Tojima T (2012) Intracellular signaling and membrane trafficking control bidirectional growth cone guidance. Neurosci Res 73:269–274.

Tojima T, Akiyama H, Itofusa R, Li Y, Katayama H, Miyawaki A, Kamiguchi H (2007) Attractive axon guidance involves asymmetric membrane transport and exocytosis in the growth cone. Nat Neurosci 10:58–66.

Tojima T, Hines JH, Henley JR, Kamiguchi H (2011) Second messengers and membrane trafficking direct and organize growth cone steering. Nat Rev Neurosci 12:191–203.

Tojima T, Itofusa R, Kamiguchi H (2009) The nitric oxide-cGMP pathway controls the directional polarity of growth cone guidance via modulating cytosolic Ca2+ signals. J Neurosci 29:7886–7897.

Tojima T, Itofusa R, Kamiguchi H (2010) Asymmetric Clathrin-Mediated Endocytosis Drives Repulsive Growth Cone Guidance. Neuron 66:370–377.

Tojima T, Itofusa R, Kamiguchi H (2014) Steering Neuronal Growth Cones by Shifting the Imbalance between Exocytosis and Endocytosis. J Neurosci 34:7165–7178.

Tomas-Martin P, Lopez-Guerrero AM, Casas-Rua V, Pozo-Guisado E, Martin-Romero FJ (2015) Cellular Signalling. Cellular Signalling 27:545–554.

Tomida T, Hirose K, Takizawa A, Shibasaki F, Iino M (2003) NFAT functions as a working memory of Ca2+ signals in decoding Ca2+ oscillation. The EMBO Journal 22:3825–3832.

Torborg CL, Hansen KA, Feller MB (2004) High frequency, synchronized bursting drives eye-specific segregation of retinogeniculate projections. Nat Neurosci 8:72–78.

Tosney KW, Landmesser LT (1985) Growth Cone Morphology and Trajectory in the Lumbosacral Region of the Chick-Embryo. Journal of Neuroscience 5:2345–2358.

Toth AB, Shum AK, Prakriya M (2016) Regulation of neurogenesis by calcium signaling. Cell Calcium 59:124–134.

Tovey SC, de Smet P, Lipp P, Thomas D, Young KW, Missiaen L, De Smedt H, Parys JB, Berridge MJ, Thuring J, Holmes A, Bootman MD (2001) Calcium puffs are generic InsP(3)-activated elementary calcium signals and are downregulated by prolonged hormonal stimulation to inhibit cellular calcium responses. Journal of Cell Science 114:3979–3989.

Tsai F-C, Seki A, Yang HW, Hayer A, Carrasco S, Malmersjö S, Meyer T (2014) A polarized Ca2+, diacylglycerol and STIM1 signalling system regulates directed cell migration. Nat Cell Biol 16:133–144.

Usachev YM, Thayer SA (1997) All-or-none Ca2+ release from intracellular stores triggered by Ca2+ influx through voltage-gated Ca2+ channels in rat sensory neurons. Journal of Neuroscience 17:7404–7414.

Usachev YM, Thayer SA (1999) Ca2+ influx in resting rat sensory neurones that regulates and is regulated by ryanodine-sensitive Ca2+ stores. J Physiol.

Van Vactor D (1998) Adhesion and signaling in axonal fasciculation. Current Opinion in Neurobiology.

Venkatachalam K, van Rossum DB, Patterson RL, Ma H-T, Gill DL (2002) The cellular

and molecular basis of store-operated calcium entry. Nat Cell Biol 4:E263–E272.

Venkiteswaran G, Hasan G (2009) Intracellular Ca2+ signaling and store-operated Ca2+ entry are required in Drosophila neurons for flight. Proc Natl Acad Sci U S A 106:10326–10331.

Verkhratsky A (2005) Physiology and Pathophysiology of the Calcium Store in the Endoplasmic Reticulum of Neurons. Physiol Rev 85:201–279.

Vig M, DeHaven WI, Bird GS, Billingsley JM, Wang H, Rao PE, Hutchings AB, Jouvin M-H, Putney JW, Kinet J-P (2008) Defective mast cell effector functions in mice lacking the CRACM1 pore subunit of store-operated calcium release-activated calcium channels. Nat Immunol 9:89–96.

Vig M, Peinelt C, Beck A, Koomoa DL, Rabah D, Koblan-Huberson M, Kraft S, Turner H, Fleig A, Penner R, Kinet JP (2006) CRACM1 is a plasma membrane protein essential for store-operated Ca2+ entry. Science 312:1220–1223.

Vigont V, Kolobkova Y, Skopin A, Zimina O, Zenin V, Glushankova L, Kaznacheyeva E (2015) Both Orai1 and TRPC1 are Involved in Excessive Store-Operated Calcium Entry in Striatal Neurons Expressing Mutant Huntingtin Exon 1. Front Physiol 6:377–379.

Vitriol EA, Zheng JQ (2012) Growth Cone Travel in Space and Time: the Cellular Ensemble of Cytoskeleton, Adhesion, and Membrane. Neuron 73:1068–1081.

Volkers M, Dolatabadi N, Gude N, Most P, Sussman MA, Hassel D (2012) Orai1 deficiency leads to heart failure and skeletal myopathy in zebrafish. Journal of Cell Science 125:287–294.

Wada F, Nakata A, Tatsu Y, Ooashi N, Fukuda T, Nabetani T, Kamiguchi H (2016) Myosin Va and Endoplasmic Reticulum Calcium Channel Complex Regulates Membrane Export during Axon Guidance. CellReports 15:1329–1344.

Walker AS, Goings GE, Kim Y, Miller RJ, Chenn A, Szele FG (2010) Nestin Reporter Transgene Labels Multiple Central Nervous System Precursor Cells. Neural Plasticity 2010:1–14.

Wang GXG, Poo M-MM (2005) Requirement of TRPC channels in netrin-1-induced chemotropic turning of nerve growth cones. Nature 434:898–904.

Wang J-Y, Sun J, Huang M-Y, Wang Y-S, Hou M-F, Sun Y, He H, Krishna N, Chiu S-J, Lin S, Yang S, Chang W-C (2014) STIM1 overexpression promotes colorectal cancer progression, cell motility and COX-2 expression. Oncogene 34:4358–4367.

Wang Y, Deng X, Hewavitharana T, Soboloff J, Gill DL (2008) STIM, Orai and TRPC channels in the control of calcium entry signals in smooth muscle. Clin Exp Pharmacol Physiol 35:1127–1133.

Warp E, Agarwal G, Wyart C, Friedmann D, Oldfield CS, Conner A, Del Bene F, Arrenberg AB, Baier H, Isacoff EY (2012) Emergence of Patterned Activity in the Developing Zebrafish Spinal Cord. 22:93–102.

Wei C, Wang X, Chen M, Ouyang K, Song L-S, Cheng H (2009) nature07577. Nature 457:901–905.

Weissman TA, Riquelme PA, Ivic L, Flint AC, Kriegstein AR (2004) Calcium waves propagate through radial glial cells and modulate proliferation in the developing neocortex. Neuron 43:647–661.

Welnhofer EA, Zhao L, Cohan CS (1999) Calcium influx alters actin bundle dynamics and retrograde flow in Helisoma growth cones. Journal of Neuroscience 19:7971–7982.

Wen Y, Eng CH, Schmoranzer J, Cabrera-Poch N, Morris EJS, Chen M, Wallar BJ, Alberts AS, Gundersen GG (2004a) EB1 and APC bind to mDia to stabilize microtubules downstream of Rho and promote cell migration. Nat Cell Biol 6:820–830.

Wen Z, Guirland C, Ming G-L, Zheng JQ (2004b) A CaMKII/Calcineurin Switch Controls the Direction of Ca^2^+-Dependent Growth Cone Guidance. Neuron 43:12–12.

Wen Z, Han L, Bamburg JR, Shim S, Ming G-L, Zheng JQ (2007) BMP gradients steer nerve growth cones by a balancing act of LIM kinase and Slingshot phosphatase on ADF/cofilin. The Journal of Cell Biology 178:107–119.

Westerfield M, Eisen JS (1987) Neuromuscular specificity: pathfinding by identified motor growth cones in a vertebrate embryo. Trends in Neurosciences 11:18–22.

Westerfield M, Liu DW, Kimmel CB, Walker C (1990) Pathfinding and synapse formation in a zebrafish mutant lacking functional acetylcholine receptors. Neuron 4:867–874.

Westerfield M, McMurray JV, Eisen JS (1986) Identified motoneurons and their innervation of axial muscles in the zebrafish. Journal of Neuroscience 6:2267–2277.

Williams RT, Manji S, Parker NJ, Hancock MS, Van Stekelenburg L, Eid JP, Senior PV, Kazenwadel JS, Shandala T, Saint R, Smith PJ, Dziadek MA (2001) Identification and characterization of the STIM (stromal interaction molecule) gene family: coding for a novel class of transmembrane proteins. Biochem J 357:673–685.

Williams RT, Senior PV, Van Stekelenburg L, Layton JE, Smith PJ, Dziadek MA (2002) Stromal interaction molecule 1 (STIM1), a transmembrane protein with growth suppressor activity, contains an extracellular SAM domain modified by N-linked glycosylation. Biochim Biophys Acta 1596:131–137.

Williamson T, Gordon-Weeks PR, Schachner M, Taylor J (1996) Microtubule reorganization is obligatory for growth cone turning. Proc Natl Acad Sci U S A 93:15221–15226.

Willoughby D, Everett KL, Halls ML, Pacheco J, Skroblin P, Vaca L, Klussmann E, Cooper DMF (2012) Direct binding between Orai1 and AC8 mediates dynamic interplay between Ca2+ and cAMP signaling. Science Signaling 5:ra29.

Winberg ML, Mitchell KJ, Goodman CS (1998) Genetic analysis of the mechanisms controlling target selection: complementary and combinatorial functions of netrins, semaphorins, and IgCAMs. Cell 93:581–591.

Wojda U, Salinska E, Kuznicki J (2008) Calcium ions in neuronal degeneration. IUBMB Life 60:575–590.

Wu HD, Xu M, Li RC, Guo L, Lai YS, Xu SM, Li SF, Lu QL, Li LL, Zhang HB, Zhang YY, Zhang CM, Wang SQ (2012) Ultrastructural remodelling of Ca2+ signalling apparatus in failing heart cells. Cardiovascular Research 95:430–438.

Wu MM, Covington ED, Lewis RS (2014) Single-molecule analysis of diffusion and trapping of STIM1 and Orai1 at ER-plasma membrane junctions. Mol Biol Cell.

Xia J, Pan R, Gao X, Meucci O, Hu H (2014) Native store-operated calcium channels are functionally expressed in mouse spinal cord dorsal horn neurons and regulate resting calcium homeostasis. J Physiol 592:3443–3461.

Xu P, Lu J, Li Z, Yu X, Chen L, Xu T (2006) Aggregation of STIM1 underneath the plasma membrane induces clustering of Orai1. Biochemical and Biophysical Research Communications 350:969–976.

Xu X, Fu AKY, Ip FCF, Wu C-P, Duan S, Poo M-M, Yuan X-B, Ip NY (2005) Agrin regulates growth cone turning of Xenopus spinal motoneurons. Development 132:4309–4316.

Yamada KMK, Spooner BSB, Wessells NKN (1971) Ultrastructure and function of growth cones and axons of cultured nerve cells. J Cell Biol 49:614–635.

Yamamoto H, Fukunaga K, Goto S, Tanaka E, Miyamoto E (1985) Ca2+, Calmodulin-Dependent Regulation of Microtubule Formation via Phosphorylation of Microtubule-Associated Protein 2, τ Factor, and Tubulin, and Comparison with the Cyclic AMP-Dependent Phosphorylation. Journal of Neurochemistry 44:759–768.

Yang I-H, Tsai Y-T, Chiu S-J, Liu L-T, Lee H-H, Hou M-F, Hsu W-L, Chen B-K, Chang W-C (2012) Involvement of STIM1 and Orai1 in EGF-mediated cell growth in retinal pigment epithelial cells. J Biomed Sci 20:41–41.

Yang Y-M, Fedchyshyn MJ, Grande G, Aitoubah J, Tsang CW, Xie H, Ackerley CA, Trimble WS, Wang L-Y (2010) Septins regulate developmental switching from microdomain to nanodomain coupling of Ca(2+) influx to neurotransmitter release at a central synapse. Neuron 67:100–115.

Yeromin AV, Zhang SL, Jiang W, Yu Y, Safrina O, Cahalan MD (2006) Molecular identification of the CRAC channel by altered ion selectivity in a mutant of Orai. Nature 443:226–229.

Yoo AS, Cheng I, Chung S, Grenfell TZ, Lee H, Pack-Chung E, Handler M, Shen J, Xia WM, Tesco G, Saunders AJ, Ding K, Frosch MP, Tanzi RE, Kim TW (2000) Presenilin-mediated modulation of capacitative calcium entry. Neuron 27:561–572.

Yu CR, Power J, Barnea G, O'Donnell S, Brown HEV, Osborne J, Axel R, Gogos JA

(2004) Spontaneous neural activity is required for the establishment and maintenance of the olfactory sensory map. Neuron 42:553–566.

Yuan JP, Zeng W, Dorwart MR, Choi Y-J, Worley PF, Muallem S (2009) SOAR and the polybasic STIM1 domains gate and regulate Orai channels. Nat Cell Biol 11:337–343.

Yuan JP, Zeng W, Huang GN, Worley PF, Muallem S (2007) STIM1 heteromultimerizes TRPC channels to determine their function as store-operated channels. Nat Cell Biol 9:636–645.

Zelenchuk TA, Brusés JL (2011) In Vivo labeling of zebrafish motor neurons using an mnx1 enhancer and Gal4/UAS Kulesa PM, Dickinson ME, Hadjantonakis A-K, eds. Genesis 49:546–554.

Zeller J, Granato M (1999) The zebrafish diwanka gene controls an early step of motor growth cone migration. Development 126:3461–3472.

Zeller J, Schneider V, Malayaman S, Higashijima S-I, Okamoto H, Gui J, Lin S, Granato M (2002) Migration of Zebrafish Spinal Motor Nerves into the Periphery Requires Multiple Myotome-Derived Cues. Developmental Neurobiology 252:241–256.

Zhang H, Wu L, Pchitskaya E, Zakharova O, Saito T, Saido T, Ford KJ (2015) Neuronal Store-Operated Calcium Entry and Mushroom Spine Loss in Amyloid Precursor Protein Knock-In Mouse Model of Alzheimer's Disease. J Neurosci 35:13275–13286.

Zhang J, Granato M (2000) The zebrafish unplugged gene controls motor axon pathway selection. Development 127:2099–2111.

Zhang J, Lefebvre JL, Zhao S, Granato M (2004) Zebrafish unplugged reveals a role for muscle-specific kinase homologs in axonal pathway choice. Nat Neurosci 7:1303–1309.

Zhang M, Song J-N, Wu Y, Zhao Y-L, Pang H-G, Fu Z-F, Zhang B-F, Ma X-D (2014) Suppression of STIM1 in the early stage after global ischemia attenuates the injury of delayed neuronal death by inhibiting store-operated calcium entry-induced apoptosis in rats. NeuroReport 25:507–513.

Zhang SL, Yu Y, Roos J, Kozak JA, Deerinck TJ, Ellisman MH, Stauderman KA, Cahalan MD (2005) STIM1 is a Ca2+ sensor that activates CRAC channels and migrates from the Ca2+ store to the plasma membrane. Nature 437:902–905.

Zhang X-F, Forscher P (2009) Rac1 Modulates Stimulus-evoked Ca2+ Release in Neuronal Growth Cones via Parallel Effects on Microtubule/Endoplasmic Reticulum Dynamics and Reactive Oxygen Species Production. Mol Biol Cell 20:3700–3712.

Zheng JQ (2000) Turning of nerve growth cones induced by localized increases in intracellular calcium ions. Nature 403:89–93.

Zheng JQ, Felder M, Connor JA, Poo MM (1994) Turning of nerve growth cones induced by neurotransmitters. Nature 368:140–144.

Zheng JQ, Poo M-M (2007) Calcium Signaling in Neuronal Motility. Annu Rev Cell Dev Biol 23:375–404.

Zheng JQ, Wan JJ, Poo MM (1996) Essential role of filopodia in chemotropic turning of nerve growth cone induced by a glutamate gradient. Journal of Neuroscience 16:1140–1149.

Zheng L, Stathopulos PB, Li G-Y, Ikura M (2008) Biophysical characterization of the EF-hand and SAM domain containing Ca2+ sensory region of STIM1 and STIM2. Biochemical and Biophysical Research Communications 369:240–246.

Zheng L, Stathopulos PB, Schindl R, Li G-Y, Romanin C, Ikura M (2011) Auto-inhibitory role of the EF-SAM domain of STIM proteins in store-operated calcium entry. Proc Natl Acad Sci U S A 108:1337–1342.

Zhou F-Q, Waterman-Storer CM, Cohan CS (2002) Focal loss of actin bundles causes microtubule redistribution and growth cone turning. J Cell Biol 157:839–849.

Zhou Y, Mancarella S, Wang Y, Yue C, Ritchie M, Gill DL, Soboloff J (2009) The short N-terminal domains of STIM1 and STIM2 control the activation kinetics of Orai1 channels. J Biol Chem 284:19164–19168.

Zhou Y, Wang X, Wang X, Loktionova NA, Cai X, Nwokonko RM, Vrana E, Wang Y, Rothberg BS, Gill DL (2014) STIM1 dimers undergo unimolecular coupling to activate Orai1 channels. Nature Communications 6:8395–8395.

Zitt C, Zobel A, Obukhov AG, Harteneck C, Kalkbrenner F, Lückhoff A, Schultz G (1996) Cloning and functional expression of a human Ca2+-permeable cation channel activated by calcium store depletion. Neuron 16:1189–1196.